EXTRACTION OF METALS FROM CONTAMINATED MATERIALS, SEDIMENTS AND INDUSTRIAL SOLID WASTE USING A NOVEL TECHNOLOGY (SERVO PROCESS)

CORINNE ALLIMANN-LECOURT

A thesis submitted in partial fulfilment of the
requirements of the University of Hertfordshire
for the degree of Doctor of Philosophy

The programme of research was carried out in the Department of Physical Sciences, Division of Chemical Sciences of the University of Hertfordshire

October 2004

ACKNOWLEDGEMENTS

I would like to thank some of the many people who have helped me throughout this research work:

My supervisors, Professor Michael Cox and Mr Terence Bailey for their continuous advice and support.

All the technicians, especially Mark, Roy, Carl, Chris, Peter, Dave, Judith for their technical support.

All my fellow research students Sandrine, Cyril, Jose, El-Said, Liam, Christina, Sacha, Kaj, Raza, Rakesh and Guillaume, as well as Oriol, Jose and Meindert who have contributed to some of the work.

Finally, my family and beloved husband Dominique for their patience, support and encouragements.

This thesis is dedicated to my much-regretted father,
he would have been so proud to see the outcome of such long studies.

Cette thèse est dédiée à mon regretté père qui, je suis certaine, aurait été fier de voir le résultat de si longues années d'étude.

"Je veux a fait des miracles,
je vais essayer a fait de grandes choses,
mais je voudrais n'a jamais rien fait.
Vouloir, c'est pouvoir, c'est la devise de tout homme"

Antoine St. Exupery

ABSTRACT

Selective Extraction and Recovery using Volatile Organic compounds is an emerging technology developed during the 1970s. This process can achieve the extraction of heavy metal contaminants from a matrix using a volatile organic reagent which passes through the feed material and reacts selectively with the desired metal salt, producing a volatile metal complex, removed from the matrix by a carrier gas. Such complexes may be decomposed to produce a pure metal product and regenerate the organic reagent for recycle. Previous studies demonstrated the possible extraction of nickel from low grade laterite ores using β-diketones (2,4-pentanedione (Hacac)) and Schiff bases (bis(pentan-2,4-dionato)propan-1,2-diimine (H_2pnaa).

The current research is directed towards the selective extraction of different metals such as zinc, lead, cadmium, molybdenum, and vanadium from contaminated sediments and industrial wastes (Orimulsion ash, Municipal Solid Waste fly ash (MSW), Pulverized Coal Combustion technology fly ash (PCC)).

New extractants and their metal complexes have been synthesised to determine their thermal stability and their volatility. Of those synthesised the metal complexes of tetra-propyldithiophosphoramide (Hprps) are the most thermally stable.

Using a thermogravimetric analyser the reaction kinetics of the SERVO process have been studied. Equipment to study the SERVO process on a laboratory scale has been designed and constructed. This equipment has been used to study the extraction of metals from four different matrices (sediments, Orimulsion ash, and two types of fly ash) using three different extractants, with promising results. These sources have been ranked from the best to the least applicable for the technology: Orimulsion ash > sediments > MSW fly ash > PCC fly ash.

Of the three extractants studied, Hacac, H_2pnaa and Hprps, the latter is the most efficient in terms of the range of metals which can be extracted, the volatilisation temperature, the extent of degradation and reaction time, but unfortunately is also the most expensive. For the fly ashes, of the three ligands studied, Hprps is the preferred extractant followed by H_2pnaa. Hacac is not recommended for these sources because extraction is too low.

CONTENTS

Title page		I
Acknowledgments		II
Dedication		III
Abstract		IV
Contents		V
Nomenclature		XI
Chapter 1: Introduction		
1.1	**Introduction**	
1.1.1	**Aim of the project**	1
1.1.2	**General Introduction**	1
1.2	**Properties of Sediments**	3
1.2.1	**Clay minerals**	3
1.2.2	**Humic Substances**	7
1.2.3	**Sediments reactions: ion exchange, pH and redox**	8
1.3	**Properties of Fly Ash**	10
1.3.1	**Coal**	10
	1.3.1.1 Composition and properties of coal	10
	1.3.1.2 Combustion of coal	11
	1.3.1.3 Properties and metal content of coal fly ash	12
	1.3.1.4 Utilisation of coal fly ash	13
1.3.2	**Hazardous Waste**	14
	1.3.2.1 Composition and properties of hazardous waste	14
	1.3.2.2 Hazardous waste combustion	15
	1.3.2.3 Properties and metal content of fly ash from hazardous waste	16
1.3.3	**Orimulsion fuel**	17
	1.3.3.1 Properties of Orimulsion fuel	17
	1.3.3.2 Orimulsion fuel incinerators	18
	1.3.3.3 Properties and metal content of Orimulsion ash	18
1.4	**Speciation and mobility of heavy metals**	19
1.4.1	**Literature review of metal speciation**	20
1.4.2	**Reactions changing solubility of metals in sediments and fly ash**	21
	1.4.2.1 Reaction decreasing solubility of heavy metals	21
	1.4.2.2 Reaction increasing solubility of heavy metals	22
1.5	**Heavy metal contamination**	24
1.5.1	**Site investigation procedure**	24
1.5.2	**Origin of heavy metal pollution**	26
1.5.3	**Metal toxicity**	27
1.5.4	**Waste disposal**	28
1.6	**Treatment technologies**	29
1.6.1	**Extraction technologies (mobilisation)**	30

1.6.1.1 Biological treatments 30
1.6.1.2 Chemical treatments 32
1.6.1.3 Soil washing 34
1.6.2 Stabilisation technologies 35
1.6.2.1 Biological treatments 35
1.6.2.2 Chemical treatments 38
1.6.2.3 Physical treatments 39

1.7 Preliminary studies of the SERVO process 40

1.7.1 Extractive metallurgy 40
1.7.1.1 Hydrometallurgy 41
1.7.1.2 Pyrometallurgy 41
1.7.1.3 Mond vapour phase process 42
1.7.2 SERVO process literature review 42
1.7.3 Recent studies of the SERVO process 46

Chapter 2: Experimental

2.1 Analytical equipment 48

2.1.1 Infra Red Spectrometry analysis 48
2.1.2 Mass Spectrometric analysis 48
2.1.3 Thermogravimetric analysis 48
2.1.4 Inductively coupled plasma analysis 49
2.1.5 MDS 2000 Microwave digestion system 49
2.1.6 X-Ray Diffraction 50

2.2 Experimental material 50

2.2.1 Preparation of simulated contaminated materials 50
2.2.2 Sediments 53
2.2.3 Puertollano Fly ash 53
2.2.3.1 Origin and composition 53
2.2.3.2 Pellet preparation 54
2.2.4 Orimulsion ash 54
2.2.4.1 Origin, production and composition 54
2.2.4.2 Pellet preparation 55

2.3 Experimental methods 55

2.3.1 Leaching of contaminated materials 55
2.3.1.1 Reflux digestion 56
2.3.1.2 Microwave digestion 56
2.3.2 Metal sequential extraction of contaminated materials 56
2.3.3 SERVO process extraction using modified thermogravimetric analysis 58
2.3.3.1 Apparatus and operational conditions 58
2.3.3.2 Cleaning procedure 59
2.3.4 SERVO Process Extraction Apparatus 60
2.3.4.1 Process design 60
2.3.4.2 Apparatus and operational conditions 63
2.3.4.3 Cleaning procedure 65

2.3.5 Reduction of metal complexes 65

2.4 Synthesis and properties of extractants and metal complexes 67

2.4.1 2,4–pentanedione and metal complexes 67
2.4.1.1 materials 67
2.4.1.2 synthesis procedure 68
2.4.1.3 $Cu(acac)_2$ 69
2.4.1.4 $Ni(acac)_2(H_2O)_2$ 70
2.4.1.5 $Zn(acac)_2(H_2O)$ 72
2.4.1.6 $Fe(acac)_3$ 74
2.4.1.7 $MoO_2(acac)_2$ 75
2.4.1.8 $VO(acac)_2$ 77
2.4.1.9 Conclusions 78
2.4.2 Bis(pentan-2,4-dionato)propan-1,2-diimine (H_2pnaa) and metal complexes 81
2.4.2.1synthesis of bis(pentan-2,4-dionato)propan-1,2-diimine (H_2pnaa) 81
2.4.2.2 synthesis of metal complexes 82
2.4.2.3 Cu(pnaa) 83
2.4.2.4 Ni(pnaa) 84
2.4.2.5 Co(pnaa) 86
2.4.2.6 Conclusions 87
2.4.3 Dithioimidophosphinates and metal complexes 88
2.4.3.1 synthesis and properties of tetra-phenyldithiophosphoramide (Hphps) 89
2.4.3.2 synthesis and properties of tetra-isopropyldithiophosphoramide (Hprps) 90
2.4.3.3 synthesis of H(prps) metal complexes 91
2.4.3.4 $Cd(prps)_2$ 92
2.4.3.5 $Co(prps)_2$ 93
2.4.3.6 $Pb(prps)_2$ 94
2.4.3.7 $Ni(prps)_2$ 95
2.4.3.8 $Zn(prps)_2$ 96
2.4.3.9 $Cu(prps)_2$ 97
2.4.3.10 Conclusions 98

Chapter 3: Application of SERVO process to contaminated materials and sediment samples

3.1 SERVO process tests on metal carbonates 100
3.1.1 Extraction 100
3.1.2 Recovery 101
3.2 Simulated contaminated materials 102
3.2.1 Kinetic study 102
3.2.2 Extraction study 111
3.3 Study of Sediments from Voies Navigables de France 116

3.3.1 Analysis of sediments 116
3.3.2 Sequential extraction of sediments 117
3.3.3 SERVO extraction results 119
3.3.3.1 Extraction obtained using H_2pnaa 119
3.3.3.2 Extraction obtained using Hacac and Hprps extractants 121
3.3.4 Conclusion 122

3.4 General conclusion 122

3.4.1 Studies on carbonates and modified clay materials 122
3.4.2 Studies on sediments 123

Chapter 4: Application of SERVO process to industrial waste

4.1 Puertollano Fly Ash 125

4.1.1 Analysis of Puertollano Fly Ash 125
4.1.2 Sequential extraction of Puertollano Fly Ash 125
4.1.3 SERVO extraction results 128
4.1.4 Conclusion 128

4.2 Rotterdam Waste Incinerator Fly Ash 128

4.2.1 Analysis of Rotterdam Waste Incinerator Fly Ash 128
4.2.2 Sequential extraction of Rotterdam Waste Incinerator Fly Ash 129
4.2.3 SERVO extraction results 130
4.2.3.1 Single extraction 130
4.2.3.2 Repeated extraction 132

4.2.4 Conclusion 136

4.3 Orimulsion Ash 138

4.3.1 Analysis of Orimulsion Ash 138
4.3.2 Sequential extraction of Orimulsion Ash 138
4.3.3 SERVO extraction results 139
4.3.4 Conclusion 140

4.4 General conclusion 141

4.4.1 Most suitable type of ash for the process 141
4.4.2 Efficiency of the extractants 143
4.4.3 Overall conclusions 146

Chapter 5: General Conclusions and Further Work

5.1 Studies of Extractants 148

5.1.1 Thermal stability and volatility of the extractant and their metal complexes 148
5.1.2 Cost of extractants 150
5.1.3 Conclusion 152

5.2 Physico-chemical characteristics of the contaminated sources studied and extraction of metals using SERVO process 152
5.2.1 Physico-chemical characteristics of the studied sources 152

5.2.2 SERVO process extraction results 155
5.2.3 Conclusion 155

5.3 SERVO cost and comparison to other relevant technologies 156

5.3.1 General assumptions 157
5.3.2 SERVO process costs 158
5.3.2.1 Capital cost 158
5.3.2.2 Operating costs 158

5.3.3 Competing technologies 160
5.2.3.1 Dredging and Offsite disposal 160
5.2.3.2 Containment/capping 161
5.2.3.3 HCl acid leaching process 161
5.2.3.4 Electrokinetic 162
5.2.3.5 In Situ fixation of lead 163
5.2.3.6 Comparison of technologies 163

5.3.4 Conclusion 166

5.4 Future Studies 166

Chapter 6: References 168

Published Papers

C Allimann-Lecourt, T H Bailey, M Cox, L M Gilby and J Robinson, 'Extraction of heavy metals from sediments using the SERVO process', Land Contamination & Reclamation 7(4), 265-269, (1999)

C Allimann-Lecourt, T H Baileey and M Cox, 'Purification of combustion fly ashes using the SERVO process', J. Chem. Tech. Biotechnol. 77, 260-266, (2002).

Appendices (see accompanying CD)

Appendix 1: List of potential contaminants associated with main industrial sectors

Appendix 2: ICRCL 59/83 and Netherlands guideline values

Appendix 3: Technical data sheet for Sodium bentonite: Volclay MPS-1

Appendix 4: Location point and metal content of sediments

Appendix 5: Chemical composition of Fly Ash from Puertollano power plant

Appendix 6: IR , MS, TGA results for Chapter 2

Appendix 7: Some physical properties of some first row transition elements

Appendix 8: ICP results from Chapter 3

Appendix 9: ICP results from Chapter 4

Appendix 10: SEM and X-Rays results from Chapters 3 and 4

GLOSSARY

Symbol	
AFNOR	Agence Française de Normalisation
b.p.	boiling point
BCR method	Community Bureau of Reference method
CLEA	Contaminated Land Exposure Assessment
dec.	decompose
DTPA	diethylenetriaminepenta acetate
EDTA	ethylenediaminetetra-acetic acid
Eh	redox potential
ESTCP	Environmental Security Technology Certification Program
Hacac	2,4-pentanedione or acetylacetone
Hphps	tetra-phenyldithiophosphoramide
H_2pnaa	bis(pentan-2,4-dionato)propan-1,2-diimine
Hprps	tetra-isopropyldithiophosphoramide
ICP-AES	Inductively Coupled Plasma – Atomic Emission Spectrometry
ICRCL	Interdepartmental Committee for the Redevelopment of Contaminated Land
IR	Infra Red spectrophotometry
m.p.	melting point
MDS	Microwave Digestion System
MS (EI)	Mass Spectrometric analysis (Electronic Ionisation)
MSW	Municipal Solid Waste
MW	molecular weight
NTA	nitrilotriacetic acid
ODR	oxygen diffusion rate
PAHs	polynuclear aromatic hydrocarbons
PCBs	polychlorinated biphenyls
PCC	Pulverized Coal Combustion
PVC	poly(vinyl chloride)
ref.	reference
RDF	refuse-derived fuel

SERVO	**S**elective **E**xtraction and **R**ecovery of Metals using a **V**olatile **O**rganic Extractant
SEM	Scanning Electronic Microscope
str.	Stretching vibration (infra-red)
TG	thermogravimetric curve
TGA	thermogravimetric analysis

Chapter 1: Introduction

1.1 Introduction

1.1.1 Aim of the project

The purpose of the work presented in this report is to establish the optimum parameters of the SERVO Process, an emerging technology, to extract and recover heavy metals from contaminated sediments and from industrial wastes such as Orimulsion ash, Municipal Solid Waste fly ash (MSW), Pulverized Coal Combustion technology fly ash (PCC). This technology is designed to extract heavy metal contaminants with a high efficiency and also produce a clean matrix and a metal of high purity, which can be reused in industry. The clean residues may be replaced on-site, or used in other manufacturing processes.

1.1.2 General introduction

In the past, man in his quest for a better standard and quality of life has exploited the natural resources of the Earth. However, because of rapid growth in the population, and also rapid growth of industrial centres and waste disposal sites, man has accelerated the process of depletion of natural resources and has damaged the fragile balance of the ecosystem. [1, 2] Some hazardous compounds are released at every stage of product manufacture, its use and also its disposal. Some other compounds will enter the environment routinely as result of agricultural practice and transport. Release might be intentional, such as discharge of effluents produced by manufacturing industry, but it may also be unintentional arising from accidental releases. In any case, the environmental consequences are the same: our living resources, water, air and soil are globally affected. The potential effects of industrial development are no longer confined to national borders. Who would have thought that one day heavy metals and organochlorine pesticide residues would have been found in the ice sheets of both polar caps, many thousands miles away from any manufacturing industry? [2] Not only is the global environment affected but also the pollutants are very diverse in nature. A large range of organic compounds, organometallic compounds, metals and some gases are potential pollutants and their

behaviour is extremely difficult to predict and assess. Some chemicals are persistent and able to accumulate within the biota, whereas others may dissipate and become diluted in the environment. [3]

Thus man has to face the problem of pollution, as it will not be possible for him to escape from its consequences. Khrishna B. Miscra explains the "way of success": [3] *It is therefore necessary that consideration of environment, economy, and performance should become the real basis for sustainable development in the planet if life on our planet is to survive forever*. Engineers, technologists, researchers and also governments, industries and individuals have to take up this serious challenge. The only way to reduce pollution is in the first instance to understand it. Pollution is primarily an economic problem, as inhabitants of the Earth must take economic decisions about what goods and services to produce, how to produce them, how much to produce, and how to distribute them. So technologists and engineers have to develop routes to clean production and clean transportation, while maintaining a level economy and producibility. Industries have to accept the emerging clean production, reduce pollutant emissions, and stop the intentional release of pollutants to land and sea. Governments have to support any movement for a clean environment, but also sanction any damages caused to it. [4] Consumers have to stop dumping if recycling is possible, by sorting their municipal waste and favouring recycling i.e. aluminium, glass, and paper. Finally, one of the targets for environmental researchers is to remediate the strongly polluted sites, which have been identified. One possible remedial action is to clean up the soil, using methods which could extract pollutants. Unfortunately, it appears that nowadays only a few of the available techniques can treat a site with high efficiency, within a relative short treatment time, at low cost, and leaving a soil which can be considered clean.

Clean-up techniques make use of the specific differences between the properties of contaminants and the properties of contaminated material. [5] Therefore, this introduction deals firstly with the physical and chemical properties of sediments, fly ash, followed by a description of heavy metal species and their mobility in these materials. Then contaminated land is defined and the source of heavy metal pollution is shown. Subsequently, different existing and emerging

technologies to treat soils, sediments and fly ash contaminated by heavy metals are described, followed by a review of work achieved using the SERVO process.

1.2 Properties of Sediments

Sediments are soil and minerals washed from land into water, usually after rain. Soils, present in sediments, are composed of a small proportion of sand (20-200 μm), and a high proportion of silt (2-20 μm) and clay (<2 μm) that gives an overall very fine texture to the sediment. The very fine textured sediment contains humic materials. This physical property results in a strong affinity for contaminants and mobility of metals, but also in a large quantity of interstitial water in the sediment. This property arises from their large surface area for adsorption: the smaller the particle, the higher the ability to hold nutrients and water.

Two other important properties of sediments are concerned with their pH and redox potential, chemical properties that will interfere with the mobility of metals. [5, 6, 7] Acidic pH values slow microbial activity, so increase the solubility of metals. Weak to alkaline pH values increase microbial activity, so increase immobilization processes such as precipitation or adsorption. Secondly, changes in sediments redox potential have an important effect on the retention or release of metals either directly or as a result of the reaction of metals with oxidised or reduced constituents of the sediment. Metals that are present in the sediment bound to clay minerals and humic substances by cation exchange process are the most mobile, whereas metals bound within the crystal structure of clay mineral are generally immobilized.

For a better understanding of the chemical reactions, which occur in clay and organic matter, the nature of these materials is described first.

1.2.1 Clay minerals

Clay minerals are three-dimensional layered structures that have a plate-like appearance. They are the most surface-active sediment mineral components as they adsorb and hold nutrients as well as water; [8] Clays are layered silicates and consist of a combination of two structural units, tetrahedral and octahedral sheets.

Tetrahedral silica sheets are formed by SiO_4 tetrahedra sharing oxygen atoms, termed basal oxygen. The unshared oxygen atoms are called apical oxygen atoms.

These different types of oxygen atom are shown in figure 1 which represents a single silica tetrahedron and a tetrahedral silica sheet [9]:

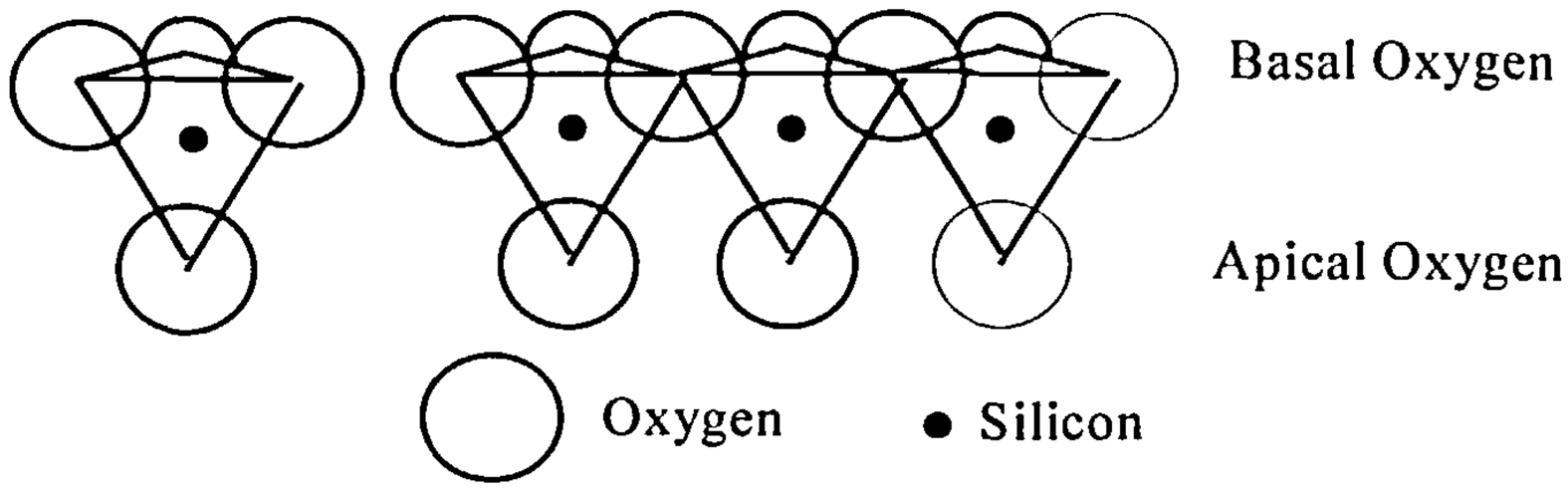

Figure 1: a single silica tetrahedron (left) and tetrahedral silica sheet (right) [9]

The interlinked basal oxygen atoms of the tetrahedral sheet are arranged to form a hexagonal (Figure 2, the diagram is not to scale to allow better visibility of the phenomenon) leaving a cavity that can mediate a negative charge resulting from isomorphic substitution in the tetrahedral silica sheet (e.g. Al^{3+} for Si^{4+}). When charged this cavity can form inner sphere or outer sphere surface complexes with aqueous solutions.

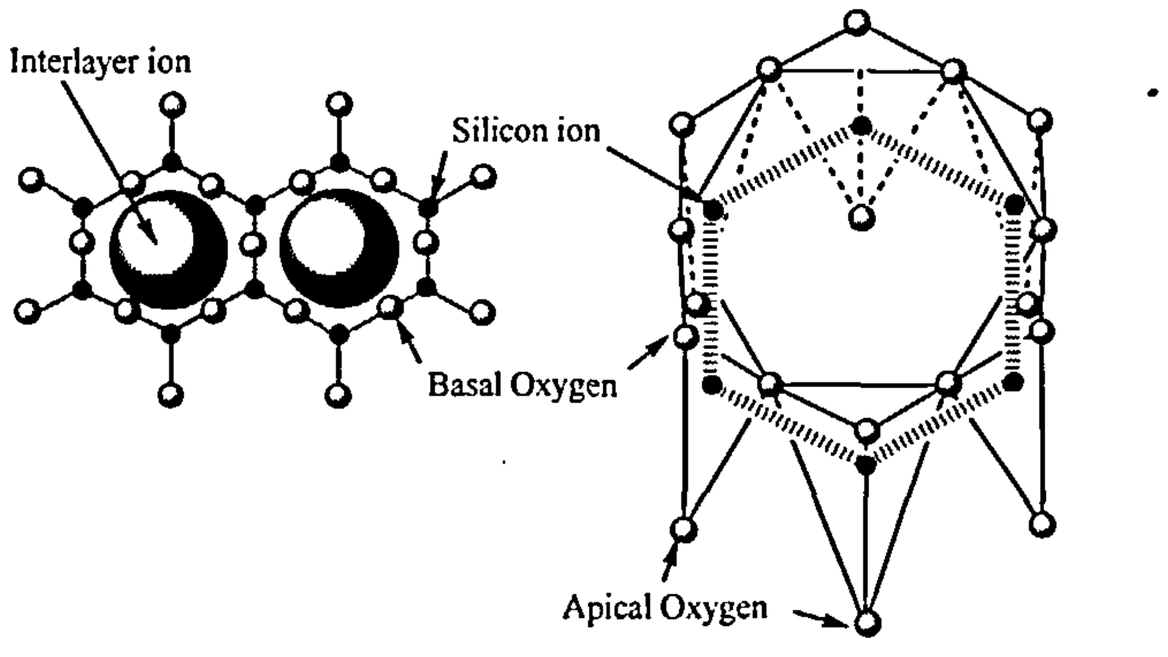

Figure 2: hexagonal arrangement of basal oxygens of the linked silica tetrahedra [9]

The amount of isomorphic substitution determines the surface charge density (z) and the cation-silicate layer interactions, and thus produces the wide range of clay minerals defined later.

The octahedral sheets are formed by cations (Al^{3+}, Fe^{2+} or Mg^{2+}), which are coordinated with six oxygen atoms or hydroxyl units in an octahedral polyhedron,

figure 3. [7] When aluminium is the octahedral cation, only two thirds of the possible positions are filled to electrically balance the structure, this is then called a dioctahedral mineral. Whereas when iron or magnesium is present, all the octahedral sites are filled to electrically balance the structure, this is then called the trioctahedral structure.

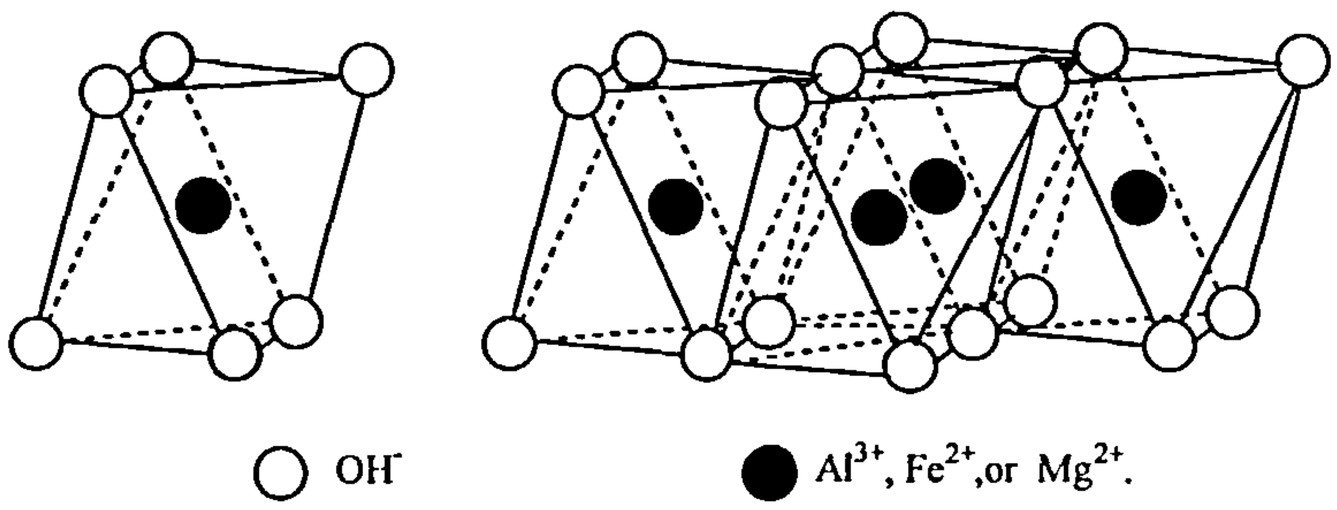

Figure 3: A single octahedral unit (left) and an octahedral sheet (right) [7].

There are several types of clays that can be structurally represented in two major categories, the 1:1 and the 2:1 type crystal lattices (figure 4).

The 1:1 type crystal lattice has one tetrahedral sheet (Si) to one octahedral sheet (Al); kaolinite is the best known example and has a non-expanding interlayer and low cation exchange capacity. The 2:1 type crystal lattice is formed with one octahedral sheet sandwiched between two tetrahedral sheets. It can be subdivided into four categories according to their layer charges, in other words the ions that bind the two crystal lattices. Talc (dioctahedral) and pyrophyllite (trioctahedral) contain no octahedral, or tetrahedral substitutions and therefore has no layer charge ($z = 0$) with van der Waal's bonding holding the layers together. These minerals have a non-expanding interlayer and no cation exchange capacity. Illite ($0.6 > z < 0.9$), mica ($z \sim 1.0$) and brittle mica ($z \sim 2.0$) also have a non-expanding interlayer composed of K^+ (inner sphere complex), but possess cation exchange capacity. Smectites ($z \sim 0.2 - 0.6$) and vermiculites ($z \sim 0.6 - 0.9$) have an expanding interlayer composed of an outer sphere complex (e.g.: Ca^{2+}, $2H_2O$) and a high cation exchange capacity. Chlorite, sepiolite and palygorskite have a variable layer charge due to a full range of substitutions that can be observed in these most complicated structures. The trioctahedral 2:1 structure has an octahedrally coordinated layer composed of cations and anionic units (e.g. $Mg_3(OH)_6$). These minerals have a high exchange capacity, and a non-expanding interlayer.

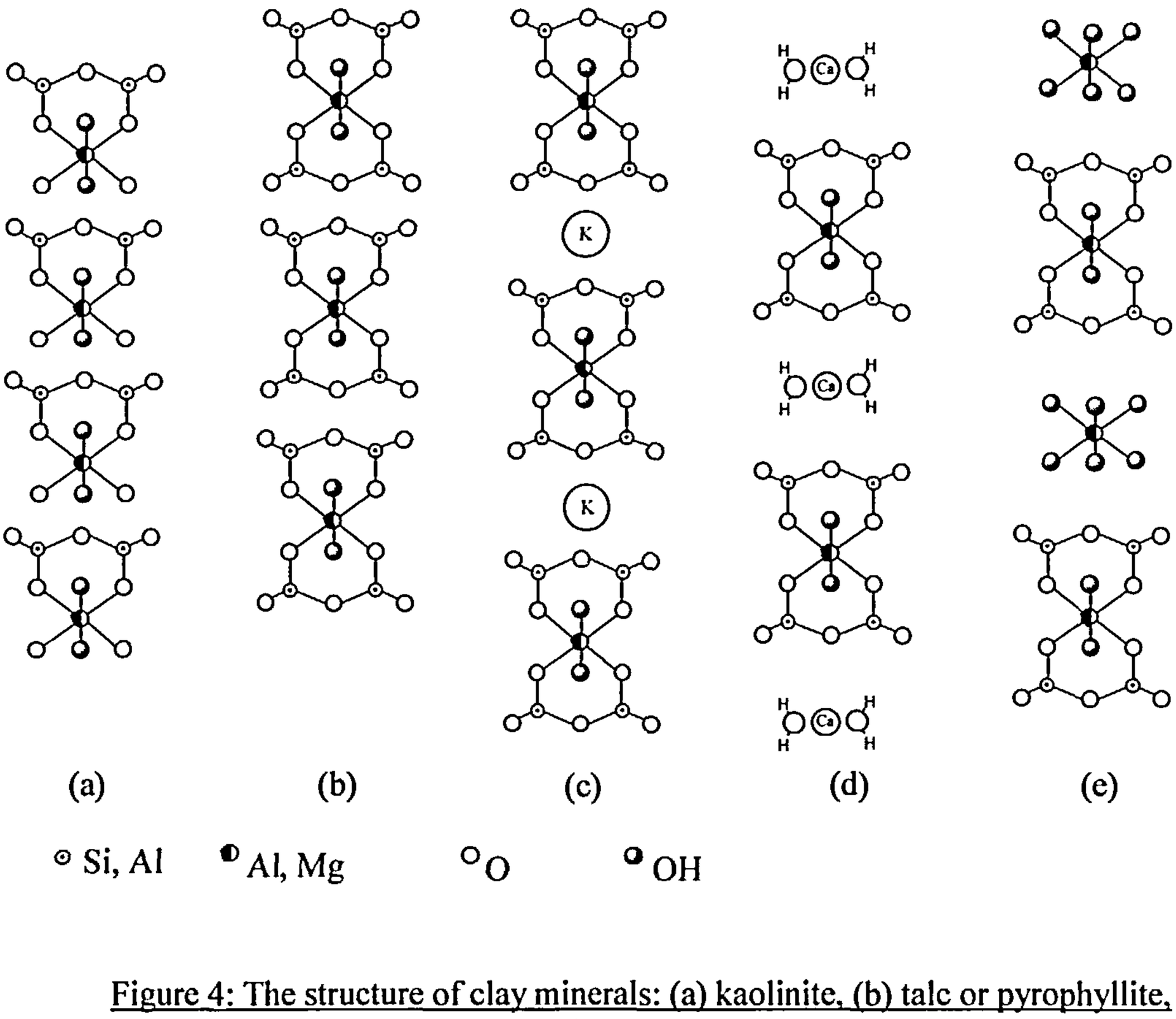

Figure 4: The structure of clay minerals: (a) kaolinite, (b) talc or pyrophyllite, (c) illite, mica or brittle mica, (d) smectites and vermiculites, (e) chlorite, sepiolite and palygorskite [7, 9]

Negative charge arises on the surface of clays as a result of the following chemical phenomenon: [7, 10, 11]

isomorphic cation substitution in the bulk structure of clays (e.g. Al^{3+} for Si^{4+} in tetrahedral silica sheet, or Mg^{2+} for Al^{3+} in octahedral sheet);

complexation in the surface of the tetrahedral sheet by inner or outer sphere complexes;

ionisation of hydroxyl ions on the mineral surface, which is pH dependent e.g.:

$$AlOH \xrightarrow{\text{change in pH}} AlO^- + H^+$$
$$SiOH \xrightarrow{\text{change in pH}} SiO^- + H^+ \qquad (1 \& 2)$$

Some ions can therefore be adsorbed on the surface of clay minerals in the diffuse layer and move about freely in aqueous solution, but remain close enough to the particle surfaces to create an effective surface charge density that balances the net structural surface charge density. Three types of surface species (inner-sphere complex, outer-sphere complex and diffuse layer) represent three modes of adsorption of aqueous ions onto a 2:1 layer type clay. The ions adsorbed in the diffuse layer will be less tightly adsorbed than the internal exchanged ion (inner-sphere and outer-sphere).

1.2.2 Humic substances

Humic substances are one of the components obtained from the degradation of humus, constituent of soil organic matter (figure 5).

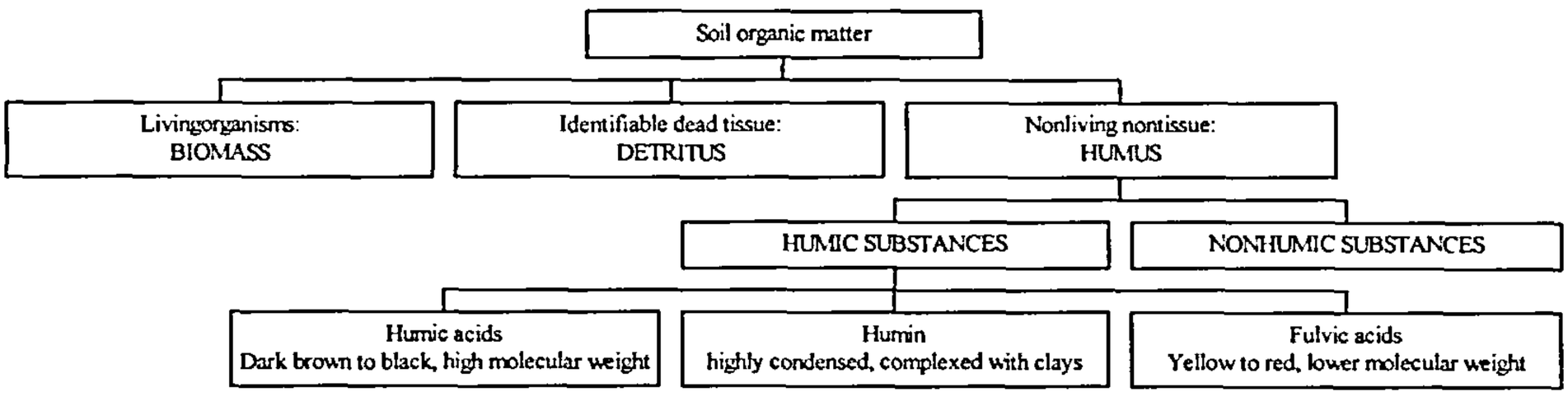

Figure 5: Soil organic matter [12]

They comprise about 60-80% of the soil organic matter and are the most stable part of humus. The three main components of humic substances, humic acid, fulvic acid and humin, have non-specific variable structures and composition and differ in their reactions. Humic substances consist of various chains and rings of carbon atoms, and contain a relatively large number of functional groups, e.g. $-CO_2^-$, -OH, >C=C<, -COOH, -SH, capable of interaction with metal ions. [12] Some of these functional groups release protons leaving negatively charged sites on the clay. This charge is variable and pH dependent. The complexity of humic substances makes them more resistant to microbial attack compared with non-humic substances, which are less complex. Non-humic substances like polysaccharides and protein-like materials constitute 20-30% of humus. Clay-humus interaction plays an important role in the protection of soil humus against microbial attacks, as clay minerals can entrap some humus in their very small pores, which then becomes physically inaccessible to

microbes.

1.2.3 Sediment Reactions: ion exchange, pH and redox

As described above, clay materials and humic substances, also called sediment colloids, have a negative surface charge that holds cations in equilibrium. Ion exchange is a reversible process in which one equivalent of an ion in solution replaces one equivalent of an ion on the exchanger. [13] The strength of the cation sorption onto colloids reflects the cationic charge. Thus the higher the positive charge on the cation, the greater the exchangeability ($Al^{3+} > Fe^{2+} > K^{+}$).

Similarly, the affinity of sediment colloids for ions with the same charge is determined by their hydrated cation radius. Thus the larger the hydrated ion, the greater is the exchange (K^{+} (0.53nm) < Na^{+} (0.79nm)). This phenomenon is explained by the fact that an ion with a larger hydrated radius is held less tightly than an ion with a smaller hydrated radius.

For expanding clays, e.g. smectites, the intercalated cations can be exchanged by other cations in the solution surrounding the clay. For non-expanding clays e.g. illites, such cations are more strongly attached in the interlayer and are non-exchangeable. So the nature of the clay mineral is important for cation exchangeability but the nature of the cation is also important.

Cation exchange takes place continuously as it is initiated by any changes in the solution surrounding the colloid. As such changes occur frequently; there is little possibility of the system reaching equilibrium. Thus changes in solution parameters can result from an addition of fertilizer, increase of potassium ions, and loss of cations by leaching, etc.

The Cation Exchange Capacity (CEC) of a sediment is defined as the number of exchange sites, which can adsorb and release cations. So it indicates the number of negative charges present per unit mass of sediment. In the past, the units for CEC were expressed as milliequivalents per 100 g of soil ($meq.100g^{-1}$), but the current conventional units are centimoles of positive charge per kilogram weight of soil ($cmol_c\ kg^{-1}$), where $_c$ is the charge of the cation. Since not all cations have the same charge, the actual amounts of ions required to balance the CEC of a soil differs between cations, e.g. if the negative charges on 1kg of soil is balanced by 0.1 cmol of

K^+ or 0.05 cmol of Ca^{2+}, then CEC can be expressed by 0.1 $cmol_{+1}\ kg^{-1}$ or 0.05 $cmol_{+2}\ kg^{-1}$. [14]

The more common exchangeable cations are Ca^{2+}, Mg^{2+}, K^+, Na^+, H^+, and Al^{3+}.

The concentration of hydrogen ions in the solution within the sediment represents the acidity as measured by the pH of the pore water. Hydrogen ions in this solution represent a minor quantity when compared to the protons present at the cation exchange sites, which may be termed the reserve acidity. Both the reserve and active acidity are in equilibrium, thus when the hydrogen ion concentration in the sediment solution is increased as a result of natural processes or human activity, the equilibrium is disturbed and a redistribution of hydrogen ions occurs between the reserve and active sites. [15] This resistance of a sediment to changes of pH is called the buffer capacity, and the higher the Cation Exchange Capacity the greater is its buffer capacity.

Sediment is also subject to variations in redox status, which mainly affects the state of elements like C, N, O, S, Fe and Mn. Some other elements like As, Cr and Hg can also be affected. Redox reactions occur where there is an exchange of electrons between the metal ion and a reducing or oxidising agent, and consequently a change in the metal oxidation state. [16]

Oxidation requires removal of electrons from the metal species to increase the oxidation state of the metal:

$$M \xrightarrow{oxidation} M^{2+} + 2e^- \tag{3}$$

$$2\underbrace{FeO}_{Fe(II)} + 2H_2O \Leftrightarrow 2\underbrace{FeOOH}_{Fe(III)} + 2H^+ + 2e^- \tag{4}$$

Oxygen gas (O_2) is a strong oxidizing agent, which can oxidize both organic and inorganic substances.

Reduction is the gain of electron(s) by the metal, so decreasing the metal oxidation state. This reaction can either be performed by a micro-organism itself, or by a reducing agent produced by the micro-organism:

$$M^{2+} + 2e^- \xrightarrow{reduction} M \tag{5}$$

$$\underbrace{NO_3^-}_{N(V)} + 2e^- + 2H^+ \Leftrightarrow \underbrace{NO_2^-}_{N(III)} + H_2O \tag{6}$$

1.3 Properties of fly ash

Fly ash is defined as the very fine particles collected in dust removal systems of exhaust gases from industrial processes such as, in the context of this project: fuel power plants and waste incinerators, and their composition will depend on the nature of the process. In the case of power plants and incinerators, the major chemical constituents are silica, alumina and oxides of iron and calcium, but the type, character and properties of the ash depend on a number of factors, the most important being the composition of the feedstock and furnace design. [17] In the following section, the role of the composition and properties of the original material, or feedstock, in the design of furnaces and the composition and properties of the resulting fly ash will be explained.

1.3.1 Coal

1.3.1.1 Composition and properties of coal

Coal is mainly composed of carbon, hydrogen and oxygen, with lesser amounts of nitrogen and sulphur, and varying amounts of moisture and mineral matter. [18] The large variety of plants and different degrees of plant conversion determine the different types of coal that vary in colour from brownish-red to dark black according to the age of the rock. Brown coal and lignite, sub-bituminous and bituminous coal, and anthracite make up a series of products with increasing carbon and decreasing oxygen content. [17]

Trace metals, also present in coal, arise from three different mechanisms. Metals may be present in the plant material and soil that form the coal, or from mud or sediment that cover the original deposits and mix with the organic matter as it is undergoing the coalification process. [19] Finally water in cracks and fractures of the deposit can carry trace metals into the coal. The concentration of metals can vary from a few percent of the total composition of the coal to a fraction of a part per

million, and their distribution reflects the distribution of trace elements in the soil.

1.3.1.2 Combustion of coal

In 1999, 87 % of coal was used as a fuel to produce energy, [18] resulting in 'gigascale' production of fly ash in the world with 65 millions tons/annum in the US and 10 millions tons/annum in the UK. Currently pulverized coal burners are most commonly used, as they offer the advantage of being able to use any type of coal, the reason being that pulverized coal burns like a gas and so fires are easily ignited and controlled. Prediction of some of the coal characteristics, i.e. grindability and moisture content, are important to ensure the best performance of the boiler. Fly ash comprises about 80% of the solid products of combustion with about 20% as bottom ash from the furnace. [17] The type of ash produced is dependent on both the boiler type but also its design.

Fluidised-bed boilers are currently replacing the low capacity stoker-fired units and smaller range pulverized coal units. In these boilers, air is injected in the furnace though distribution plates to fluidise a bed of hot inert material into which the powered coal is injected. [20] The inert material disperses the coal particles throughout the bed, helps the ignition of the particles and finally provides sufficient residence time for complete combustion. In this case between 10-90% of the solid product of combustion is fly ash with the remainder occurring as the bed drawdown.

In stoker-fired boilers, the coal fuel is injected into the boiler in three different ways: [21] underfeed, overfeed, and spreader. In these boilers, fly ash is produced as 20% of the solid product of combustion.

When coal particles are burned at high temperatures in the furnace volatile matter is vaporized and the carbon is burned off. Inorganic matter, present in form of impurities, is converted into ash. Most of this mineral matter consists of clays, pyrite and calcite. During combustion, the pyrites changes to iron oxide, and mica and clay particles are partially vitrified to form small glassy amorphous alumino-silicate spheres. [18] The coarser ashes fall to the bottom of the furnace and are collected as bottom ash, while the finer particles are separated from flue gases using electrostatic precipitators and are collected as fly ash. For every ton of coal burned 3 - 30 % of the mass remains after combustion as fly ash and bottom ash, an average of 7 - 15% ash

is common in bituminous coal. [18]

1.3.1.3 Properties and metal content of coal fly ash

(a) Physical properties

The resultant physical properties of the ash, such as moisture content, particle mass, glass composition and the portion of unburned carbon will depend on the combustion temperature at which the coal was fired, the air:fuel ratio, coal pulverization size and rate of combustion. [18] In general, fly ash consists of spherical and spongy aggregates, [22] some of which are hollow, 'cenospheres', while others may contain many spherical particles within a large glassy sphere, 'pherospheres'. As fly ash particles are extremely fine, with an average size between 7 to 12 μm, they have a pozzolanic activity, where they react with calcium oxide in the presence of water and produce highly cementitious water-insoluble products. The portion of unburned carbon (2 - 10%) is an important parameter as it determines the loss on ignition. [23]

(b) Chemical properties.

Fly ash is mainly composed of oxides of elements including silicon (SiO_2), aluminium (Al_2O_3), calcium (CaO), iron (Fe_2O_3), magnesium (MgO), titanium (TiO_2), sulphur (SO_3), sodium (Na_2O) and potassium (K_2O). [22] The proportion of these oxides depends on the nature of the feedstock. Thus fly ashes, obtained from bituminous and lignite coal are relatively rich in ferric oxide and contain less than 5% calcium oxide. Fly ashes from sub-bituminous and lignite coals are characterized by higher CaO, MgO, and SO_3 and lower SiO_2 and Al_2O_3 than the bituminous fly ashes.

(c) Metal content.

During combustion (volatilised) metals may react with sulphur or oxygen to form other combustion products. Later these will undergo condensation and enrich the fly ash particles or become fume. Some others like As_2O_3 will react with calcium oxide, alumina and/or silica to form non-volatile compounds. [18]

1.3.1.4 Utilisation of coal fly ash

The Netherlands is the country using the most fly ash with virtually 100% utilisation in industrial applications principally construction. The average level of use in the world was around 40% in 1999 [18] with only 27% for the USA, who have the largest fly ash production. By far the greatest utilisation for coal fly ash (in 1999: 49%) was as an additive to cement and concrete products. [17] The fly ash reacts with free lime within the Portland cement to produce a stronger and more durable concrete. It has been found that concrete containing coal fly ash is less susceptible to attack from chemical products in the environment, and to damage caused by freezing and thawing. Fly ash can also be used alone as a structural fill or cover material (15%). In this application, the fly ash used requires some specific properties like particle size, compaction characteristics, density, permeability and comprehensive strength of the grout material. The use of fly ash mixtures for hazardous waste stabilisation and solidification accounted for 12% of the total reuse of fly ash in 1999, and is further developed in §1.6.2.3. To a lesser extent fly ash is used in the following applications:

roadway and pavement construction as a soil stabiliser;

as an addition to construction materials to form a lightweight aggregate, but here suffers from a lack of natural plasticity and the presence of soluble salts;

zeolite synthesis, the low amount of mullite and low Si/Al ratio allows the formation of a high ion exchange capacity material with a high selectivity for polar molecules;

and in the ceramic industry where its high compressive strength and good thermal stability makes it suitable for high temperature applications including refractory materials. [17]

However in these applications there is little economical value since fly ash utilization is restricted by standards set for their environmental quality. Heavy metals traces are considered as potentially hazardous to the environment and their potential solubilization during zeolite synthesis or volatilization during fly ash firing for ceramic uses restrict the number of reusable fly ashes.

1.3.2 Hazardous waste

Annual hazardous waste production worldwide is estimated to be 350 million tons. [24] Although, municipalities and industries are reducing waste production per inhabitant, this will not decrease the total annual production because of the continuously increasing world population. High temperature incineration is currently one of the preferred technologies for managing waste, even if high capital cost discourages its use. To reduce the cost of waste incineration, the possibility of producing energy as a co-product is becoming popular, but requires some initial waste preparation or fuel addition to optimise the combustion. [25]

1.3.2.1 Composition and properties of hazardous waste

(a) Municipal solid waste (MSW)

Municipal waste solids are extremely heterogeneous in size, shape, composition and heating value. Municipal waste is composed of more than 50% of non-biodegradable material (table 1) that can be segregated by the householder for further recycling (metal, glass, paper, and some plastics). The material left after segregation, so-called refuse-derived fuel (RDF), is mainly composed of organic waste that could be used efficiently for compost preparation or as a better source of energy when incinerated. [26, 27] Municipal waste solids can also be burnt as received, when it is called mass-burning.

Waste	Paper	Glass	Metals	Plastics	Rubber and leather	Textiles
Percent	38.9%	6.3%	7.6%	9.5%	3.1%	3.2%
Waste	Wood	Food wastes	Yard trimming	Other inorganic wastes	Other materials	
Percent	7.0%	6.7%	14.5%	1.5%	1.7%	

Table 1: Municipal solid waste composition in the US 1994 [26]

(b) Medical waste.

Medical waste only represents a tiny fraction of the total waste produced

annually. Because of its nature, i.e. infectious, low level radioactive, or hazardous, [24] almost all medical waste is incinerated to reduce the volume and to prevent spreading of infection. The residue is treated as radioactive hazardous waste, and is not used for energy recovery or fly ash reuse.

(c) General chemical industry waste

Table 2 [24] shows that most of the total chemical industry waste produced in the US is classified as organic and general chemical waste. Incineration is often preferred to reducing the waste volume because the high heat capacity of the organic chemicals provides a good source of energy recovery.

Waste category	Organic chemicals	General chemicals	Explosives	Plastics and resins
Waste generation, kt yr^{-1}	60-80	40-50	10-15	6-10
Waste category	Refuse systems	Agricultural chemicals	Inorganic pigments	Alkalis/chlorine
Waste generation, kt yr^{-1}	5-8	3.5-5	2.5-4.5	2.5-4.5

Table 2: Annual waste generation in US chemical industry. [24]

1.3.2.2 Hazardous waste combustion

Current incinerators have the ability to destroy nearly 100% of liquid and 60% of solid wastes. [25]

(a) Solid waste incinerators

Municipal solid wastes, because of their high heterogeneity, are extremely difficult to burn to recover energy if they have not been previously sorted. [28] RDF does not require much preparation and thus is often much easier to handle than mass-burning refuse. For incinerators to operate without auxiliary fuel or air preheating, the waste solid must contain at least 50% moisture or 60% ash and have more than 25% combustibles. Moreover, combustion is optimised with time, temperature and turbulence. [29]

(b) Liquid waste incinerators

Liquid wastes are divided according to their heating value into high (>16MJ kg^{-1}) and low (<16MJ kg^{-1}) heating value, with the low heating value liquids requiring additional fuel or gas to help combustion. [28] Vertical furnaces, used for the combustion of liquid wastes, are constructed on a steel shell lined with high temperature refractories and consequently require higher investment than horizontal incinerators.

(c) Rotary Kiln Incinerators.

These have the ability to accept a wide range of industrial waste such as solids, heavy tars, sludges, filter cakes, and liquid wastes. Therefore they are often used for the incineration of chemical and medical wastes. [30]

1.3.2.3 Properties and metal content of fly ash from hazardous waste

The ashes obtained from combustion of municipal waste incinerators may be classified under 3 categories, namely: bottom ash, APC residues (Air Pollution Control) also called fly ash, and combined (APC and bottom ash combined). [31]

(a) Physical properties.

Bottom ashes produced from hazardous waste incineration are quite heterogeneous in size, with 20% of the bottom ash having a particle size > 10^5 μm, and the remaining fraction more uniform in size with up to 10% smaller than $2*10^5$ μm. [31, 32] Fly ash (APC residues) has an average particle size larger than 20 μm, but smaller than 250 μm and contains planar, cylindrical, as well as spherical particles and sintered agglomerates and has been described as "shredded sponge". [33]

(b) Chemical properties.

As mentioned before because of the high heterogeneity of waste components, the fly ash obtained from the combustion of municipal waste is quite complex. The bottom ash consists of ferrous and non-ferrous metals, slag and construction materials. Fly ash particles are dry to semi-dry particles, which consist of the reaction products of calcium chloride and unreacted lime. Due to the high concentration of

soluble salts, fly ashes are usually highly soluble in water (25 - 85% by weight). [31] Most of the available literature report different interpretations of the X-ray analyses of fly ash. [33-34] For example, a careful analysis of municipal solid waste fly ash [33] showed the presence of $Na_{21}MgCl_3(SO_4)_{10}$, $K_2Ca(SO_4)_2.H_2O$, SiO_2, $PbCl_2$, $PbSO_4$, $CaSO_4$ and $PbTi_3O_7$. Another X-ray analysis [32] reports the main components as $K_2Ca(SO_4)_2.H_2O$, $(K,Na)_3Na(SO_4)_2)$, $CaSO_4$, with other crystalline phases like $KNaSO_4$, NaCl, $Ca_3Al_2SiO_{10}$, SiO_2, $CaCO_3$, Fe_2O_3, $(Na,KAlSiO_8)$, $2CaSO_4.H_2O$, TiO_2, Fe_3O_4.

(c) Metal content.

Metal distribution within the various particle size fractions is important to determine the association of metal within the fly ash matrix. For instance, aluminium, potassium, magnesium and iron have been found throughout the various sized particles [34], whereas cadmium, chromium and lead were present in the highest concentration in the smallest particle size fractions. [32]

The elemental metal content of more than thirty municipal solid waste components have been identified and quantified. [35] The target of this study was to determine the contribution of each waste component to the total metal content. For example, cadmium was found in coloured newsprint, residual mixed paper, plastic film, plastic house wares, lawn waste, food containers and Ni-Cd batteries. Certain paper fractions like coloured newsprint and magazines, which may be candidates for composting and recycled paper, contain the highest concentration of metals. This study shows that almost all waste components contain some heavy metals that are considered as toxic, and therefore it remains difficult to remove metals prior to combustion.

1.3.3 Orimulsion fuel

1.3.3.1 Properties of Orimulsion fuel

Below the Orinoco belt of Venezuela exists the world biggest reserve of natural bitumen. [36, 37] This "non-flammable" and very inert bitumen is a very highly viscous material that requires dispersion in water to reduce its viscosity to a transportable level. Orimulsion is the trade name given to Orinoco natural bitumen

(70%) dispersed in water (29.8%) that is used as a fuel for electric utility boilers, with the aim of replacing heavy fuel oil by a cheaper alternative. Water and bitumen do not mix naturally, so a small quantity of surfactant and magnesium-based additive is added to the mixture. [38] Until recently (end 1998) the additives used were phenol ethoxylate and magnesium nitrate (0.2%), but these have since been replaced by tridecylalcohol ethoxylate (0.13%) and monoethanolamine (0.03%), together with magnesium hydroxide to improve fuel storage capacity and minimize high-temperature corrosion. These modifications result nowadays in two different formulations of Orimulsion: Orimulsion or Orimulsion 100 for the original formula and Orimulsion 400 for the current product. [38]

Typical constituents of Orimulsion [36] are carbon (55 - 62%), hydrogen (7 - 7.5%), sulphur (2.4 - 3%), vanadium (270 - 340$\mu g.g^{-1}$), nickel (60 - 70 $\mu g.g^{-1}$), sodium (15 - 50%), magnesium (300 - 450 $\mu g.g^{-1}$) and water (27 - 30%). These percentages are defined in term of ranges, corresponding to a number of Orimulsion ash analyses, with carbon the most variable constituent.

1.3.3.2 Orimulsion fuel incinerators

From the perspective of combustion, Orimulsion does not differ much from coal or heavy oil; it ignites easily in boilers, results in stable flames and is compatible with existing ignition and flame detection systems. Since Orimulsion fuel has a high content of sulphur and vanadium, the potential of sulphur trioxide (SO_3) emission is higher than for other fuels. [39] Therefore, Orimulsion fuel incinerators were originally designed for coal and fuel firing, modified with good emission pollutant control. Use of ammonia injection is for example required to reduce sulphur trioxide emission to levels similar to those from other fuels. [40] Another modification required on combustors is the fitting of electrostatic precipitators to limit the emission of particulates. [37]

1.3.3.3 Properties and metal content of Orimulsion ash

(a) Physical properties

The fly ash produced from Orimulsion combustion is less dense than the fly ash from other fuels, with particulate matter less than ten microns in diameter,

producing handling problems. [37] Therefore granulation of the fly ash on site is often carried out for easy handling and transportation.

(b) Chemical properties and metal content

The main constituents of Orimulsion ash are not really well documented. Typical analysis shows 55 - 70% of oxides and sulphates of magnesium, 8 - 10% of vanadium, 1.5 - 2.5% of nickel, 0 - 2% of unburnt carbon, and 0.1% other trace elements and remaining oxygen compounds. [37] An X-ray diffraction study [41] shows that the fly ash contains 11% vanadium oxysulphate ($VOSO_4$, xH_2O), 7% ammonium nickel sulphate ($(NH_4)_2Ni(SO_4)_2$), 75% ammonium magnesium sulphate ($(NH_4)_2Mg(SO_4)_2$), 10% aluminium sulphate ($Al_2(SO_4)_3$), and 4% ammonium iron sulphate ($(NH_4)_2Fe(SO_4)_2$).

1.4 Speciation and mobility of heavy metals

To understand the chemistry of heavy metals and their interaction with other components of the system, such as clay minerals or organic matter, and to assess their mobility and retention, it is necessary to determine the speciation of the metals in the matrix. [42] This is normally determined by selective extraction, partitioning into the following groups: exchangeable phase; acidic phase (or bound to carbonates); oxidizable phase (organically bound for soil/sediment and bound to sulphidic compounds for fly ash); reducible phase (occluded in Fe/Mn oxides); and finally structurally bound in silicates. Metals are associated with these phases in various ways including ion exchange, adsorption, precipitation and complexation. Metal mobility depends upon numerous factors. McLean et al [43] have described this phenomenon as:

> *"Metal mobility in soil-waste systems is determined by the type and quantity of soil surfaces present, the concentration of metal of interest, the concentration and type of competing ions and complexing ligands, both organic and inorganic, pH, and redox status. Generalization can only serve as rough guides of the expected behaviour of metals in such systems"*

Based on the above description it is clear that a comprehensive description of mobility of metals in soil is well beyond the scope of this thesis. Thus, the following

sections explain the mobility of elements found in the water-soluble and exchangeable fractions by defining the reactions that increase and decrease solubility. [42]

1.4.1 Literature review of metal speciation

Sequential extraction procedures for the speciation of particulate trace metals in sediment were first established by Tessier in 1979 [44] to partition trace metals like cadmium, cobalt, copper, nickel, lead, zinc, iron and manganese into five fractions: exchangeable, bound to carbonates, bound to Fe-Mn oxides, bound to organic matter and residual. This procedure is still currently used as a reference method. [45] Several modifications of this procedure including varying the soil/extractant ratio, the extractant concentration, the extraction time, and the order of extractants have been proposed, allowing a wide range of procedures over Europe. In recent years, the Community Bureau of Reference (BCR) launched a research programme to establish a unique reference method for the sequential extraction of metals from sediment. [46] As a result of this programme a three-step procedure has been developed and validated in which metals are partitioned to acid-soluble/exchangeable, reducible and oxidizable species. [47] Nevertheless, a comparative study [45] has revealed some sources of uncertainty in the application of the BCR three-stage extraction procedure that suggests some improvements are still required.

It is also important to determine heavy metal speciation in other solid particles like coal fly ash or waste incineration fly ash as their mobility and possible leachability in landfill has recently attracted a lot of attention. Again a modified Tessier procedure has been developed [34] whereby the fraction leached in the fourth step with hydrogen peroxide is bound to sulphide compounds. The BCR procedure has also been applied to fly ash [48] but with only an extraction efficiency of 85% which was attributed to incomplete dissolution of the final residue.

1.4.2 Reactions changing solubility of heavy metals in sediments and fly ash

1.4.2.1 Reactions decreasing solubility of heavy metals

(a) Non-specific adsorption of cations and anions

This is the reversible ion exchange process described earlier with the sorption mechanism based on electrostatic attraction. [49]

The ion exchanger in the system (sediment or fly ash) can be organic matter, clay minerals or hydrous oxides e.g. hydrous iron oxide, hydrous manganese oxide. The residual charge on these colloidal exchangers depends on the pH of the system. Thus iron oxide is positively charged below an approximate pH of 7 and negatively charged above this value. Organic matter is positively charged below a soil pH of 2.5, and negatively charged above. However clay minerals are always negatively charged due to the isomorphous substitution described earlier. Nevertheless, at low pH, these negative charged surfaces may also have some surface hydrous oxides of aluminium, iron or which are able to adsorb anions.

Adsorption of cations and anions occurs on negative and positive sites respectively on the colloidal fraction of the soil. Cation exchange occurs where a higher concentration of cations is held on the negatively charged colloid than in the soil solution. The cation exchange capacity of a soil increases as pH rises to 7.0 [49] as the number of negative sites increases. Most of the heavy metals occur as cations apart from arsenic, boron, molybdenum, vanadium and selenium that are generally present as anions under normal soil conditions.

To summarise, pH is the most important physico-chemical parameter controlling the sorption and desorption of metals in a system and thus their mobility.

(b) Specific adsorption

This phenomenon is not well defined [49] and was introduced when it was found that some cations have a higher exchange power than others, and could selectively form complexes with the hydroxyl groups of the hydrous oxides of iron, manganese and aluminium. Once these complex MOH^+ species are formed, they are not easily decomposed and require strong acids or complexing agents to reverse the reaction.

The strength of such specific adsorption of heavy metals is defined as: [50]

$$Cd > Ni > Co > Zn > Cu > Pb > Hg$$

(c) Chemisorption of elements

Chemisorption [49] occurs when a metal like cadmium can replace an element such as calcium in the mineral structure of calcium carbonate. The sorption process is based on strong formal bonding between the metal and the substrate and can only be broken by matrix destruction.

1.4.2.2 Reactions increasing solubility of heavy metals

(a) Organic complexation of metals [51]

The type of interaction between organic ligands and metals can be predicted from some characteristics of the metal and ligand.

Inorganic elements have been classified by Sparks [51] into three different groups according to their hydrolytic properties. Group 1 elements form non-dissociated oxocomplexes, e.g. SO_4^{2-}, and oxyacids, e.g. $As(OH)_3$. Group 2 elements are highly hydrolysed, but can also occur as hydrated cations, e.g. Fe(III). Group 3 elements do not have very stable hydroxo complexes.

Elements can also be classified based on their hard and soft characteristics. Hard acids e.g. group I metals like Na^+, K^+, Al^{3+} and Mg^{2+} have high positive charge and small size and do not have easily excited outer electrons. Hard acids, not polarizable, interact via electrostatic and/or ionic reactions with hard bases e.g. PO_4^{3-}, OH^- of low polarizability and high electronegativity. Soft acids e.g. group III metals like Cu^+, Cd^{2+} and Au^+ have a low charge and large size, and have some easily excited outer electrons. Soft acids are polarizable and form covalent bonds with soft bases e.g. CN^-, I^- of high polarizability and low electronegativity. Transition metals e.g. group II metals like Ni^{2+}, Mn^{2+} form complexes of intermediate strength with intermediate bases e.g. Br^-, NO_2^-.

Organic ligands can be classified under three different categories according to their binding strength. Simple inorganic ligands, majority of which are anions, tend to complex with hard metals, as their donor atom is oxygen. The hard donor sites of

natural organic matter consist of mainly carboxyl and phenolic sites, whereas the soft donor sites of natural organic matter are mainly those containing sulphur donor atoms.

The determination of the stability or formation constants for hard and soft metal complexes provides information on the affinity of a metal for an organic ligand.

(b) Precipitation and co-precipitation

Precipitation reactions involve sediment components like carbonates, phosphates, silicates, sulphides, and basic salts. [49, 52]

Precipitation occurs when the concentrations of metal and accompanying ions exceed the solubility product of an insoluble form K_{sp}:

$$MX_{n\,(s)} \Leftrightarrow M^{n+}_{(aq)} + nX^{-}_{(aq)} \qquad (7)$$

$$K_{sp} = [M^{n+}][X^{-}]^{n}$$

where M = metal and X^{-} = sediment component.

Co-precipitation processes occur when a metal ion precipitates in association with a secondary mineral such as: iron, manganese and aluminium oxides, calcium carbonate and clay minerals. Heavy metals normally found co-precipitated in soil by these secondary minerals are listed below: [52]

Fe oxides: Cu, Mn, Mo, Ni, Zn and V

Mn oxides: Co Fe, Ni, Pb and Zn

Al oxides: Pb, Cu, Ni, Co, Zn and Mg

Ca carbonate: V, Mn, Fe, Co, Cd

Clay minerals: V, Ni, Co, Cr, Zn, Cu, Pb, Ti, Mn, and Fe.

Co-precipitation is higher with Fe and Mn oxides than with Al oxides and clay minerals, the reason being the higher solubility of the former two minerals.

The redox status of sediment plays an important role in the behaviour of some pollutants. Firstly, some elements such as cadmium, which form insoluble sulphide precipitates (CdS) under strongly reducing conditions, are very firmly fixed in waterlogged soils. However, if these soils become aerobic, the sulphide oxidises as a

result of bacterial action to form sulphate and then the liberated Cd(II) is very mobile. Secondly, the redox potential of the soil determines the presence of sorptive iron and manganese oxides that under reducing conditions will dissolve and therefore liberate all the metal ions previously co-precipitated.

1.5 Heavy metal contamination

"Contaminated Land" is the term given to land containing substances that when present in sufficient concentrations, may cause harm to humans, animals and the environment. [53]

To determine if land is contaminated, a series of investigations have to be followed usually consisting of a three stage site investigation to assess the extent of contamination.

1.5.1 Site investigation procedure

When there is a suspicion that possible contamination of land has occurred, a study is usually first carried out on the previous land use. Ordnance Survey maps, publicly available historical records, and details of past industrial use are all studied. A list of potential contaminants associated with the main industrial sectors is available to establish the kind of contaminant that might be found following industrial use (appendix 1). [53]

Having identified potential sources of contamination, an initial sample survey is carried out to establish the nature and concentration of the contaminant and the type of risk involved. The site investigation also involves a geophysical survey. [54] As soil site conditions frequently limit the selection of a treatment process, it is necessary to have data such as soil size distribution, soil homogeneity and isotropy, bulk density, particle density, soil permeability, soil moisture, soil pH, E_h (redox potential), humic and clay content, total organic carbon, biochemical oxygen demand, chemical oxygen demand, availability of electron acceptors, and oil and grease content.

Once the types of contaminant and their total concentration have been defined, tables of standards and guidelines are used to check whether the concentration of contaminants is above or below the guideline limit. Such

contaminated land guidelines differ from one country to another, in contrast to guidelines for atmospheric pollutants that are recognised and applied worldwide. The United Kingdom Government guidance (ICRCL 59/83 relevant up to March 2002, since superseded by CLEA) on soil remediation standards for contaminated soils is based on two trigger values, a "threshold" and an "action" value (appendix 2 A2-1). [53] These two values define three situations and consequent actions:

all concentrations are below threshold values, so no remedial action is necessary;

some or all of the concentrations are between the threshold and the action value. Here there is a need to consider whether remedial action is required and a more detailed risk assessment will be required to define the nature of the contaminants and their most likely effect on the environment, considering the most likely pathways a contaminant would take to provoke harm;

some or all concentrations are equal to or exceed the action value. Appropriate remedial techniques are proposed and remedial action launched.

The Netherlands have their own list known as the "A, B, C Dutch list" (appendix 2 A2-2). [53] The A, B, C values were originally introduced in 1986, and have been superseded by "Target" and "Intervention" values. The A value is a base reference for a clean soil; B defines the value at which more detailed sampling is required before taking any decision; and C is the intervention value at which clean up is required, and finally the "target" value is the concentration to be aimed for in the longer term.

The United States are more concise in the sense that there is only one action value, which corresponds to the UK threshold value.

In determining treatment goals, the question of whether to remediate a site and what degree of clean up is necessary should be addressed. A screening logic is needed that takes into account specific site factors, the degree of protection required, cost, availability and reliability of clean-up alternatives. Sampling data are taken into account when selecting an initial list of treatment options. Then a detailed evaluation of this initial list, based on selected and appropriate criteria, produces a short list of feasible and effective technologies.

1.5.2 Origin of heavy metal pollution

There are two main sources of heavy metals in soils: weathering of the parent material, which is considered as a natural source, and external contaminating sources. [52, 55] Heavy metals naturally occur in parent rocks from which they are released as a consequence of weathering. Thus heavy metals become accessible and are subject to chemical reactions like oxidation or reduction and consequently become either retained or transported depending on the solubility of their final products.

External contaminating sources can be subdivided into two categories:

primary sources where heavy metals are added to soil as a result of working the soil. [54] Three particular sources are causes of concern, because of the high levels of some of the trace elements in these materials. Historically, pesticides contributed to high levels of arsenic, lead, and mercury because of the use of chemicals such as lead arsenate, calcium arsenate and arsenite, mercuric chloride and organomercury compounds. Fortunately the use of these materials is decreasing. However, phosphate fertilisers continue to be used in large quantities and sewage sludge is also added as a soil conditioner and these are sources of cadmium, lead and arsenic; [56]

secondary sources arise when heavy metals are added to soil as a consequence of nearby industrial activity and include: [52] abandoned metalliferous mining, an important source of As, Cd, Cu, Ni, Pb, and Zn from fine particles of ore carried away by wind or weathering (ions in solution); metal smelting, producing atmospheric pollution from fine particles of ore, aerosol-sized particles of oxides (As, Cd, Pb, Tl) and gases like SO_2; metallurgical industries like electroplating produce solutions of metal salts, and scrap from the electronics industry where metals are used in semiconductors, batteries, contacts, circuits and solders; and finally waste disposal and the corrosion of metals used in structures and paints.

Reduction in the release of pollutants into the environment is the first step in the fight against pollution. Good prevention and good remediation are the only weapons man has in the serious challenge of reducing pollution. It is essential for the future of the planet that industry addresses the problem of environmental pollution. To do so, industries should minimise direct discharge and introduce a cleaner

technology.

Cleaner technology refers to a technology that considers all aspects of a process from "cradle to grave" and seeks to minimise pollution at every stage. Currently industries that already have an established process do not have to close their operations, because they do not have a clean technology, but would have to add some treatment facilities upstream and downstream to the current operational process phase that would reduce the quantity of pollutant released in the environment and make the best use of raw materials and energy. However, companies starting new operations have to consider installing new cleaner processes to replace the older polluting technology.

Remediation processes currently under development are also looking at the possible recovery of the pollutant. As natural resources are depleted new resources of raw material are required. Therefore if clean-up techniques can recover the pollutants contained in contaminated land, this could be a new resource of raw material, and provide an interesting way of reducing remediation costs.

1.5.3 Metal toxicity

Metal ions can be potentially toxic to human. This toxicity can be related to the position of the metal in the periodic table, and will decrease with an increase in the stability of the electron configuration. Among the highly electropositive metal ions of the periodic table group 1 and group 2 elements which occur in biological systems primarily as free cations, toxicity increases with atomic number [56]:

$$1: Na < K < Rb, Cs$$

$$2: Mg < Ca < Sr < Ba$$

According to Fergusson [56], the increase of toxicity reflects the metal affinity for amino, imino, and sulfydryl groups, therefore metals from the periodic table groups 1, 2 and 13 to 18 are less toxic than metals from groups 3 to 12. However, this generalisation has to be considered with caution. The position of cadmium in the periodic table would suggest that alkyl-Cd compounds are quite toxic, but unlike alkyl-Hg compounds, alkyl-Cd compounds are unstable in aqueous solutions. The toxicity of metals also depends upon the physico-chemical forms in which they occur and the ease with which they are accumulated. Some metals like

iron or copper are essential for living organisms, but in excess, as well as in deficiency, may have serious consequences. Selenium, for example is a prerequisite for human health when taken in small amounts [57] and can protect against heart diseases. But selenium becomes toxic when present with other metals like arsenic, silver or copper, with which it forms complexes.

1.5.4 Waste disposal

Wastes may be classified by their physical characteristics, i.e. solid waste (less than 70% water); liquid waste (less than 1% suspended solid); and sludge (intermediate between solid and liquid). [58] They can also be classified according to their hazard criteria, as non-hazardous waste (no immediate harm to human); hazardous waste (contain leachable toxic constituents); and special waste (from industry with special waste guidelines).

Until recently, landfilling was the preferred option for disposal of wastes. Before the mid-80's, disposal of waste material was not regulated, and landfill consisted of just covering the waste with an adequately thick protective clay cap to prevent volatilisation and dusting. No protection was generally considered to prevent the eventual movement of the pollutants to the ground water, resulting in extensive water pollution. Modern landfills are now equipped with pollutant monitoring wells, a management system and leachate barriers. Because of these new landfill designs and new regulations, including introduction of landfill tax, it is now becoming increasingly expensive to landfill wastes. [58] Thus now it is necessary to reduce the amount of waste to be landfilled, and the primary alternatives to landfill are combustion, source reduction, and recycling.

Combustion or incineration involves the reduction in mass (75%) and volume (90%) of waste at high temperatures. The heat produced can then be used to generate electricity. This relatively expensive technique can contribute to air pollution and still requires the disposal of fly ash products in which the metallic pollutants are concentrated. Nevertheless, this fly ash may be used as a raw material to substitute a part of the constituents in concrete; as a component in building bricks, replacing up to 40% of the raw material; in the ceramic industry; in the removal of heavy metals from waste water; and can also be converted into zeolites. However in these

applications, the use of fly ash is restricted by its environmental quality with the presence of hazardous components like heavy metals, and by its technical quality with wide differences of composition and mechanical properties. These restrictions have to be addressed so that fly ash can be completely reused and not landfilled.

Source reduction, unlike incineration, involves the prevention of waste such as the reduction of material used for packaging.

Recycling involves the separation of recyclable material from the rest of the waste. The regeneration of spent catalysts used in industrial plants is a good example to demonstrate these two definitions. The recovery of heavy metals would avoid the problems of waste disposal and offer the economical possibility of reusing the recovered metals.

1.6 Treatment technologies

Remediation technologies can be classified in terms of where operations take place, i.e.: *ex-situ* (processes applied to excavated soil/sediment), *in-situ* (processes occurring in un-excavated soil/sediment, which remain relatively undisturbed). [59] The major advantages of *ex-situ* compared with *in-situ* processes include better control of process conditions; improved accessibility of contaminants to the treatment process; and easier control of process emissions and wastes. Nevertheless, soil structure and fertility are less damaged when soil is treated *in-situ*, and this option also excludes the cost of excavation and replacement and/or disposal of the soil/sediment/waste.

On-site processes refer to processes that take place on the contaminated site and may be *ex-situ* or *in-situ*. [60] Off-site processes treat soils/sediments that have been removed from the excavated site, therefore incur some transportation cost. Finally in-vessel processes are *ex-situ* processes that take place inside a mechanically contained system such as a bioreactor, and may be on-site or off-site. These latest offer the advantages of optimised extraction conditions.

The selection of the most appropriate remediation technique for an area of contaminated land is a complex and specific procedure. [61] It will depend on: (a) the site, its location and history; (b) soil/sediment/industrial waste characteristics; (c) the nature, physical and chemical state of the contaminants; (d) the degree of pollution;

(e) the desired final land use; (f) the technical and financial means available; and (g) environmental, legal, geographical and social issues. Generally no single technology can remediate an entire site and several treatments are combined to form what is known as a treatment train.

Metals, non-destroyable and immutable, can be removed (extraction), or rendered less toxic (stabilisation). Therefore, treatment methods described below are divided into extraction (mobilisation) and stabilisation (immobilisation) technologies. Further categorisation results in the consideration of biological, chemical and physical treatment technologies, where biological treatments rely on processes carried out by living organisms, chemical treatments rely on a range of chemical reactions, and physical treatments rely on the exploitation of differences in physical, chemical and thermal properties between metals and the contaminated land.

1.6.1. Extraction technologies (mobilisation)

1.6.1.1 Biological treatments

Two biological processes involve the mobilisation of heavy metals. Phytoextraction uses plants or algae that can accumulate heavy metals from soils or sediments. Bioleaching relies on the biochemically mediated mobilisation of the metal contaminant into a solution that is then separated from the soil or fly ash and the metal recovered.

Initial research in phytoremediation was centred on the use of pre-existing plants, which accumulate metals. Ernst [62] reviewed the response of these plants, also called hyperaccumulators, to metals and showed that even if some plants have a good resistivity to metals and are able to accumulate them (e.g. *Thlaspi Coerulescens* for zinc, cadmium, copper) they are restricted by a very slow rate of growth. In fact high levels of metals in soil actually induce a lower production of biota and a lower turnover of nutrients during decomposition of metal enriched litter. [62] Even if some plant species are shown to be resistant, it is difficult to consider using this method for the decontamination of metal polluted soil because of the time scale. Ernst explains that decontamination of tailings from a zinc-cadmium smelter would require several thousand years to reduce the contamination to the Dutch clean soil standard. [62] Moreover, enhancement of the metal uptake by plants was shown to be

difficult as some factors like increase of the soil acidity would also decrease the metal availability to plants. But due to their small biomass, slow growth rates and unknown agronomic potentials, these hyperaccumulators have been superseded by harvested plants that may be composted, landfilled, incinerated or extracted to recover valuable metals. [63]

Scott McGregor studied a second type of biological accumulator [64]. He demonstrated that metal uptake by trees is related to metal availability as well as the metal itself. Also, the accumulations of heavy metals occur mainly in bark and twigs and to a lesser extend in wood. Trees did not accumulate all metals, and the level of metals found were lower than in plants, but the benefit of using trees is that following metal accumulation, they can still be use for paper production, chipboard industries, etc.

Microbial remediation is based on reactions that occur between metals and microbes. As metals may become toxic to micro organisms at high concentrations, some micro organisms have developed mechanisms to protect themselves from such toxic effects. These mechanisms provide a basis for the treatment of metal contaminated sites. [65, 66] Microbial leaching is a simple and effective technology which has been used for metal extraction from low-grade ores [67] and mineral concentrates. [68] The first bioleaching process was applied in the 18th century for the extraction of copper in Rio Tinto, Spain. The process was then considered to be hydrosolubilisation of copper but it was actually the influence of a bacterium, *Thiobacillus*, which was discovered to be the cause of this phenomenon only 40 years ago. *Thiobacillus* is an acidic sulphur-oxidizing bacterium, which fixes CO_2 and derives its energy from the oxidation of sulphur compounds to sulphate.

$$4H_2O + S^{2-} \rightarrow SO_4^{2-} + 8H^+ + 8e^- \qquad (8)$$

This metabolic process results in the acidification of the environment, which induces a metal leaching process. Bioleaching shows best results under anaerobic condition [5], i.e. with sediments, where metals occur predominantly in sulphidic and other reduced forms. In this case pH is low enough and the metals are quickly oxidised and

efficiently solubilised. Under aerobic conditions, metallic species in the sample are mostly oxidised and are subject to chemical transformations, which make metals more strongly bound to soil, therefore the bioleaching process will be longer and pH used will be lower.

Special techniques have been developed to optimise the operational conditions [5, 66] e.g. soil slurry reactor and on-site heap leaching. In the reactor soil slurry, good mixing and aeration are needed as well as the presence of sulphur compounds and pH control. In the on-site heap leaching, a solution of sulphur compounds and an appropriate micro organism are sprayed on the surface of the soil to be treated. This second mode has the advantage of no excavation, which obviously reduces the overall costs. An impervious membrane that allows the leachate to be recovered for treatment confines the leached metals.

This bioleaching process for contaminated land is still at bench or pilot scale, with only a few examples developed so far for bioremediation of soil and sediment. [69, 70, 5] *Thiobacillus* is also considered for bioleaching of metal oxides from fly ash [71] where the addition of sulphur for bacterial acid production is a cheap option. Another advantage is the gradual in fall pH, which will enhance sequential metal passage into solution, and therefore an easy separation of metals.

1.6.1.2 Chemical treatments

Oxidation, which requires the removal of electrons from the metal species to increase the oxidation state of the metal, [16] and chemical leaching, which uses leachants like acids, alkalis, surfactants, and organic solvents are two chemical processes involved in the solvent/chemical extraction of metals.

Solvent/chemical extraction is an *ex-situ* process that requires excavation and pre-treatment such as screening, crushing, dewatering and pH adjustment. The prepared feed material is then mixed with the solvent in the extraction step, followed by physical separation of the decontaminated solids and contaminant loaded extraction solvent. A final recovery and recycle step removes the solvent from the contaminant allowing the solvent to be recycled and the contaminant collected for disposal. [72]

A variety of chemical extraction processes exist which employ a number of

solvents chosen on the basis of contaminant solubility. This process is well developed for the removal of polychlorinated biphenyls (PCBs), and polynuclear aromatic hydrocarbons (PAHs), but is not as well developed for the removal of heavy metals. [73] Recently ethylenediaminetetra-acetic acid (EDTA) has been tested as a potential chelating agent for remediation of contaminated soil, and was successfully demonstrated for the complete extraction and recovery of lead from contaminated soil. [74] The lead is recovered by addition of cationic precipitants in the alkaline pH range, allowing EDTA to be reused.

MSW, coal and Orimulsion fly ashes can also be treated using chemical leaching. Acid and alkaline leaching has been most commonly used on MSW fly ash with good extraction efficiency for metals like Zn, Pb, and Cr. [33, 75] Orimulsion ash has been leached with alkaline solutions such as NaOH. [76] With 30% NaOH solution 94% extraction of vanadium was achieved with a total recovery of the vanadium using 30% H_2SO_4 for neutralisation and NH_4Cl for precipitation. Leaching of vanadium using 2 mol dm^{-3} H_2SO_4 acid [36] was also quite effective with a maximum of 88.5% vanadium extraction and 84.2% recovery using $NaClO_3$ to oxidise the vanadium at the solution boiling temperature and a pH = 2.3. Chelating agents such as EDTA, diethylenetriaminepenta-acetate (DTPA), nitrilotriacetic acid (NTA) have also been tested on MSW and coal fly ashes with good extraction of Cr, Cu, Pb and Zn. [75] The maximum extractions: 50% Cr, 95% Cu, 100% Pb and Zn, were obtained with a 0.3 - 1.0% concentration of the chelating agents in a pH range of 3 - 9. Moreover the iron and silicon were stable against extraction. Leaching by acid/alkaline solution is achieved by dissolving or destroying the solid structure of the residues. [77,78] Consequently, further amounts of heavy metals, which were previously integrated in the matrix, such as Fe, Mg and Al, will be released more easily after disposal of the residues.

Soil flushing is an *in-situ* chemical mobilisation process, which uses water, aqueous solutions, or gaseous mixtures to increase contaminant solubility. [75] The idea is to accelerate reactions like desorption, acid/base reactions, oxidation/ reduction, ion pairing or complexation, which induce leaching of contaminants and also increases the mechanisms of the subsurface contaminant transport, like advection and molecular diffusion. Soil contaminants are then transferred to an

aqueous leachant, which is recovered, from the subsurface and treated by conventional effluent treatment processes. Soil flushing can be carried out in two ways [79] depending on the depth of contamination. For shallow depths, the flushing solution is pumped onto the soil surface, where it percolates slowly downwards through the contaminated soil and carries contaminants towards extraction wells that pump out the contaminated solution. Wells may be installed both vertically or horizontally depending on the geological factors and engineering considerations. For greater depths or for treating sediments, a pump and treat system is used where the flushing solution is injected through injection wells in the contaminated soil/sediment and, as above, extraction wells will remove the contaminated solution. Reagents, which are used in soil flushing, can be acids, alkalis, or complexing agents, and are generally used in low concentration. Unfortunately sometimes they appear to be environmentally damaging. Thus the use of acid like HCl to mobilise metals was successful but acidification again dissolved part of the solid matrix. [78] Chelating agents like EDTA, which do not require acidic conditions, have been shown to be the most appropriate reagents for soil flushing. [80] Some column tests using 0.01mol dm^{-3} EDTA showed a good extraction yield of 48% for Cd and 31% for Pb.

Soil flushing is more effective in homogeneous permeable soils. Even though it offers the advantage of being an *in-situ* process with no requirement for excavation, the process still produces large amounts of contaminated wastewater, which need to be handled and treated.

1.6.1.3 Soil washing

Soil washing uses a mixture of processes such as physical separation or chemical solvent extraction to remove contaminants. It is actually an *ex-situ* water-based system, which uses dilute aqueous surfactant solutions to remove contaminants through physical extraction. [81]

The process is not a complete treatment by itself, but it is better considered as a pre-treatment technique, which can reduce the volume of the contaminated soil by up to 90%, by separating the clean soil from the 10-30% of residual contaminated concentrate, which then requires further treatment.

Being an *ex-situ* process, soil washing requires excavation of the

contaminated matrix, and some mechanical screening to remove the oversize fraction. Then, by mixing with water and using for example, multistage hydrocyclones, the screened soil/water slurry is separated into coarse and fine grain material. Following this separation process, the coarse grained material is washed again, and the fine material is directed to a sludge thickener and filter press where it is converted to dry solid filter cakes. The filtrate and spent wash waters are treated to remove any contaminants and recycled.

The washing process may involve the addition of a leaching agent, surfactant, or complexing agent like EDTA to aid decontamination and even when water is used alone some pH adjustment may be necessary.

The two most important soil parameters, which affect the efficiency of this process [81] and also limit its use, are:

grain size distribution, as soils which contain at least 50% of coarse material, sand and silt, are more appropriate for soil washing;

cation exchange capacity, as the higher the CEC, the lower the efficiency of soil washing as, unless careful pH control is applied, the metals tend to be retained.

Soil washing was successfully demonstrated on a pilot scale in New Jersey in 1992 [82] with complete removal of Cr, Ni, and Cu. Since this date it has become established as a useful approach to soil treatment. However the process still shows severe limitations in the cases of soils rich in fines like clay.

1.6.2. Stabilization technologies

1.6.2.1 Biological treatments (microbial remediation)

Biomineralisation and biosorption are two phenomena where metal-microbe interaction induces immobilisation of metals. [83, 84] Biomineralisation is a passive process where insoluble metal precipitates are formed by interactions with microbial metabolic products. Biosorption is an active process where metals are directly sequestered by live or dead biological matter.

(a) Biomineralisation

Sulphate ions can be reduced under anaerobic conditions by sulphate reducing bacteria like *desulfovibio*, and *desulfotomaculum* to form hydrogen sulphide, as shown in equation 11. [83-85] Then, the hydrogen sulphide reacts with soluble metals forming insoluble metal sulphides as shown in equation 12.

$$SO_4^{2-} + 10H^+ + 8e^- \Leftrightarrow H_2S + 4H_2O \qquad (9)$$

$$H_2S + M^{2+} \longrightarrow MS_{(s)} + 2H^+ \qquad (10)$$

Precipitation of metal sulphides by such sulphate-reducing bacteria constitutes the second phase of a combined sulphur oxidation/reduction biotreatment for soil decontamination [86] where metals like Cu, Zn and Cd have been precipitated successfully. Because of their low solubility product, most heavy metal sulphides are readily precipitated. Metal sulphide precipitation is nowadays well understood and is often considered for the bioremediation of contaminated soil in association with bioleaching to recover metals from the leached solution. [84, 87]

Precipitations enhanced by other microbial metabolic products can occur. Metal phosphate precipitation can be obtained as a result of biologically produced phosphate under anaerobic conditions. Thus *Pseudomonas aeruginosa* and *Pseudomonas putida* have been used to remove Cd, Zn, Cu, Fe, Co and Ni from metal-citrate wastes. [88] In an alkaline environment, following for example sulphate reduction, the respiration of some bacteria will transform CO_2 into carbonate in the periplasm to form metal-bicarbonate precipitation, [83] with subsequent formation of some metal hydroxides or oxides. [66]

Reductive precipitation of a metal to a lower redox state can be driven by some micro organisms rendering them less mobile and less toxic. For example, chromate ions can be reduced to insoluble trivalent chromium with soluble reductase enzymes generated by *E. Coli.* [89]

(b) Biosorption

Methylation of metals is a biosorption process that can be promoted by bacteria and fungi. The addition of methyl or alkyl groups to metallic species increases their lipophilicity and permeability across biological membranes. Methylation of metals also enhances the volatilisation of metals and both of these properties increase their toxicity. [62] Metals currently known to convert from an inorganic to organo-metallic form are mercury, arsenic, cadmium, and lead. However it is unlikely that biological methylation would be employed at contaminated sites, as the volatility of the metal contaminant may pose an emission problem.

Extracellular complexation is also a biosorption process that occurs from interaction of metals with extracellular polymers, like polysaccharides or glycoproteins, excreted by bacteria or from organic matter accumulated from the dead microbes. Indigenous bacteria can be stimulated to produce specific extracellular polysaccharides. [90] Another class of microbial chelating agents are siderophores, which are low molecular weight ligands synthesised and excreted by bacteria, fungi cyanobacteria or algae for capturing and supplying iron to support metabolic activity. Other metals like Cr(III), Cu or Ni may also complex these ligands. [90]

Intracellular accumulation can be considered as a two-stage biosorption process. First, metal ions are bound passively to the surface of the bacterial cell wall by physical/chemical processes. Then the metal ions are transferred to the interior of the cell by the microbial energy system normally associated with magnesium and potassium transport. [66, 91]

The mechanism by which bacteria resist heavy metals resulted from several biomolecular functions in the bacterial cell walls that specifically bind metals. [90, 94] Secretion of peptidoglycan, a cysteine rich polypeptide, in bacterial cell walls is an example of a process for binding essential metals like Cu, Co, Zn, Ni, as well as non-essential metals like Cd using ion exchange reactions. Further development of polypeptides and proteins by careful screening of bacteria may produce systems that are selective for immobilising specific toxic metals.

1.6.2.2 Chemical treatments

Chemical stabilisation converts contaminants into less soluble and less toxic species by chemical reactions, thus minimising the leaching of the contaminants. [93] Several commercial technologies have been developed and two examples are described below.

THIO RED is a commercial *in-situ* or *ex-situ* detoxification and stabilisation technology, which involves the use of an organic reagent, able to reduce metals to their lowest state and render them insoluble as stable complexes. The technology [94] uses a liquid detoxifying reagent (a polymeric organosulphur reagent), which forms metallic thiocarbonates in contact with metals and their compounds. These metallic thiocarbonates do not leach under either acidic or alkaline conditions, and are not hazardous or toxic. For *in-situ* use, this technology has to face the problem of widely diverse concentrations of heavy metals throughout the site. The amount of reagent required to complex the metal depends on the different levels of contamination; therefore the technology uses a dosing system which controls the quantity of reagent percolated into the soil by the use of an electronic sensor. This technology has the advantage, compared to the flushing process, of not using water so that the volume of the soil is not increased and it can also be applied simultaneously, when necessary, with biological treatment for the destruction of organic contaminants.

The Soluble Phosphate process is another stabilisation process that involves the addition of a stabilization agent, orthophosphate (PO_4^{3-}) under controlled pH conditions to produce insoluble metal phosphates. [95, 96] Even though the process has been commercially used to stabilise Zn, Cu, Cd, and Pb in fly ash, it still has the disadvantage of possible redissolution of the metal phosphates under acidic conditions. Moreover not all toxic metals form insoluble metal phosphates, thus solubilities of these species and the effectiveness of this technique depends on the metal ion and pH. Nevertheless, the advantage of these stabilisation processes compared to others is the minimum effect on the soil following treatment, which is not hardened, retains its particulate nature, and shows no volume change.

Addition of sorbing components like Fe(III) and Al(III) salts to MSW bottom fly ash together with reduction of the pH to 7-8 enables the simultaneous precipitation of Cu(hydr)oxides and oxyanions, such as molybdates [97].

1.6.2.3 Physical treatments

The principle physical treatment to immobilise contaminants is solidification where they are physically bound within a stabilised mass to form a mixture which sets to a firm impervious species.

Inorganic cementitious solidification technologies use well-established hydraulic cement processes that have been used for more than two decades. [93] The primary reagents have their origin in natural limestone and clay formation, and therefore have an advantage concerning reagent cost to treat contaminated materials like fly ash. The reagents and the contaminated materials tend to contain the same active ingredients i.e. SiO_2, CaO + MgO and $Al_2O_3 + Fe_2O_3$. Operational conditions require the pH to be above 10 and enough free water in the system to complete the cementation reaction. Two different variations are available for remediation, the soluble silicate process and the slag process. The soluble silicate process [93] involves a mixture of soluble silicates with a source of multivalent metal ions, e.g. cement or lime. The soluble silicates can either be accelerators or anti-inhibitors in cementitious systems to reduce leachability.

The slag process [93] involves mixing waste slag with fly ash, kiln dust (both waste materials), lime or Portland cement and is widely used for highly acidic contaminated soils. These hydraulic cement processes offer advantages of being less expensive than other solidification processes. However in both cases the product is a waste solid containing the contaminants in a concrete matrix, which has to be disposed or used in for example construction. [93]

The Modified Sulphur Cement Process was developed for the solidification of pre-dried material like contaminated soils, sludges and industrial metalliferous wastes. [93] It requires the melting of modified sulphur cement at about 119°C, followed by mixing with the feed to give homogeneous molten slurry, which is then cooled and stored for disposal. Compared with the previous hydraulic cement process, this sulphur cement process offers several advantages. As no water addition is made, chemical reactions, which can occur in the hydraulic process, are avoided. Moreover chemical resistivity of the sulphur concrete is better than conventional concrete, [93] but is rather more expensive.

Vitrification is a thermal process, which converts contaminated soils and waste material into a stable glassy form. Two types of system are available to treat heavy metals. *In-situ* vitrification uses an electric current to melt the soil at extremely high temperatures (~1,200°C) whereby the metal contaminants are incorporated as their oxides form into a matrix of vitrified glass and crystalline material. [96] Water vapour and organic pyrolysis combustion products are captured by a hood, which directs the gases into a treatment system to remove any contaminants. The vitrification product is both chemically stable and leach resistant. The process is very effective for most types of contaminants as heavy metals are retained within the molten soil and organic compounds are thermally destroyed, [98, 99] however it is very expensive. Thermal vitrification, the second available system, [93] requires the excavation of soil and uses a rotary kiln to melt the soil, generally with the addition of other materials such as silica and lime to produce a stable glass (often used with pre-treatment to reduce volume). For an overall destruction efficiency of 99.99%, there are unfortunately some non-negligible limitations to vitrification. High moisture content in the feed increases the energy cost, which already represents more than 40% of the overall cost. Thus vitrification processes tend to be used for disposal of contaminated materials where cost is of secondary importance, like nuclear waste and radioactively contaminated soils.

1.7 Preliminary studies of the SERVO process

The SERVO Process (Selective Extraction and Recovery of metals using Volatile Organic compounds) was designed in the early 1970s at the University of Hertfordshire as an alternative process for the extractive metallurgy of low grade ores [100].

This section introduces the technology of extractive metallurgy and the development of the SERVO Process.

1.7.1 Extractive metallurgy

Extractive metallurgy is the recovery of metals naturally occurring in ore. It can be divided into three main types of process: [101, 102]

1.7.1.1 Hydrometallurgy

Hydrometallurgy involves the leaching of the valuable metal out of the ore using an aqueous solution, and recovering the metal from the leach liquor after separating from the residual waste ore. [103, 104]

Separation of the leach liquor from the unwanted material is mainly achieved by the following three techniques:

decantation is a slow batch or continuous process, where the unwanted material is allowed to settle under gravity, leaving a clear solution;

thickening is a combined process using settlement and decantation with some form of slow agitation of the solid phase to provide densification of the solids;

filtration is a process where a porous physical barrier is used to collect the solid material and allow the liquid filtrate to permeate.

Unfortunately the leaching operation is rarely selective so the leachate contains many different metals in solution in addition to the one required, so that processes to separate these, such as liquid-liquid extraction using an organic reagent in an organic phase, or ion exchange are required. Many different organic reagents and resins are now commercially available to carry out such separations. Both these processes are capable of producing a pure concentrated aqueous solution of the desired metal, which can be recovered by other techniques such as electrolytic deposition to produce a pure metal product.

Hydrometallurgy is an important technology for producing a number of metals, especially aluminium and gold but also metals like copper, cobalt and nickel. Here the reduction in the grade of the ore and the increasing use of oxidic ores less suitable for pyrometallurgy have increased the proportion of these metals produced by hydrometallurgy.

1.7.1.2 Pyrometallurgy

Pyrometallurgy involves a number of established thermodynamic processes and involves heating operations like roasting, calcination, chemical reduction or smelting to extract metals. This type of operation depends on metal speciation in the ore. [101] However this process is not universally applicable, and some metals

cannot be reduced by smelting e.g. titanium, vanadium, and chromium. Pre-treatment are often required to remove the ore minerals from waste rock leading to problems of disposal of waste, e.g. jarosite in zinc smelting. In addition smelting produces its own environmental problems such as emission of SO_2.

1.7.1.3 Mond vapour phase process. [105]

This process, developed in 1902, is based on the reaction of carbon monoxide with nickel at temperatures around 100°C to produce a volatile nickel carbonyl, $Ni(CO)_4$, which, on further heating to 200-300°C, decomposes to give the metal and carbon monoxide: [105]

$$Ni + 4CO \xrightarrow{100°C} Ni(CO)_4 \xrightarrow{200\text{-}300°C} Ni + 4CO \qquad (11)$$

Formation of iron and cobalt carbonyls is also possible. To minimise the co-extraction of these two metals, reaction conditions are used which make the formation of nickel carbonyl highly selective. [105] The Mond Nickel process is used commercially by Inco at Sudbury, Ontario to refine impure nickel powders.

This process combines the selectivity of hydrometallurgy and the one-step operation of pyrometallurgy, but has disadvantages in that nickel carbonyl is very volatile and very toxic.

This process provided the basis of the SERVO process, which combines selective extraction process, able to treat low grade feed material, and with a simple one/two stage operation. [106]

1.7.2 SERVO Process literature review

This patented process extracts metals from a matrix using a volatile reagent, which passes through the feed material and reacts selectively with the desired metal: [100]

$$H(Ext)_{gas} + M^{+}(Matrix)_{solid} \xrightarrow{T} M^{+}(Ext)^{-}_{gas} + H^{+}Matrix_{solid} \qquad (12)$$

Products of this reaction are metal complexes which can be removed from the gangue

by a carrier gas, and may be reduced in the vapour phase to produce a metal product and regenerate the reagent for recycle.

$$M^{+}(Ext)^{-}_{gas} \quad + \quad H_2 \quad \xrightarrow{T} \quad M_{(sol)} \quad + \quad H(Ext)_{gas} \qquad (13)$$

The SERVO Process flowsheet is shown in figure 6. The Mond nickel process showed that it was possible to extract metal using a volatile reagent, with formation of a metal complex, combining selectivity and a one-step process. However the carbon monoxide used as extractant reacted only with nickel atoms in the zero oxidation state, so that the choice of another type of extractant was necessary. In hydrometallurgy selective extraction is achieved using organic chelating reagents, which can react specifically with some metals like copper, nickel, and cobalt. [104]

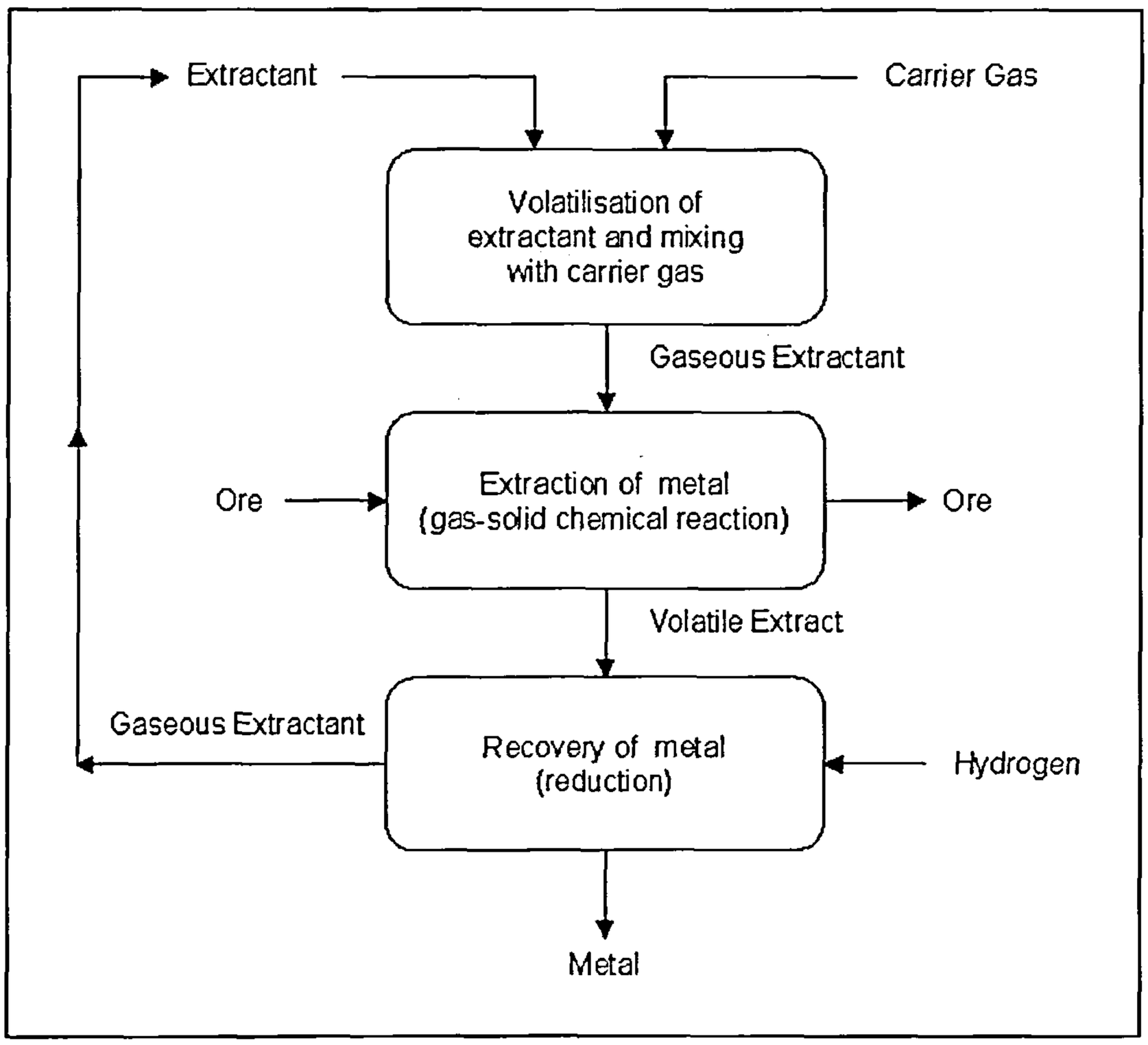

Figure 6: SERVO Process flowsheet

Moreover Allis and Chalmers [106] demonstrated that after extraction by a liquid-liquid process, nickel and cobalt complexes could be separated by volatilisation of the more volatile complex, in this case the cobalt complex as a vapour.

Gas chromatographic studies by Sievers [107] demonstrated that β-diketonates of a number of metals had low volatilisation temperatures, which allowed their separation on a column. Fluorinated analogues of β-diketones like hexafluoro-acetylacetone, which had been successfully used by Sievers, were considered for the extraction of metals from ore. This reagent was tried on roasted chalcopyrite but although reaction with copper oxide had been successfully demonstrated, in the presence of ferric iron, the latter reacted preferentially.

Thus the development of an extractant volatile at low temperature, which was selective over iron (III) and which could form reducible metal complexes was required. Ferric ion being trivalent and copper ion divalent, the desired reagent had to be acidic and exploit the difference in stereochemistry of the divalent and trivalent metals, i.e. square planar and octahedral. This led to the study of Schiff base ligands (figure 7) that favoured such stereochemistry of the metal. So in 1985, twenty such reagents and their corresponding metal complexes were studied by P. W. Duke. [108, 109]

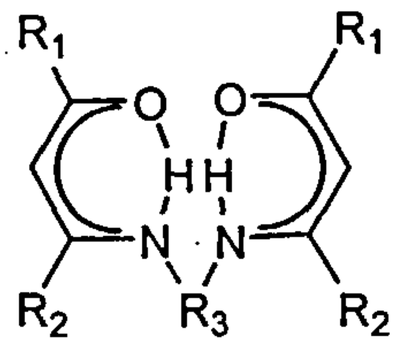

Figure 7: Schiff Base reagent

Two parameters were used in the choice of reagents: the first selection criterion was the volatility and transport of the reagent and subsequent metal complexes with little or no decomposition. Secondly, the metal complex should be capable of reduction to produce the metal and regenerate the reagent. Studies of extraction and reduction demonstrated that the compound, bis-(pentan-2,4-dione)propane-1,2-di-imine (figure 8) was the most suitable for extraction and

recovery of divalent metals like copper, nickel and cobalt from their ores.

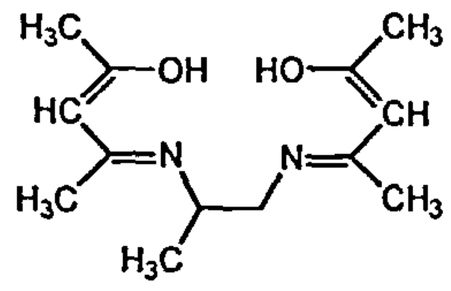

Figure 8: Bis-(pentan-2,4-dione)propane-1,2-di-imine

Following these studies, the combined extraction and reduction of copper from a sulphide ore (chalcopyrite) was carried out following an oxidative roast prior to extraction and a nitrogen/hydrogen carrier gas mixture. The product of these experiments was a pure copper metal (>99.9%) and no iron(III), confirming the selectivity of the reagent.

In 1989 D. W. Barr, directed the research towards adapting the SERVO Process for the selective extraction of nickel over iron from low-grade nickel laterite ore. [106, 110] This study optimised operational conditions for the extraction and recovery of nickel from New Caledonian laterite ore. It appeared that the better the physical contact between the ore and the volatile reagent, the higher the extraction. So optimum flow rate and temperature would correspond to the conditions where the concentration of the reagent in the vapour is at its greatest.

Subsequently preliminary reaction kinetics of the chelating process in the vapour phase and thermal stability of the extractant with identification of any degradation products were necessary to demonstrate that the SERVO process was a feasible approach to extractive metallurgy from low grade ore. [106, 110] These studies were carried out using a redesigned thermal balance, where the weight loss could be measured against time. Chemical reaction data obtained from these kinetic studies were limited when using a fast flow rate and low reaction temperature. Nevertheless rate of reaction data suggested that the process is largely diffusion controlled.

A study on the thermal stability of the organic reagent showed some reagent degradation, which could be reduced by decreasing the reagent heating rate.

Dr A .A. Pichugin extended the work done by Barr, concerning the kinetic

factors affecting the extraction process. [111] These results showed that size of the ore, column dimensions, column temperature, and carrier gas flow rate influenced the extraction. Moreover, there is an induction period where the extractant seems to accumulate within the ore before the extraction starts. The extraction rate between the end of this induction period and the end of the extraction is linear.

All these results suggest the following mechanisms of nickel extraction: [111]

adsorption of the extractant;

condensation of the extractant in the pores;

reaction between liquid extractant and nickel;

desorption of nickel complex;

accumulation of nickel complex in liquid extractant;

volatilisation of nickel complex into the carrier gas.

Thus optimum extraction conditions will be those, which allow the condensation of the extractant in the pores to occur.

Research on the degradation of the reagent was also extended and it was demonstrated that there were four possible degradation routes: [111]

thermal degradation;

degradation caused by oxygen and water in the carrier gas;

degradation caused by chemical reaction within water from the ore;

degradation caused by chemical reaction with other components in the ore.

1.7.3 Recent studies of the SERVO process

Originally devised for the treatment of low grade ores, the SERVO process has recently been studied for the treatment of metalliferous wastes. The sources considered below contain some new challenging metals to be extracted i.e. molybdenum, vanadium, lead and zinc:

sediments from canal and rivers with high concentrations of metals like zinc and lead;

Orimulsion ash containing vanadium, nickel, and magnesium;

Puertollano fly ash from a coal fired electricity generating plant;

MSW Rotterdam fly ash from a waste incineration plant.

A programme of experiments was designed to study the application of the SERVO process for these materials that included:

synthesis of new extractants and their metal complexes, and a study of their volatility to determine the operational conditions of the SERVO process;

modification of a thermogravimetric analyser with the ability to record the weight loss or gain and record operational temperature;

preparation of simulated materials for testing with this modified equipment;

design and construction of laboratory scale equipment to test the new extractants on actual waste samples.

Chapter 2: Experimental

2.1 Analytical Equipment

The analytical equipment used to identify the extractants and metal complexes prepared and to analyse the elements extracted will initially be described.

2.1.1 Infra Red Spectrometry analysis

Infrared Spectroscopy (IR) is used to determine the functional groups of the ligands and the metal complexes. Discs, prepared using dry potassium bromide (KBr), were scanned using a Perking Elmer Paragon 1000 FT-IR spectrometer through the wavelength range from 400 to 4000 cm^{-1}. [112] This range covers the vibration of the covalent bonds in the molecule; such vibrations have frequencies, which depend on the masses of the vibrating atoms and on the strength of the bond between them. Such vibrational modes are characteristic of the groups in the molecule. Spectra obtained from unknown substances are compared to tables of characteristic infrared absorption bands to determine the main functional groups in the compounds.

2.1.2 Mass Spectrometric analysis

Mass Spectrometry (MS) is used to complement the determination of the functional groups obtained by IR.

IR gives information about the functional groups in a molecule, but tells little about its size. MS provides the molecular weight and involves the ionisation of molecules in a high vacuum, and correlates the molecular fragments arising from ionisation processes according to their masses and records the abundance of such fragments. [113]

2.1.3 Thermogravimetric analysis

Thermogravimetry (TGA) is a technique in which a change in the weight of a substance is recorded as a function of time or temperature. The basic instrumental requirement for gravimetry is a precision balance with a furnace programmed for a linear rise of temperature with time. The thermogravimetric curve (TG) is a record of

the weight [114] change as a function of temperature or time. TGA was used here for two purposes. Firstly, it was modified as detailed in § 2.3.3 so it could be used as to simulate the SERVO process extraction reactor, and secondly it was used to investigate the volatilisation temperature of ligands and metal complexes. The equipment was normally used with a temperature ramp of 10°C min^{-1} up to 300°C, with argon carrier gas at the flowrate of 60 cm^3 min^{-1}, operational conditions optimised by Dr. Pichugin. [111]

2.1.4 Inductively Coupled Plasma – Atomic Emission Spectrometry (ICP-AES)

A Perkin Elmer Plasma 40 Emission spectrometer was used for the analysis of metal ions in solution. Metal ions present in solution are flushed through a plasma torch where the high temperature causes excitation of the atomic species. [115] In their excited form, electrons in the metal atoms are transferred to higher and unstable energy levels and then return to the original energy level, emitting energy at a specific wavelength, which is measured. Standard solutions containing known amounts of metals are first flushed through the plasma at the chosen wavelength and used as references to determine the concentration of the element present in the unknown solutions.

2.1.5 MDS 2000 Microwave Digestion System

This equipment was used to digest solid samples in a closed vessel using microwave heating. The resulting solution was used to determine the metal concentration by spectroscopic methods. Microwaves offer a faster heating rate and consequently a faster dissolution rate than conventional heating.

A mixture of 0.3 g sample, 3 cm^3 of distilled water, 3 cm^3 of HNO_3 (70 %), 3 cm^3 of HCl (37 %) and 3 cm^3 of HF (40 %) were placed in an Advanced Composite Vessel.

All the samples, accurately weighed, were run for 30 minutes at full power (630 W) and cooled for a minimum of 5 minutes to stabilize the pressure before removing the vessel from the turntable of the system. After heating in the microwave furnace the solution was transferred to a volumetric flask, following filtration. The vessel was rinsed with 2 mol dm^{-3} HNO_3 and the flask filled up with distilled water to keep a suitable acidity for the spectroscopic analysis (ICP-AES).

2.1.6 X-Ray Diffraction

X-ray diffraction is a technique used to investigate the organisation of solids, at the atomic scale, and is recognise as the most useful approach for identification of minerals. [1116] X-ray diffraction occurs in accordance with Bragg's Law: $n\lambda = 2d\sin\theta$, where λ is the wavelength of monochromatic X-rays, d is the interplanar spacing, θ is the critical angle for constructive interference of scattered rays, and n is an integer. In these studies the samples were presented as powders.

2.2 Experimental material

2.2.1 Preparation of simulated contaminated materials

Air floated sodium bentonite (Volclay Minerals Limited Grade MPS-1, a high purity, air floated sodium bentonite, that contains 99.75% minimum montmorillonite) was used to prepare the different contaminated clay samples, and a technical data sheet provided by the supplier is included in appendix 3. [117] Montmorillonite, a dioctahedral smectite, was chosen for its high absorption capacity of organic compounds, which is related to its large surface area (760×10^3 m^2 kg^{-1}) and also for its cation exchange capacity (1 $cmol_c$ kg^{-1}).

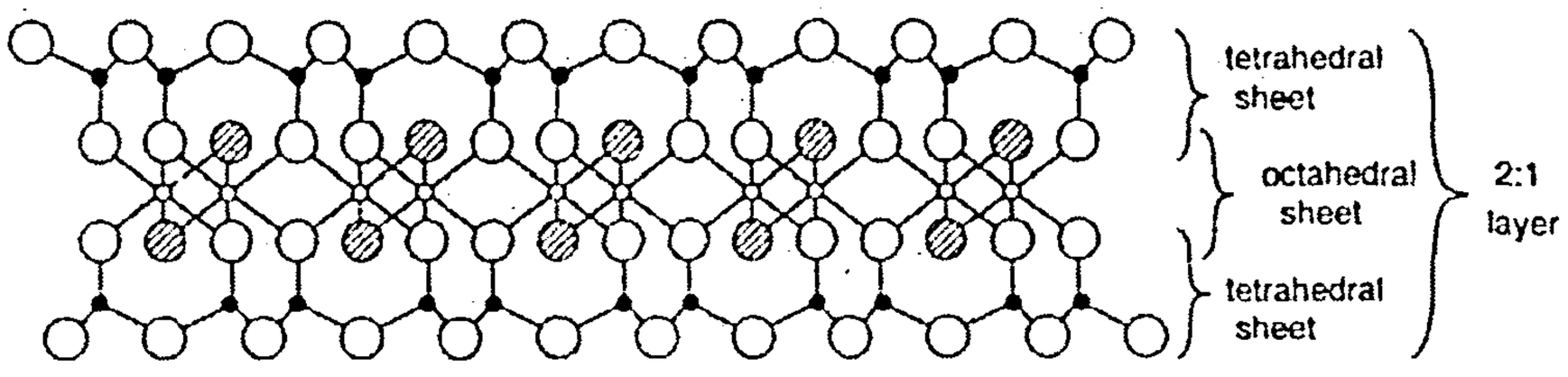

Figure 9a: Schematic drawing of Montmorillonite Clay [117]

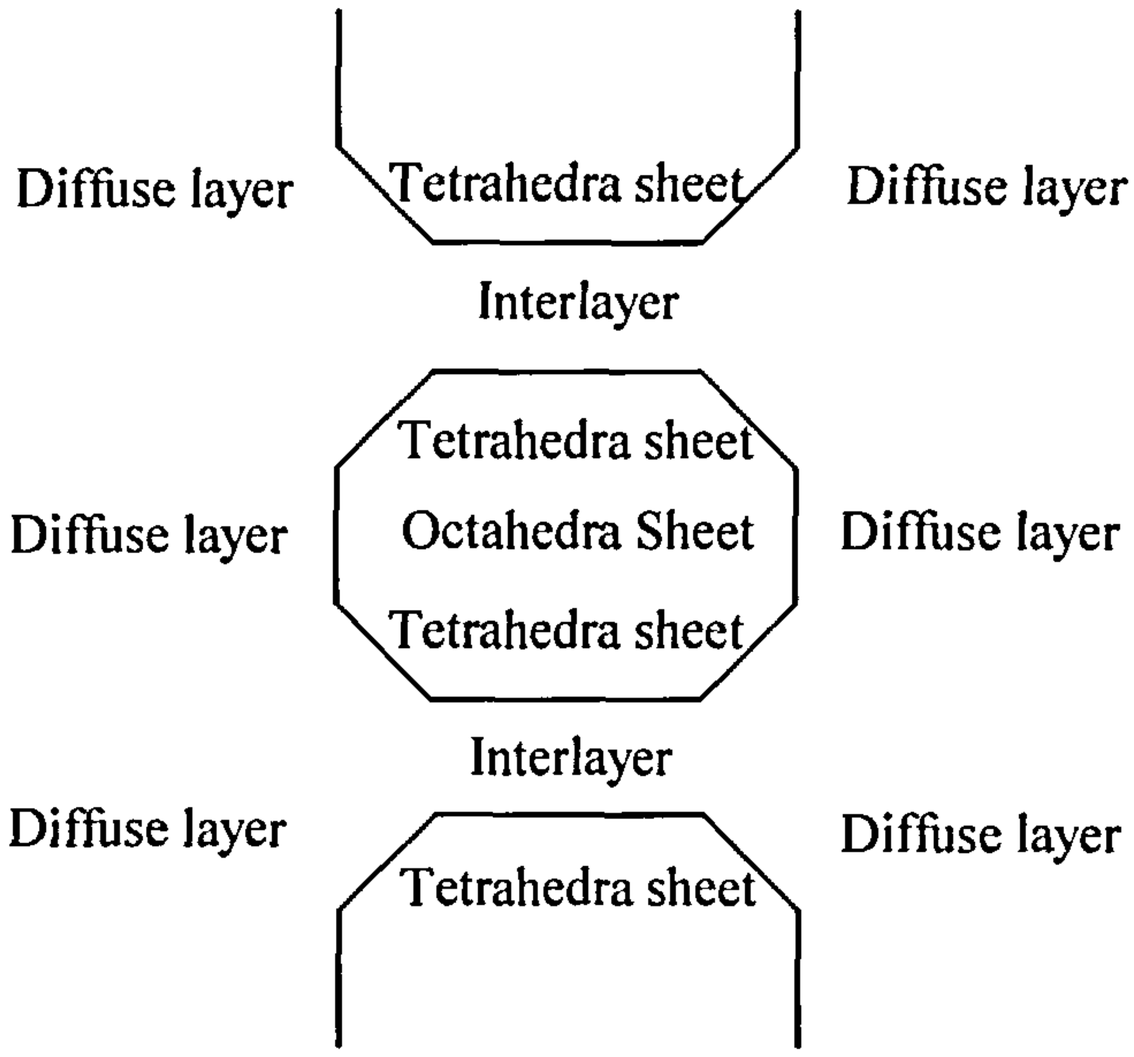

Figure 9b: Schematic representation of Montmorillonite Clay

Montmorillonite has a 2:1 clay structure with two sheets of tetrahedral silicate species sandwiching a sheet of octahedral aluminosilicate. The tetrahedral cations are Si^{4+} and the octahedral cations are Al^{3+}, Fe^{2+} and Mg^{2+}. Its ideal half cell chemical formula is $M_{0.33}$, H_2O, $Al_{1.67}(Fe^{2+}, Mg^{2+})_{0.33}$ $Si_4O_{10}(OH)_2$ (figures 9a & b). [10]

Four different types of clay were prepared, two were fully exchanged with either copper or nickel ions and the two other were partially exchanged with either copper or nickel ions only in the interlayer region.

Materials used for the substitution were:

copper sulphate solution (5 g dm^{-3});

nickel sulphate solution (5 g dm^{-3})

sodium hydroxide solution (0.1 mol dm^{-3}).

Procedure:

Clay (40 g) was added to the copper solution (500 cm^3), the mixture was stirred for two hours, and then centrifuged. The supernatant solution was analysed by ICP. The resulting clay was then dried at room temperature until no variation of weight was observed. Once dried the clay was separated into two portions:

the first part was mixed and stirred with a sodium hydroxide solution (500 cm^3) for 2 hours. It was filtered, and dried, ready to be ground and stored (clay 1).

the second part was washed for 2 hours with distilled water (500 cm^3, pH 7) to remove the copper ion exchanged outside the interlayer, and centrifuged. The supernatant solution was analysed by ICP AES. The resulting clay was dried at room temperature until no further variation of weight occurred. It was then mixed and stirred with a sodium hydroxide solution (400 cm^3) for another two hours, filtered, and dried, ready to be ground and stored (clay 2).

The same procedure was used with the nickel solution and the resulting clays were respectively identified as clay 3 and clay 4. Figure 10 indicates the four different types of clays obtained:

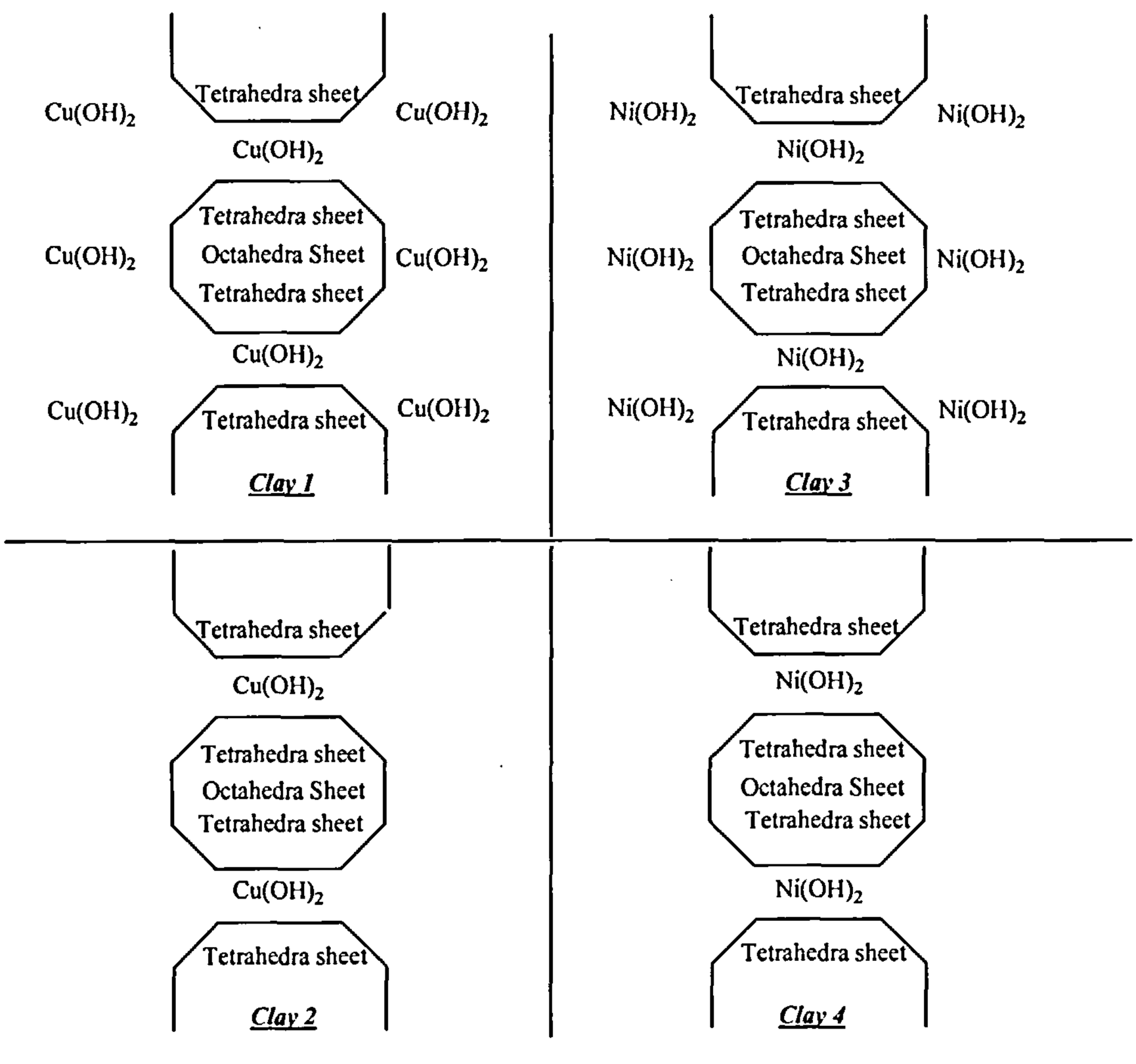

Figure 10: Schematic representation of the prepared types of clays

These four types of clays were leached as described later in §3.3.1.1 to determine their metal content.

2.2.2 Sediments

Sediments were sampled by technicians of *Voies Navigables de France* from a French canal in Roubaix (June 97) (appendix 4).

The surface sediments were sampled using a multisampler. [118] After dismantling the sampler, the sediments were collected in a basket and mixed so that the sample was homogeneous. The sediments were stored in glass containers and delivered to the University for laboratory experiments.

Metal contents determined by the Pasteur Institut from previous sampling (May 97) at the same location are shown in appendix 4. These sediments were considered as highly contaminated with zinc and lead. Canal sediments generally include clays, quartz (SiO_2), feldspar (potassium, calcium, and/or sodium aluminium silicates), various silicate minerals, gibbsite ($Al(OH)_3$) and calcite ($CaCO_3$).

On receipt at the University, sediments were dried at room temperature until no weight loss could be observed, ground and sieved to produce agglomerates sizes ranging from 710 µm to 1mm. Finally these sediments were leached as described later in §3.3.1.1 to determine their metal content for comparison with the data provided by the Pasteur Institut.

2.2.3 Puertollano Fly ash

2.2.3.1 Origin and composition

The fly ashes used in this study came from the Puertollano power plant, central Spain, which uses Pulverized Coal Combustion technology (PCC). Puertollano fly ash was obtained directly from the electrostatic precipitators of the plant, and consequently showed a low moisture content (1%). The major crystalline phases identified in these ashes were 17% quartz (SiO_2), 3.2% mullite ($Al_6Si_2O_{13}$), 1.3% magnetite (Fe_3O_4) and 78.5% glass. [23] Because of the high content of silica and alumina, and a low ratio SiO_2/Al_2O_3 (2:1), these fly ashes have potential applications for ceramics and zeolite synthesis. Moreover, treatment of these fly ashes at high temperature (1050°C) involves mineral transformations, i.e. the interaction of the quartz content and the glass matrix, forming large amount of Al minerals like mullite ($Al_6Si_2O_{13}$). [23]

An important consideration for subsequent use is the trace element concentration in fly ash. Because of potential environmental impact which can occur during zeolite synthesis and in ceramic use from the solubilization and volatilization of hazardous elements, a low content of heavy metals in fly ash is desired. The Puertollano fly ash has limited application because of its very high concentration of As, Cd, Ge, Hg, Pb and Zn. The complete chemical composition of Puertollano fly ashes is recorded in appendix 5. [23] Application of the SERVO process could be useful for the removal of these contaminants and offer the possibility to use the treated fly ash as a raw material for the preparation of ceramics and zeolites.

These fly ashes were leached as will be described in §3.3.1.2 to determine their metal content and compare it with the data provided by the Puertollano power plant.

2.2.3.2 Pellet preparation

Particles of fly ash were agglomerated at room temperature using clay (2.5%) from Volclay (described in § 3.2.1 and analysis provided by the supplier in appendix 3) as a binding agent. The mixture was moistened with distilled water and the pellets were rolled by hand. The pellets were left at room temperature to dry for 24 hours.

2.2.4 Orimulsion Ash

2.2.4.1 Origin, production and composition

As described earlier, Orimulsion is a low cost carbonaceous fuel from Venezuela that consists of a water-in-oil emulsion of a Venezuelan heavy crude oil with a magnesium stabiliser. Trials of the use of Orimulsion as a fuel have been carried out at several power stations in the UK but potential problems were found with its use especially concerning the disposal of the combustion ash. This is easily leached under landfill conditions and with the high proportion of vanadium constitutes a potential hazardous waste. Therefore some means of removing this element was required. This Department had previously been involved in the development of a successful hydrometallurgical process to recover the vanadium and nickel content of the ash and so the opportunity was taken to compare the SERVO process with its simple flowsheet, with the traditional hydrometallurgical route. Orimulsion ash was provided as a fine powder by Reakt with a size distribution between 1-10 μm and a moisture content about 15%. The ash generated from Orimulsion appears to be less dense than fly ash from other fuels. The chemical

composition of Orimulsion ash used in this study is summarized in table 3. [1] The major components are ammonium magnesium sulphate (75%); aluminium sulphate (10%); ammonium iron sulphate (4%); vanadyl and nickel sulphates; magnesium, nickel and vanadium oxides; some oxygen compounds and residual carbon. [37]

Since these studies began the proposed use of Orimulsion as a fuel in this country has been suspended.

Element	% wt		Element	% wt
V	7.600		Al	0.030
Ni	1.730		Cr	0.006
Mg	17.600		Ti	0.090
Ca	0.260		Fe	0.300
Cu	0.003		K	0.300
Zn	0.006		Co	0.005
Na	0.720		Mn	0.006
Si	0.070		Mo	0.070

Table 3: Chemical composition of Orimulsion ash [118]

Orimulsion ash was leached as described later in §3.3.1.2 to determine their metal content and compare it with the above data provided by Reakt.

2.2.4.2 Pellet preparation

Particles of fly ash were agglomerated at room temperature using clay (10%) from Volclay as a binding agent. The mixture was moistened with distilled water and the pellets were rolled by hand. The pellets were left at room temperature to dry for 24 hours.

2.3 Experimental Methods

2.3.1 Leaching of contaminated materials

Digestion under reflux was used for samples of sediments and clays. Microwave digestion was used for fly ash and Orimulsion ash.

2.3.1.1 Reflux digestion

The materials accurately weighed (0.5 g) were digested in aqua regia solution (10 cm^3, 1:3 concentrated HNO_3/HCl) under controlled reflux for five hours. The solution was filtered washed with nitric acid and diluted to 100 cm^3 in a volumetric flask. The solution was analysed using ICP-AES to determine the metal content.

2.3.1.2 Microwave digestion

This was carried out as described earlier (§2.1.5). The resulting solution was filtered, rinsed with nitric acid (2 mol dm^{-3}) and distilled water and diluted to volume in a 50 cm^3 volumetric flask.

The solution was analysed by ICP-AES to determine the metal content.

2.3.2 Metal speciation extraction of contaminated materials

This technique was used on fly ash samples and dried sediments (0.5g of material accurately weighed). [47] The extraction was performed in 100 cm^3 polypropylene tubes using a wheel mechanical shaker to allow end-over-end shaking at 30 ± 2 rpm, at room temperature 25 ± 2°C. The polypropylene tubes were carefully chosen to fit the centrifuge MSE Falcon 61300. After extraction, the tubes were placed in a centrifuge at a speed of 3000 rpm and temperature of 4 °C to separate solid residues from the supernatant liquid, which was then removed using a Pasteur pipette. The supernatant liquid was stored at 4 °C in high-density polyethylene containers with a V shaped bottom to allow the collection of some residual solids, which may arise despite careful pipette manipulation. Residues were washed by adding distilled water (20 cm^3), shaking for 15 min, and centrifuged. The supernatant washing solution was stored in the same conditions as the extracting solutions. The "cake" obtained upon centrifugation was broken up prior to the next step. Solutions from steps 1 to 3 were analysed by ICP-AES without dilution to determine the metal content. For the last step a dilution of the obtained solution in a 100 cm^3 volumetric flask was necessary to allow its analysis by ICP-AES.

Extractants were prepared according to the following procedures:

Solution 1: Acetic acid, (0.11 mol dm^{-3}): glacial acetic acid (25 cm^3) was diluted in a 1 dm^3 volumetric flask to form an acetic acid solution of 0.43 mol dm^{-3}.

250 cm^3 of this solution was then diluted to 1 dm^3 to form the required acetic acid concentration of 0.11 mol dm^{-3}.

Solution 2: Hydroxylamine hydrochloride, 0.1 mol dm^{-3}: hydroxylamine hydrochloride (6.95 g) was dissolved in 900 cm^3 of water. The solution was acidified with concentrated nitric acid to pH 2 and made up to 1 dm^3. pH of the solution was always checked if the solution was not prepared and used the same day.

Solution 3: Hydrogen peroxide, 30 % was used as supplied by the manufacturer, and was acid stabilised to pH 2.0 - 3.0.

Solution 4: Ammonium acetate, 1.0 mol dm^{-3}: ammonium acetate (77.08 g) was dissolved in 900 cm^3 of water and the solution was acidified to pH 2 with concentrated nitric acid and made up to 1dm^3.

The four step procedure is detailed in table 4:

Step	Fraction	Reagent	Shaking time and temperature
1	Acid soluble (e.g. carbonates)	20 cm^3 solution 1	16 h at 25°C (overnight)
2	Reducible (e.g. Fe-Mn oxides)	20 cm^3 solution 2	16 h at 25°C (overnight)
3	Oxidizable (e.g. sulfides)	a) 5 cm^3 solution 3 b) 5 cm^3 solution 3 c) 25 cm^3 solution 4	1h at 25°C covered, 1h at 85°C covered, and concentrated to low volume. 1h at 85°C covered, and concentrated to low volume. 16 h at 25°C (overnight)
4	Residual (Al-Si-O species)	1 cm^3 HCl 35% w/w + 2 cm^3 HF 48% w/w + 4 cm^3 HNO_3 70% w/w + 5 cm^3 H_2O.	26 min in microwave

Table 4: Sequential extraction procedure for 0.5 g of dried starting material [47]

2.3.3 Servo process extraction using modified thermogravimetric analysis

2.3.3.1 Apparatus and operational conditions

The thermogravimetric analyser was modified for use as the SERVO process reactor for preliminary studies on the simulated contaminated materials (Figures 11a and b). The furnace tube was connected using an exhaust tube to a trap where metal complexes were collected. This exhaust tube was heated using a heating tape to avoid the condensation of the extractant and complex before the cooled trap.

A Pyrex "extractant boat" was designed so it can be placed under the pan.

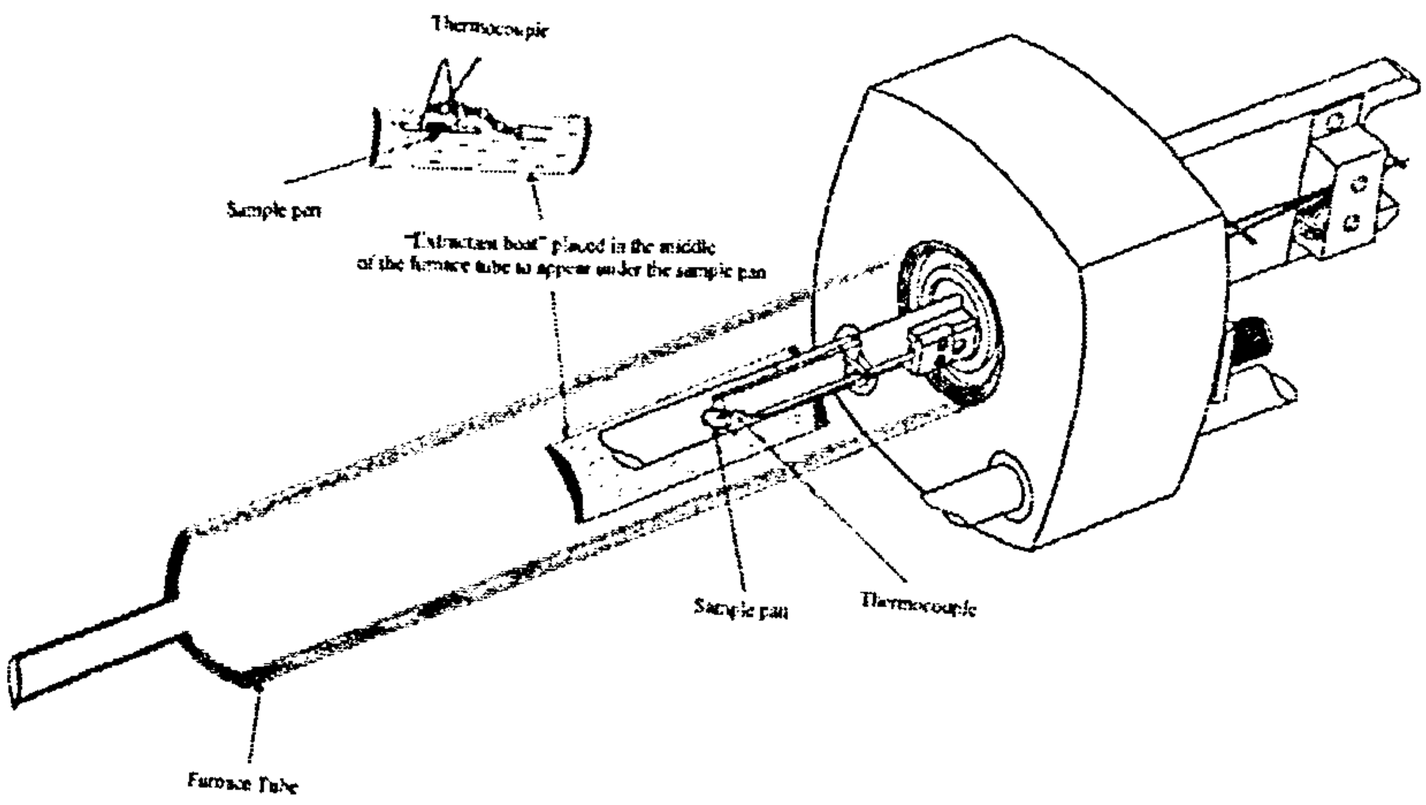

Figure 11a: modified TGA for SERVO process extraction, cross section

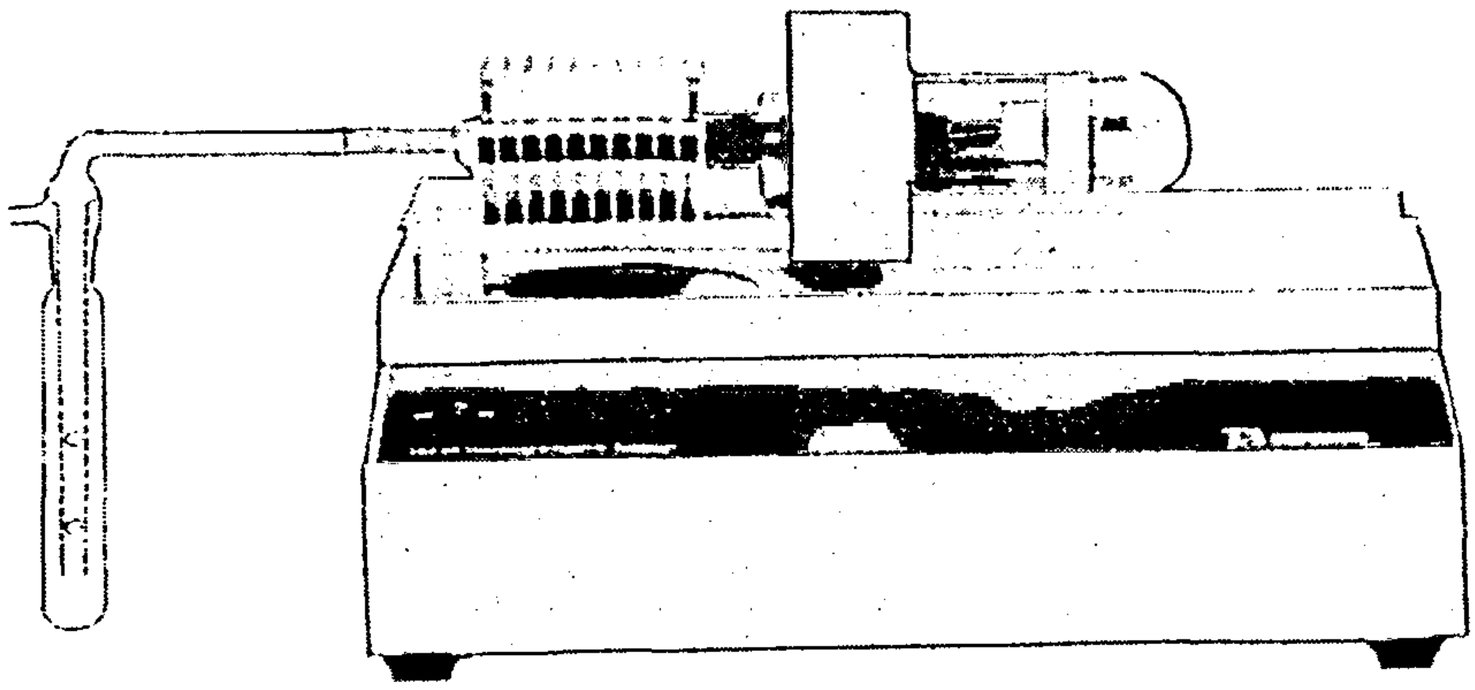

Figure 11b: modified TGA for SERVO process extraction

The general experimental procedure is described below for the extraction of copper from the loaded clays.

Clay materials were accurately weighed in the sample pan (20 ± 3mg) and H_2pnaa (ca. 0.7 ± 0.04g) extractant was placed in the "extractant boat" under the sample pan, and argon was flushed through the heated system at a flowrate of 60 cm^3 min^{-1}. This corresponds approximately to 1 mole of metal for 10 moles of extractant so that the extractant would be in large excess over the normal stoichiometric conditions to ensure a saturation of the atmosphere around the clay material. The system was gradually heated from room temperature to 230°C. Once this temperature was reached, it was monitored for 3 hours. Metal complexes were collected in the cooled trap placed at the end of the equipment.

In a second set of experiments, the clay materials and H_2pnaa were mixed prior to the experiment in different molar ratios from 1:1 to 1:4 and an amount of approximately 20 ± 2 mg of the mixture was placed in the pan. The system was then heated as before and the metal complexes were collected in the cooled trap.

In a third set of experiments, clay materials and H_2pnaa were mixed prior the experiment in a 1:1 ratio and an amount of approximately 30 ± 3 mg of the mixture was placed in the pan. The system was heated as before and, after cooling, the residue was rehydrated overnight with distilled water at pH 7 and the heating procedure repeated. This sequence was repeated.

Finally the first experiment was repeated with the system heated from room temperature to 350°C. Once this temperature was reached, it was monitored for 3 hours. Metal complexes were collected as before in the cooled trap placed at the end of the equipment.

2.3.3.2 Cleaning procedure

At the end of the experiment, the residual clay was collected and digested with *aqua regia* as described earlier; the tube containing the metal complexes was cleaned with nitric acid. The two solutions were then analysed by ICP-AES to determine the metal contents.

2.3.4 SERVO Process Extraction Apparatus

2.3.4.1 Process Design

The apparatus used for the SERVO process was constructed using electrical parts from RS Components Ltd, and electrothermal tapes from Electrothermal Engineering Ltd. It is composed of 5 major parts as shown in figure 12:

two ovens connected to temperature controllers;

one thermocouple 12 way selector switch connected to a digital temperature indicator and 4 thermocouples;

one Electrothermal heating tape shaped into a doughnut connected to a transformer. This shape was considered for practical purposes as it was to be placed between the two ovens;

one Electrothermal heating tape shaped into a sock connected to a transformer to be placed between the second oven and the cooled trap.

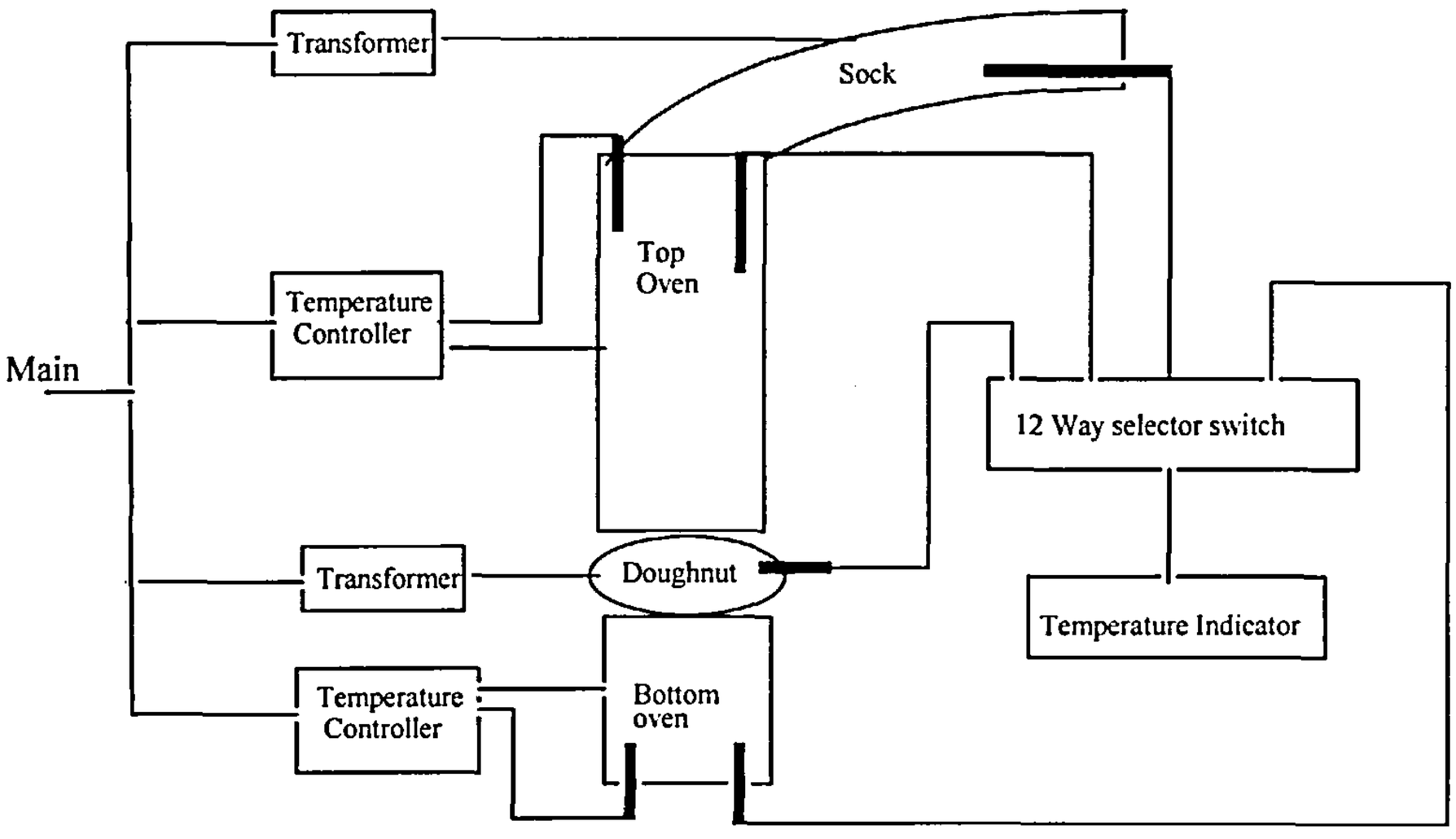

Figure 12: Schematic representation of the 5 major parts composing the Extraction section of the SERVO process equipment

1) Ceramic ovens

Ceramic ovens (Lindberg® electric heating units) were made of stainless steel resistance wire spirally wound and encapsulated as shown in figure 13. A glass fibre cover was designed to avoid heat loss.

To control the temperature of these ovens, temperature controllers (type K sensors, 0 -400°C, RS 344-120) were connected to each oven. The electric system for the temperature controllers is shown in figure 14. The system was adjusted to allow control of the temperature between ± 3°C of the set value

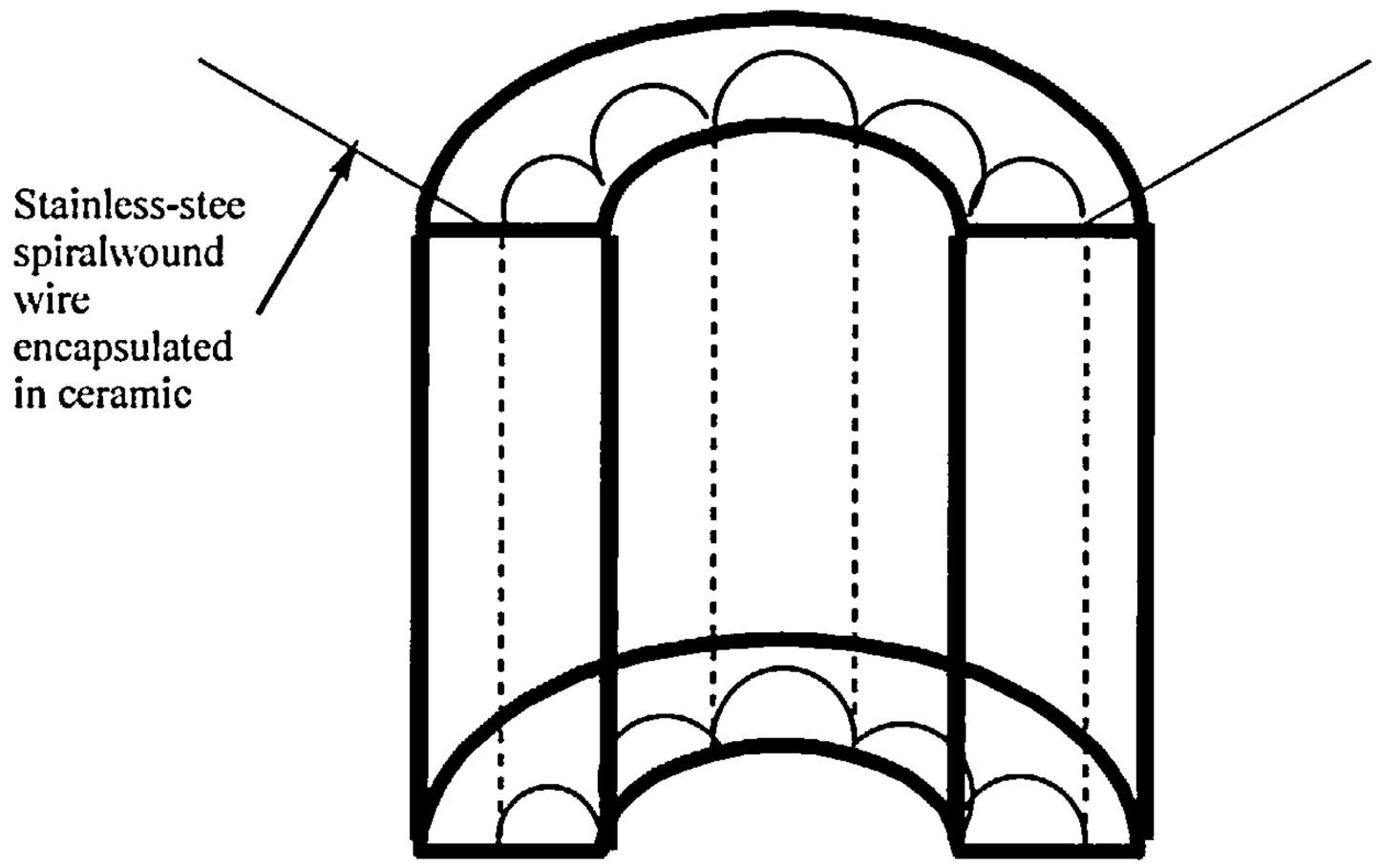

Figure 13: Half ceramic oven

2) Temperature Controller

A thermocouple 12 way selector switch (type K, RadioSpares (RS) C219-4602) was connected to 6 thermocouple probes (type K, RS 159-023) using thermocouple extension wires (type K, RS 151-209) protected with a solid glass fibre insulators and miniature connectors (type K). These thermocouple probes were placed in the regions where temperature needs to be controlled. A digital temperature indicator (type K, RS 258-108) was also connected to the selector switch to enable the temperatures to be monitored.

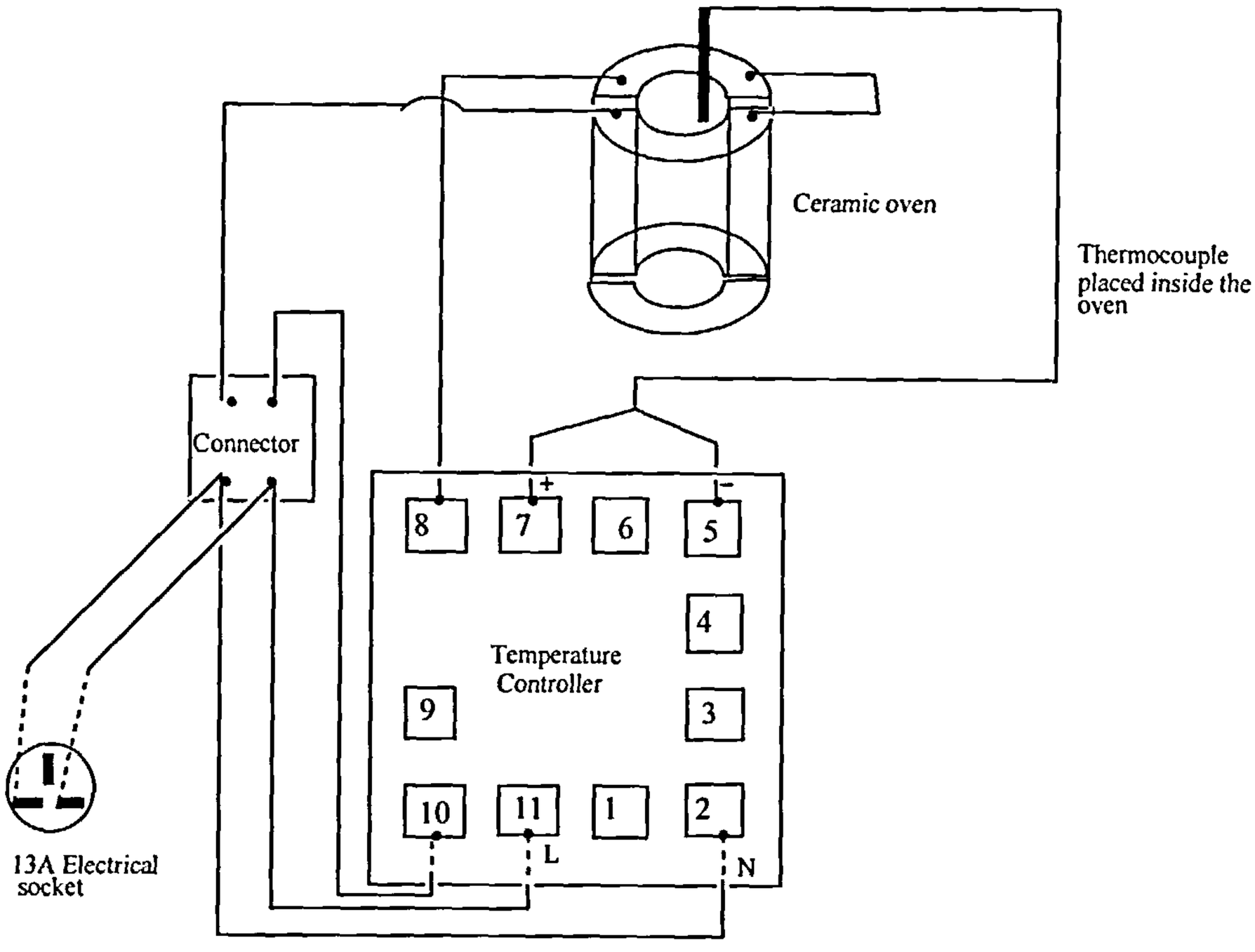

Figure 14: Electric system of the temperature controllers

3) Doughnut electrothermal tape

The heating tape (Electrothermal HT75502 MK1, 230V, 50-60Hz, 100W, 2ft) was rolled to form a doughnut shape. A glass fibre cover was designed to hold the shape and avoid any heat loss. The doughnut was connected to a transformer (RS 207-914, 8A, 230V, 47-400HZ) to control the energy input.

4) Sock electrothermal tape

As with the doughnut, this was an Electrothermal heating tape (Electrothermal HT75506 MK1, 230V, 50-60Hz, 300W, 6ft) rolled to form a sock shape. A glass fibre cover was designed to hold the shape and avoid any heat loss. The sock was connected to a transformer (RS 207-914, 8A, 230V, 47-400HZ) to control the energy input.

2.3.4.2 Apparatus and operational conditions

The apparatus used was the same for all experiments, although the volatilisation reactor was different for liquid and solid extractants. An outline of the SERVO process extraction equipment is shown in figure 15.

Two different types of reactor 1 were designed to contain either a liquid extractant (figure 15: left) or a solid extractant (figure 15: right). Reactor 2 was a cylinder fitted with standard joints and a coarse glass frit placed on top of the reactor 1, and contained the contaminated matrix. This was connected to a heated horizontal tube and a cooled receiver to contain the volatilised metal complexes, excess reagent and decomposition products. All experiments were run under 60 cm^3 min^{-1} of N_2 gas. The two reactors were first heated up to temperature T_1 for 90 min, so complexation could occur in reactor 2, then the reactor 2 was heated up to T_2, allowing volatilisation of the metal complex. The metal complexes were collected in trap cooled with liquid nitrogen or a trap containing a high boiling solvent e.g. petroleum ether, boiling range 100-120°C.

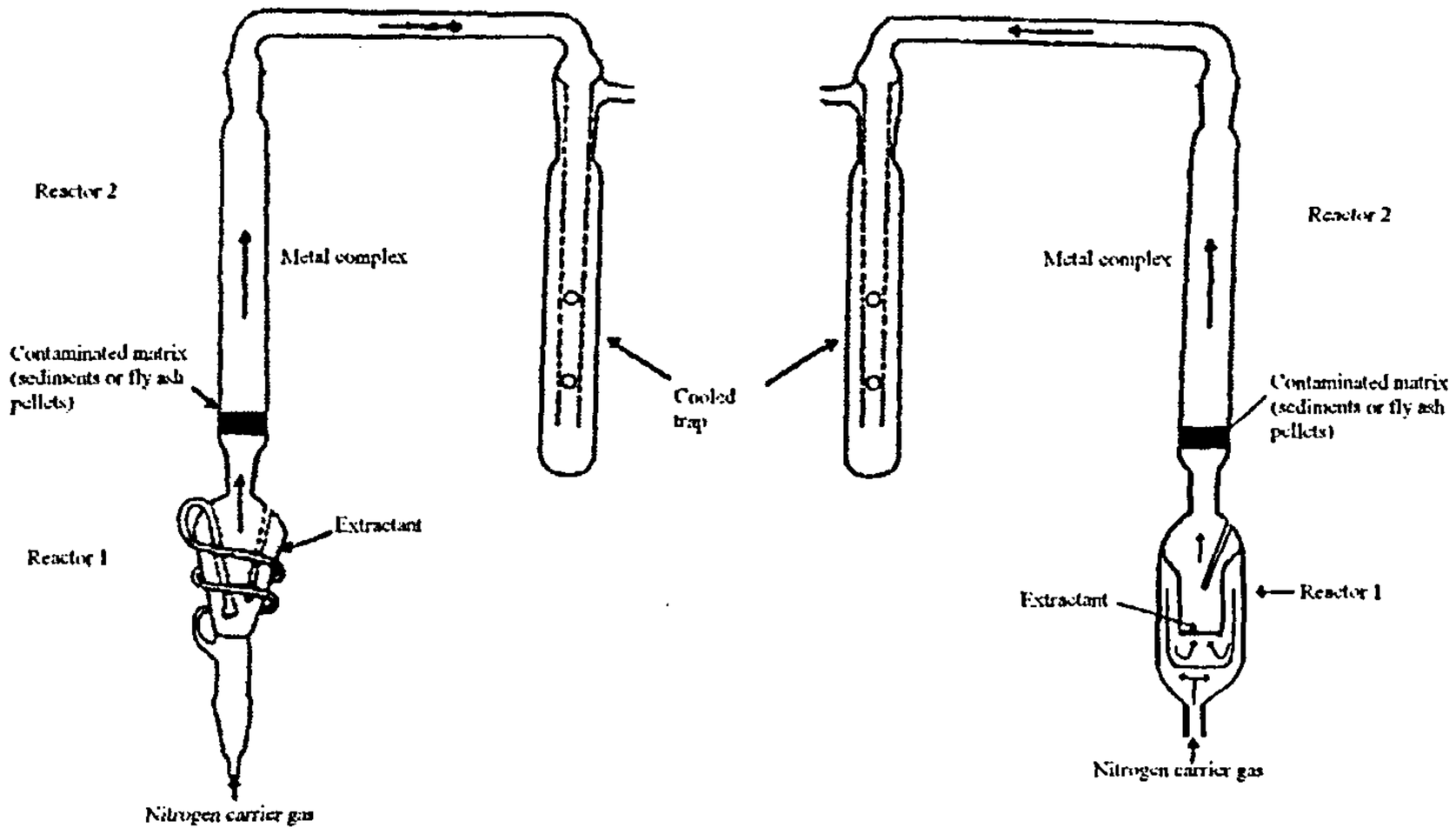

Figure 15: SERVO process extraction apparatus
(left: liquid extractant, right: solid extractant)

To test the possible extraction of metals using the new SERVO process extraction apparatus, metal carbonates, i.e. copper carbonate, zinc carbonate, nickel

carbonate and cobalt carbonate, were used as starting material and placed in the reactor 2 with either Hacac, H_2pnaa, or Hprps in reactor 1. The operational temperatures used in the reactor 1 were defined by the thermal stability of each extractant. The operational temperatures T_2 used in the reactor 2 were chosen according to the optimum volatilisation of the required metal chelate (DTG temperatures) (table 5).

Metal carbonates	Hacac (T_1 = 120°C)	H_2pnaa (T_1 = 230°C)	Hprps (T_1 = 250°C)
$CuCO_3$	T_2 = 250°C	T_2 = 250°C	T_2 = 260°C
$ZnCO_3 2Zn(OH)_2 H_2O$	T_2 = 160°C	T_2 = 175°C	T_2 = 290°C
$CoCO_3$ 0.5H_2O	T_2 = 250°C	T_2 = 250°C	T_2 = 290°C
$2NiCO_3 3Ni(OH)_2 4H_2O$	T_2 = 270°C	T_2 = 240°C	T_2 = 230°C

Table 5: Operational temperatures T_1 and T_2 used for extraction test

Metal carbonates (0.1 g accurately weighed) were used with either Hacac (20 cm^3), H_2pnaa (5g accurately weighed), or Hprps (2g accurately weighed). The quantity of extractant was determined by the volume of the extractant reactor. Only 2 g of Hprps were used, to reduce the cost of the experiment. Each experiment was repeated three times to establish reproducibility.

When the SERVO process extraction apparatus was used with contaminated materials like sediments, fly ashes or Orimulsion ashes, operational conditions used are shown in the table 6 for 2 g of material.

Quantity of extractant used per 2 g of material	Temperature T_1	Temperature T_2
20 cm^3 of Hacac	120°C	200°C
5g of H_2pnaa	230°C	270°C
2g of Hprps	250°C	280°C

Table 6: Operational conditions for the SERVO process extraction apparatus

Some experiments were carried out to exhaustion, where 5g of the initial material was placed in the reactor with Hacac (20 cm^3), H_2pnaa (5 g), or Hprps (2 g). Following the first experiment 0.5 g, accurately weighed, of the contaminated sample was removed for analysis, and the remaining 4.5 g were subjected to another

extraction run with the same quantity of extractant. This procedure was carried out until no sample was left.

2.3.4.3 Cleaning Procedure

In the above experiments, the material after extraction was shaken to provide homogeneity and a sample of 0.5 g, accurately weighed, was removed, and digested as described previously. Otherwise, 1 g, accurately weighed, of material was digested and analysed. The remaining sample was stored.

The traps containing the metal complexes were cleaned after each batch using dichloromethane for H_2pnaa and Hprps, and petroleum ether for Hacac. Solutions were then stripped 5 times with hydrochloric acid (10 cm^3, 5 mol dm^{-3}). The obtained solutions were then diluted ten fold.

2.3.5 Reduction of metal complexes

Reduction of the synthesised metal complexes was studied using the extraction process reactors modified to enable the introduction of hydrogen gas between reactors 1 and 2 as shown in figure 16. Glass balls (20g, 1-2mm diameter) were introduced into reactor 2. The collection trap contained petroleum ether (100-120°C) to recover the ligand. After each run, reactor 2 and the glass balls were washed with 2 mol dm^{-3} nitric acid to leach the deposited metal and the solution analysed by ICP-AES. The recovered ligand was analysed by IR to check if any decomposition had occurred during the reduction of the metal complex.

Metal complexes like copper, nickel, and cobalt were believed from previous studies to be reducible. [108, 109, 120, 121] Operational conditions of each run are defined in table 7. Generally temperature T1 was selected to allow volatilisation of the metal complex and avoid any thermal decomposition. Temperature T2 was selected at 280°C to be low enough to avoid thermal decomposition. Previously [108, 109] Cu(pnaa) and Ni(pnaa) had been reduced at T2 = 340 °C and T2 = 325 °C respectively. It was not possible to check the reduction of Cu(pnaa) and Ni(pnaa) at these temperature because the maximum temperature that could be achieved with the reactors were 300°C so it was only possible to check for reduction at 280°C. The nitrogen flowrate was kept at 60 $cm^3\,min^{-1}$. Gas flowrate was set at 20 $cm^3\,min^{-1}$ at a 3:1 ratio of nitrogen:hydrogen shown previously to be most effective. [119]

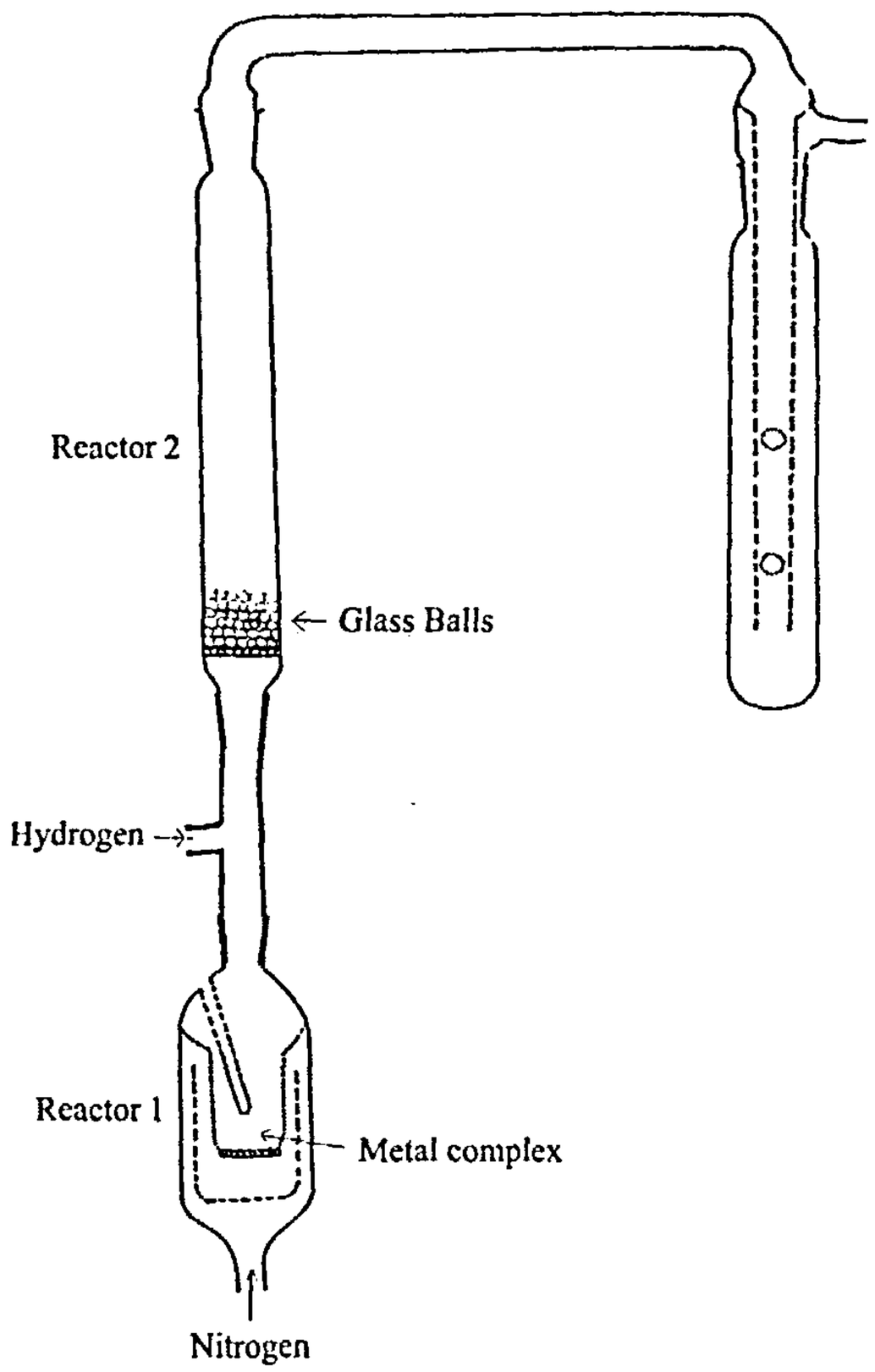

Figure 16: SERVO process reduction apparatus

Metal complexes	Quantity of metal complex used accurately weighed	Temperature T1	Temperature T2
$Cu(acac)_2$	0.1g	218°C	270°C
$Ni(acac)_2$	0.01g	218°C	270°C
Cu(pnaa)	0.05g	260°C	280°C
Ni(pnaa)	0.05g	260°C	280°C
$Co(prps)_2$	0.1g	270°C	280°C
$Ni(prps)_2$	0.1g	270°C	280°C

Table 7: Operational conditions for the reduction of metal complexes

2.4 Synthesis and properties of extractants and metal complexes

All experimental work has been carried out under good laboratory conditions fulfilling the University safety regulations. All instrumental analysis (IR, TGA and MS) of the prepared compounds are presented in appendix 6.

2.4.1 2,4-pentanedione and metal complexes

2.4.1.1: Materials

2,4-pentanedione (Hacac) was obtained from Aldrich and used as received.

Bp: 140°C

TGA: Volatilisation temperatures: 22°C → 148°C

Percentage residue after volatilisation: 0.1%

IR (cm^{-1}): 3487 (OH str.), 2925 (C-H str., alkyl group), 1710-1729 (C=O str. asymmetric), 1624 (C=C str.), 1304-1250 (C-O aliphatic ketone).

MS (EI): m/z: 100 (M^+, 17%), 85 (23%), 57 (5%), 43 (100%).

The volatilisation temperatures of this ligand indicate an extremely volatile compound (22°C → 148°C) that is also thermally stable (only 0.1% of residue is formed after volatilisation). IR analysis confirms the structure of Hacac, a β-diketone with the specific C=O stretching frequency at 1710 cm^{-1}.

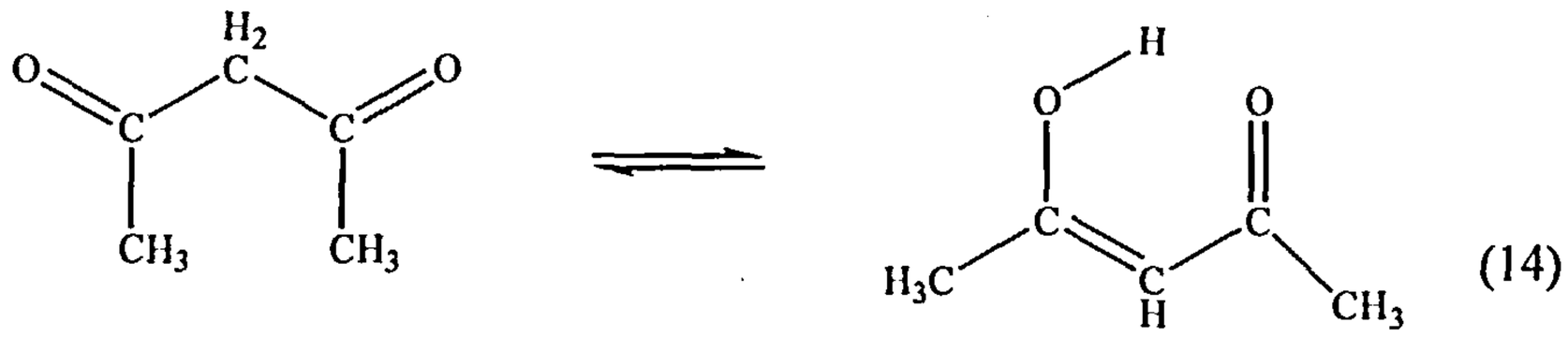

keto form (diketo) enol form (keto-enol) (14)

As with all β-diketones, Hacac exists in tautomeric equilibrium between the diketo and keto-enol forms [122] (equation 14).

In the later form, Hacac contains one acidic and one basic functional group and coordinates as an anion through both oxygen atoms. Upon reaction with a metal ion, the positive charge on the latter is reduced by one unit for each ligand anion

coordinated. Where the coordination number of the metal is twice the positive charge on the ion, chelation with the ligand produces a neutral molecule (equations 15, 16):

$$M^{n+} + n(Hacac) \Leftrightarrow M(acac)_n + nH^+ \qquad (15)$$

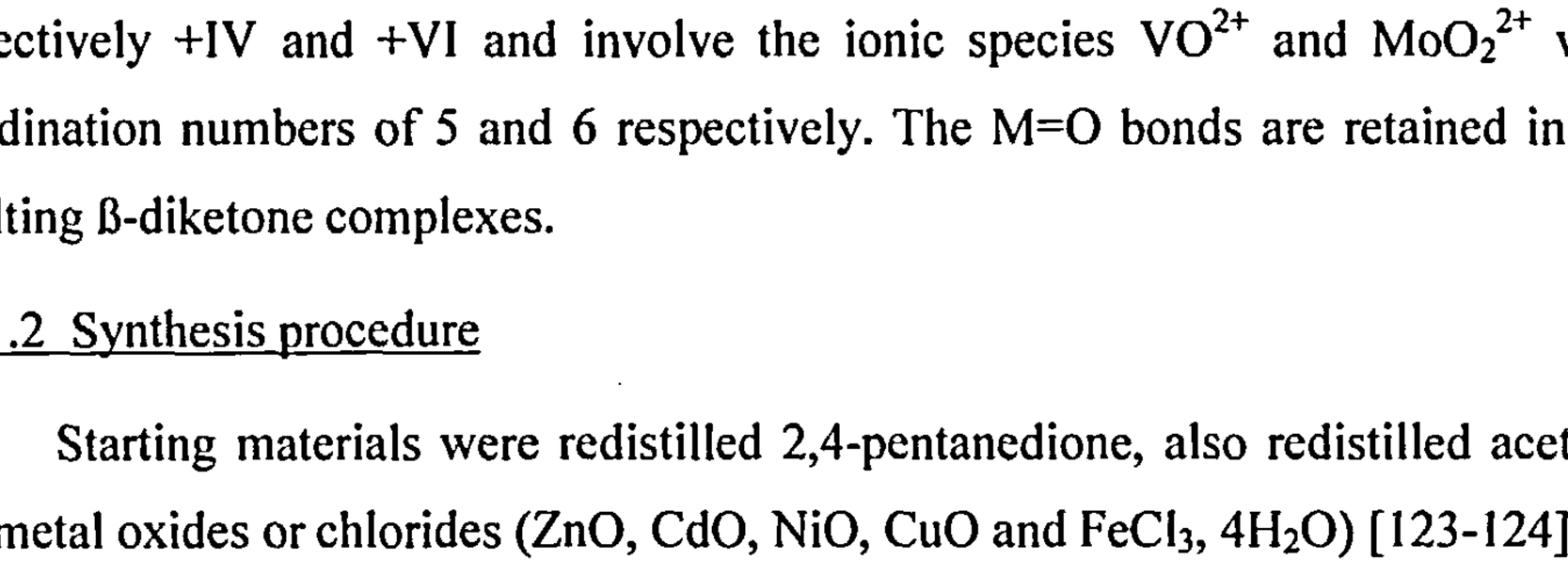

(16)

This is the situation for divalent metals ions like Cu^{2+}, Ni^{2+}, Zn^{2+} with coordination number 4 and trivalent metals ions like Fe^{3+} or Cr^{3+} with coordination number 6.

In the case of vanadium and molybdenum, the most stable oxidation states are respectively +IV and +VI and involve the ionic species VO^{2+} and MoO_2^{2+} with coordination numbers of 5 and 6 respectively. The M=O bonds are retained in the resulting ß-diketone complexes.

2.4.1.2 Synthesis procedure

Starting materials were redistilled 2,4-pentanedione, also redistilled acetone and metal oxides or chlorides (ZnO, CdO, NiO, CuO and $FeCl_3$, $4H_2O$) [123-124].

The method of preparation involved the addition of 2,4-pentanedione (0.097 moles ~ 10 cm^3) to a suspension of the corresponding metal oxides or chlorides (approx 0.048 moles) in dry acetone (ZnO: 3.95g, CdO: 6.22g, NiO: 3.62g, CuO: 3.85g and $FeCl_3$, $4H_2O$: 6.42g). The reaction mixture was shaken by hand and heated gently under reflux for 10 minutes. The solution was filtered to remove any insoluble material and the solvent evaporated under reduced pressure to give a coloured solid (as specified in the following table), which was recrystallised from petroleum ether.

Metal 2,4 - pentanedionate	Colour	Mp	Yield
$Zn(acac)_2$	White fibre	136°C	17%
$Cd(acac)_2$	Reddish crystals	235°C	23%
$Ni(acac)_2$	Green crystals	112°C	45%
$MoO_2(acac)_2$*	Light Green crystals	172°C (d)	-
$VO(acac)_2$*	Green powder	210°C (d)	-
$Cu(acac)_2$	Blue	127°C	74%
$Fe(acac)_3$	Orange/red crystals	173°C	56%

* Compounds supplied by Dr Liam Gilby

Table 8: Specifications of metal 2,4-pentanedionates

2.4.1.3 Cu $(acac)_2$

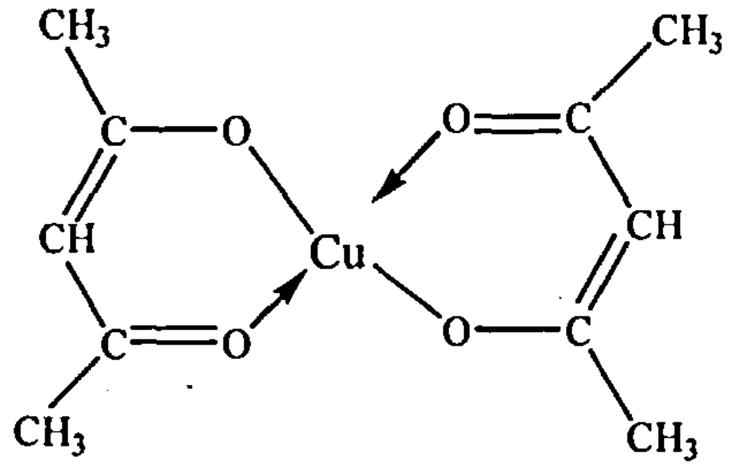

Figure 17: $Cu(acac)_2$

The complex was prepared as described earlier (§ 2.4.1.2)

Yield: 74 %

Mp: 127°C followed by sublimation at 170°C

(Reported decomposition above 230°C [125])

TGA: Volatilisation temperatures: 163°C → 270°C

Percentage residue after volatilisation: ≅ 0.2 %

(Reported 172°C → 224°C (0%) [126])

IR (cm^{-1}): 3474 (OH str.), 2900 (C-H str., methyl), 1600 (C=O str. broad band,

ß diketones), 1033 (C-H deformation vib.), 692 (C-C str).

MS(EI): m/z: 263 ($^{65}M^+$, 39%), 261 ($^{63}M^+$, 83.5%), 246 (49%),
233 (22%), 231 (4 8%), 164 (37%), 162 (58%),
150 (47%), 148 (83%), 100 (21%), 85 (31%), 43 (100%).

$Cu(acac)_2$ melts at 127°C but literature data shows only decomposition above 230°C. The TGA thermogram shows a single weight loss from 163 - 270°C, indicating that the chelate obtained is anhydrous and quite volatile. The residue of only 0.2% after volatilisation indicates a good thermal stability. The reported sublimation temperatures of 172 - 224°C were recorded using a TG-DSC thermogram using heating rate of 5°C min^{-1}, [127] and the different technique and experimental conditions can explain the difference between the reported data and that found in the current work. The IR spectrum confirms the main structural characteristics of the chelate. MS (EI) shows the presence of the two isotopes of copper (appendix 7), ^{63}Cu, 83.5% and ^{65}Cu, 39%. The calculated equivalent abundance ratio ^{63}Cu : ^{65}Cu 100 : 46.7, is close to the theoretical value (100 : 44.5). Molecular ion also confirms the composition.

2.4.1.4 $Ni(acac)_2(H_2O)_2$

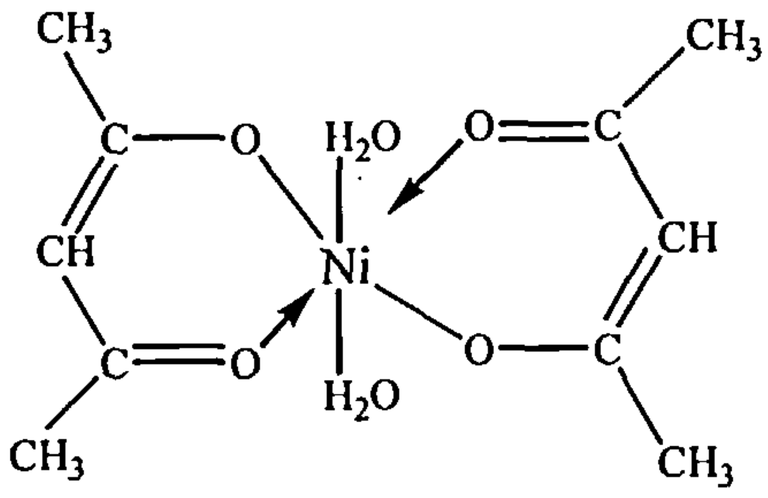

Figure 18: $Ni(acac)_2$

The complex was prepared as described earlier (§ 2.4.1.2)

Yield: 45 %

Mp: 112°C followed by sublimation at 152°C
(Reported decompose above 230 [125])

TGA: Volatilisation temperatures: 146°C → 280°C

Percentage residue after volatilisation: ≅ 28.6 %

(Reported ranges of volatilisation 157°C → 214°C [127] and 190°C → 326°C (22%) [128])

IR (cm^{-1}): 3402 (OH str.), 2988 (C-H str., methyl), 1610 (C=O str. broad band, ß diketones)), 1520 (C=C str.), 1262 (C=O), 1196 (C-O), 1020 (C=O str.), 658 (C-C str.)

MS (EI): m/z: 260 ($^{62}M+$, 1.4%), 258 ($^{60}M+$, 11%), 256 ($^{58}M+$, 27%), 241 (25%), 157 (43%), 142 (14%), 100 (15%), 85(23%), 43 (100), 28 (47%).

Nickel 2,4-pentanedionate is reported to be trimeric ($[Ni(acac)_2]_3$) in solid state and monomeric $Ni(acac)_2$ in dilute solutions, in the vapour phase, or when the compound is isolated in an inert solid matrix. [126] A melting point is not recorded in the literature only decomposition above 230°C. [125] The compound synthesised in this work was found to melt at 112°C and sublimes above 152°C.

The TGA thermogram shows a double weight loss. The first loss of 12% appears between 50 - 145.5 °C, and is equivalent to two molecules of water (2*18/292.7 = 12.3%), confirming the chelate obtained is dihydrated. The second weight loss of 58.6% from 145.5 - 280° leaving a residue of 28.6%, showing thermal degradation of $Ni(acac)_2$ above 280°C. Reported sublimation temperatures of 157 - 214°C [127] were recorded using a TG-DSC thermogram at a heating rate of 5°C min^{-1} with no residue reported, and 190 - 326°C [127] using TGA at a heating rate of 5°C min^{-1}, that showed thermally instability with a residue of 22%. Again different techniques and experimental conditions can explain these differences in the final volatilisation temperature. Moreover the composition of the compound synthesised by Belcher et al [128] was not stated, but in the preparation, it is mentioned that the compound was purified by repeated sublimation which should produce the anhydrous nickel acetylacetonate. The residue left (22%) after sublimation [127] confirms the thermal instability obtained in this study for $Ni(acac)_2(H_2O)_2$ (28.6%). The IR confirms the main characteristics of the structure.

MS(EI) shows the presence of the main three isotopes of nickel (appendix 7), ^{58}Ni, 27%; ^{60}Ni, 11% and ^{62}Ni, 1.4%. The equivalent abundance ratios ^{58}Ni: ^{60}Ni: ^{62}Ni were measured at 100 : 40.7: 5.2, which are close to the theoretical values (100 :

38.2 : 5.25). The two other nickel isotopes were present but in extremely low concentration so that they were barely distinguishable in the MS spectrum.

2.4.1.5 $Zn(acac)_2(H_2O)_2$

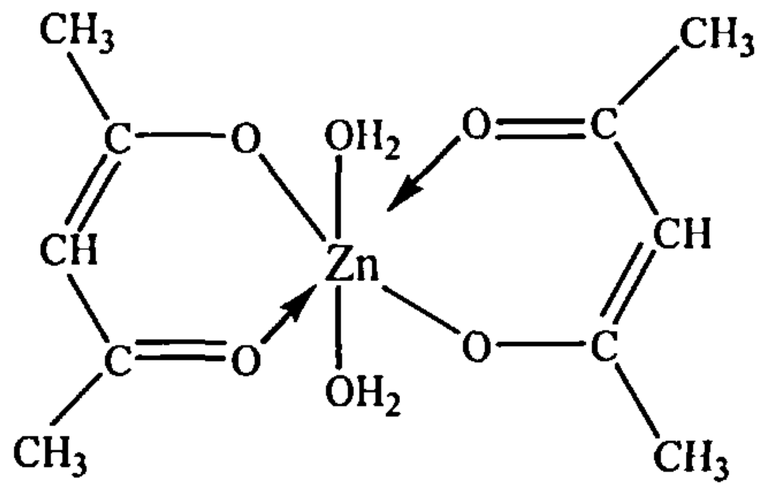

Figure 19: $Zn(acac)_2(H_2O)_2$

The complex was prepared as described earlier (§ 2.4.1.2)

Yield: 17 %

Mp: 136°C

TGA: Volatilisation temperatures: 122°C → 200°C

Percentage residue after volatilisation: ≅ 9.7 %

IR (cm^{-1}): 3446 (OH str.), 2925 (C-H str. methyl), 1594 (C=O str. Broad band, ß diketones)), 1266 (C=O), 1021 (C-O str.), 928 (C-H vib.)

MS (EI): m/z: 266 ($^{68}Zn(acac)_2^+$, 16.5%, 33), 265 ($^{67}Zn(acac)_2^+$, 3.75%, 7.5), 264 ($^{66}Zn(acac)_2^+$, 20.6%, 41.2), 262 ($^{64}Zn(acac)_2^+$,50%, 100), 167($^{68}Zn(acac)^{2+}$, 21.4%, 37.5), 166 ($^{67}Zn(acac)^{2+}$, 4.7%, 8.2), 165 ($^{66}Zn(acac)^{2+}$, 35.9%, 63), 163 ($^{64}Zn(acac)^{2+}$,57%, 100), 150 (31.1%), 100 (15.6%), 85 (22.6%), 43 (100%).

The melting point obtained (135°C) is close to the reported value of 138°C [124] and the IR confirms the main structural characteristics of the chelate.

MS (EI) shows the presence of the main isotopes of zinc (appendix 7). Zinc isotopes (^{64}Zn, ^{66}Zn, ^{67}Zn, and ^{68}Zn) appear complex with two molecules of Hacac as expected in clusters of ions 266 ($^{68}Zn(acac)_2^+$, 16.5%, 33), 265 ($^{67}Zn(acac)_2^+$, 3.75%, 7.5), 264 ($^{66}Zn(acac)_2^+$, 20.6%, 41.2), and 262 ($^{64}Zn(acac)_2^+$,50%, 100). The measured equivalent abundance ratios 100 : 41.2 : 7.5 : 33 are close to the theoretical ratios 100 : 57.4 : 8.4 : 38.7 with a 28% error in the ^{66}Zn data.

Zinc isotopes also appear with one molecule of Hacac in the ions 167 ($^{68}Zn(acac)^+$, 21.4%, 37.5), 166 ($^{67}Zn(acac)^+$, 4.7%, 8.2), 165 ($^{66}Zn(acac)^+$, 35.9%, 63), and 163 ($^{64}Zn(acac)^+$, 57%, 100). The measured equivalent abundance ratios of 100 : 63 : 8.2 : 37.5 are close to the theoretical ratios with this time only a 9.7% error in the ^{66}Zn data. The final zinc isotope ^{70}Zn was not observed but this is expected as its abundance is low at 0.6%.

The TGA thermogram shows a triple weight loss and a residue of 9.7%, i.e. a thermally unstable compound. The amount of residue at 300°C is insufficient to suggest the presence of zinc, as this would require at least 23%, so the residue is presumably mainly carbon products. The first weight loss of 14.21% (= 39.87 g mol^{-1}) appears from 58 - 87°C, would be the loss of water from the compound. Two molecules of water corresponds to 36 g mol^{-1} suggesting that compound is dihydrated and not a monohydrate as previously reported from a different synthesis to that used here [129]. The third weight loss 59.1% (= 163.50 g mol^{-1}) from 127.5 - 200°C seems the easiest to identify as it corresponds to the molecular weight of $Zn(acac)^+$. The second 16.28% (= 49.95 g mol^{-1}) from 87 - 127.5°C could correspond to the loss of a molecule of CH_3CO (= 43 g mol^{-1}) resulting from the decomposition of the second molecule of acac. This observation would mean that upon volatilisation, $Zn(acac)_2.(H_2O)_2$ is unstable and split into three parts as shown in figure 20 and equation 18.

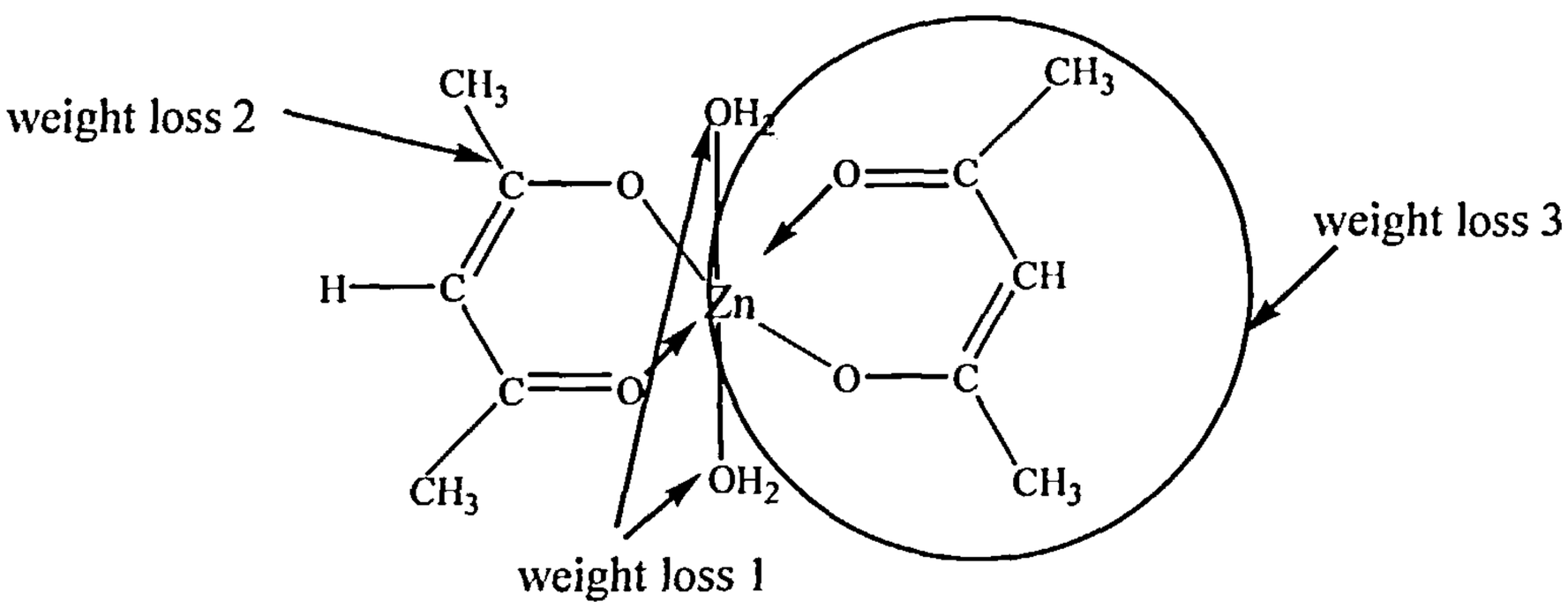

Figure 20: Thermal decomposition of $Zn(acac)_2.(H_2O)_2$

$$Zn(acac)_2(OH_2)_2 \rightarrow \underbrace{2H_2O}_{\text{weight loss 1}} + \underbrace{CH_3CO}_{\text{weight loss 2}} + \underbrace{Zn(acac)^+}_{\text{weight loss 3}} + \text{Residue} \qquad (17)$$

The degradation process of 2,4-pentanedionates of divalent metals has been studied using a combined TG-DTA-MS technique, [129] and general fragmentation pattern has been proposed (figure 21):

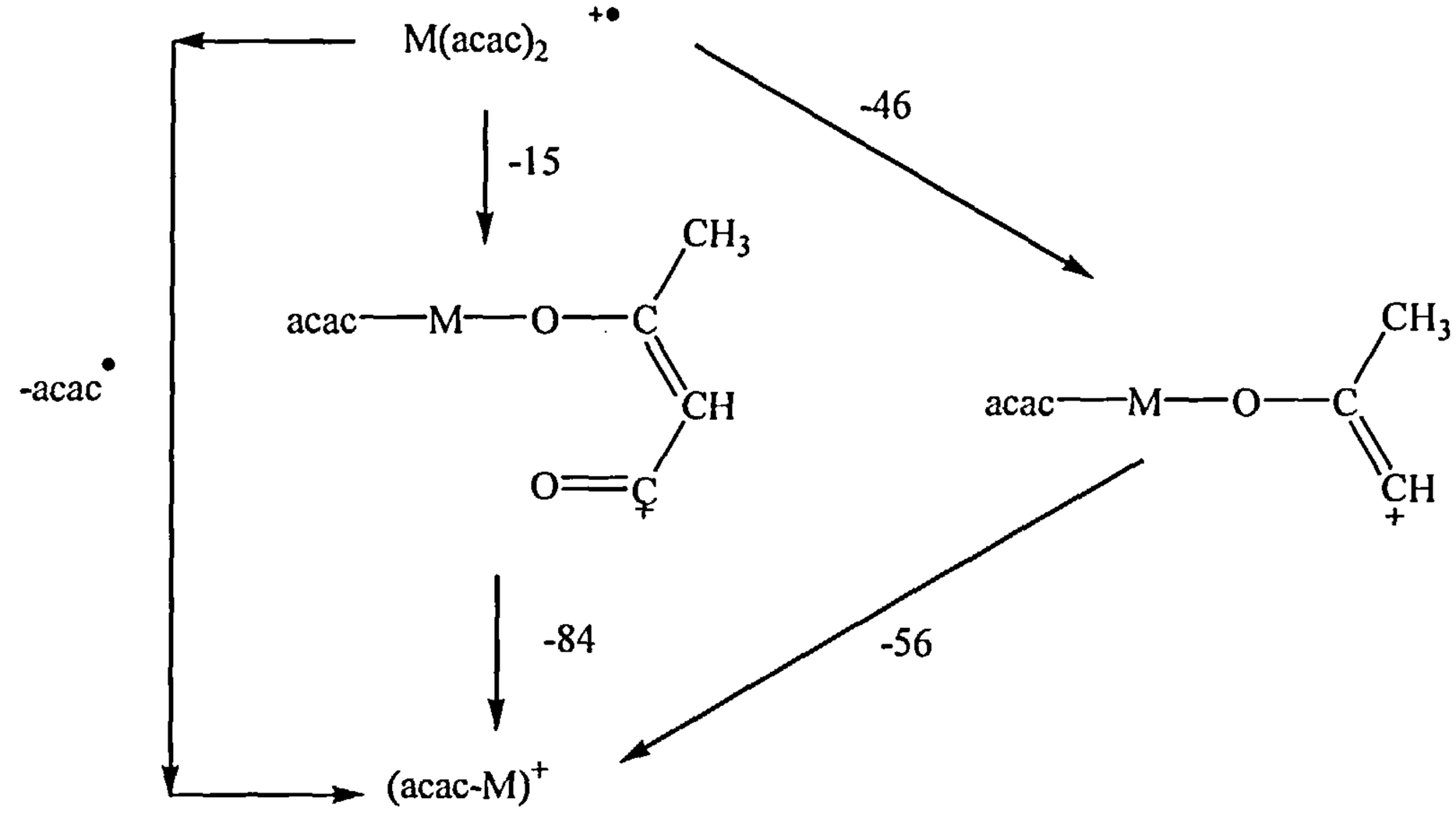

Figure 21: Fragmentation pattern of metal 2,4-pentanedionates ([129])

This general fragmentation pattern confirms the formation of $Zn(acac)^+$ as the third weight loss but does not support the formation of the CH_3CO fragment observed in the splitting pattern of the zinc complex prepared above. However as this is probably the dihydrate rather than the monohydrate certain variations might be expected.

2.4.1.6 $Fe(acac)_3$

The complex was prepared as described earlier (§ 2.4.1.2)

Yield: 56 %

Mp: 173°C

TGA: Volatilisation temperatures: 92°C → 275°C

Percentage residue after volatilisation: ≅ 3.65 %

(Reported temperature range from 203°C → 290°C [130])

IR (cm^{-1}): 3469 (OH str.), 1614 (C=O str. broad band of ß diketones)), 1539 (C=C str.), 1367 (C-H), 1291-1148 (C-O), 732 (C-C).

MS (EI): m/z: 362 (^{56}Fe ,49.6%, 100), 333 (58.4%), 312 (14.1%), 293 (16.1%), 283 (10.7%), 209 (13.4%), 159 (45%), +43 (100%).

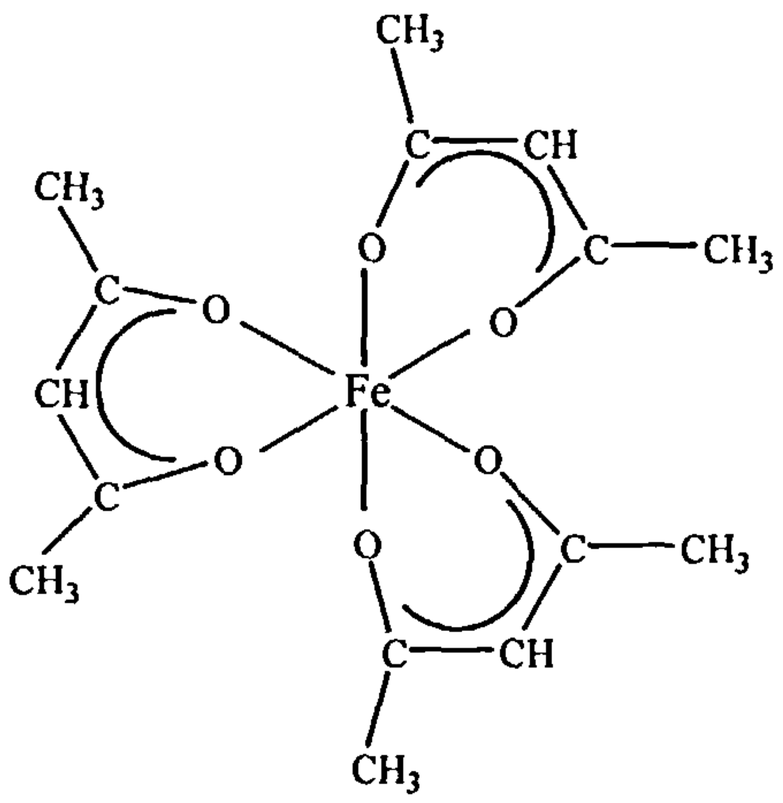

Figure 22: $Fe(acac)_3$

The TGA thermogram shows a single weight loss from 92 - 275°C, indicating that the chelate obtained is anhydrous and quite volatile. The residue after volatilisation is 3.65%, showing good thermal stability. Reported sublimation temperatures of 203 - 290°C [130] were recorded using a TG-DSC thermogram at a heating rate of 5°C min^{-1} but no residue was reported. As before the different technique and experimental conditions used can explain the difference in the final volatilisation temperature from that obtained in this work. The IR spectrum confirms the main characteristic of the chelate structure. Some presence of moisture is shown by the OH stretching at 3469 cm^{-1}. This comes from the presence of water in the originally prepared compound that was then stored under vacuum before TGA, leaving the time for drying. MS (EI) shows only the presence of the main isotope of iron (appendix 7), ^{56}Fe with an intensity of 49.6%. Three other isotopes were expected ^{54}Fe ^{57}Fe and ^{58}Fe, with the theoretical abundance ratios ^{54}Fe: ^{56}Fe: ^{57}Fe: ^{58}Fe of 6.3:100:2.4:0.3. However as the intensity of the ^{56}Fe obtained was 49.6%, the expected intensity of ^{54}Fe ^{57}Fe and ^{58}Fe would be 3.1%, 1.2% and 0.15% which are too low to be detected in the spectra.

2.4.1.7 $MoO_2(acac)_2$

The complex was supplied by Dr Liam Gilby. [131]

Mp: decomposes at 210°C

TGA: Volatilisation temperatures: 130°C → 256°C

Percentage residue after volatilisation: ≅ 55 %

IR (cm^{-1}): 3433 (OH str.), 1585 (C=O str. broad band, ß diketones)), 1506 (C=C str.), 1262 (C-O), 1024 (C=O str.), 915 (Mo-O str. vibration) [131], 669 (C-C).

MS (EI): m/z: 330 (^{100}M, 3%, 25), 328 (^{98}M, 12.12%, 100), 327 (^{97}M, 3.94%, 32.5), 326 (^{96}M, 7.6%, 62.5), 325 (^{95}M, 7.3%, 60), 324 (^{94}M, 2.72%, 22.5), 322 (^{92}M, 4.85%, 40), 288 (^{100}M, 19.5%, 39) 286 (^{98}M, 50%, 100), 285 (^{97}M, 29.5%, 59), 284 (^{96}M, 39.5%, 79), 283 (^{95}M, 36%, 72), 282 (^{94}M, 22.5%, 45), 280 (^{92}M, 27%, 54), 231(^{100}M, 32.1%, 41), 229 (^{98}M, 78.2%, 100), 228 (^{97}M, 48.5%, 62), 227 (^{96}M, 67.6%, 86), 226 (^{95}M, 54.0%,69), 225 (^{94}M, 29.7%,38), 223 (^{92}M, 40.9%, 52).

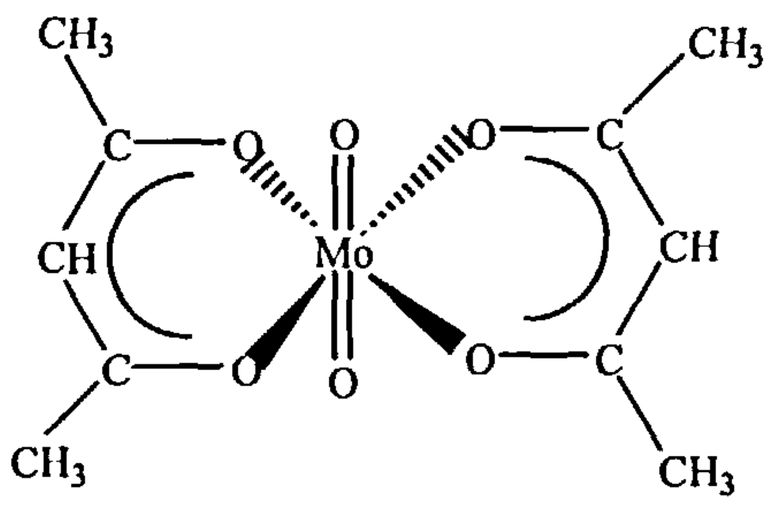

Figure 23: $MoO_2(acac)_2$

The melting point shows the thermal instability of the chelate as it decomposes at 210°C. The TGA thermogram shows a double weight loss: the first weight loss of 38.5% appears from 130 - 256°C and the second loss of 6.0% from 256 - 350°C, is not a smooth curve and shows some irregularities. The 55% residue left after the run shows extensive thermal decomposition of $MoO_2(acac)_2$. The IR confirms the main structural characteristics of the chelate. The presence of some moisture is shown by the OH stretching at 3433 cm^{-1}. Following the IR analysis and before thermal analysis the compound was stored under vacuum to dry.

MS (EI) shows the presence of several clusters of seven isotopes of molybdenum (appendix 7), with only three noted in the table 9. The isotope ratios obtained are given in table 9 are close to the literature values with however some

large errors, up to 55.4%, in their intensity. The ratios for cluster 1, the most important as it shows the different isotopes of molydenum for the $MoO_2(acac)_2$ molecule ion, is calculated from the smallest cluster in the spectrum and therefore measurements are less precise and involve higher errors. On the other hand cluster 3 ratios, showing the best results of the three (apart from the 2 isotopes ^{97}Mo and ^{96}Mo), is calculated for the most intense cluster.

Isotopes	Cluster 1ratios Mw 330-322	Cluster 2 ratios Mw 288-280	Cluster 3 ratios Mw 231-223	Theoretical Ratios
^{100}Mo	25 (37%)	39 (2.2%)	41 (2.7%)	39.9
^{98}Mo	100	100	100	100
^{97}Mo	32.5 (17.9%)	59 (49%)	62 (55.4%)	39.6
^{96}Mo	62.5 (10%)	79 (14.5%)	86.4 (25.2%)	69
^{95}Mo	60 (9%)	72 (9.1%)	69 (4.5%)	66
^{94}Mo	22 (41%)	45 (17.5%)	38 (0.1%)	38.3
^{92}Mo	40 (33%)	54 (12.1%)	52 (15.4%)	61.5

Table 9: Molybdenum isotope ratios obtained by MS(EI)

2.4.1.8 $VO(acac)_2$

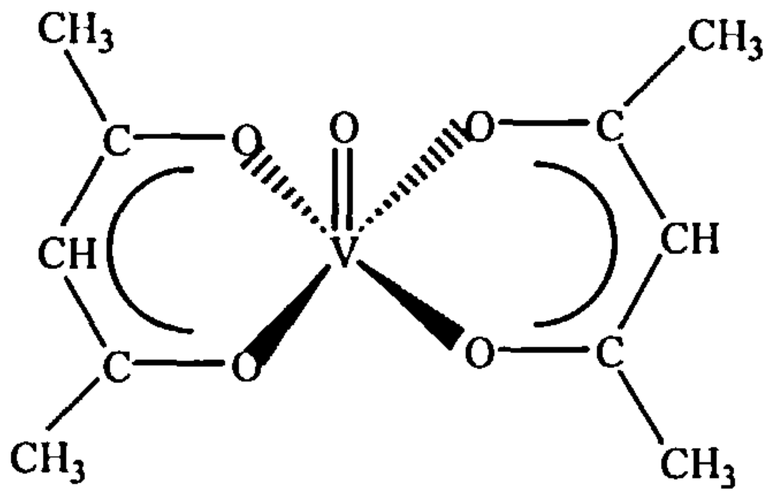

Figure 24: $VO(acac)_2$

The complex was supplied by Dr Liam Gilby

Mp: decomposes at 172°C

TGA: Volatilisation temperatures: 131°C → 230°C

Percentage residue after volatilisation: ≅ 12 %

(reported 140°C → 230°C [132])

IR (cm^{-1}): 3446 (OH str), 1528 (C=C, C=O conjugated str.), 1286 (C-O), 1017 (C=O str.), 966 (V=O str.), 684 (C-C).

MS (EI): m/z: 265 ($^{51}M^{+}$, 100%, 100), 250 (27%), 183 (50%), 166 (86%), 150 (9%), 126 (7%), 125 (3%), 124 (3%), 123 (7%), 67 (12%), 43 (30%).

The melting point determination shows that $VO(acac)_2$ decomposes at 172°C, but the TGA thermogram shows that volatilisation starts at 131°C with a smooth single weight loss curve. Reported sublimation temperatures of 140 - 230°C [132] were again recorded using a TG-DSC thermogram at a heating rate of 5°C min^{-1} but no residue was reported. The different technique and different experimental conditions used can explain the difference obtained in the starting volatilisation temperatures with the current work.

The IR confirms the main characteristics of the chelate structure.

MS (EI) spectra shows the presence of the main isotope of vanadium ^{51}V (appendix 7) complex with an intensity of 100%. The second isotope ^{50}V does not appear in the spectrum as its expected intensity is too low (0.25%).

2.4.1.9 Conclusions

All the 2,4-pentanedionato compounds were identified and confirmed as being the required compounds. The most important physical characteristics are the thermal stability and the volatilisation temperatures and these are presented in table 10 with further comments.

Results in table 10 show that nickel, copper and iron 2,4-pentanedionates are thermally stable below 280°C and can be recovered after sublimation. The residue after volatilisation is an indicator of the thermal stability of the chelate, assuming all compounds are initially of equal purity. Thus the most stable chelate is copper 2,4-pentanedionate with a thermal degradation of only 0.2%, followed by iron and nickel complexes with residues of 3.6% and 29.4% respectively. A literature report [127] indicates that the copper and nickel complexes are thermally unstable leaving a large residue after sublimation, which is verified in this work for nickel but not copper.

Compound:	Volatilisation temperature (°C)	Residue	Thermal stability
$Cu(acac)_2$	(163 →270) ± 4	0.2%	stable
$Ni(acac)_2(H_2O)_2$	(146 →280) ± 4	28.6%	dec > 280°C
$Zn(acac)_2(H_2O)$	(122 →200) ± 4 (Zn(acac))	9.7%	dec. to $Zn(acac)^+$ volatile
$Fe(acac)_3$	(92 →275) ± 4	3.6%	stable
$MoO_2(acac)_2$	(130 →256) ± 4 (MoO_2)	55.0%	dec > 130°C
$VO(acac)_2$	(131 →230) ± 4	12.0%	dec > 172°C

Table 10: Summary of thermal properties of synthesised compounds

Another 2,4-pentanedionate which could be recovered after sublimation is the vanadyl(IV) complex when heated below its decomposition temperature of 172°C. Upon heating, the dioxomolybdenum(VI) and zinc 2,4-pentanedionates decompose and therefore cannot be recovered. To conclude, an order of stability can be established from the most stable to the least stable complexes: Cu > Fe > V > Ni > Zn > Mo. A similar order of thermal stability, based on the temperature at which decomposition begins, has been published. [124] This order of Fe > Ni > Cu, shows iron to be the most stable. This was not confirmed in the current study as the decomposition temperature of $Cu(acac)_2$ was above it, but the observation that Fe > Ni is in accordance with the order proposed from our work. However decomposition temperatures are difficult to reproduce as they tend to vary with the heating rate.

The volatility of the metal 2,4-pentanedionates is the second important property, which requires more discussion. The iron(III) chelate is volatile over the largest temperature range from 92 - 275°C, and the zinc chelate is volatilised over the smallest temperature range from 122 - 200°C. Therefore selective extraction of iron(III) might be possible if the temperature of the extraction reactor in the SERVO apparatus were kept at 100°C. The next most volatile compounds are molybdenum and vanadium 2,4-pentanedionates at 130°C, with the least volatile being the nickel compound starting at 146°C and finally copper 2,4-pentanedionate at 163°C. The ease of volatility of these compounds can be explained by several physical characteristics such as the shape and size of the molecule, but also the molar heat of sublimation. In table 11, the shape, coordination number [127] and molar heat of

sublimation (ΔH_{sub}) [124, 126, 129, 130,132] of the studied chelates are summarised and classified in order of volatility. Large discrepancies have been found in the literature for the molar heat of sublimation of some metal acetylacetonate complexes depending on the technique used (e.g. ΔH_{sub} data for $Fe(acac)_3$ range from 19.5 kJ $mole^{-1}$, [124] obtained by the isoteniscopic method, to 104 kJ $mole^{-1}$ [129] obtained by DSC). The molar heats of sublimation in table 11, for copper, iron, oxovanadium, anhydrous nickel and zinc complexes were obtained using DSC under the same experimental conditions and can therefore be compared directly. In the case of the hydrated zinc and nickel chelates, the molar heats of sublimation were obtained from fusion and vaporisation enthalpy calculations, and by the isoteniscopic method respectively.

Volatility order	Compounds	Coordination number:	Spatial arrangement of chelates in solid phase [127]	ΔH_{sub} (kJ $mole^{-1}$)
1	$Fe(acac)_3$	6	Octahedral	103.9 ± 5.5 [132]
2	$Zn(acac)_2H_2O$ $(Zn(acac)_2)_3$	5	Intermediate between square pyramidal and trigonal bipyramid	74 ± 2 [124] 117 ± 3 [124]
3	$MoO_2(acac)_2$	6	Octahedral	-
4	$VO(acac)_2$	5	Pyramidal	140.7 ± 4.0 [132]
5	$Ni(acac)_2(H_2O)_2$ $(Ni(acac)_2)_3$	4	Planar Octahedral	69 [124] 108.2 ± 4.9 [126]
6	$Cu(acac)_2$	4	Planar	107.1 ± 5.7 [126]

Table 11: Physical characteristics of metal 2,4-pentanedionates which could affect their volatility

From table 11 it can be seen that the more volatile chelates have higher coordination numbers and a more symmetrical structure about the metal, i.e. octahedral > pyramidal > planar. In addition the more volatile compounds tend to be coordinately saturated and therefore cannot participate in any intermolecular bonding. The molar heat of sublimation data presented in table 11 does not reflect this; thus, considering only the anhydrous chelates, the observed molecular heats of

sublimation increase in the order: $Fe(acac)_3 < Cu(acac)_2 \sim (Ni(acac)_2)_3 < (Zn(acac)_2)_3 < VO(acac)_2$. Iron was found the most volatile and the molar heat of sublimation confirms this. But copper was found to be the least volatile whereas from the ΔH_{sub} it should be the second most volatile complex. However it should be noted that the ΔH_{sub} data were compiled from a number of studies that may not be strictly comparable.

$MoO_2(acac)_2$ molar heat of sublimation could not be found in the literature, and cannot be placed in this volatility order.

2.4.2 Bis(pentan-2,4-dionato)propan-1,2-diimine (H_2pnaa) and metal complexes

2.4.2.1 Synthesis of bis(pentan-2,4-dionato)propan-1,2-diimine (H_2pnaa)

Starting materials used were 2,4-pentanedione, 99%, bp:140°C and 1,2-diaminopropane, 99%, bp:120°C.

Bis(pentan-2,4-dionato)propan-1,2-diimine is obtained by the slow addition of 1,2-diaminopropane (0.487 moles ~ 42 cm^3), to continuously stirred 2,4-pentanedione (0.974 moles ~ 100 cm^3 at 0°C) according the chemical reaction (equation 18) : [111]

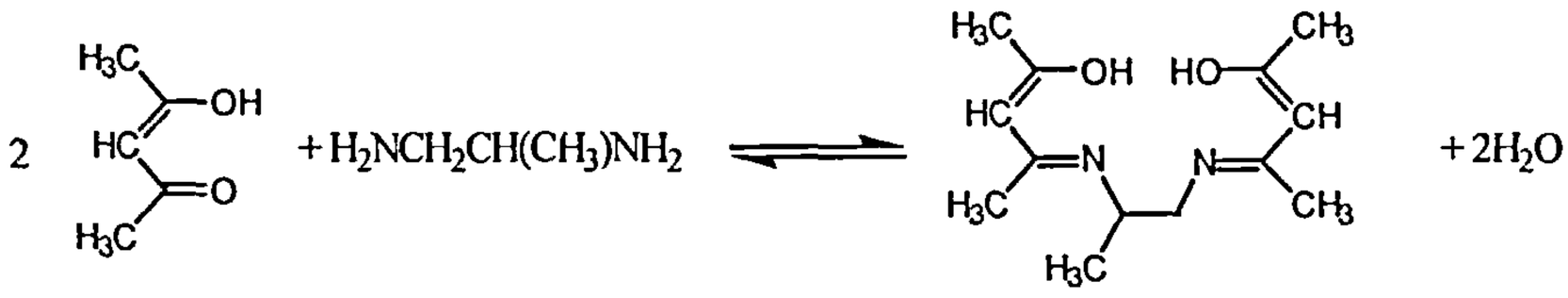

(18)

Because the reaction is exothermic and reversible, it is important to control the temperature and addition of diaminopropane. Once the reaction was complete, the crystals were filtered under suction, washed with ice-cold heptane, air-dried and recrystallised from heptane to give a white crystalline solid (mp: 88°C, yield: 73%).

As with β-diketones, H_2pnaa exists in a tautomeric equilibrium [133] (equation 19) and contains two acidic and two basic functional groups, and coordinates as a dianion through the oxygen and nitrogen atoms as a tetradentate Schiff base ligand.

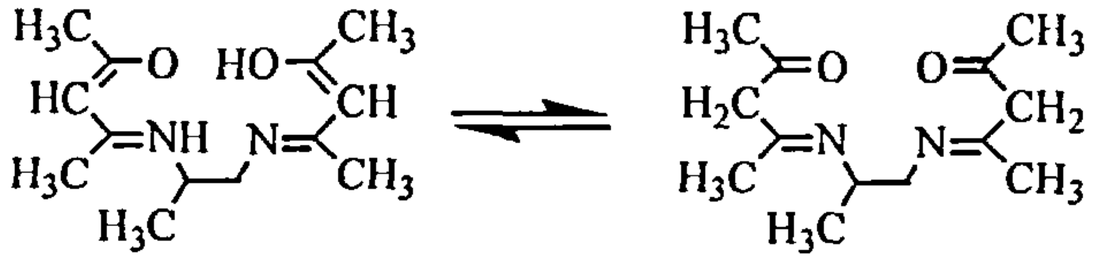

enol form (keto-enol) ⇌ keto form (diketo) (19)

This ligand has the potential to be more selective as, to produce neutral complexes, it requires that the ions have a charge of +2, a coordination number of four and favour square planar or square pyramidal coordination. Therefore, copper(II), nickel(II), cobalt(II), zinc(II), palladium(II), platinum(II), and oxovanadium(IV) can be expected to form volatile derivatives with Schiff bases. [134] These ligands and their metal chelates are less volatile than the corresponding bidentate β-diketones [134] but are more thermally stable, [127].

Properties of H_2pnaa:

Yield: 73 %

Mp: 91°C

TGA: Volatilisation temperature range: 100°C → 250°C

Percentage residue after volatilisation: ≅ 4 %

IR (cm^{-1}): 3500 (H- bonded OH str.), 2998 (H-bonded N-H str.), 2970 (C-H str., alkyl group), 1578-1772 (C=O str.), 1607 (C=N), 1436 (C-C), 1285-1000 (C-O, series of strong peaks), 736 (C-C).

MS (EI): m/z: 239 (M^++1, 12%), 195 (2%), 139 (14%), 126 (100%), 112 (13%), 98 (18%), 43 (39%).

The volatilisation temperature range shows it to be quite volatile (100 - 250°C), and also thermally stable with only 4% residue. IR analysis confirms the structure of H_2pnaa, as a Schiff base with the specific C=O stretching at 1710 cm^{-1}, and a vibration at 3500 cm^{-1} indicating hydrogen bonding between O-H and N-H .

2.4.2.2 Synthesis of metal complexes

These metal complexes were obtained by reaction between the metal 2,4-pentanedionate and bis(pentan-2,4-dionato)propan-1,2-diimine (~ H_2pnaa). [134]

Bis(pentan-2,4-dionato)propan-1,2-diimine (8.4×10^{-3} moles ~ 2g) dissolved in ethanol (10 cm^3) was added to the corresponding calculated molecular ratio (1:1) of metal 2,4-pentanedionate (8.4×10^{-3} moles) dissolved in ammonia (1 mol dm^{-3}, 30 cm^3). The reaction mixture was then heated on a steam bath for 20 minutes. The metal complexes were precipitated by the addition of water, filtered, and recrystallised from acetone.

H_2pnaa-metal complexes	Colour	Mp	Yield
Cu(pnaa)	Deep blue crystals	Sublimes at 250°C	69 %
Ni(pnaa)	Brown crystals	145°C	49 %
Co(pnaa)	Purple crystals	154°C	34 %

Table 12: H_2(pnaa) -metal complexes specifications

Several attempts to prepare the Zn(pnaa) using the above method failed to produce an identifiable product.

2.4.2.3 Cu(pnaa)

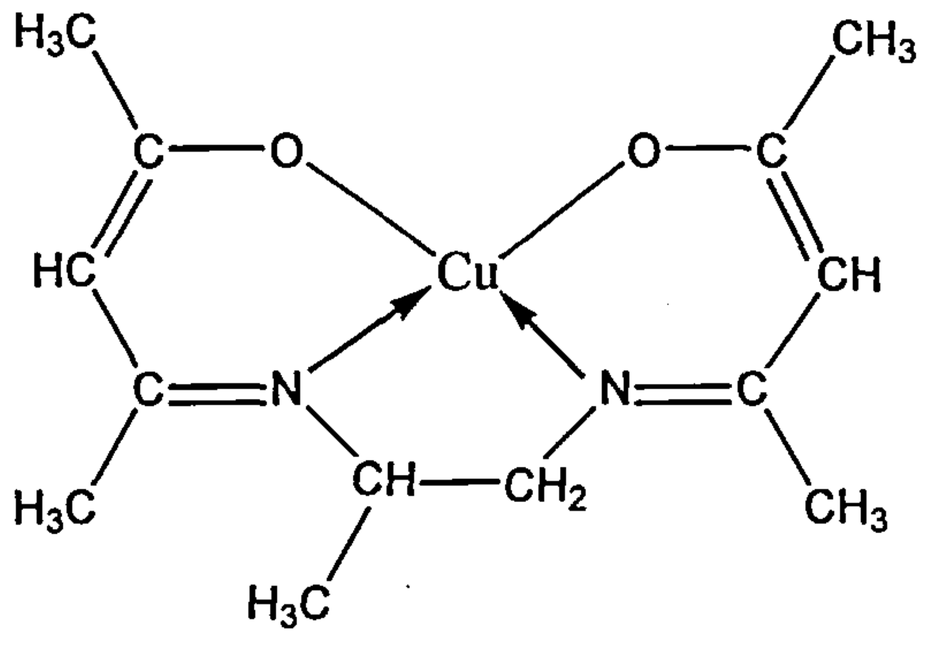

Figure 25: Cu(pnaa)

The complex was prepared as described earlier (§ 2.4.2.2)

Yield: 69%,

Mp: sublimes at 250°C (reported mp = 122°C [134])

TGA: Volatilisation temperatures: 142 °C → 192°C

Percentage residue after volatilisation: ≅ 1.6%

Reported 105°C → 305°C (1%) [135]

IR (cm^{-1}): 3446 (OH str.), 2920 (C-H str.), 1660 (C=N),1533 (C=C str.), 1419

(C-C), 1354 (C-H vib.), 1275 (C-O).

MS (EI): m/z: 303 ($^{65}M^+$, 5.8%), 301($^{63}M^+$, 12.9%), 239 (5%), 112 (8%), 85 (33%), 43 (100%).

Cu(pnaa) sublimes at 250°C but literature data shows a melting point of 122°C, and the TGA thermogram shows a single weight loss from 142 - 192°C, indicating that the chelate obtained is anhydrous and sublimes from 142°C and not at 250°C as seen from the melting point determination. TGA is a more reliable instrument than the melting point apparatus and so the sublimation temperature starting at 142°C is more precise. The residue after volatilisation is only 1%, showing good thermal stability. A sublimation temperature range 105 - 305°C has been recorded [134] using a TGA thermogram with a heating rate of 5°C min^{-1}, and the different experimental conditions used can explain the difference from results obtained in the current study. The residue reported in this earlier study (1%) is the same as currently found and supports the thermal stability of the compound. The IR spectrum confirms the main characteristics of the structure. A small O-H vibration at 3446 cm^{-1} shows the presence of some moisture. This probably comes from the presence of water in the originally prepared compound that was then stored under vacuum before the TGA study to dry. MS (EI) shows the presence of the two isotopes of copper (appendix 7), ^{63}Cu, 12.9% and ^{65}Cu, 5.8%. The calculated equivalent abundance ratio ^{63}Cu : ^{65}Cu of 100 : 45.0 is close to the theoretical value (100 : 44.5).

2.4.2.4 Ni(pnaa)

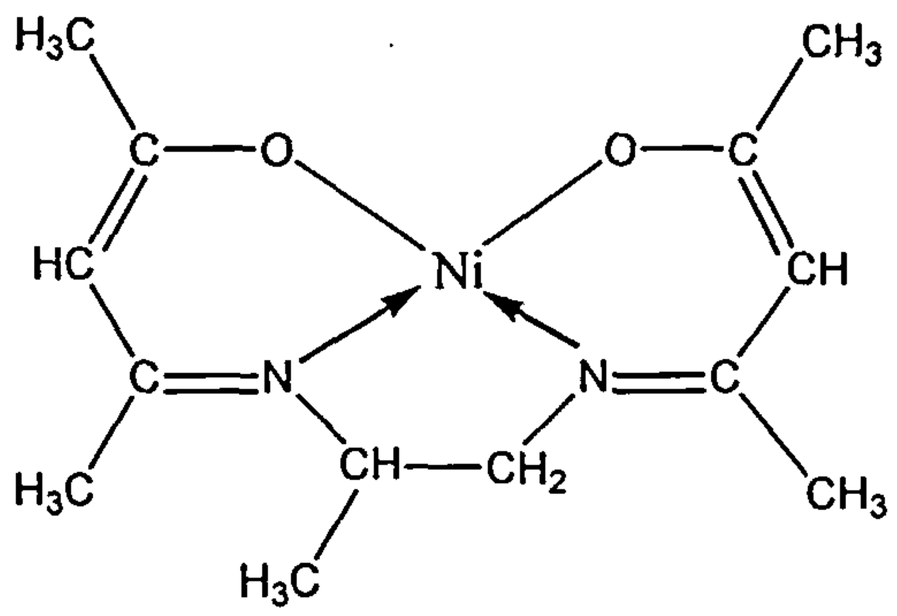

Figure 26: Ni(pnaa)

The complex was prepared as described earlier (§ 2.4.2.2)

Yield: 49 %

Mp: 145°C (reported mp = 157°C [134])

TGA: Volatilisation temperatures: 194°C → 300°C

Percentage residue after volatilisation: ≅ 4 %

Reported values 85°C → 360°C (8%) [135]

IR (cm^{-1}): 3500-3000 (broad OH str.), 2941 (C-H str.), 1600 (C=N), 1520 (C=C str.), 1436 (C-C), 1260–1019 (series of strong peaks C-O).

MS (EI): m/z: 298 ($^{62}M^+$, 9%), 296 ($^{60}M^+$, 42%), 294 ($^{58}M^+$, 100%), 281 (M-CH_3, 32.3 %), 99 (21.7%), 58 (butyl, 10%), 43 (C_3H_9, 12.97%).

Ni(pnaa) melts at 145°C which is close to the literature value of 157°C [134], and the TGA thermogram shows a single weight loss from 194 - 300°C. The residue after volatilisation is 4%, showing good thermal stability. The reported sublimation temperature range 85-360°C [134] was recorded using a heating rate of 5°C min^{-1}, and as noted above these different experimental conditions can explain the variation in the final volatilisation temperature, and the difference in reported final residue of 8% compared to 4% found in our work. The IR spectrum confirms the main characteristics of the structure. A broad O-H vibration between 3500-3000 cm^{-1} shows the presence of OH in the structure, possibly indicating some coordination of water to the nickel. The compound as originally prepared was stored under vacuum before the thermal analysis studies giving time for the compound to loose water thus explaining the absence of any water loss in the TGA.

MS(EI) shows the presence of the main three isotopes of nickel (appendix 7), ^{58}Ni, 100%; ^{60}Ni, 42%, and ^{62}Ni, 9%. The calculated equivalent abundance ratios ^{58}Ni : ^{60}Ni : ^{62}Ni of 100 : 42 : 9, are close to the theoretical values (100 : 38.2 : 5.25). The two other nickel isotopes were not observed being in too low an abundance.

2.4.2.5 Co(pnaa)

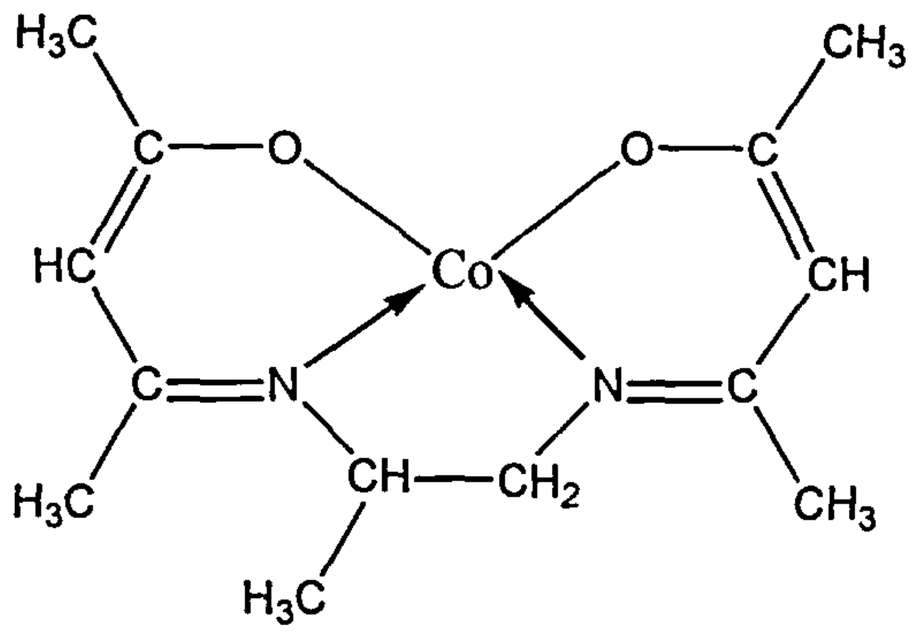

Figure 27: Co(pnaa)

The complex was prepared as described earlier (§ 2.4.2.2)

Yield: 34%

Mp: 154°C

TGA: Volatilisation temperatures: 167°C → 292°C

Percentage residue after volatilisation: ≡ 0.4 %

Reported 80°C → 350°C (6%) [134]

IR (cm^{-1}): 3419 (broad OH str.), 2923 (C-H str.), 1610 (C=N), 1522 (C=C str.), 1463 (C-C), 1401 (C-H), 1260-1019 (C-O).

MS (EI): m/z: 297 ($^{59}M^{+}$, 54.4%, 100), 279 (98%), 238 (20%), 183 (100%), 169 (35.6%), 126 (5%), 99 (24%), 43 (14%).

There are no reported data for the melting point of Co(pnaa), the current work showed that Co(pnaa) melts at 154°C. The thermogram shows a single weight loss from 167 - 292°C, indicating that the chelate is anhydrous. The residue after volatilisation is 0.4%, showing good thermal stability. Reported sublimation temperatures 80-350°C [134] were recorded using a TGA thermogram with a heating rate of 5°C min^{-1}, and as before different experimental conditions can explain differences in the data. The IR confirms the main characteristics of the structure of the chelate. The broad O-H vibration between 3419 cm^{-1} indicates the presence of some water in the compound but this was probably surface moisture as it was not detected in the TGA analysis. MS (EI) shows the presence of the single isotope of

cobalt (appendix 7) for the molecular ion at 297 with a good abundance of 54.4%, together with the characteristic fragmentation pattern of H_2pnaa.

2.4.2.6 Conclusions

All metal compounds of H_2pnaa were identified and confirmed as being the required complexes. For this study, the most important physical characteristics are the thermal stability and the volatilisation temperatures and these are summarised in table 13.

Complex	Melting Point (°C)		Volatilisation range (°C)	Residue after volatilisation	Thermal stability
	Exp.	Lit.			
H_2(pnaa)	91 ± 2	90	(100 → 250) ± 4	(4.0 ± 0.2) %	Moderately stable
Cu(pnaa)	119 ± 2	122	(142 →292) ± 4	(1.0 ± 0.2) %	Stable
Ni(pnaa)	145 ± 2	155	(194 → 300) ± 4	(4.0 ± 0.2) %	Moderately stable
Co(pnaa)	154	-	(167 →292) ± 4	(0.4 ± 0.2) %	Stable

Table 13: Volatilisation study of the synthesised pnaa metal complexes

Results in table 13 show that Co(pnaa) is the most stable followed by Cu(pnaa) and Ni(pnaa). Thus in general the metal complexes offer good thermal stability, with a single weight loss and condensation of the sublimate shows little or no decomposition. Copper may be expected to volatilise before nickel which may allow selective extraction of copper from cobalt and nickel. From the above studies, the order of volatility is H_2pnaa > Cu(pnaa) > Co(pnaa) > Ni(pnaa). The nature of the metal complexed by H_2pnaa can influence the volatility of the metal chelate in many ways. [134] The most important property of the metal atom is its Lewis acidity that will affect the tendency to interact with Lewis-base sites within the complex involving nitrogen or oxygen donors. This type of interaction is supported by the existence of stacking chains of metal in the crystal structures of ß-ketoimide complexes (figure 28). The lower volatility observed for the nickel and cobalt complexes relatively to copper is consistent with the greater capacity of coordinated nickel(II) and cobalt(II) atoms to act as Lewis acids.

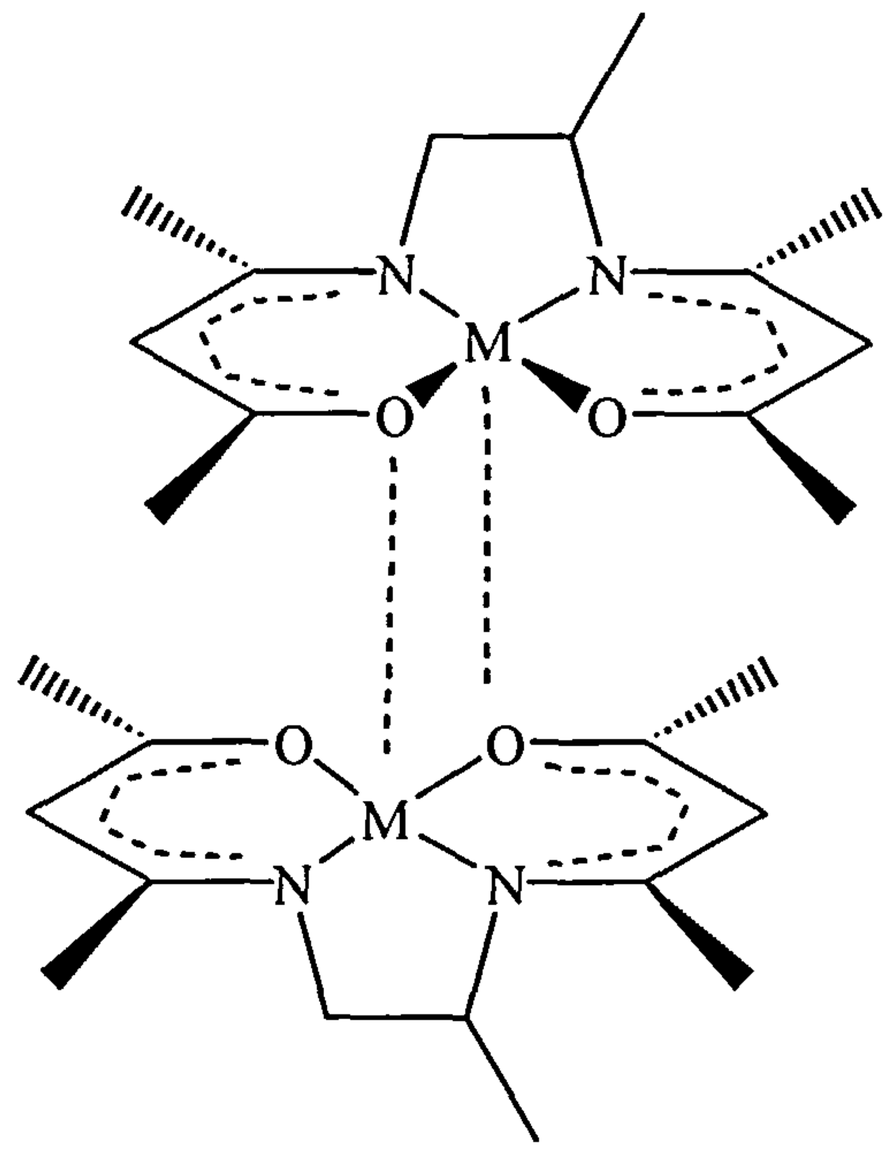

Figure 28: Lewis acid activity of the central metal ion in M(pnaa) [128]

2.4.3 Tetra-alkyldithioimidophosphine and metal complexes

Tetra-alkyldithioimidophosphinates of zinc, cadmium, nickel, copper, cobalt, molybdenum, and vanadium [136, 137, 138] have been studied in recent years. The structure and bonding in the dithioimidophosphinates ligands make them unique among sulfur donors in several respects:

(1) tautomeric equilibrium between the imido $(Ph_2PS)_2NH$ and thiol structures $(Ph_2PS)(Ph_2PSH)N$ [133] (equation 20). The imido structure contains one acidic and one basic functional group, and coordinates as a mono-anion through the sulphur atoms;

(2) stereochemical trends in complexing with divalent metals to form neutral complexes by deprotonation of the ligand at the amine N-H (imido structure as shown in equation 21) [133];

(3) tetrahedral geometry about the central metal atoms;

(4) nonrigidity of the six membered MS_2P_2N ring geometry with either pseudo-chair or pseudo-boat conformation depending on the metal involved within the chelate ring [133] reveal square planar structures.

The ability of these ligands to form neutral complexes with divalent metals led to their selection as potential ligands for the SERVO process.

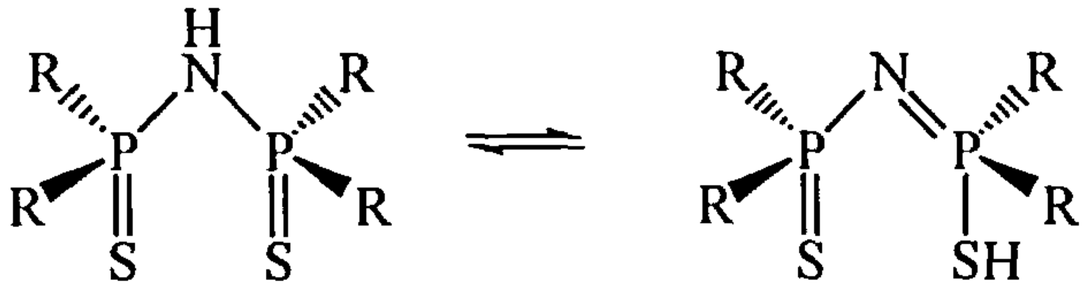

imido structure thiol structure R=Ph or ^{i}Pr (20)

2.4.3.1 Synthesis and properties of tetra-phenyldithiophosphoramide H(phps)

Tetra-phenyldithiophosphoramide was obtained after sulphurisation of the reaction product between hexamethyldisilazane and chlorodiphenylphosphine. [133, 136, 138] (equation 21).

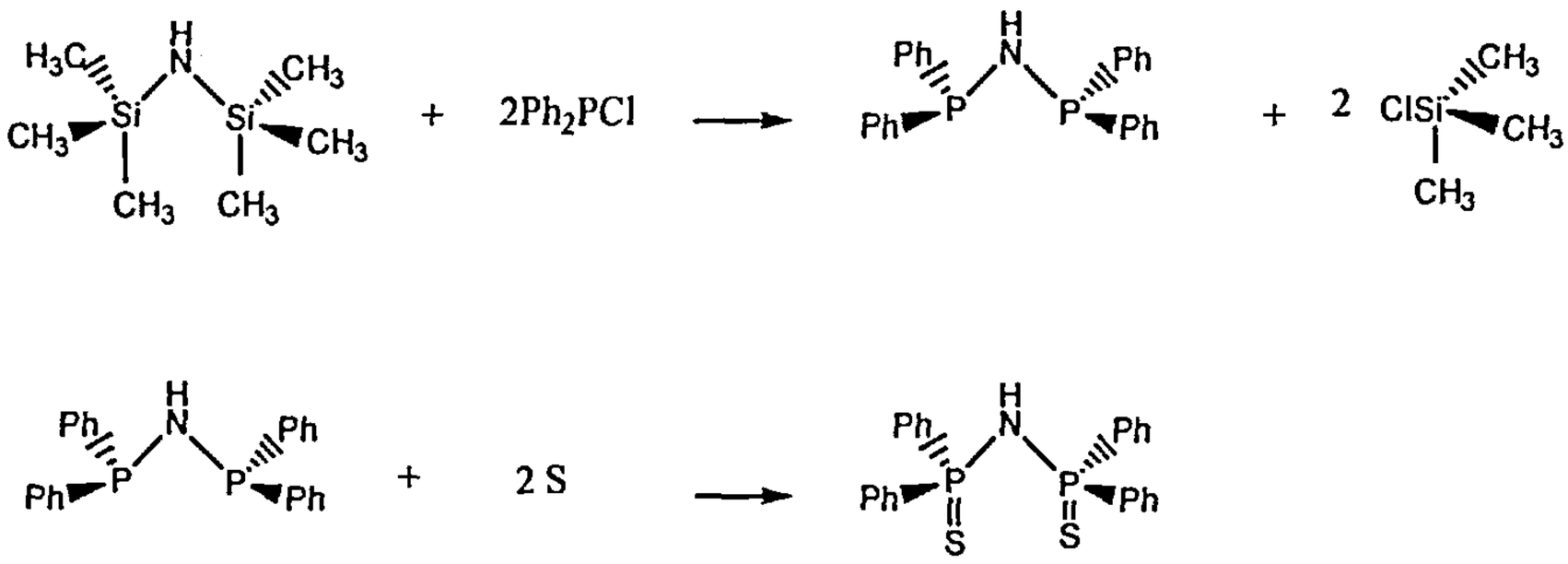

(21)

A solution of hexamethyldisilazane (0.071 moles ~ 15cm^3) in toluene 100 cm^3 was placed in a two-neck round bottom flask provided with a dropping funnel and a condenser adapted for distillation. The distillate was collected in a round bottom flask and the system closed with a calcium chloride drying tube. The flask was heated with a heating mantle and the mixture stirred with a Teflon-coated magnetic stirrer.

A solution of chlorodiphenylphosphine (0.141moles ~ 25 cm^3) in toluene (100 cm^3), placed in the dropping funnel, was added drop-wise to the solution of hexamethyldisilazane while heating between 80-90°C for 3 hours to completely remove the chloromethylsilane product. Then the mixture was heated further and toluene (100 cm^3) removed. The mixture was cooled to room temperature, the dropping funnel replaced with a stopper, elemental sulphur (4.5 g) added to the flask,

and the mixture heated again to 80-90°C overnight. Upon cooling, the precipitate was filtered onto a glass frit, washed with toluene, carbon disulfide, petroleum ether, dried in air and recrystallised from toluene to give a white crystalline solid.

Properties of H(phps):

Yield: 50.1 %

Mp: 208°C (reported mp = 213°C [132])

TGA: Volatilisation temperatures: 274°C → 500°C

Percentage residue after volatilisation: ≅ 30.8 %

IR (cm^{-1}): 3049 (N-H str. vibration), 2631 (N-H), 1690 (C=C str. phenyl), 1438 (C-C str. phenyl), 1437 (N-H str.), 925 (P-N-P medium), 778 (P_2N weak), 691(P=S), 648 (P=S)

MS (EI): m/z: 481 (M+, 36%), 395 (36%), 310 (100 %), 286 (54%).

The volatilisation temperatures for H(phps) are quite high and show the low volatility of the compound (274°C → 500°C). Moreover a residue of 30.8% is left at 500°C indicating thermal instability. IR analysis confirms the structure of Hphps, with specific vibrations of N-H and P-N-P at 1320 cm^{-1} and 932 cm^{-1} respectively. MS analysis shows the presence of the molecular ion of the ligand: 481 g mol^{-1}.

2.4.3.2 Synthesis and properties of tetra-iso-propyldithiophosphoramide (Hprps)

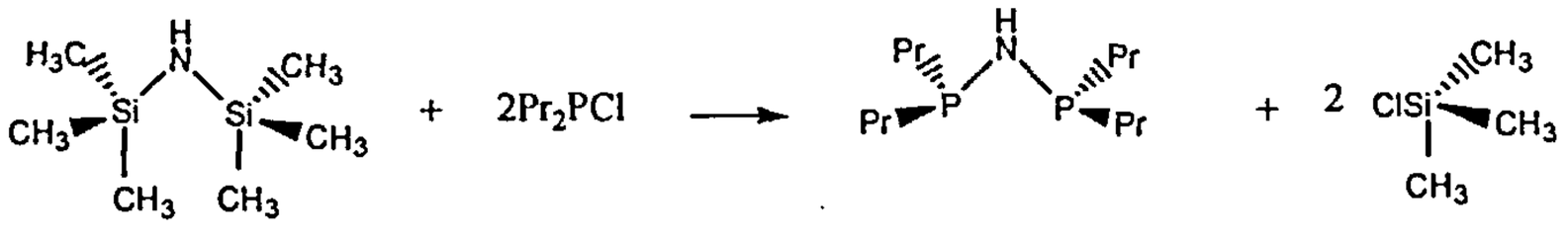

(22)

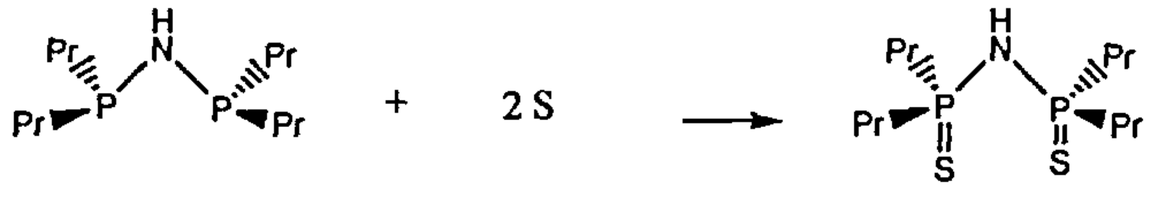

Tetra-isopropyldithiophosphoramide was prepared using the same procedure as for tetra-phenyldithiophosphoramide substituting chlorodiisopropylphosphine for chlorodiphenylphosphine (equation 22). The crude product was recrystallised from toluene to give a white crystalline solid.

Properties of Hprps:

Yield: 57 %

Mp: 173°C (reported mp = 165°C [135])

TGA: Volatilisation temperatures: 180°C → 300°C

Percentage residue after volatilisation: ≅ 0.84 %

IR (cm^{-1}): 3238 (N-H str. vibration), 2600 (NH), 1454 (C-C str.), 1386 (N-H str), 935 (P_2N vibration), 905 (C-H), 880 (C-H), 774 (P_2N vibration), 698 (P=S), 646 (P=S).

MS (EI): m/z: 313 (M+, 49%), 270 (24%), 228 (100 %), 149 (65%), 107 (22%), 43 (55%).

The volatilisation temperature for Hprps is quite low and shows reasonable thermal stability with only a small residue (0.84%) at 300°C. IR analysis confirms the structure of Hprps, with specific vibrations of N-H and P-N-P at 1326 cm^{-1} and 935 cm^{-1} respectively. MS analysis shows the presence of the molecular ion at 313.

2.4.3.3 Synthesis of H(prps) metal complexes

Metal complexes were prepared following published procedures. [139-141] Starting materials were metal carbonates and the ligand tetra-iso-propyldithiophosphoramide. The metal complexes were obtained by addition of excess metal carbonate (0.1g) to a solution of the ligand (~0.3 g) in dichloromethane (30 cm^3) to ensure complete reaction of the ligand, and the mixture was refluxed for 3 hours. The precipitate was filtered and recrystallised from dichloromethane/ petroleum ether (40-60°C). Crystals were then dried at room temperature. More details of the complexes prepared are provided in table 14.

Metal carbonate used (0.1g)	Amount of ligand used	M.p of the metal complex	Crystal colour	Yield
$ZnCO_3{\cdot}2Zn(OH)_2\ H_2O$	0.3 g	147°C	White	84 %
$CdCO_3$	0.23 g	163°C	Colourless	83 %
$CoCO_3.0.5H_2O$	0.4 g	168°C	Deep blue	68 %
$NiCO_3{\cdot}3Ni(OH)_2\ 4H_2O$	0.1 g	173°C	Light green	65 %
$PbCO_3$	0.24 g	125°C	Yellow-orange	54 %
$CuCO_3{\cdot}Cu(OH)_2$	0.16 g	152°C	Purple	75 %

Table 14: Specifications of Hprps-metal complexes

2.4.3.4 $Cd(prps)_2$

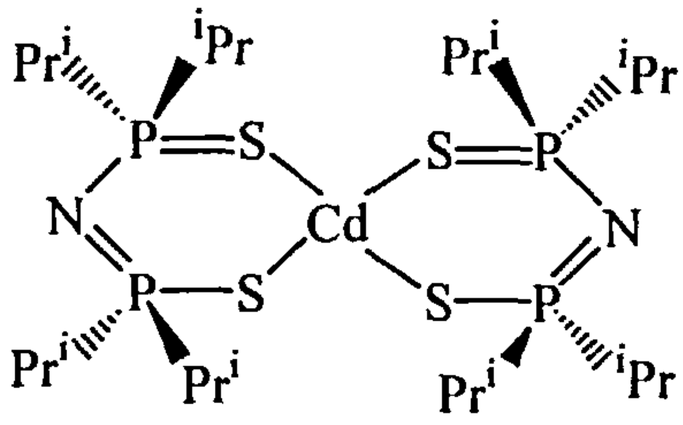

Figure 29: $Cd(prps)_2$

The complex was prepared as described earlier (§ 2.4.3.3)

Yield: 83 %

Mp: 161°C (reported mp = 161°C [136])

TGA: Volatilisation temperatures: 140°C → 300°C

Percentage residue after volatilisation: ≅ 6.3 %

IR (cm^{-1}): 1457 (C-C), 1288 (C-C), 786 (P_2N vibration), 680 (P=S)

MS (EI): m/z: 738 (13%), 697 ($^{116}M^+$, 40.5%, 40.5), 695 ($^{114}M^+$, 100%, 100), 694 ($^{113}M^+$, 59.5%, 59.5), 693 ($^{112}M^+$, 84.8%, 84.8), 692 ($^{111}M^+$, 45.6%, 45.6), 691 ($^{110}M^+$, 34.2%, 34.2), 428 ($^{116}M^+$, 15.2%, 22.6), 426 ($^{114}M^+$, 67%, 100), 425 ($^{113}M^+$, 38%, 56.6), 424 ($^{112}M^+$, 59.5%, 88), 423 ($^{111}M^+$, 30.4%, 45.3), 422 ($^{110}M^+$, 29.1%, 43.4), 313 (23%), 270 (13%), 278 (39%), 113 (4%), 149 (44%), 73 (10%), 41 (40%), 28 (77%).

The melting point (161°C) is the same as reported [135].

The IR confirms the main characteristics of the structure.

MS (EI) confirms the presence of the most abundant isotope of cadmium ^{114}Cd complexed with two molecules of Hprps in the molecular ion at 738. The presence of other cadmium isomers can be found with clusters appearing in the region 697 - 691 and 428 - 422. The first cluster (appendix 7) (^{116}Cd, ^{114}Cd, ^{113}Cd, ^{112}Cd, ^{111}Cd, and ^{110}Cd) indicates the metal complexed to two molecules of prps less one propyl group from 697 - 691. The measured equivalent abundance ratios of 40.5 : 100 : 59.5 : 84.8 : 45.6 : 34.2 are close to the theoretical ratios 26.1 : 100 : 42.5 : 84 : 44.6 : 43.5. The second cluster (^{116}Cd, ^{114}Cd, ^{113}Cd, ^{112}Cd, ^{111}Cd, and ^{110}Cd) indicates cadmium complexed with one molecule of prps in a cluster of ions from

428 to 422. The equivalent abundance ratios measured as 22.6 : 100 : 56.6 : 88 : 45.3 : 43.4, extremely close to the theoretical values.

The TGA thermogram shows a single weight loss from 140 - 300°C, indicating that the chelate obtained is anhydrous and quite volatile. The residue left after complete volatilisation is 6.3%, showing that some thermal degradation has occurred.

2.4.3.5 $Co(prps)_2$

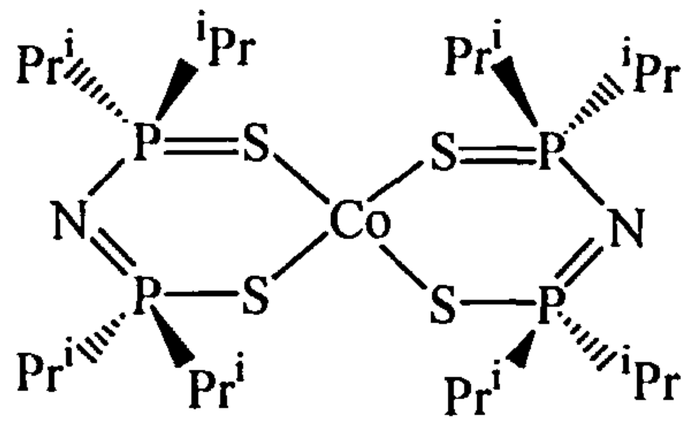

Figure 30: $Co(prps)_2$

The complex was prepared as described earlier (§ 2.4.3.3)

Yield: 15 %

Mp: 168°C (reported mp = 174°C [139])

TGA: Volatilisation temperatures: 158°C → 300°C

Percentage residue after volatilisation: ≅ 4 %

IR (cm^{-1}): 3500 (OH str.), 1464 (C-C), 1301 (C-C), 780 (P_2N), 697 (P=S)

MS (EI): m/z: 683 ($^{59}M^+$, 2.6%), 667 (5.3%), 624 (17.3%), 608 (24%), 313 (28%), 228 (61%), 149 (47%), 43 (100%)

The melting point obtained (168°C) is slightly different from the reported value of 174°C [142], and therefore indicates some impurities.

$Co(prps)_2$ was analysed by TLC to examine the solvent system for purification of the chelate on a silica column. It was found that good separation of the spots was obtained using 1:20 ethylacetate/petroleum ether. Upon purification the compound was unstable and degraded overnight. The IR confirms the main characteristics of the structure of the chelate.

MS (EI) shows the presence of the single isotope of cobalt ^{59}Co (appendix 7) complexed with two molecules of prps as expected but with a quite low intensity of 2.6

The thermogram shows a single weight loss from 158°C to 300°C, indicating that the chelate obtained is anhydrous and quite volatile. The residue, left after complete volatilisation (4 %), shows some thermal degradation of the cobalt chelate, certainly the impurities demonstrated by the melting point.

2.4.3.6 $Pb(prps)_2$

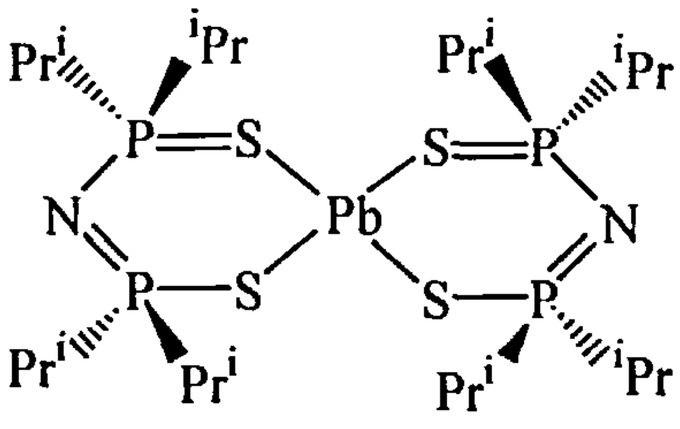

Figure 31: $Pb(prps)_2$

The complex was prepared as described earlier (§ 2.4.3.3)

Yield: 54 %

Mp: 125°C

TGA: Volatilisation temperatures: 175°C → 300°C

Percentage residue after volatilisation: ≅ 1.5 %

IR (cm^{-1}): 3600-3100 (small OH str.), 1619 (C=N), 1464 (C-C), 1355 (C-C), 775 (P_2N), 692 (P=S).

MS (EI): m/z: 832 ($^{208}M^+$, 7%, 100), 831 ($^{207}M^+$, 1.3%, 18), 830 ($^{206}M^+$, 2.4%, 34), 790 (100%), 748 (23%), 313 (32%), 270 (4%), 149 (32 %), 73(20%), 43 (18%), 28 (42%).

There is no recorded data on $Pb(prps)_2$, so no literature comparison can be made.

The IR spectrum confirms the main characteristics of the structure of the chelate, but a small OH stretching from 3600 to 3100 cm^{-1} shows the compound is not fully dried.

MS (EI) shows the presence of a cluster in the molecular ion of the three main isotopes of lead (^{208}Pb, ^{207}Pb, ^{206}Pb) (appendix 7) complexed with two molecules of prps as expected in the range 832 - 830. The measured equivalent abundance ratios 100 : 18 : 34 are close to the theoretical values of 100 : 21.2 : 46.

The thermogram shows a single weight loss from 175 - 300°C, indicating that the chelate obtained is quite volatile. The residue after volatilisation is only 1.5%, showing reasonable thermal stability.

2.4.3.7 $Ni(prps)_2$

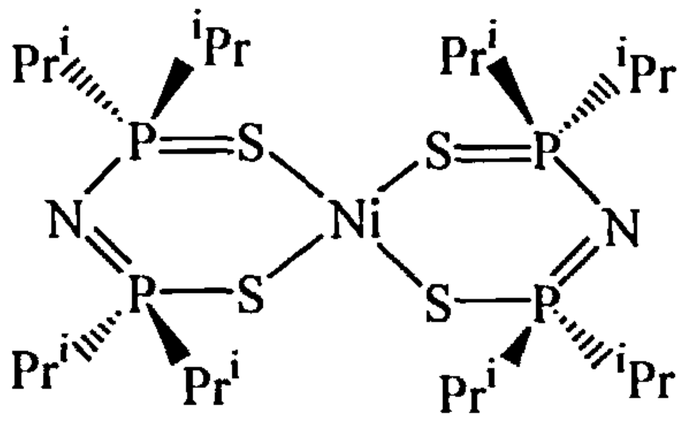

Figure 32: $Ni(prps)_2$

The complex was prepared as described earlier (§ 2.2.3.3)

Yield: 12 %

Mp: 173°C (reported mp = 126°C [136])

TGA: Volatilisation temperatures: 160°C → 300°C

Percentage residue after volatilisation: ≅ 1.45 %

IR (cm^{-1}): 3600-3300 (weak OH str.), 3224 (vibration N-H), 1464 (C-C), 1301 (C-C), 1097 (C-H), 932 (P_2N), 771 (P_2N), 699 (P=S).

MS (EI): m/z: 684 ($^{60}M^+$, 40%), 682 ($^{58}M^+$, 97%), 664 (46%), 648 (82%), 624 (36%), 604 (22%), 313 (46%), 270 (27%), 228 (100%), 149 (64%), 107 (21%), 43 (44%).

The melting point obtained (173°C) is different from the reported value of 126°C [139], so the complex was prepared using two different methods and both products had the same melting point. The identity of the compound was confirmed by the molecular ion.

The IR confirms the main characteristic of the structure of the chelate, but a small OH stretching from 3600 to 3300 cm^{-1} shows the compound was not fully dried.

MS (EI) shows the presence of the two main isotopes of nickel ^{58}Ni and ^{60}Ni (appendix 7) complexed with two molecules of Hprps as expected but at a quite high intensity of 97% and 40% respectively. The measured equivalent abundance ratio of 100 : 41 is close to the theoretical ratio 100 : 38.2 and therefore confirms the presence of $Ni(prps)_2$.

The thermogram shows a single weight loss from 160 - 300°C, indicating that the chelate obtained is anhydrous and quite volatile. The residue after volatilisation is 3.1%, showing some thermal degradation of the nickel chelate.

2.4.3.8 $Zn(prps)_2$

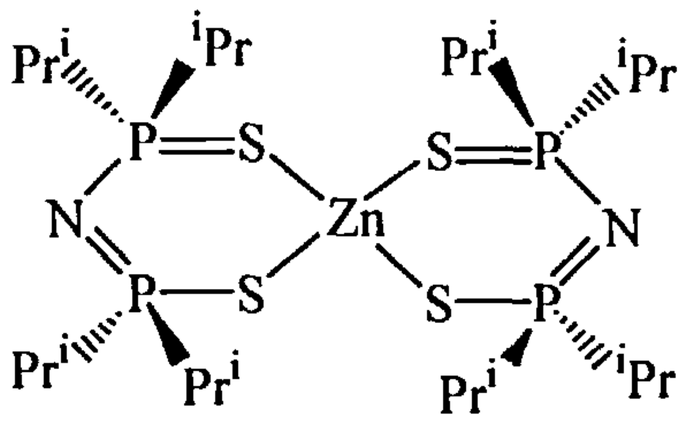

Figure 33: $Zn(prps)_2$

The complex was prepared as described earlier (§ 2.4.3.3)

Yield: 84%

Mp: 147°C (reported mp = 144°C [136])

TGA: Volatilisation temperatures: 150°C → 300°C

Percentage residue after volatilisation: ≅ 0.7 %

IR (cm^{-1}): 3600-3240 (weak OH str.), 3240 (vibration N-H), 1464 (C-C), 1310 (C-C), 775 (P_2N), 695 (P=S).

MS (EI): m/z: 692 (^{68}Zn, 14%, 35), 690 (^{66}Zn, 25%, 62.5%), 688 (^{64}Zn, 40%, 100), 651 (^{70}Zn, 15.2%, 15), 649 (^{68}Zn, 50.6%, 50), 648 (^{67}Zn, 29.1%, 29), 647 (^{66}Zn, 72%, 72), 645 (^{64}Zn, 100%, 100), 382 (^{70}Zn, 4%, 6), 380 (^{68}Zn, 30.4%, 42.8), 379 (^{67}Zn, 12.65%, 17.8), 378 (^{66}Zn, 46.8%, 66), 376 (^{64}Zn, 71%, 100), 313 (13%), 270 (5%), 228 (29%), 149 (28%), 73 (14%), 65 (3%), 41 (45%).

The melting point obtained (147°C) is similar to the reported value of 144°C [136], and the IR spectrum confirms the main characteristics of the chelate, but a small OH stretching from 3600 to 3240 cm^{-1} shows the compound is not fully dried.

MS (EI) shows the presence of the main isotopes of zinc (^{68}Zn, ^{66}Zn, ^{64}Zn) (appendix 7) complexed with two molecules of Hprps but in a relatively high intensity of 14%, 25% and 40% respectively. The equivalent abundance ratios of 35 : 62.5 : 100 are close to the theoretical ratios 38.7 : 57.4 : 100. The other two isotopes of zinc (^{67}Zn and ^{70}Zn) did not appear but this is expected as their expected intensities are low. Another two clusters of zinc appear from 651-645 and 382-376 and correspond to $Zn(prps)_2$-^{i}Pr and $Zn(prps)^{+}$ respectively.

The thermogram show a single weight loss from 150 - 300°C, indicating that the chelate obtained is anhydrous and quite volatile. The residue left after complete volatilisation is 0.7%, showing virtually no thermal degradation.

2.4.3.9 $Cu(prps)_2$

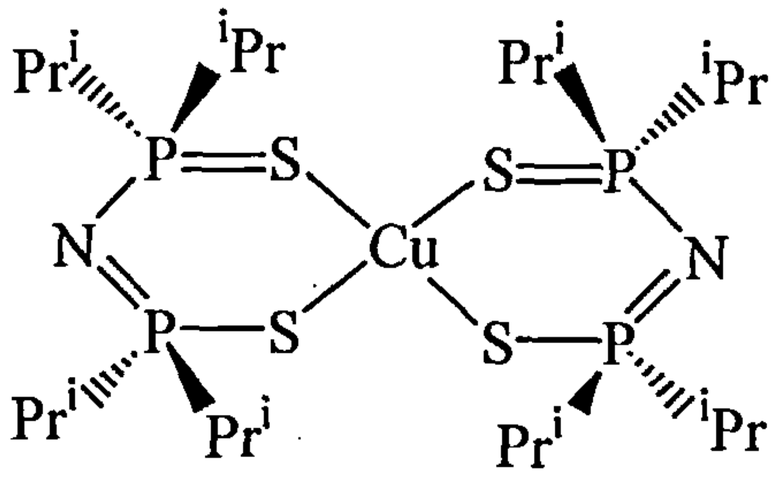

Figure 34: $Cu(prps)_2$

The complex was prepared as described earlier (§ 2.4.3.3)

Yield: 75%

Mp: 152°C

TGA: Volatilisation temp.: 185°C → 300°C (two observed weight losses)

Percentage residue after volatilisation: ≅14.51 %

IR (cm^{-1}): 2597 (NH), 1460 (C-C), 1307 (C-C), 774 (P_2N), 695 (P=S)

MS (EI): m/z: 695 (40%), 689 (^{65}Cu , 8%, 36.6), 687 (^{63}Cu, 22%, 100), 377 (^{63}Cu, 20%, 37), 375 (^{65}Cu, 53.3%, 100), 313 (57.3%), 270 (17%), 228 (100%), 149 (50%), 73 (27%), 43 (30%).

There is no reported data on the $Cu(prps)_2$, and therefore no comparison can be made. The IR spectrum confirms the main structural characteristic of the chelate.

MS (EI) shows the presence of the main isotopes of copper (^{63}Cu and ^{65}Cu) (appendix 7) complexed with two molecules of Hprps in a relatively low intensity of 8% and 22% respectively. The measured equivalent abundance ratio of 36.6 : 100 is close to the theoretical ratio of 44.5 : 100. Another cluster appears from 377 - 375 and corresponds to $Cu(prps)^+$.

The thermogram shows a single weight loss from 134 - 300°C, indicating that the chelate obtained is anhydrous and quite volatile. The residue after volatilisation is 14.9%, showing some thermal degradation of the copper chelate.

2.4.3.10 Conclusions

All Hprps compounds were identified and confirmed as the required compounds by their physical properties. As before the most important properties, the thermal stability and the volatilisation temperatures are summarised in the table 15.

Compounds :	Melting Point (°C)		Volatilisation temperature (°C)	Residue % left after complete volatilisation	Thermal Stability
	Exp.	Lit.			
Hphps	208 ± 2	214	(274 → 500) ± 4	(30.8 ± 0.2) %	Not stable
Hprps	173 ± 2	165	(150 → 300) ± 4	(0.8 ± 0.2) %	Stable
$Zn(prps)_2$	147 ± 2	144	(150→300) ± 4	(0.7 ± 0.2) %	Stable
$Ni(prps)_2$	173 ± 2	126	(160→300) ± 4	(1.4 ± 0.2) %	Stable
$Pb(prps)_2$	125 ± 2	-	(175 →300) ± 4	(1.5 ± 0.2) %	Stable
$Co(prps)_2$	168 ± 2	174	(158→300) ± 4	(4 ±0.2) %	Stable
$Cd(prps)_2$	163 ± 2	161	(140 → 300) ± 4	(6.3 ± 0.2) %	Moderately stable
$Cu(prps)_2$	152	-	(150→300) ± 4	(14.9 ± 0.2) %	Not stable

Table 15: Volatilisation study of the dithiophosphoramide metal complexes

Results in table 15 show that volatilisation of Hprps and its metal chelates occurs over a suitable temperature range for the SERVO process with, except for copper, little or no decomposition. Hphps does not have the volatility required for the SERVO process and was therefore not studied further. These results also show that $Zn(prps)_2$ is the most stable complex followed by $Ni(prps)_2$, $Pb(prps)_2$, $Co(prps)_2$ and $Cd(prps)_2$. $Cu(prps)_2$ is thermally unstable.

$Zn(prps)_2$, $Cd(prps)_2$ and $Cu(prps)_2$ have a similar or lower initial volatilisation temperature than the extractant itself, followed by $Ni(prps)_2$ and $Co(prps)_2$, and finally $Pb(prps)_2$. All the metal complexes are volatile at the temperature of 176°C, and volatilisation is complete at 300°C or below. An order of volatility can be established:

$$Cd(prps)_2 > Hprps \sim Zn(prps)_2 \sim Cu(prps)_2 > Co(prps)_2 > Ni(prps)_2 > Pb(prps)_2.$$

As with H_2pnaa, the Lewis acidity of the metal can influence the volatility of the metal Hprps chelate. Again it can be noticed that the lower volatility for $Ni(prps)_2$ and $Co(prps)_2$ relatively to $Cu(prps)_2$ is consistent with the greater capacity of coordinated nickel(II) and cobalt(II) ions as Lewis acids, leading to the type of interaction shown in figure 28. The volatility order obtained for Hprps metal chelates is similar to that obtained for H_2pnaa metal chelates.

Chapter 3: Application of the SERVO process to contaminated materials and sediment samples

3.1 SERVO process tests on metal carbonates

3.1.1 Extraction

To test the possible extraction of metals using the new SERVO process extraction apparatus, some metal carbonates, i.e. copper carbonate, zinc carbonate, nickel carbonate and cobalt carbonate, were used as starting material and placed in the reactor 2 with either Hacac, H_2pnaa or Hprps in reactor 1 with the thermal conditions noted in table 5 (§2.3.4.2).

Metal carbonates	Hacac	H_2pnaa	Hprps
$CuCO_3$	87.8 % ± 4.8	39.4 % ± 7.9	0.6 % ± 0.2
$ZnCO_3.2Zn(OH)_2H_2O$	17.9 % ± 0.9	15.7 % ± 8.0	42.3 % ± 9.5
$CoCO_3.0.5H_2O$	24.2 % ± 1.5	94.7 % ± 3.0	83.2 % ± 1.9
$2NiCO_3.3Ni(OH)_2.4H_2O$	1.4 % ± 0.4	19.4 % ± 10.0	56.0 % ± 17.8

Table 16: Extraction results obtained from metal carbonates with the different extractants (mean of replicates presented in appendix 8 tables A8-1 to A8-3).

This table shows that the extraction of metal carbonates is possible using the new SERVO process design. $CuCO_3$ did not react with Hprps, but a black residue was found in the reactor 2 after the run and thermal degradation must have occurred. Hacac is the most efficient extractant for $CuCO_3$, followed by H_2pnaa. The optimum extractions for zinc and nickel carbonates were obtained using Hprps, but remain low (42% and 56 % respectively) compared to the expected results. Moreover, the extraction of these metals carbonates using H_2pnaa and Hacac are below 20%. Cobalt carbonate is the most easily extracted metal with up to 95% extraction using H_2pnaa and 83% using Hprps.

3.1.2 Recovery

After extraction, it will be necessary to recover the metal from the volatile metal chelate and recycle the ligand. The most convenient method of metal recovery is deposition of the metal by reduction of the metal chelate with hydrogen in the vapour phase. This technique of chemical vapour deposition has received a lot of interest for a number of applications, e.g. production of high-density copper film on connection plates, [120] nickel metallization of ferrites and as decorative and corrosion resistant coatings. [121] Metal 2,4-pentanedionates of copper(II), nickel(II), and cobalt(III) have already been successfully reduced in the vapour phase by hydrogen, and the metal deposited. [119-121] Chelates of H_2pnaa with copper [143] and nickel [134] have also been successfully reduced in a similar way. But to date no attempts have been reported on the reduction of metal chelates with Hprps.

Reduction of some of the synthesised metal chelates such as $Cu(acac)_2$, $Ni(acac)_2$, Cu(pnaa), Ni(pnaa), $Co(prps)_2$ and $Ni(prps)_2$ has been attempted under the conditions described under §2.3.5. Only the two first chelates have been successfully reduced with metal deposited on the glass wall of reactor 2 under the fritted glass. Table 17 provides a resume of the results observed and the conditions under which they have been obtained, and compared with the literature. [119, 121,134, 143]

Metal chelates	Temperature of reactor T2 and result observed	Temperature of reactor where reduction occurred in literature
$Cu(acac)_2$	270°C, reduction with deposition	Above 220°C [143]
$Ni(acac)_2$	270°C, reduction with deposition	Above 250°C [121]
Cupnaa	280°C, no reduction, no degradation observed	At 340°C (no reduction below) [143]
Nipnaa	280°C, no reduction, no degradation observed	At 325°C (no reduction below, and decomposition above) [134]
$Co(prps)_2$	280°C, no reduction, no degradation observed	-
$Ni(prps)_2$	280°C, no reduction, no degradation observed	-

Table 17: Operational temperatures for hydrogen reduction of metal chelates and results observed

Previous works [134, 143] have shown that Cu(pnaa) and Ni(pnaa) were reduced at T2 = 340 °C and T2 = 325 °C respectively. It was not possible to check the reduction of Cu(pnaa) and Ni(pnaa) at these temperature because the maximum temperature that could be achieved with the reactors was 300°C so it was only possible to check these two complexes were not reduced at 280°C. Also hydrogen reduction of metal chelates occurs above temperatures, which are specific for each metal chelate. Some metal chelates which are thermally unstable like Ni(pnaa), will require reduction over a small temperature range of 2 or 3°C, i.e. above the minimal reduction temperature and below the decomposition temperature. This would cause some difficult operational conditions where optimum precision in the oven temperature has to be defined. No reduction of $Co(prps)_2$ and $Ni(prps)_2$ could be observed at 280°C, although it might be achieved at a higher temperature. To date hydrogen reduction of the Hprps chelates has not been achieved and recovery of the metal and extractant by absorption into organic solvents and subsequent treatment with dilute hydrochloric acid is suggested as a possible alternative.

3.2 Simulated contaminated materials

3.2.1 Kinetic study

This study is based on the schematic representation of clay montmorillonite shown in figures 9b and 10 in chapter 2. These figures show that the original clay and Clay 2 have the same free outer layer, and Clays 1 and 2 have in common an interlayer which is fully exchanged by copper hydroxide. Analysis of the metals contained in the four prepared clays, using ICP AES, is given in table 18:

Clays	Clay 1	Clay2	Clay3	Clay4
% of metal content (dry material)	2.88 ± 0.20 % copper	2.57 ± 0.06 % copper	1.90 ± 0.15 % nickel	1.70 ± 0.03 % nickel

Table 18: Metal content in the different clays (mean of three replicates presented in appendix 8 tables A8-4 to A8-7)

From this analysis the ratios of adsorption of copper and nickel hydroxides in the interlayer and diffuse layer of montmorillonite can be deduced and are presented in table 19.

Thus the total concentration of copper hydroxides adsorbed by montmorillonite is 2.88% (Clay 1 is fully exchanged with copper hydroxides), and as the concentration of copper adsorbed within the montmorillonite interlayer is the copper content of Clay 2, i.e. 2.57% (Clay 2 being exchanged with copper only in the interlayer), the concentration of copper adsorbed by the outer layer of montmorillonite will be 2.88 - 2.57 = 0.31%.

	Clay 1 (copper)	Clay 2 (copper)	Clay 3 (nickel)	Clay 4 (nickel)
Interlayer content	2.57%	2.57%	1.70 %	1.70 %
Diffuse layer content	0.31%	0%	0.20 %	0 %
Total content	2.88%	2.57%	1.90 %	1.70 %
Ratio content of interlayer:diffuse layer	89.2 : 10.8	100 : 0	89.7 : 10.3	100 : 0

Table 19: Content in the interlayer and outer layer of Clays 1 – 4

Thus from these data the ratio of copper adsorbed by the outer layer compared to the total amount of copper adsorbed will be (0.31 / 2.88) × 100 = 10.8%, and the ratio of copper adsorbed by the interlayer compared to the total amount of copper adsorbed would be (2.57 / 2.88) × 100 = 89.2%. Similarly for the nickel system the total concentration of nickel adsorbed by montmorillonite is 1.90% (Clay 3 is fully exchanged with nickel), and the concentration of nickel adsorbed by the interlayer of montmorillonite is the content of Clay 4, 1.702%, so the concentration of nickel adsorbed by the outer layer of montmorillonite is 1.898 - 1.702 = 0.196 %. Thus the ratio of nickel adsorbed by the outer layer compared to the total amount of nickel adsorbed will be (0.196 / 1.90) × 100 = 10.3%, and the ratio of nickel adsorbed by the interlayer compared to the total amount of nickel adsorbed will be (1.70 / 1.90) × 100 = 89.7%. Therefore it can be concluded that similar adsorption ratios of 90:10 of copper and nickel hydroxides in the interlayer and diffuse layer of montmorillonite is obtained.

Figures 35-39 show the TGA thermograms of the five different types of clay, heated up to 600°C similar characteristic features occur in all figures. The first weight loss corresponds to the loss of adsorbed bound water and the second weight loss to the loss of crystalline water. [9] Notice that the original Clay contains less

water than the modified samples 1 to 4. Thus the original clay contains 9.56% of adsorbed bound water and 1.50% of crystalline water, whereas clays 1 to 4 contain about 11% of adsorbed and bound water and 3% of crystalline water. So the preparation of the modified clays does affect the crystalline structure of the montmorillonite clay.

Figure 40 shows the weight change of clay when heated in presence of H_2pnaa placed in a boat just below the pan of the TGA instrument. This TGA figure shows a weight loss of 8.4% (± 0.2), corresponding to loss of adsorbed water, followed by a weight increase of 1.15% (± 0.2), corresponding to the first absorption of H_2pnaa followed by a plateau and a second weight increase of 10.0% (± 0.2), corresponding to a second absorption of H_2pnaa. This is then followed by a gradual weight loss up to 230°C indicating slight loss of H_2pnaa as the temperature increases.

Figures 41 and 42 show the same experiment using Clay 2 and Clay 1 respectively. From figure 40 the initial weight loss of 8.5% (± 0.2), corresponding to the loss of adsorbed water, is followed by a weight increase of 1.16% (± 0.2), corresponding to a first absorption of H_2pnaa, a plateau and then another weight increase of 0.3% (± 0.2), corresponding to a second absorption of H_2pnaa. Figure 41 the first weight loss of 8.6% (± 0.2), corresponding to the loss of adsorbed water is followed by a single weight increase of 0.8% (± 0.2), corresponding to absorption of H_2pnaa.

The original Clay and Clay 2 both have the diffuse layer free of copper and it can seen in figures 40 and 41 that the same weight increased is observed (1.16%) corresponding to the absorption of H_2pnaa on this diffuse layer, suggesting that the first H_2pnaa absorption is onto the diffuse layer. Then H_2pnaa is adsorbed in the interlayer. Again in figure 42 the absorption of H_2pnaa in the interlayer is significant reaching 10%, compared to the first absorption on the diffuse layer of 1.15%. Looking at the ratio of these two values, the total absorption of H_2pnaa in clay equals $1.15 + 10 = 11.15\%$, so $(10 / 11.15) \times 100 = 89.7\%$ of the total H_2pnaa is adsorbed in the interlayer and $(1.15 / 11.15) \times 100 = 10.3\%$ is adsorbed in the diffuse layer. This ratio of H_2pnaa absorption in the interlayer and diffuse layer is similar to that found when adsorbing nickel and copper on the clay i.e. approximately 10% in the outer layer and 90% in the interlayer. This indicates that H_2pnaa occupies the same sites as copper and nickel hydroxides.

In the case of Clay 1, figure 42, both the interlayer and diffuse layer are fully exchanged by copper, and the only weight increase (0.8%) is the absorption of H_2pnaa in the diffuse layer, as the interlayer sites are blocked by copper. Strictly, as Clay 1 is fully exchanged by copper hydroxides, and as H_2pnaa is adsorbing on the same sites as the latter, no absorption of H_2pnaa on Clay 1 should occur. But some absorption could be possible by reaction of the adsorbed copper hydroxides with H_2pnaa to form the copper pnaa complex directly; this is then volatilised and explains the recorded second weight loss.

In the case of Clay 2, figure 41, the interlayer is fully exchanged by copper, leaving the diffuse layer free. The same absorption as that observed for the original Clay (figure 44) shows that H_2pnaa adsorbs on these free sites. The second observed absorption can be explained in a similar way to Clay 1 with the reaction of the copper with H_2pnaa to form the copper pnaa complex.

A rough estimate of the rate of absorption of the extractant on the clay can be made from these data and table 20 shows that the higher the free diffuse layer space, the faster the H_2pnaa is adsorbed.

Type of clay:	Original Clay	Clay 2	Clay1
Time at which the clays start to adsorb the H_2pnaa (min-sec)	11min 54s	22 min 36s	25 min

Table 20: Absorption time of the different clays

Finally the rate of absorption of the extractant on the clay is dependent on temperature. This can be seen in figure 40 where the slope of absorption decreases as the temperature stops rising and becomes constant; i.e. an absorption slope of 1.26% min^{-1} when the temperature rise at 20°C min^{-1} compared with a slope of 0.09% min^{-1} when temperature is constant at 230°C. The weight changes in the thermograms of Clay 3 and Clay 4 (figures 43 and 44) can be similarly interpreted.

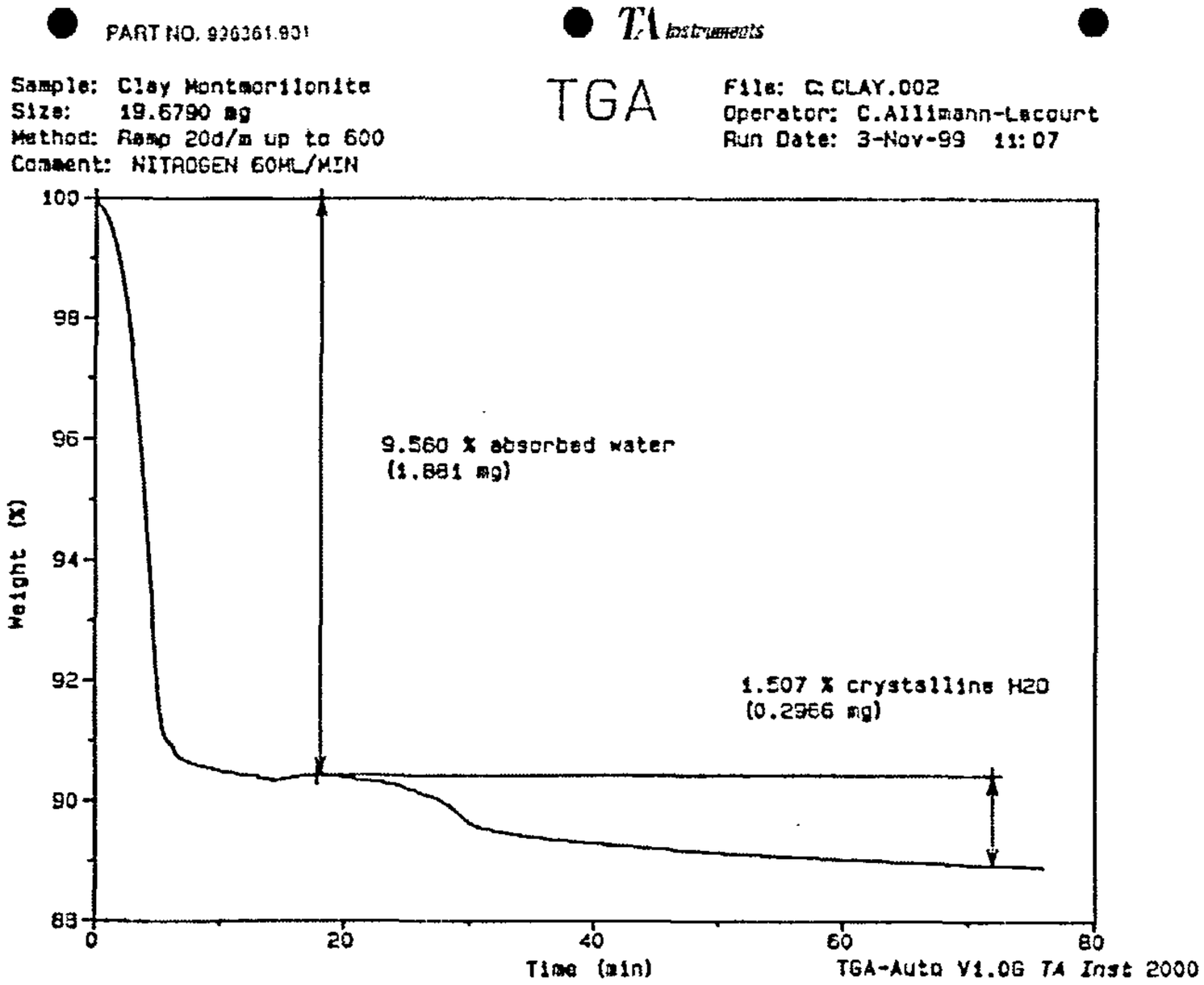

Figure 35: TGA thermogram of Clay

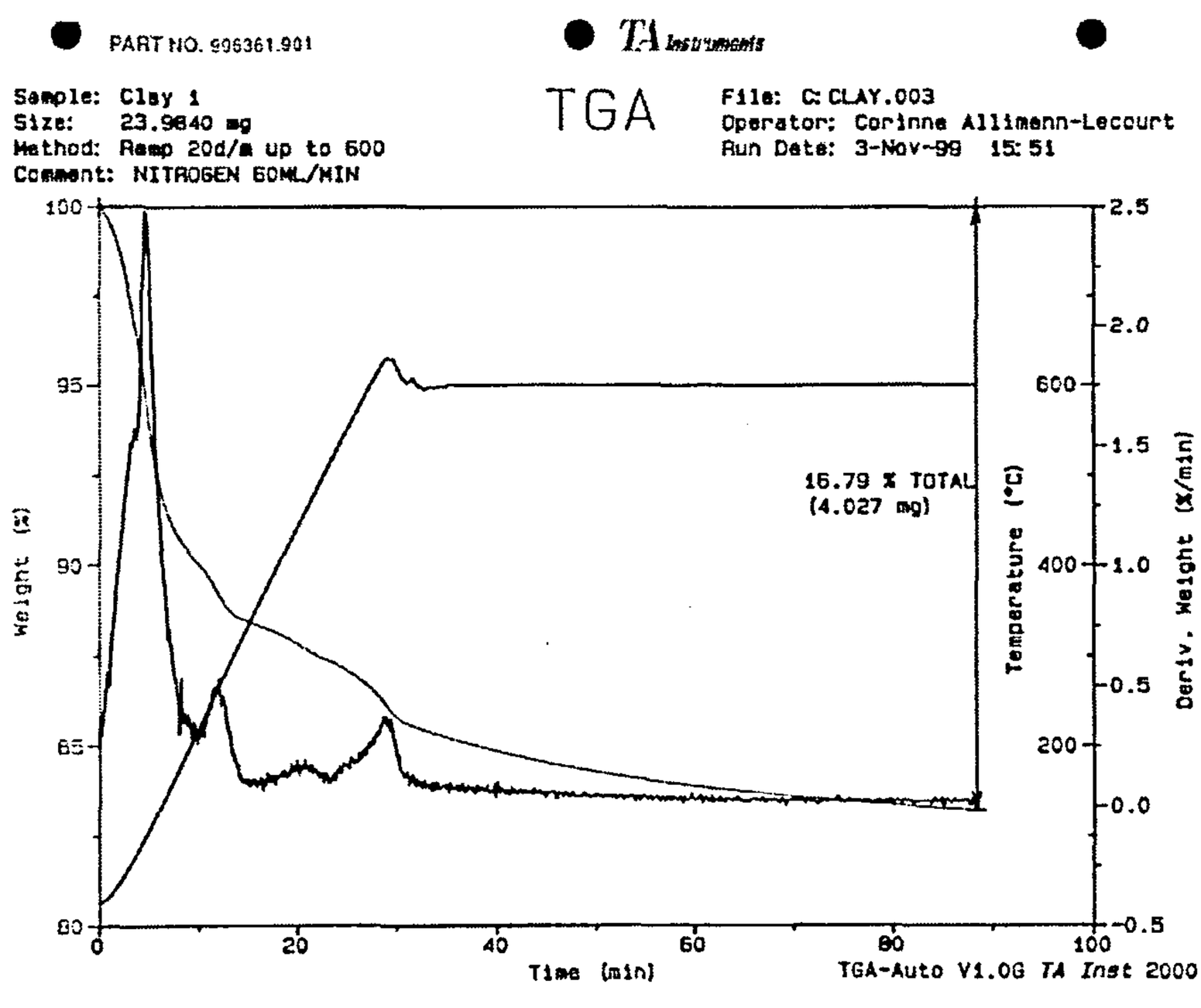

Figure 36: TGA thermogram of Clay 1

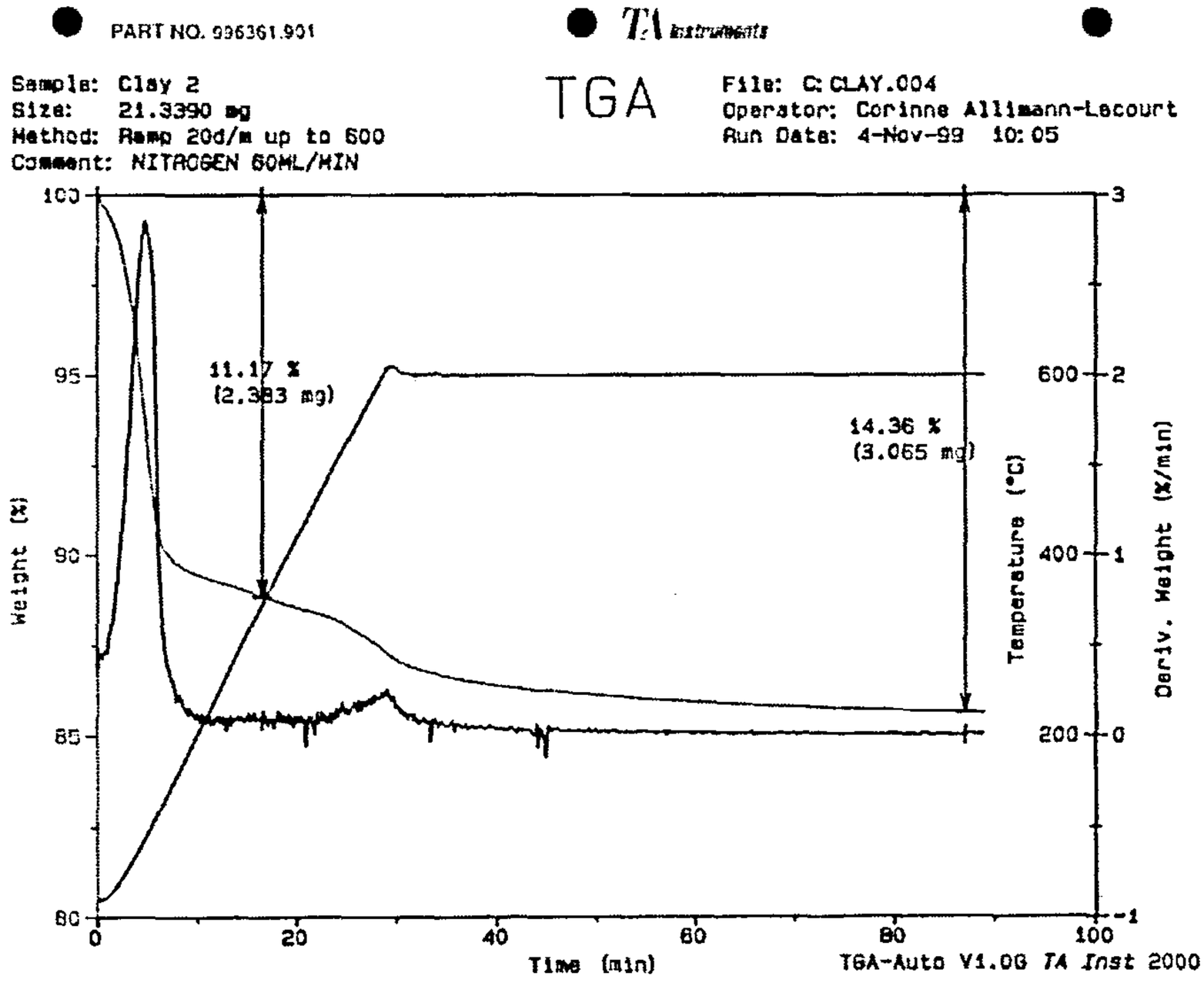

Figure 37: TGA thermogram of Clay 2

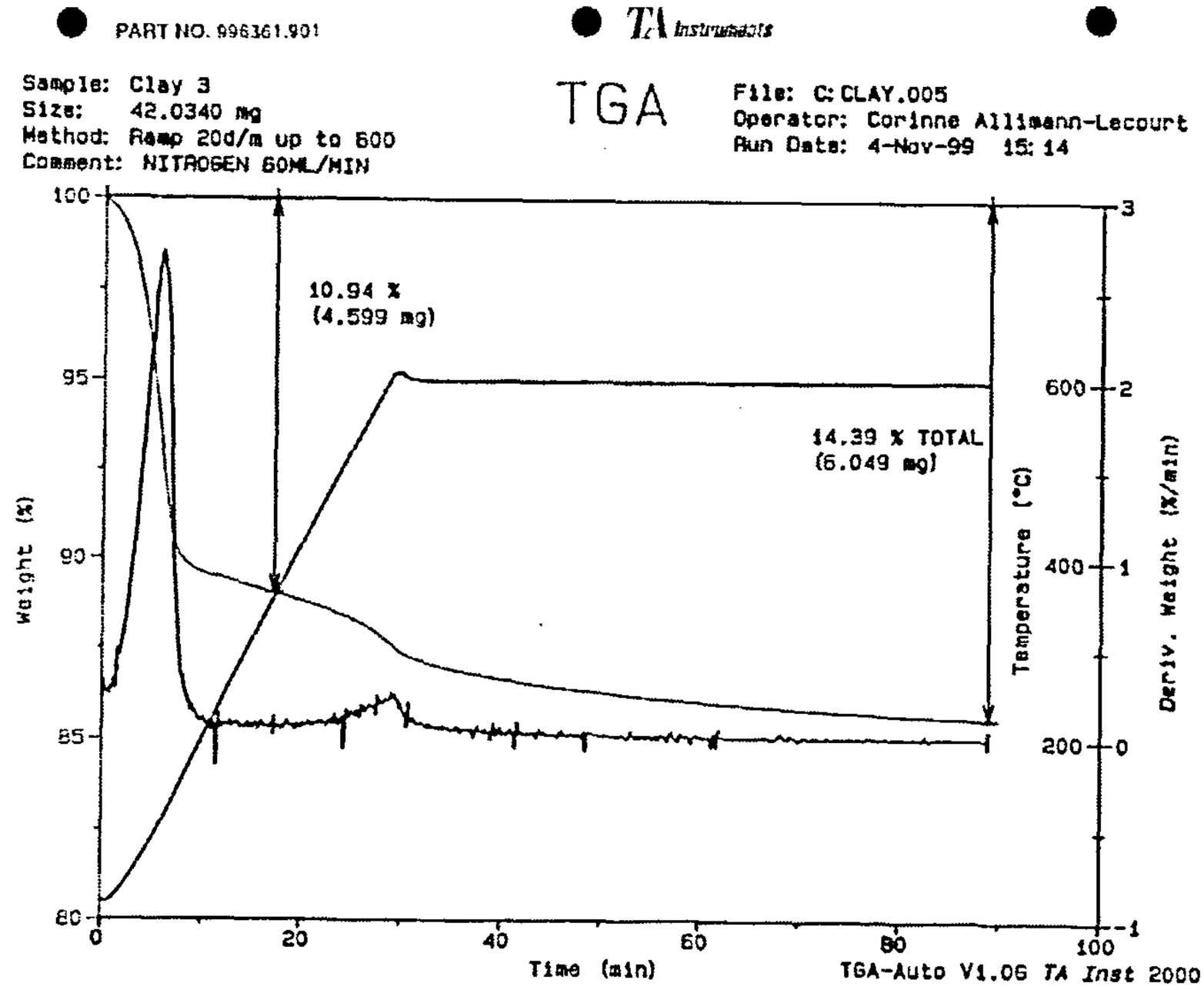

Figure 38: TGA thermogram of Clay 3

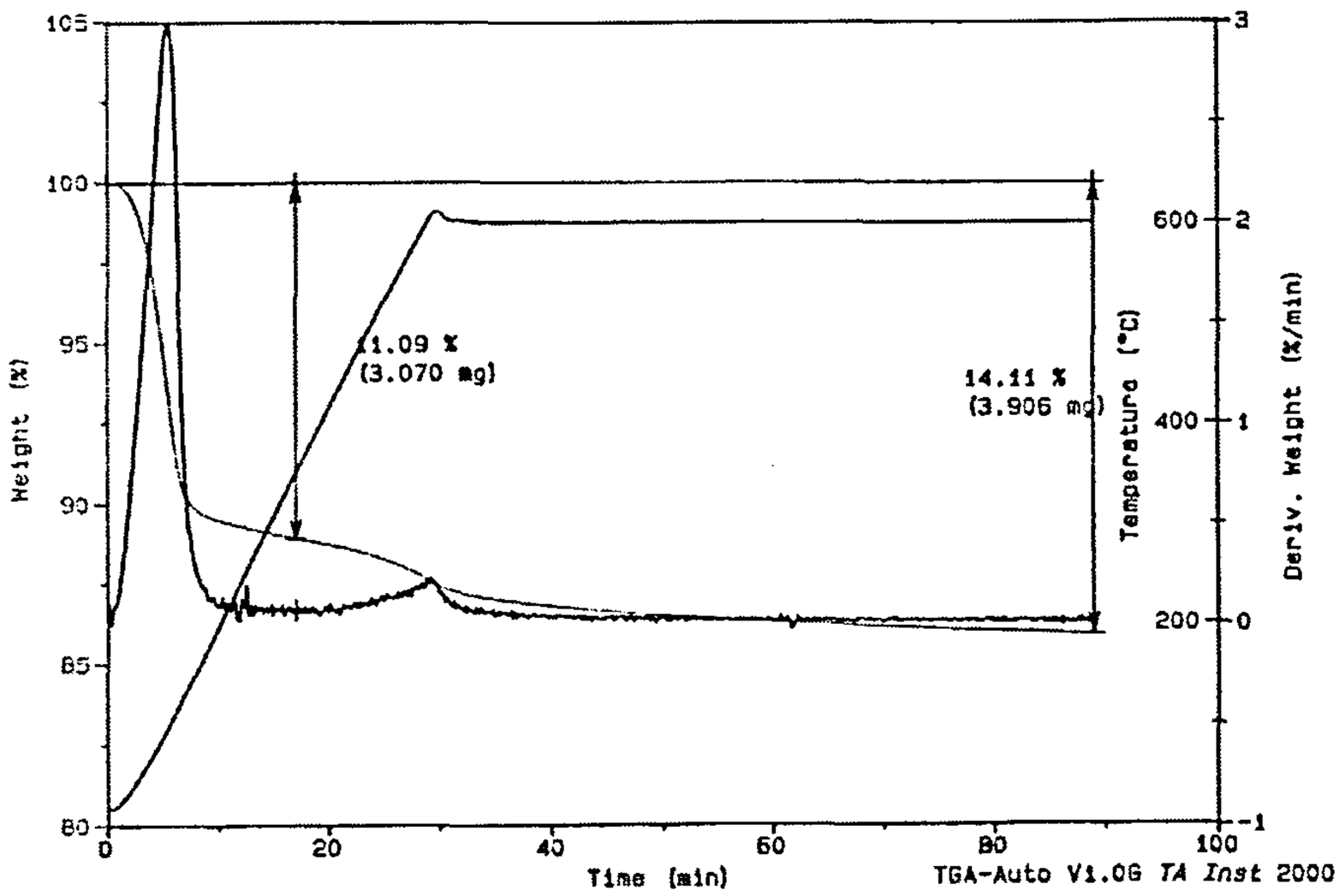

Figure 39: TGA thermogram of Clay 4

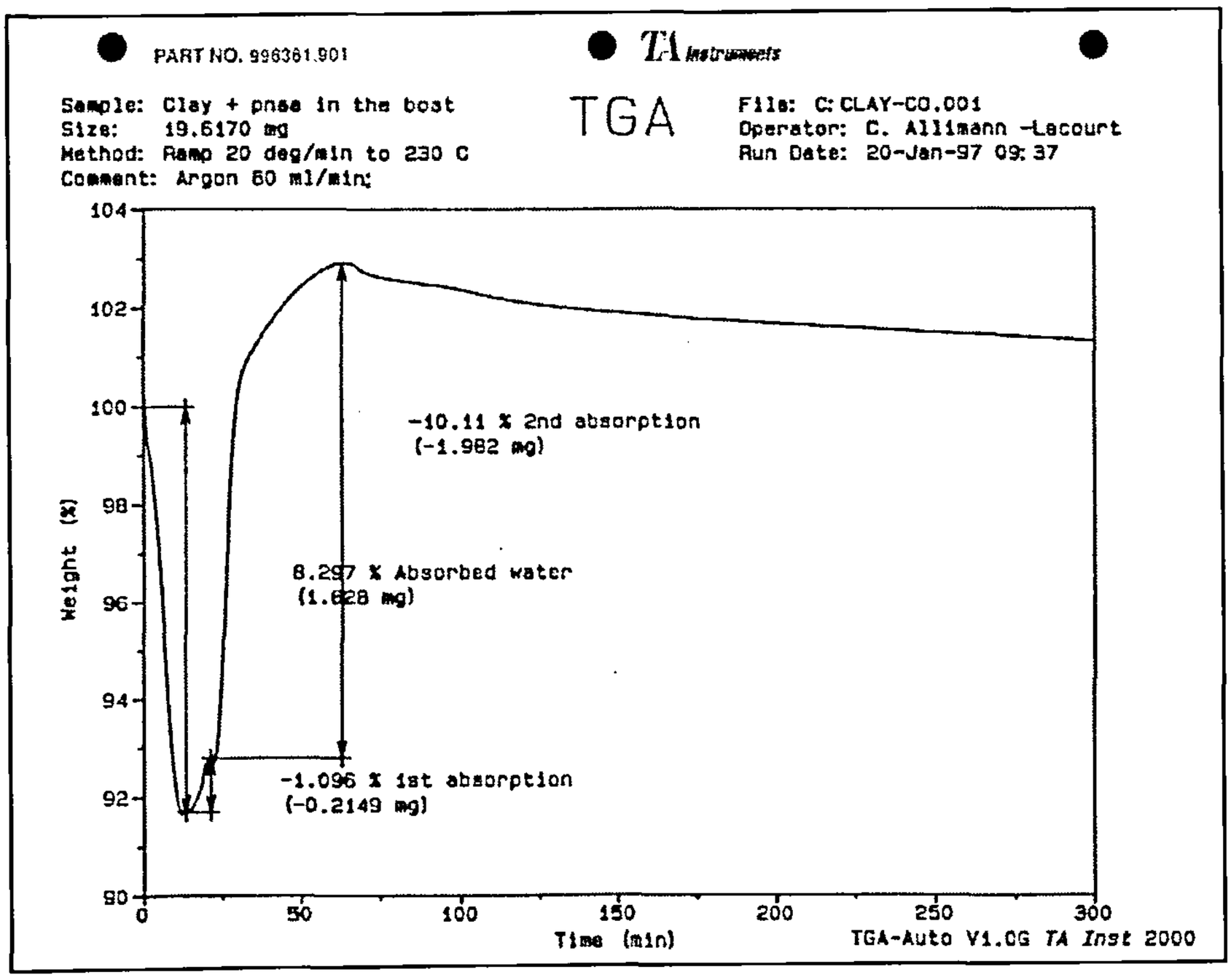

Figure 40: TGA thermogram of Clay + H_2pnaa in the boat.

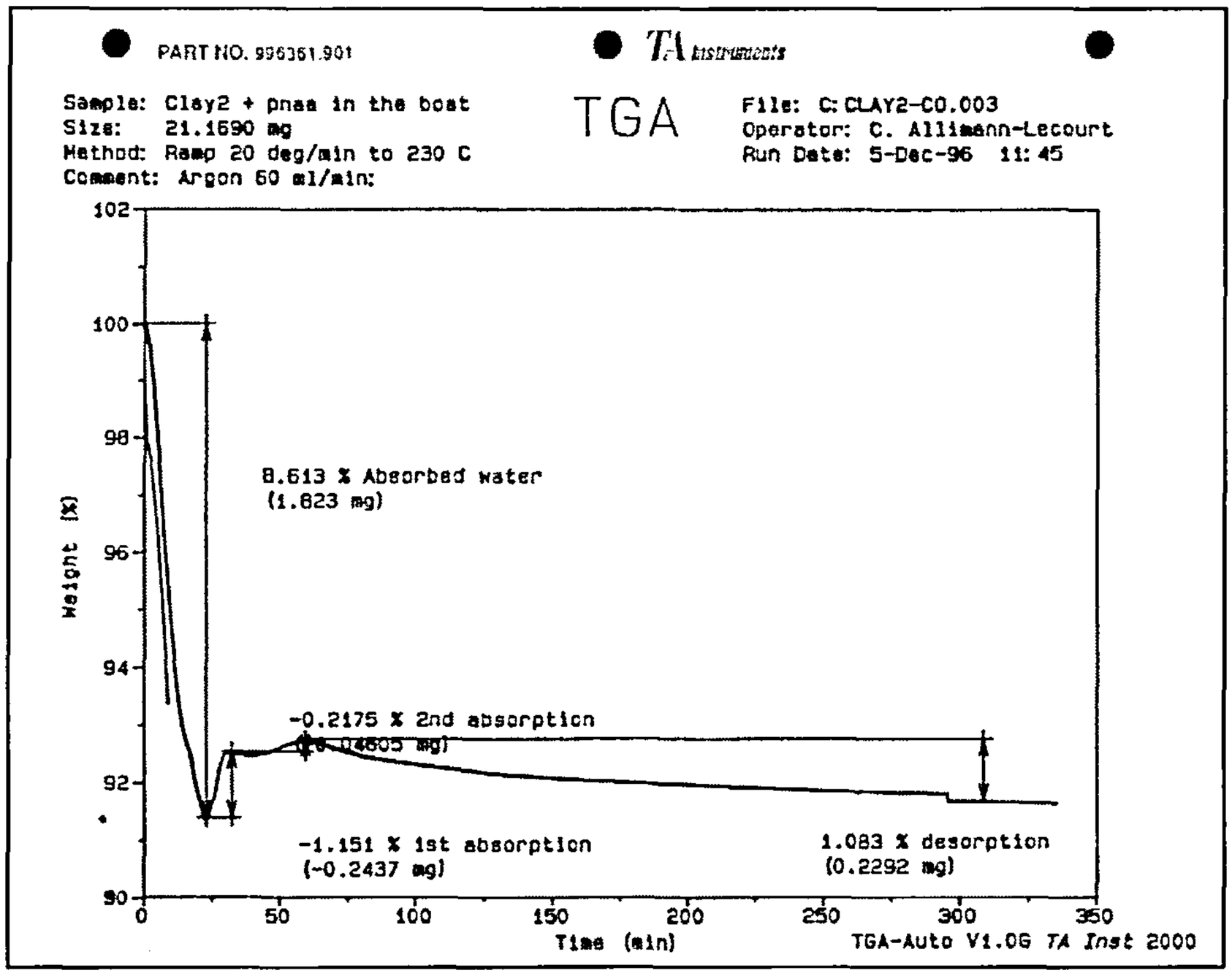

Figure 41: TGA thermogram of Clay 2 + H_2pnaa in the boat.

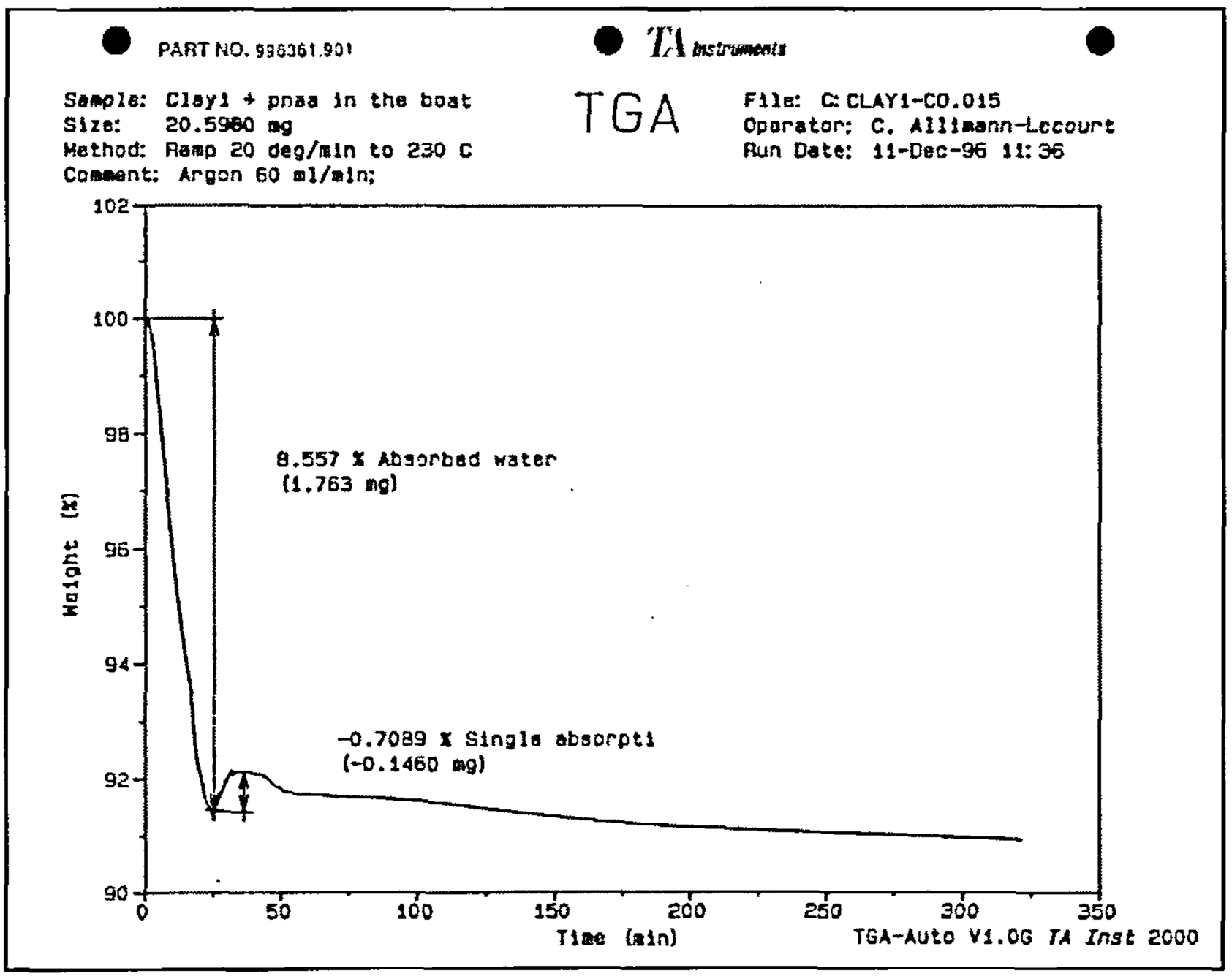

Figure 42: TGA thermogram of Clay 1 + H_2pnaa in the boat.

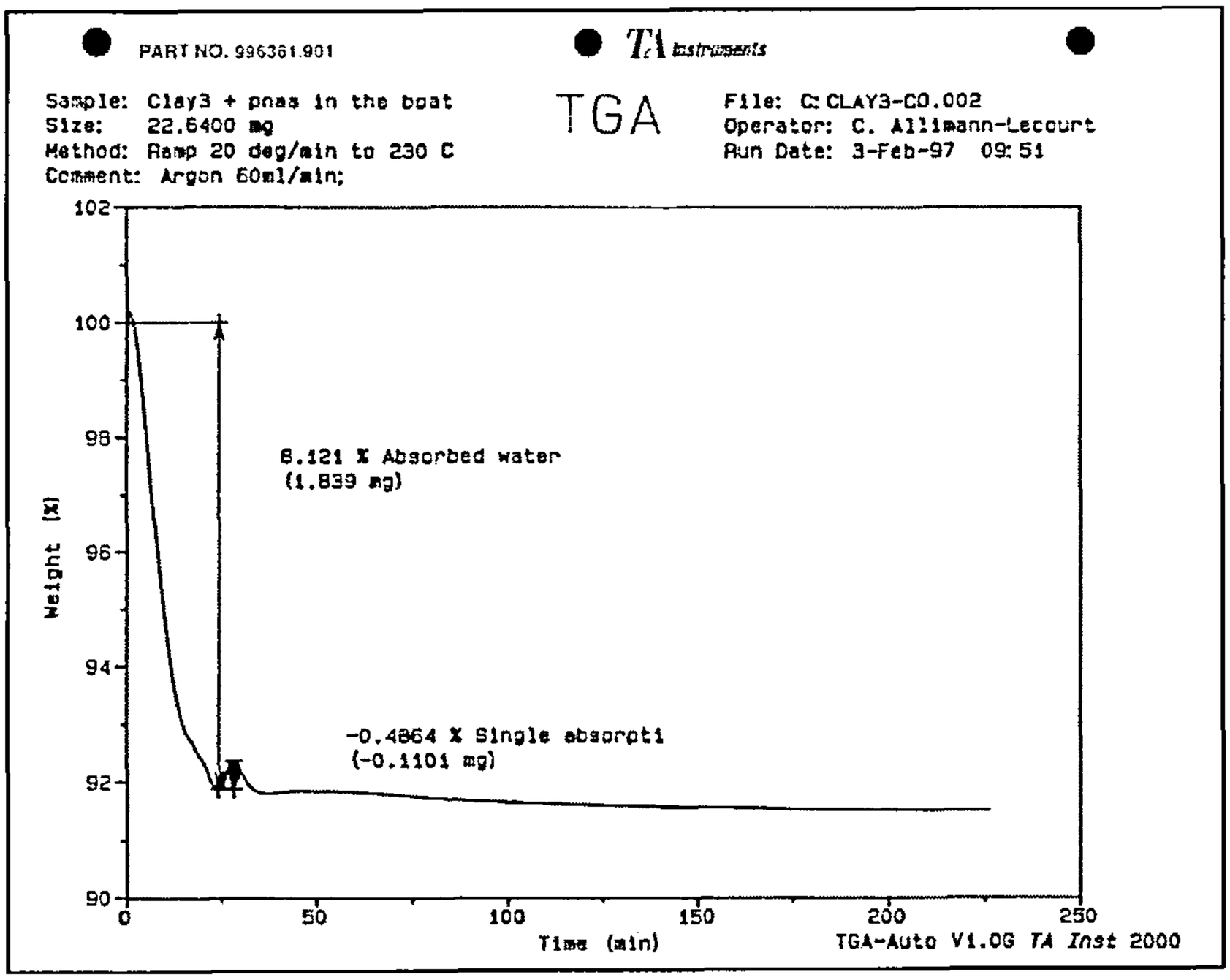

Figure 43: TGA thermogram of Clay 3 + H_2pnaa in the boat.

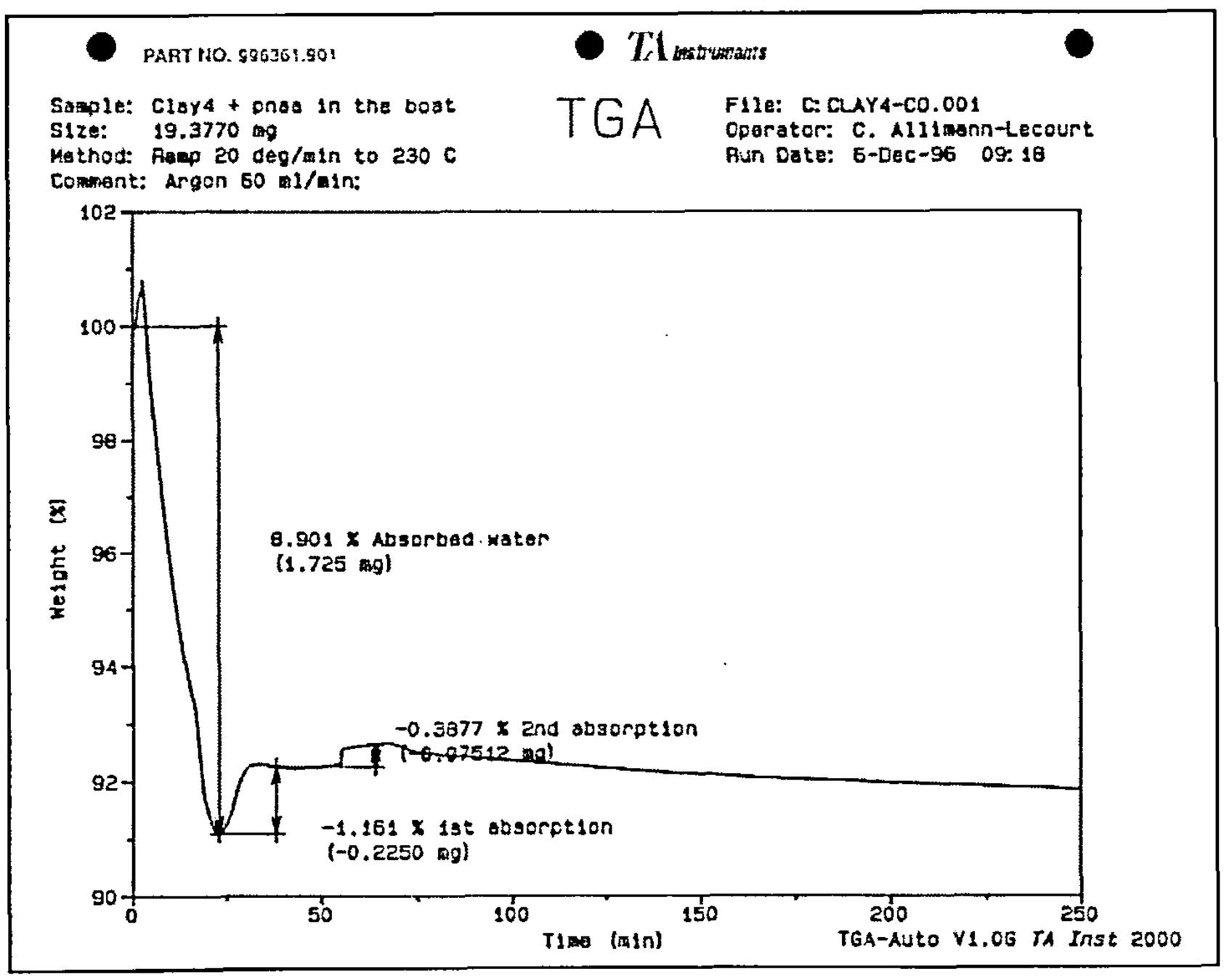

Figure 44: TGA thermogram of Clay 4 + H_2pnaa in the boat.

3.2.2 Extraction study

The first set of experiments used H_2pnaa which had been previously studied by P. Duke. [108]

The analysis of Clay 1 and Clay 2 after completion of the above experiments where the H_2pnaa was placed in a boat under the pan (figures 40- 44) show some extraction of copper and nickel (table 21):

Clay material used	Clay 1	Clay 2	Clay 3	Clay 4
Metal extracted (%) (mean values of 3 experiments)	Copper 36.8% ± 2	Copper 24.6% ± 2	Nickel 35.2% ± 2	Nickel 25.0% ± 3

Table 21: Extraction results obtained from Clays1 – 4 using H_2pnaa after heating at 230°C for 3 hours
(mean of three replicates presented in appendix 8 tables A8-8 to A8-11)

The analysis of the volatile extract showed the presence of no metal. However a black deposit was found in the exhaust tube of the equipment. Analysis of this very small deposit by electron microscopy indicated the presence of carbon and traces of copper and nickel respectively. Thus the metal complex seems to have been thermally degraded at the exit of the reactor.

Although, the H_2pnaa was sorbed in excess of the normal stoichiometric amount these extraction results are low compared to the 60% extraction obtained by Pichugin from a nickel laterite ore. [111] It can also be seen that the extraction of metals from the fully exchanged clays are better than these of the clays exchanged only in the interlayer. This indicates that the extraction of metal, from the outer layer of the clay is easier than the extraction of metal in the interlayer spaces. This is confirmed by figures 40-44 where desorption of the resulting metal complexes is observed as the last weight loss in the thermograms. In the case of Clay 1 and Clay 3, complete desorption of the metal complexes occurs but with Clay 2 and Clay 4 this is not the case. Thus the metal species in the interlayer of the clay are more difficult to volatilise than those present on the outer layers. Later studies (figure 47) showed that a higher temperature and longer contact time will help the complete release of the metal complexes present in the interlayers of the clays.

These preliminary results were used as a basis to improve the extraction of metals and reduce the amount of H_2pnaa used. Therefore, to improve the condensation of the H_2pnaa though the clay, it was decided to mix the clay and extractant in different molar ratios before running the experiments. This would avoid the previously required volatilisation step, which could result in an initial lost of H_2pnaa before contacting the clay. The molar ratios of copper: H_2pnaa used were from 1:1 to 1:4 and results of these experiments are shown in figure 45.

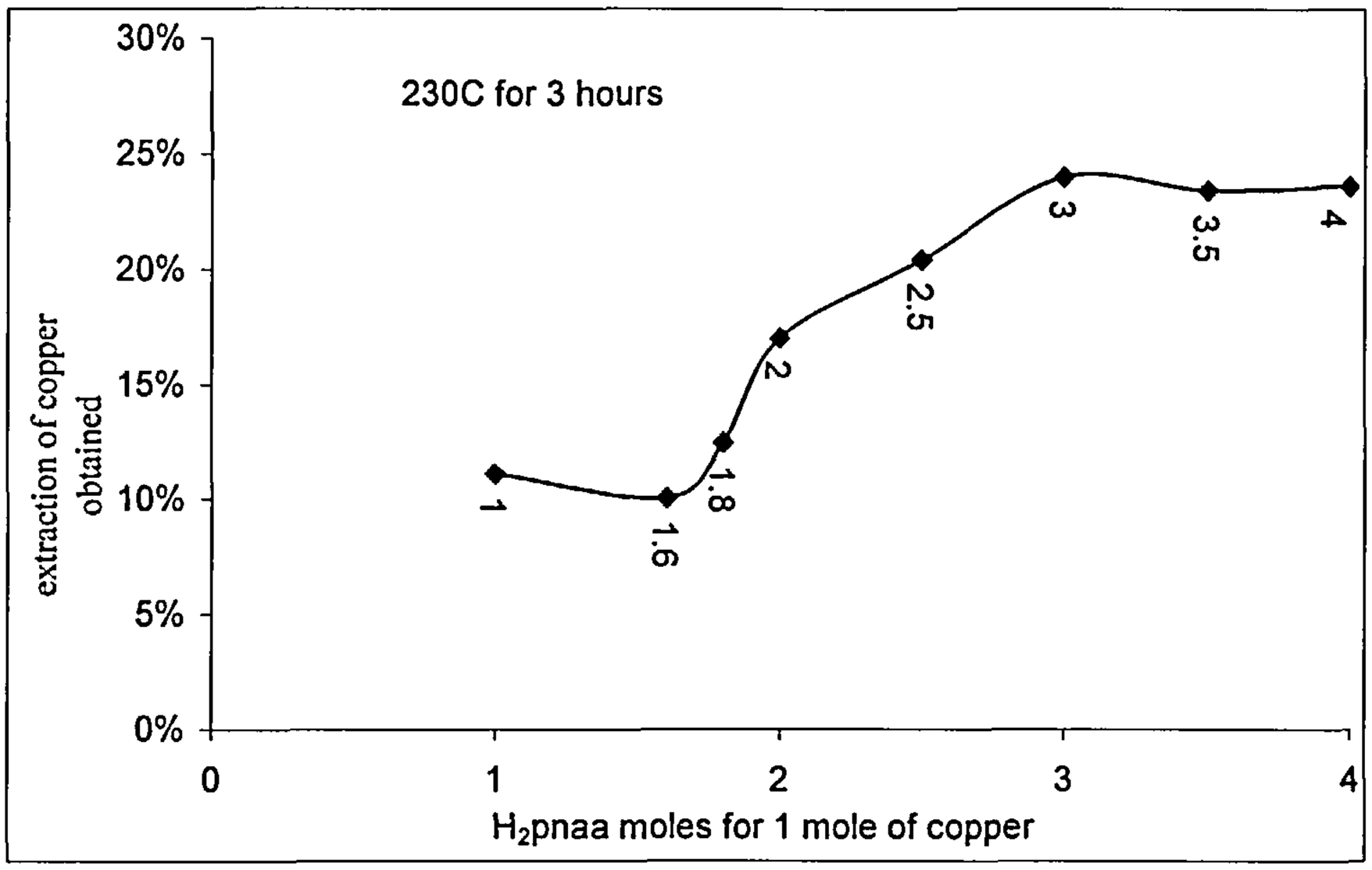

Figure 45: Extraction results obtained with mixtures of Clay 1 and H_2pnaa at different molar ratios copper: H_2pnaa maintained at 230°C for 3 hours (mean of three replicates presented in appendix 8 tables A8-12 to A8-19)

The extraction of copper increases as the ratio of H_2pnaa increased up to 3 times the stoichiometric requirement. At this point the extraction of copper no longer improves and a plateau of around 23.5% extraction is achieved which is still lower than the 36.8% obtained when H_2pnaa was present in the boat under the pan (table 20). Thus this attempt to improve the condensation of H_2pnaa within the pores by mixing the Clay 1 and H_2pnaa before the experiment was not wholly successful. Nevertheless, when mixtures of Clay 1-H_2pnaa were stored in a closed glass container, after 48 hours the colour of the mixture changed from dark green to purple; moreover the larger the amount of H_2pnaa in the mixture the quicker the change in colour. This purple colour indicates the formation of Cu(pnaa). The

mixture ratios 1:2, 1:3, and 1:4 were repeated 7 days after their preparation, when all mixtures were purple in colour. No improvement in the extraction could be observed.

The highest extraction (24%) at ratio 1:3 is still lower than the extraction obtained on the Clay1 (36.8%), but the amount of H_2pnaa involved is much less.

To improve the extraction, the residual clay was rehydrated after each run, before mixed again with the required amount of H_2pnaa to simulate repeated batch extraction. Samples of Clay 1 and Clay 2 were used for these experiments and the results are presented in figures 46 and 47.

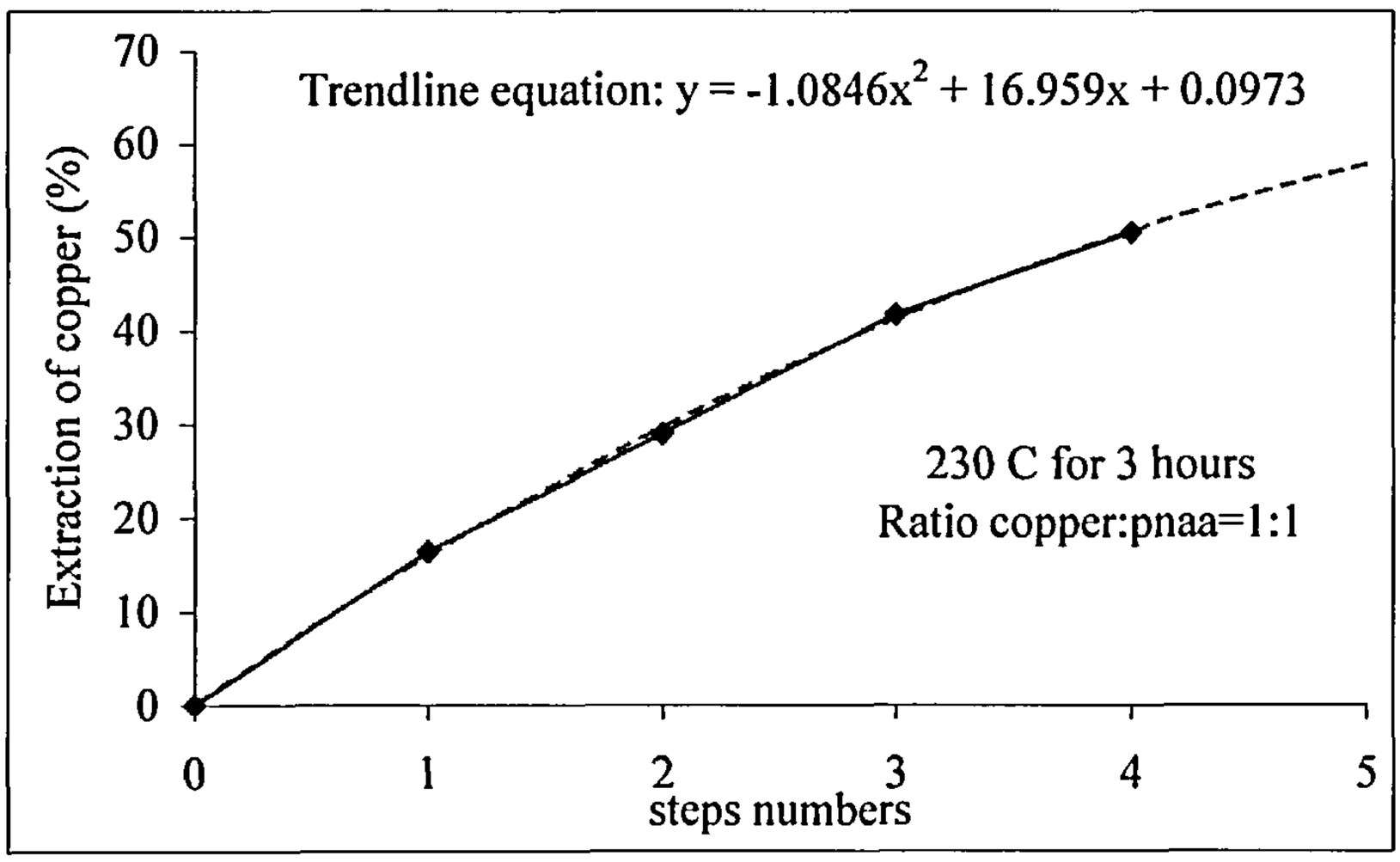

Figure 46: Extraction of copper obtained from Clay 1 ground with H_2pnaa at a ratio 1:1 in 4 steps, at 230°C for 3 hours
(mean of two replicates presented in appendix 8 table A8-20)

The curve presented in figure 46 shows increasing extraction of copper up to 50% after the fourth step. The curve tends to a plateau, and was fitted to a trend-line equation, which indicated that the amount of copper extracted after the 10^{th} step would be 62.2%. This value can be compared with the extraction obtained (36.8%) in the first experiment with H_2pnaa placed in the boat, at the same copper: H_2pnaa ratio. These results show the extraction of copper is much improved when mixing H_2pnaa with the clay before the experiment and repeating the process 10 times.

The results for extraction of Clay 2 shown in figure 47 indicate extraction of 32% of copper after the eighth step. This value can be compared to the extraction obtained (23.5%) when placing the H_2pnaa in the boat at the same ratio of copper:

H_2pnaa. Again it can be concluded that the extraction of copper is much improved by mixing the H_2pnaa with the clay before running the experiment and repeating the process.

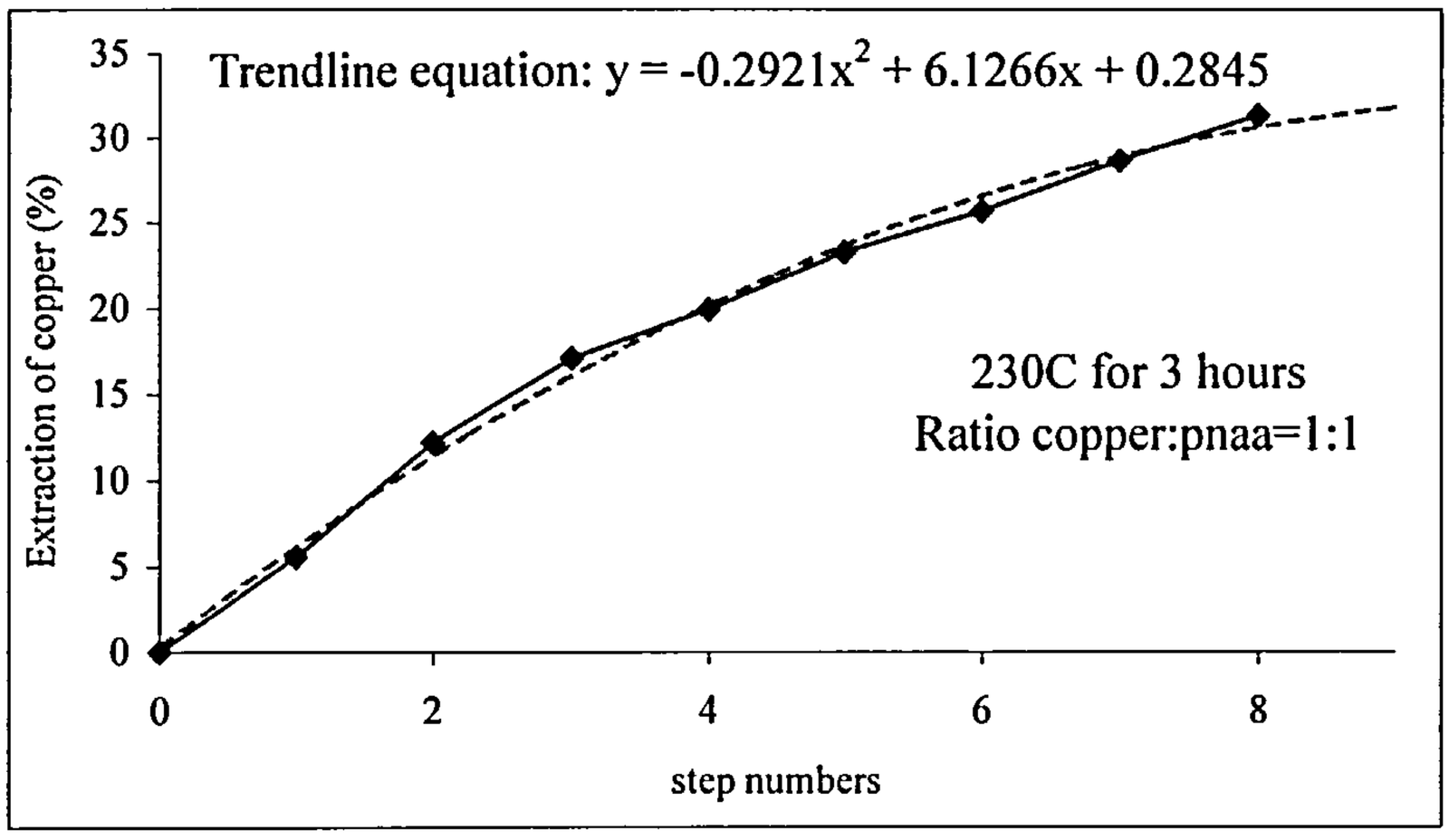

Figure 47: Extraction of copper obtained from Clay 2 ground with H_2pnaa (ratio 1:1) in 8 steps at 230°C for 3 hours (one replicate presented in appendix 8 table A8-21).

Although a higher extraction is obtained with the same amount of H_2pnaa, the overall process takes a long time so it is now necessary to try to reduce the overall reaction time. Thus the initial experiment, with the H_2pnaa placed in a boat with a ratio of copper: H_2pnaa 1:10, was carried out at a higher temperature (350°C for 3 hours) to help release the metal complexes. Figure 48 shows a thermogram of Clay 2 run under these conditions. It can be noticed that the release of copper complexes is completed at 350°C. Thus in future experiments the process should be carried out at temperatures high enough to allow the complete volatilisation of the metal complexes formed.

The extraction results obtained from these experiments are shown in table 22.

Clay material used	Clay 1	Clay 2
Copper extracted (%) (mean values of 3 experiments)	39.5 % ± 1	37 % ± 1

Table 22: Extraction results obtained from Clay 1 and Clay 2 maintained at 350°C for 3 hours; molar ratio copper: H_2pnaa 1:10

The results in table 22 show that although the higher temperature helps the release of the metal complexes in the interlayer, the extraction is still not complete. Also, while the extraction obtained from Clay 1 has not changed much when heated up to 350°C (39.5% compared to 36.9%), the higher temperature does ensure the complete volatilisation of the copper complexes formed.

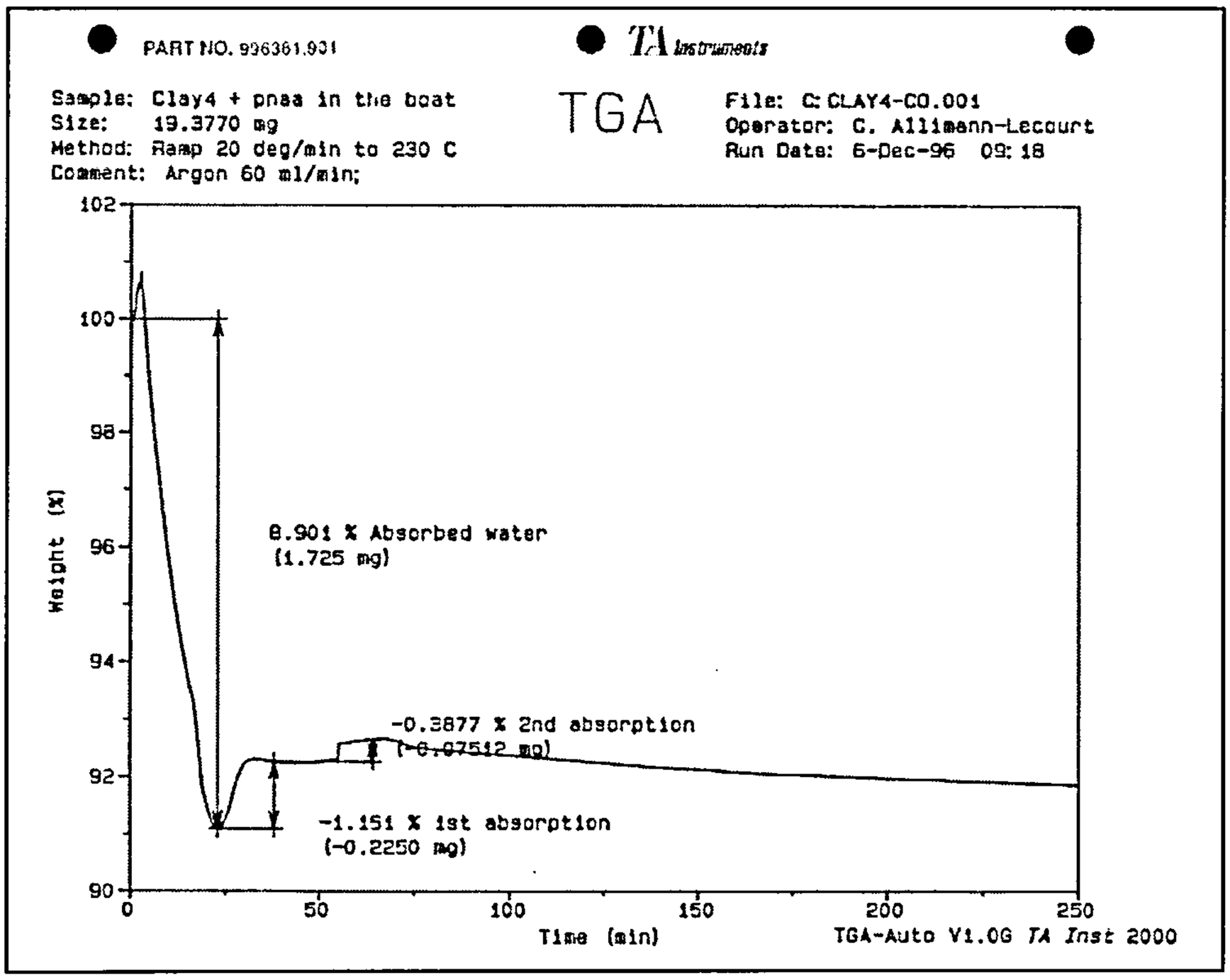

Figure 48: TGA Spectra of Clay 4 + H_2pnaa in the boat.

3.3 Study of the Sediments from Voies Navigables de France

3.3.1 Analysis of Sediment

On receipt at the University, the sediments were dried at room temperature until no further weight loss occurred (after 10 days, 60% weight loss). The resulting dried sediments were ground to a fine texture and sieved to remove the organic detritus (6.4%) and agglomerates of sizes ranging from 710 μm to 1 mm were selected for testing with the SERVO process. These sediments were heated up to 105 °C in the TGA, and 5% of water was found present in the pores. Analysis of the leached sediments is shown in table 23.

Reference analysis shows the metal content found by the Pasteur Institut from previous sampling (May 97) at the same location after the same leaching and analysis procedure as described in §2.3.1.1. The difference between the results is significant for cadmium, copper and nickel, but not for lead and zinc. Nevertheless repeated sampling of material cannot be done at exactly the same point and differences of just few centimetres in the location are enough to provide completely different analyses. In spite of the variation, these sediments still have concentrations exceeding the French AFNOR normes especially for zinc and lead.

Metals	Cd	Cu	Ni	Pb	Zn	Fe
Analysis of digested sediments (June 97) ($\mu g\ g^{-1}$)	50.3± 2	310 ± 2	47.7 ± 2	1600 ± 2	8549 ± 2	12104 ± 2
Reference Analysis from Institut Pasteur (May 97) ($\mu g\ g^{-1}$)	84	350.1	91.2	1815.5	8279.8	-
AFNOR normes French regulation limits ($\mu g\ g^{-1}$)	2	100	50	100	200	-

Table 23: Analysis of the leached sediments from Voies Navigables de France (mean of three replicates presented in appendix 8 table A8-22)

An X-Ray powder diffraction study of the sediments showed an extremely complex system that is difficult to interpret, with only some crystalline components giving lines that could not be easily assigned.

A more complete analysis of these sediments was then carried out to determine the speciation of the different pollutants and to provide a better

understanding of the subsequent metal ligand reactions to ensure the complete removal of the metal pollutants.

3.3.2 Sequential Extraction of Sediments

The metal speciation was determined using the BCR three-stage sequential extraction procedure (§2.3.2) proposed by the European Community Bureau of Reference [47] that distinguishes the speciation of the elements by their ease of extraction with various aqueous media. Results are presented in figure 49 and table 24. An internal check was performed on these results by comparing the total amount of metals removed in the procedure with the results of total digestion. In previous studies of river sediments, [144] recoveries in the range of 89-110% compared with the certified values, for chromium, copper, lead, manganese, vanadium and zinc and 82% for nickel were obtained. In the present work, recoveries are in the range (99-112%) for copper, zinc, and iron. But a larger amount of nickel (146%) was released by sequential extraction than by total digestion. Since no suitable reference materials were available to validate either the sequential extraction or the *aqua regia* digestion of sediments, it is not possible to determine the source of this variability.

The sequential extraction results show that iron is mostly present in the oxidisable and residual phases, and to a lesser extend in the reducible phase. Nickel is present as acid soluble and oxidizable species and to a lesser extent in the reducible phase, but absent from the residue. On the other hand, copper is present mostly in the oxidisable phase (83.3%) with the remaining 16.7% in the residue. Zinc is present in all the phases, with approximately equal amounts in the acid soluble, oxidisable and reducible phases and 15% in the residue.

In tables A8-26, appendix 8, the replicate E analysis result for zinc was rejected in steps 3 and 4. This replicate showed a lower concentration of zinc in the residual phase (785.2 $\mu g\ g^{-1}$ against a mean of 1314.6 $\mu g\ g^{-1}$ for the other replicates) and a higher concentration in the oxidisable phase (2140.3 against a mean of 3305.8 $\mu g\ g^{-1}$). If particular attention is drawn to replicate E (table 25), the zinc quantity released from all layers by sequential extraction is 9283 $\mu g\ g^{-1}$ and a recovery of 108.6% is obtained, which on its own is a good result. The distribution of zinc in replicate E agrees in steps 1 and 2 with the results of the other four replicates, but varies considerably in steps 3 and 4. No similar observations could be made for

copper, iron, or nickel. But the variation shown here demonstrates the high variability of zinc between the two different samples.

	Fe (12104 µg g^{-1})	Ni (48 µg g^{-1})	Cu (310 µg g^{-1})	Zn (8550 µg g^{-1})
Step 1 (available, i.e. carbonates)	126 ± 34 (1%)	29.9 ± 1.0 (42%)	0	2953 ± 137(27.2%)
Step 2 (reducible, i.e. Fe-Mn oxyhydroxides)	2481 ±240 (20.5%)	14 ± 0.6 (19%)	0	3271 ± 160 (30.2%)
Step 3 (oxidisable, i.e. sulfides)	4577 ± 400 (37.7%)	28 ± 3.6 (39%)	255 ±28 (83.3%)	3306 ± 111 (30.5%)
Step 4 (residue, i.e. Al-Si-O)	4947 ± 118 (40.8%)	0	52 ± 5.6 (16.7%)	1315 ± 74 (15.4%)
Total	12131	72	306	10844
Recovery (%)	100.2	145.8	98.7	126.8

Table 24: Sequential extraction of sediments from Voies Navigables de France (mean of three replicates presented in appendix 8 tables A8-23 to A8-26)

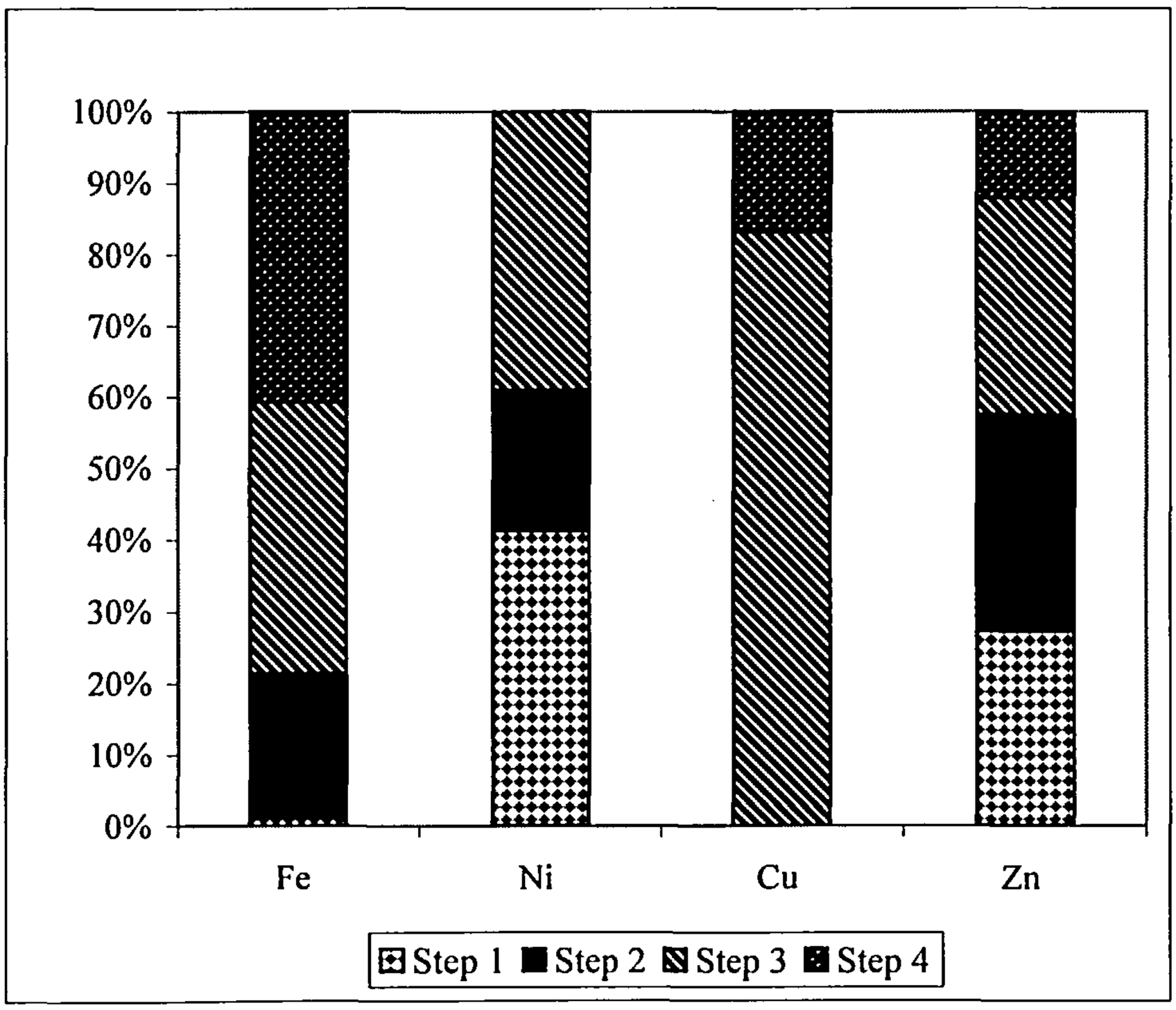

Figure 49: Sequential extraction of sediments from Voies Navigables de France

	Replicate E (μg g^{-1})	Mean of replicates (μg g^{-1}) presented in table 23
Step 1	2977 (32%)	2953 (27.2%)
Step 2	3381 (36.4%)	3271 (30.2%)
Step 3	2140 (23.1%)	3306 (30.5%)
Step 4	785 (8.5%)	1315 (15.4%)
Total	9284	10844
Recovery (%)	108.6	126.8

Table 25: Comparison of the zinc sequential extraction obtained for replicate E and the mean of other replicates

It is important to note that these speciation analyses were carried out on dried sediments, and during the drying process some oxidation of both the sulfide and the organic matter may be expected. [144] All the elements studied here were oxidised, and redistributed from the immobile residual phase to more mobile phases (reducible). Thus iron, present in the reducible phase, can be attributed to species such as iron oxyhydroxides (e.g. ferrihydrite ($5Fe_2O_3.9H_2O$), hematite (α-Fe_2O_3) or goethite (FeOOH)), that occur as a result of oxidation of the sediment during drying. These iron oxyhydroxides can adsorb metals from the oxidisable phase rendering them capable of reduction and therefore more mobile. It has been shown that ferrihydrite and hematite can adsorb metals according to the order Cu > Zn > Ni, and goethite in the order Cu > Zn. [52,144] From the results in table 23 an order of mobility can be established as follows: Zn > Ni > Cu. This agrees with the increasing affinity of ferrihydrite and hematite for zinc and nickel, but not for copper.

3.3.3 SERVO Extraction from sediments

Extraction of nickel, zinc, copper, and iron was achieved using the three different ligands Hprps, H_2pnaa and Hacac.

3.3.3.1 Extraction obtained using H_2pnaa

Treatment of the sediments with H_2pnaa under the operational conditions specified in §2.3.4.2 gave extraction of only 15 % of nickel, 22% of copper and 16% of zinc. As with the clay materials, sequential experiments were carried out with 5 g of initial material with 5 g of H_2pnaa. Following this initial experiment, 0.5 g of the material was removed for analysis, and the remaining 4.5 g were re-extracted and this procedure was repeated four times. These results are shown in figure 50.

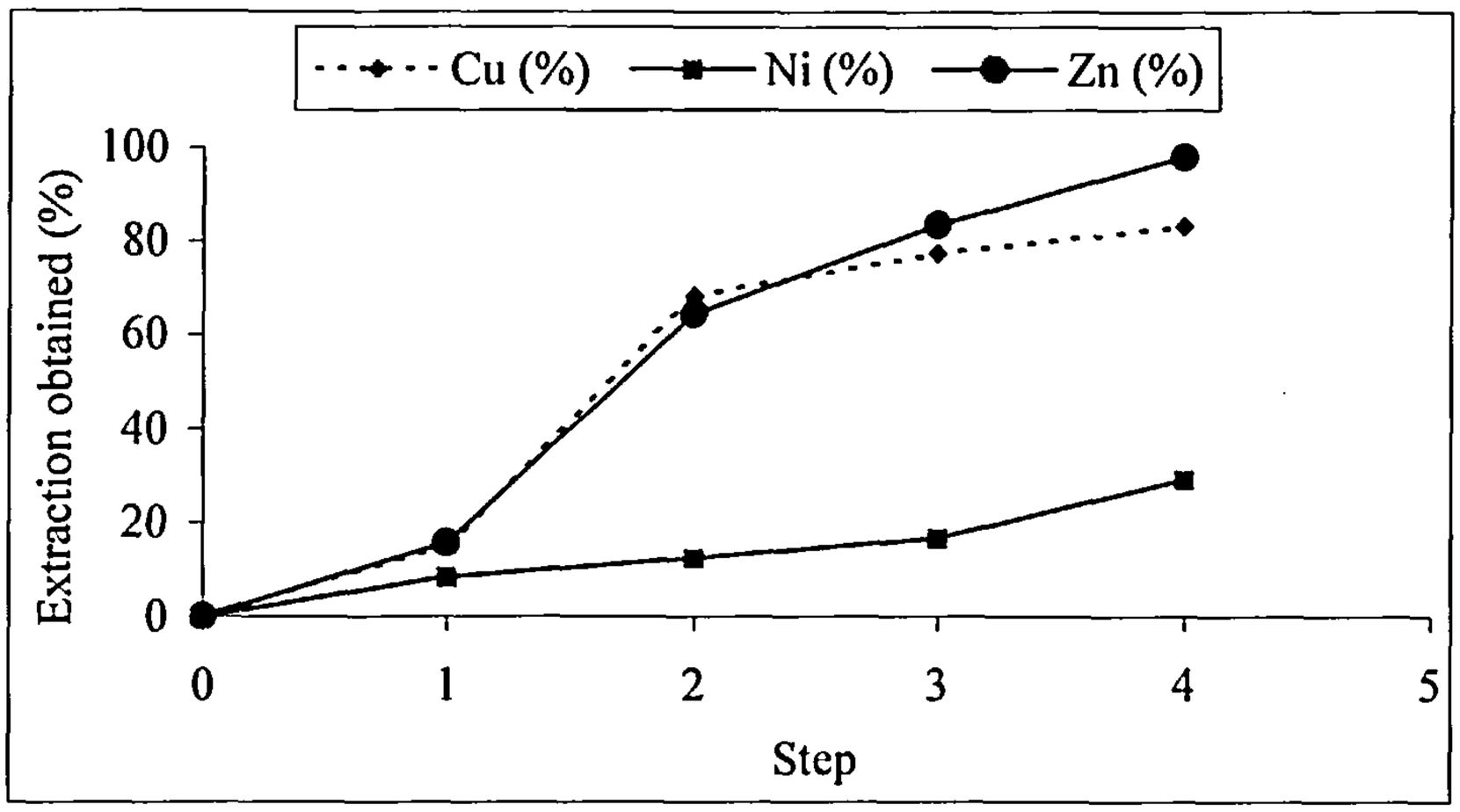

Figure 50: Extraction obtained from sediments using H_2pnaa in SERVO system (mean of three replicates presented in appendix 8 tables A8-27 to A8-29):

The results obtained after 20 hours (four steps) show that up to 80 % of the copper is extracted, leaving a final concentration in the sediment of 46 μg g^{-1}, far below the AFNOR normes (100 μg g^{-1}). This extraction agrees with the results of copper speciation obtained earlier, where it was shown that 16.3% of copper is bound in the residual phase and therefore cannot be extracted by the SERVO process, and 80% out of the 83.7% of copper present as oxidisable phase is extracted after 20 hours.

The extraction of zinc follows the same trend as copper up to ten hours, although the speciation of these elements within the sediment is different. The maximum extraction obtained after 20 hours is 98%, i.e. all the zinc was extracted. From the sequential extraction analysis, it was shown that zinc is present in all the phases, but there was significant variation between the two samples. The extraction of nickel shows a completely different trend, with only 28% of nickel extracted after 20 hours. This does not agree with the sequential extraction results that indicate that all the nickel should be extractable. Extraction of nickel might be improved by increasing the extraction time but as the residual concentration of nickel after 20 hours was reduced to 34 μg g^{-1}, i.e. below the AFNOR norms, no further experiments were performed.

3.3.3.2 Extraction obtained using Hacac and Hprps extractants

Using these extractants, only a single heating cycle for 5 hours was required to obtain similar extraction performance to that found with H_2pnaa after 20 hours (four steps). Thus figure 51 shows that after 5 hours the extraction of zinc and copper is much higher with Hprps and Hacac than H_2pnaa, but nickel extraction still remains low with these extractants.

Looking in detail at the results with Hprps, the extraction of zinc is in agreement with the sequential extraction results shown in figure 49. But only 37 % of copper of the 83.7% present in oxidisable phase is extracted. A longer extraction time may improve this extraction. It is moreover important to recall that $Cu(prps)_2$ showed some thermal degradation (14.5%) at 300°C, and at the temperature of the process (280°C), some decomposition might also be expected. Hprps extracts a small quantity of iron (4.7 %). To date no thermal data are available on possible complexes of iron with Hprps, for although $Fe(phps)_2$ was successfully synthesised following the established procedure, [139] attempts to prepare $Fe(prps)_2$ following the same procedure was unsuccessful.

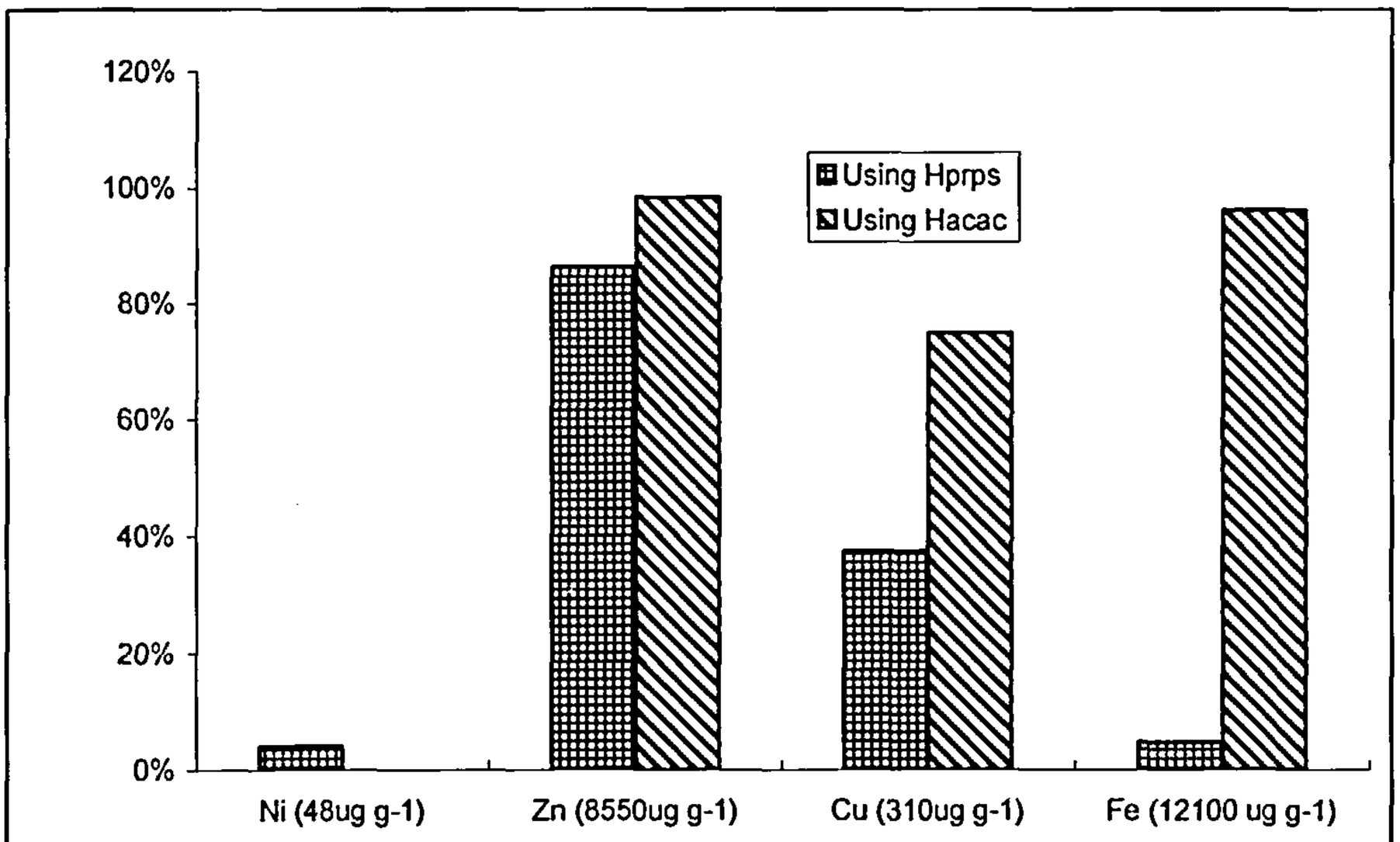

Using Hprps	4.1% ±2	86.4% ±1.6	37.6% ±0.6	4.7% ±1.4
Using Hacac	0.0%	98.5% ±0.3	74.9% ±1.7	96.2% ±0.1

Figure 51: Extraction of nickel, zinc, copper and iron from canal sediments using Hacac and Hprps extractants
(mean of three replicates presented in appendix 8 tables A8-30 to A8-36)

Hacac extracts up to 96% of zinc and iron and up to 75% of copper but no nickel could be extracted. The volatilisation temperatures of $Ni(acac)_2$ and $Cu(acac)_2$ are similar so this parameter cannot explain the non-extraction of nickel. However, $Ni(acac)_2$ is not thermally stable and 28.6% degradation was previously observed at 280°C (§2.2.1.4), therefore some losses are expected for this element. The good extraction of zinc and iron by Hacac (96%) does not agree with the sequential extraction result where 41% of these two elements were found in the residual phase and therefore should not be extracted. However it should be noted that 2,4-pentanedione is particularly active towards iron and $Fe(acac)_3$ can be formed by the action of the ligand with metallic iron or steel. $Fe(acac)_3$ and $Zn(acac)_2$ are also more volatile than $Cu(acac)_2$ and $Ni(acac)_2$, so their better extraction might be expected. The copper extraction obtained with Hacac (75%) agrees with the 83.7% of copper present in oxidisable phase.

3.3.4 Conclusion

Using the extractants Hacac and Hprps only a single heating cycle for 5 hours at 230° C was required to obtain similar extraction performance to that found with H_2pnaa after 25 hours. However, it should be noted that the extraction of iron with Hacac would be detrimental to the operation of the SERVO process for the removal of toxic metals as the iron extraction would deplete the amount of extractant available in the system.

The extraction results do not always agree with the results expected from the sequential extraction studies, especially for zinc and iron. It is difficult without further extensive studies on further materials to come to any firm conclusions as to the reasons for this anomaly.

3.4 General conclusions

3.4.1 Studies on carbonates and modified clay materials:

Preliminary tests on metal carbonates have shown that extraction of these elements was possible using the new design of SERVO process equipment. Copper carbonate is most easily extracted using Hacac (88%), followed by H_2pnaa (39%). The optimum extractions for zinc and nickel carbonates were obtained using Hprps, but remain low (42% and 56 % respectively) compared to the expected results.

Cobalt carbonate is the most easily extracted metal with up to 95% extraction using H_2pnaa and 83% using Hprps.

Some modified clays were prepared by the adsorption of copper carbonate or nickel carbonate in the interlayer and the diffuse layer of the clays. The composition of these clays are shown in table 19 (p103).

It was shown that the preparation of Clays 1 to 4 does affect the crystalline structure of the montmorillonite clay.

The ratio of H_2pnaa absorption in the interlayer and diffuse layer is similar to that found when adsorbing nickel and copper on the clay i.e. approximately 10% in the outer layer and 90% in the interlayer. This indicates that H_2pnaa is occupying the same sites as copper and nickel hydroxides when adsorbed in the clay structure.

Preliminary studies of the extraction of copper in Clay 1 and Clay 2 on the modified TGA showed that the extraction of metals from the fully exchanged clays (Clay 1) are better than these of the clays exchanged only in the interlayer (Clay 2). Thus the metal complex in the interlayer of the clay is more difficult to volatilise than the one present on the diffuse layer. Some mixing studies of the clay and H_2pnaa extractant in different molar ratios before running the experiments showed improved extraction of copper but it reaches a plateau that is still lower than the extraction obtained when H_2pnaa was present in the boat under the pan. It can also be noticed that the release of copper complexes is completed at 350°C. Thus future experiments should be carried out at temperatures high enough to allow the complete volatilisation of the metal complexes formed.

3.4.2 Studies on sediments

The canal sediments used were first dried, ground, and sieved. Agglomerate sizes ranging from 710 μm to 1mm were used in SERVO process without any other pre-treatment. These agglomerates had a fine texture with a high proportion of silt, clay and humic materials that provide high porosity, they also contained some gibbsite ($Al(OH)_3$) and calcite ($CaCO_3$), that increase the exchange capacity. The sediments as received contained a large quantity of interstitial water (60%), which provided the sediments with not only a high porosity, permeability, aeration and sorptive capacity, but also makes the metals more likely to be oxidised and redistributed to more mobile phases (reducible) during the drying process. Metal

speciation showed that nickel is present as both acid soluble and oxidizable species and to a lesser extent in the reducible phase, but absent from the residue. On the other hand, copper is present mostly in the oxidisable phase (83.3%) with the remaining 16.7% in the residue. Zinc is present in all the phases, with approximately equal amounts in the acid soluble, oxidisable and reducible phases and 15% in the residue.

The SERVO process using H_2pnaa after 20 hours extracted up to 80% copper, 98% zinc, and 28% nickel. Only the extraction result obtained for copper is in agreement with the speciation analysis of the elements of study.

When using Hacac as extractant, only a single heating cycle of 5 hours at 200°C was required to obtain similar extraction performance to that found with H_2pnaa after 20 hours. Hacac extracted up to 96% zinc and iron, up to 75% copper, but no nickel. However, the extraction of iron would be detrimental to the operation of the SERVO process as this would deplete the amount of extractant available in the system.

Using Hprps a single heating cycle for 5 hours at 280°C extracted 4% of iron and nickel, 37.6% copper, and 85% zinc. This time only the extraction result obtained for zinc is in agreement with the speciation analysis of the elements of study. Copper is less well extracted than expected, which might be due to some thermal degradation of the $Cu(prps)_2$ complex.

Even if the Hprps and Hacac extractants only required a single heating cycle of 5 hours, H_2pnaa remains the extractant of choice for the SERVO process as Hprps does not extract all the extractable copper and only little nickel is removed and Hacac extracts all the iron and no nickel. Despite its longer heating cycle, H_2pnaa removed all the zinc and copper, did not extract iron, and gave the highest extraction (28%) of nickel.

Chapter 4: Application of SERVO Process to Industrial Waste

4.1 Puertollano Fly Ash:

4.1.1 Analysis of Puertollano Fly Ash:

Because of the particle size range of the fly ash, and the possible condensation of the extractant on the particles, [111] some pressure built-up was expected in the process. Therefore, the fly ashes were sieved to give two samples: large particles (>730μm) and small particles (<730μm). Attempts to fluidise the small particles were disappointing as they were ejected from the reactor. Therefore these materials were first agglomerated at room temperature using clay as a binding agent at levels of 2.5%. The mixture was moistened with distilled water and pellets formed by rolling by hand. These were then left to dry at room temperature for 24 hours. X-Ray powder diffraction study of the fly ash showed an extremely complex system that was difficult to interpret with only some crystalline components giving lines that could not be easily assigned (appendix 10). Analyses of Puertollano fly ash following total digestion, as defined in §2.3.1.1, are presented in table 26 compared with relevant literature values [23] and were used as reference concentrations. The reference analysis shown is the analysis of a Puertollano Fly Ash from the same pulverized coal combustion run and was verified using suitable reference material [25]. Therefore an internal check was performed on the results of the total analysis by evaluating the difference (%) and the standard t test [145] to compare the experimental mean with the reference analysis.

Concentration in μg g^{-1}	Zn	Cu	V	Fe	Pb
Total analysis	1085 ± 11	83 ± 4	161 ± 5	48860 ±351	556 ±13
Reference analysis [25]	1233	75	202	51060	751
Difference (%)	14.8	10.7	20.3	23.8	25.9

Table 26: Analysis of the digested Puertollano fly ash
(mean of three replicates presented in appendix 9 table A9-1)

From table 26, it can be seen that the experimental analyses of copper, iron, and zinc differed from the reference analysis in a range of ±10% with higher differences for vanadium (-20%) and lead (-26%). These differences might be a result of a different digestion procedure used for the ash.

4.1.2 Sequential Extraction of Puertollano Fly Ash:

The major constituents of this fly ash are shown in table 27, [23] and a more detailed composition is given in appendix 5.

SiO_2	Al_2O_3	Fe_2O_3	CaO	MgO	Na_2O	K_2O	P_2O_5	TiO_2	MnO	SO_3
58.4%	29.3%	7.5%	0.9%	1.0%	0.4%	2.4%	0.1%	0.7%	0.1%	0.2%

Table 27: Major oxide contents of the Puertollano fly ash

The results of speciation studies, figure 52 and table 28, show that iron, lead, copper, and nickel are only leached following complete digestion (step 4), so these metals are present within the silicate phase of the fly ash or as resistant oxides and so will be resistant to extraction or leaching. As for previous sequential analyses, an internal check was performed on the results by comparing the total amounts of metals removed with the results of the total digestion (recovery 1).

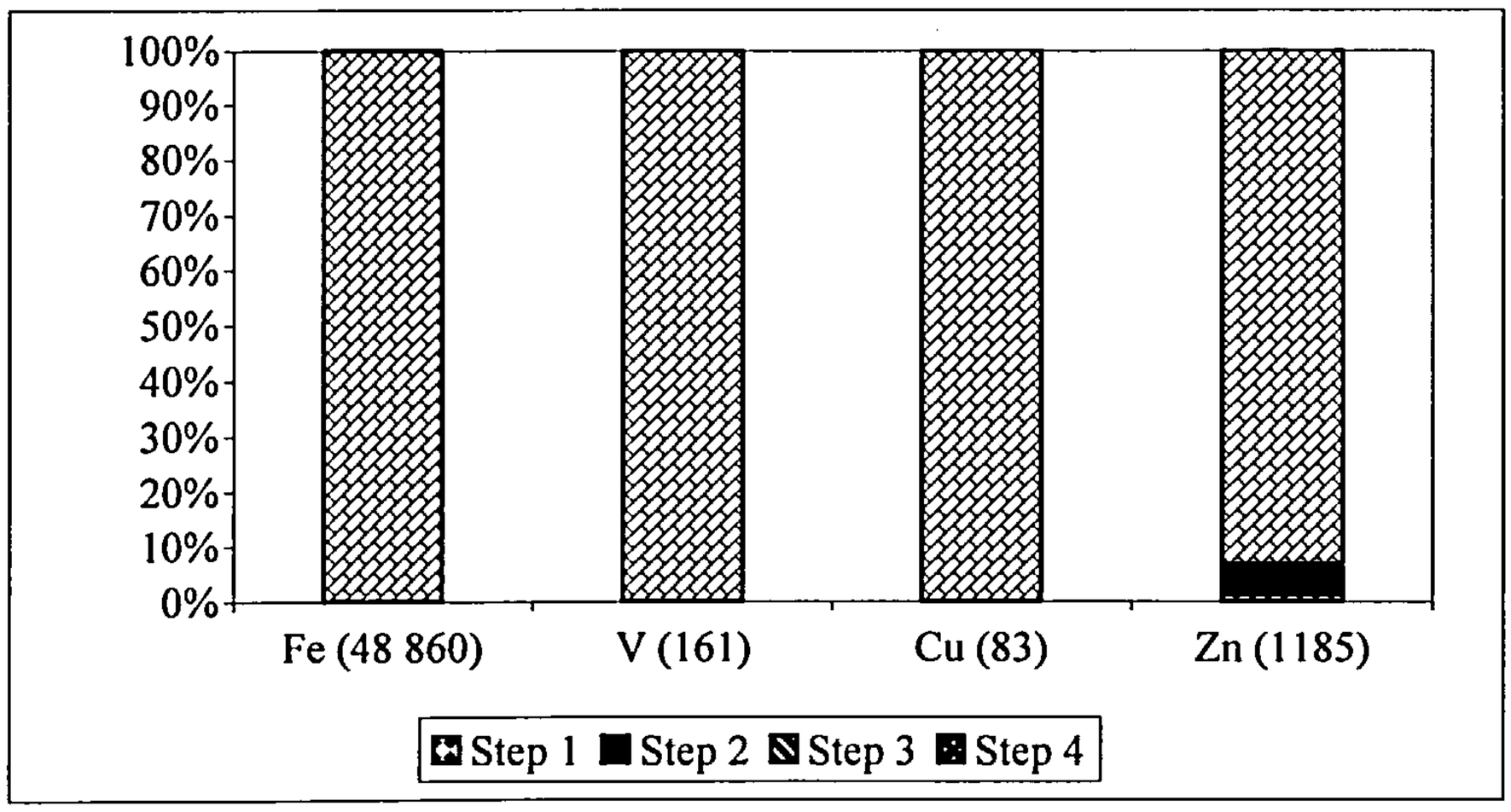

Figure 52: Sequential extraction of Puertollano Fly Ash
(mean of four replicates presented in appendix 9 tables A9-2 and A9-3)

Moreover, because a reference analysis is available, a second recovery was calculated by comparing the total amount of metals removed in the procedure with the results of the reference analysis (recovery 2).

Zinc is the only metal partially leachable using the BCR procedure with 1% of zinc extracted in step 1 (available phases), 0.6% of zinc in step 2 (reducible phases) and finally 4.6% of zinc extracted in step 3 (oxidizable phase). Thus even with zinc the majority of the element (93.7%) is only released after complete digestion and consequently is bound in the silicate phase. Recovery 1 shows a difference of up to 25% when comparing the total sequential extraction with the total content obtained after total digestion analysis (table 25). The experimental results for iron, copper, vanadium and lead in the first three steps of extraction were within experimental error and therefore appear as zero in table 28.

	Fe (48 860 $\mu g\ g^{-1}$)	V (161 $\mu g\ g^{-1}$)	Cu (83 $\mu g\ g^{-1}$)	Zn (1185 $\mu g\ g^{-1}$)	Pb (556 $\mu g\ g^{-1}$)
Step 1 (available)	0	0	0	12.3 ± 2.5 (1.04%)	0
Step 2 (reducible)	0	0	0	7.5 ± 2.3 (0.64%)	0
Step 3 (oxidisable)	0	0	0	54.3 ± 7.8 (4.58%)	0
Step 4 (residual)	50122 ±1056	121.3 ±14.1	66.5 ± 8.7	1021 ± 144 (93.74%)	686 ±78
Total	50122	121	66	1095	686
Recovery 1 (%)	102.6	75.2	79.8	101	123.3
Recovery 2 (%)	98.2	59.9	88	88.8	91.3

Table 28: Sequential extraction of Puertollano Fly Ash
(mean of four replicates presented in appendix 9 tables A9-2 and A9-3)

Recovery 1 shows that zinc and iron are extracted in the same proportions as for the full digestion, and Recovery 2 confirms this as approximately 10% of copper and zinc were not extracted when compared to the reference value (table 26). Recovery 2 value obtained for lead (91.6%) is higher than that in table 26 (74%) therefore better extraction of lead was obtained during the sequential extraction. But vanadium recovered during the sequential extraction was lower than the full digestion

(Recovery 2 lower than the value in table 26). Thus some losses of vanadium must have occurred in the first three steps.

Therefore the total extraction results obtained using sequential extraction are closer to the reference values than the total digestion analysis results. This confirms that the different digestion procedures used for the digestion of the ash provide a feasible explanation of the errors obtained in the full digestion analysis (table 26).

4.1.3 SERVO Extraction Results

Extraction studies, under conditions specified in §3.3.4.2, for pellets containing 2.5% clay, showed no extraction of nickel, copper, lead, or iron and only a little extraction for zinc (results presented in appendix 9 tables A9-4 and A9-5). This is expected from the sequential analysis that indicated these elements as being present in the silicate phase. Zinc extraction with Hprps (54.1 μg g^{-1} ±10.1 (5.2% ±1.0)) and H_2pnaa (68.1 μg g^{-1} ±1.6 (6.5% ±0.2)) are in line with the results of the sequential extraction where 6.2 % of zinc was shown to be extractable.

4.1 4 Conclusion

Metal speciation is very important in the SERVO process and the poor results obtained with the Puertollano PCC fly ash are explained by the metals being present in the silicate phase of the ash. It is also evident that microwave digestion used to digest fully the Puertollano PCC fly ash does not provide complete extraction of the metals.

4.2 Rotterdam Waste Incinerator Fly Ash

4.2.1 Analysis of Rotterdam Waste Incinerator Fly Ash

The fly ash as received was sieved and particles in the range 1.4 – 2 mm used. The diverse nature of the feed material to the incinerator produces a heterogeneous fly ash with particles having different physical properties. A scanning electronic microscope (SEM) study showed that some particles were burnt plant material, with a high carbon content (75%) and no trace metals (appendix 10). Other particles were more like characteristic fly ash with high concentrations of zinc and copper, and the presence of chlorine in all the particles at a significant level suggests that the wastes initially contained some PVC material.

The analysis of sieved portion of the Rotterdam fly ash following acid digestion is presented in table 29.

Metals	Fe	Pb	Cd	Zn	Cu	Ni
Concentration ($\mu g\ g^{-1}$)	8400	4850	310	13 500	1050	480

Table 29: Analysis of the digested Rotterdam waste incinerator fly ash (mean of three replicates presented in appendix 9 table A9-6)

X-Ray powder diffraction study of the fly ash showed an extremely complex system that is difficult to interpret with only some crystalline components giving lines that could not be easily assigned (appendix 10).

4.2.2 Sequential Extraction of Rotterdam Waste Incinerator Fly Ash

The speciation studies (figure 53 and table 30) showed that most of the metals are easily leachable in the first three stages of the BCR procedure, except for nickel and iron that seem to be mainly contained in the silicate phase. Zinc is the most easily leachable metal, and is also present at the highest concentration, so posing a potentially significant environmental risk.

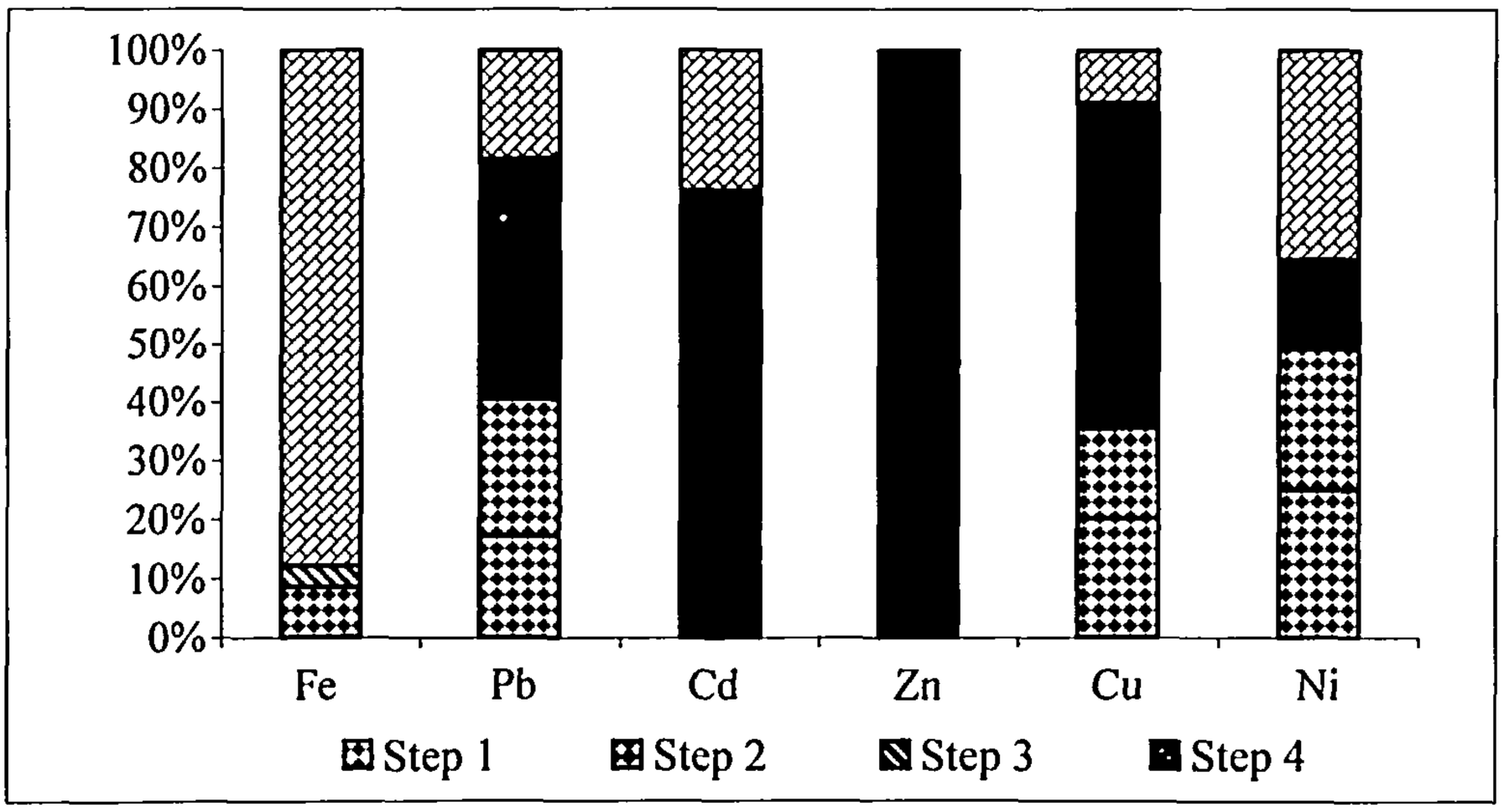

Figure 53: Sequential Extraction of Rotterdam Waste Incinerator Fly Ash (mean of five replicates presented in appendix 8 tables A9-7 to A9-12)

Moreover, most of the zinc (60%) and cadmium (71.5%) are easily leached by dilute acetic acid and so would tend to leach under acid rain conditions. In the present

study, recoveries, calculated as in §4.3.2, are in the range (89-108%) for all metals. Therefore the reported sequential extraction data are within errors of ±10%. Since no suitable reference materials were available to validate either the sequential extraction or the total digestion of these fly ashes, the variability can be attributed to the high variability of the particles and consequent sampling difficulties.

	Fe (8400 μg g^{-1})	Pb (4850 μg g^{-1})	Cd (310 μg g^{-1})	Zn (13500 μg g^{-1})	Cu (1050_μg g^{-1})	Ni (480 μg g^{-1})
Step 1, available	4.0 ± 2.0 (0.05%)	816 ± 78 (17.3%)	221 ± 6 (65.8%)	8108 ± 742 (57%)	190 ± 15 (20.1%)	116 ± 3 (25.1%)
Step 2, reducible	753 ± 74 (8.7%)	1100 ± 68 (23.3%)	24.8 ± 2.0 (7.4%)	4139 ± 285 (29%)	143 ± 21 (16%)	111 ± 8 (24.1%)
Step 3, oxidisable	318 ± 23 (0.4%)	1936 ± 291 (41%)	9.9 ± 0.4 (2.9%)	1974 ± 162 (14%)	517 ± 48 (55%)	71 ± 4 (15.4%)
Step 4, residual	7795 ± 254 (90.8%)	867 ± 17 (18.4%)	80 ± 5.7 (24%)	32.0 ± 4.2 (0.22%)	82 ± 3 (8.7%)	164 ± 9 (35.4%)
Total	8585	4720	336	14287	940	462
Recovery (%)	102.2	97.3	108.3	105.8	89.4	96.2

Table 30: Sequential Extraction of Rotterdam Waste Incinerator Fly Ash
(mean of five replicates presented in appendix 9 tables A9-7 to A9-12)

4.2.3 SERVO Extraction Results:

4.2.3.1 Single extraction

Extraction with the SERVO process, figure 54 and table 31, still requires optimisation. From the speciation results, both zinc and copper should be almost fully extracted (i.e. 87% copper and nearly 100% zinc) but the best result obtained for these metals using the three extractants is only 50% extraction with Hprps. Also with nickel only 21% of the potential 65% is extracted with Hprps and no extraction is observed with the other extractants. Similarly with lead only 37% of the potential 92% is extracted using Hprps and again there is no extraction with Hacac or H_2pnaa. However up to 76.7% of the potential 83% cadmium is extracted with Hprps but all of the extractable iron is removed with Hacac (10.4 %) and Hprps (8.3%). The low overall extraction of iron is the result of 90% of it being contained in the silicate phase. The extraction of iron and cadmium are the only results in agreement with the sequential extraction results. The low extraction obtained for the other metals may be

the result of a too brief a contact time; therefore the extraction was repeated using several batches of extraction.

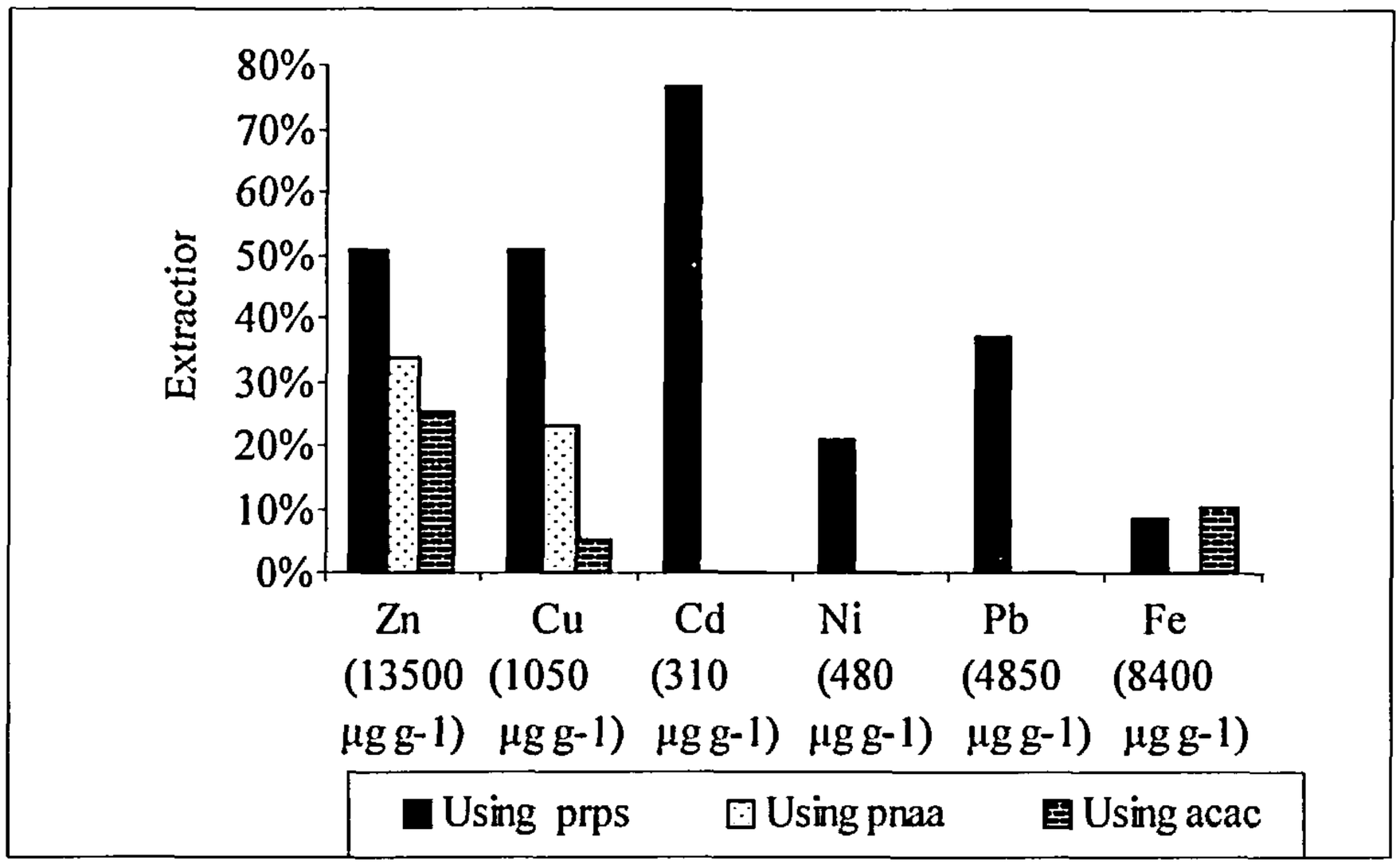

Figure 54: SERVO Extraction Results from Rotterdam Fly Ash in one step using Hprps, H_2pnaa and Hacac (mean of two experiments presented in appendix 9 tables A9-13 to A9-23)

	Hprps (µg g^{-1})	H_2pnaa (µg g^{-1})	Hacac (µg g^{-1})
Zn (13500 µg g^{-1})	6796 ± 378 (50.7%)	4493 ± 344 (33.5%)	3387 ± 193 (25.0%)
Cu (1050 µg g^{-1})	571 ± 44 (50.8%)	241 ± 37 (23%)	58 ± 16 (5.1%)
Cd (310 µg g^{-1})	234 ± 6 (76.4%)	0.0	0.0
Ni (480 µg g^{-1})	100 ± 20 (20.7%)	0.0	0.0
Pb (4850 µg g^{-1})	1789 ± 270 (36.9%)	0.0	0.0
Fe (8400 µg g^{-1})	686 ± 118 (8.3%)	0.0	859 ± 168 (10.4%)

Table 31: Concentration of zinc, copper, cadmium, nickel, lead and iron extracted from Rotterdam Fly Ash in one step using Hprps, H_2pnaa and Hacac (mean of two experiments presented in appendix 9 tables A9-13 to A9-23)

The residues after extraction were studied by scanning electronic microscopy to see whether any adsorption of the ligand on the surface of the particles had occurred

(appendix 10). No increase of the carbon content was observed on the surface of the residues, showing no organic contamination. But there was an increase in the surface phosphorous concentration following extraction with Hprps, suggesting that some of the extractant or metal complexes (i.e. $Cd(prps)_2$ or $Cu(prps)_2$) were being decomposed and the released phosphorus species were reacting with the fly ash residues.

4.2.3.2 Repeated extraction

a) Using Hacac:

Figure 55 shows that after two steps the extraction of copper and iron reaches a plateau and no further improvement is observed. The observed iron extraction (table 32) (11.7%) agrees with the sequential extraction results, as 90.8% of iron is bound to the silicate phase. Therefore all the extractable iron is removed with Hacac after two steps. In the case of copper, the observed extraction (18.6%) does not agree with the sequential extraction results, that shows only 8.7% of copper is bound to the silicate phase. However, as shown in figure 55 increasing the contact time does not improve extraction. Cadmium and nickel extraction increase with time but seem to trend towards a plateau after step 4. Therefore more than four steps would be required to obtain the optimum extraction of nickel and cadmium from Rotterdam Fly Ash with Hacac. $Ni(acac)_2(H_2O)_2$ is known to be thermally unstable (§2.2.1.4, 28.6% residue at 300°C) therefore some decomposition of the $Ni(acac)_2(H_2O)_2$ might explain the extraction obtained. Zinc extraction also increases with time but does not seem to tend towards a plateau. Therefore further investigations are required to determine the optimum extraction conditions for zinc.

The temperature used in the second reactor, where complexation occurs, was chosen to ensure the volatilisation of all metal 2,4-pentanedionates, i.e. 200°C. The incomplete extraction of "extractable" metals may be explained by incomplete complex formation. The optimum extraction of iron is obtained after two steps; this result might pose a problem as iron extraction is not required and would restrain the extraction of other metals.

	Zn (13500 µg g^{-1})	Cu (1050 µg g^{-1})	Cd (310 µg g^{-1})	Ni (480 µg g^{-1})	Fe (8400 µg g^{-1})
Step 1	3388 ± 24 (28.9%)	136 ± 23 (11.7%)	25 ± 1.5 (10.3%)	58 ± 6 (11.0%)	635 ± 229 (6.9%)
Step 2	3930 ± 68 (33.5%)	175.3 ± 28.3 (15.1%)	30 ± 0.4 (12.3%)	94 ± 17 (17.8%)	678 ± 262 (7.4%)
Step 3	4673 ± 6 (39.9%)	194.0 ± 17.3 (16.7%)	43 ± 0.1 (17.7%)	119 ± 9 (22.4%)	1014 ± 104 (11.0%)
Step 4	5795 ± 48 (49.5%)	216.1 ± 1.2 (18.6%)	55 ± 5 (22.5%)	134 ± 3 (25.3%)	1078 ± 86 (11.7%)

Table 32: Concentration of zinc, copper, cadmium, nickel and iron (µg g^{-1}) extracted from Rotterdam Fly Ash in four steps using Hacac
(mean of two experiments presented in appendix 9 tables A9-34 to A9-38)

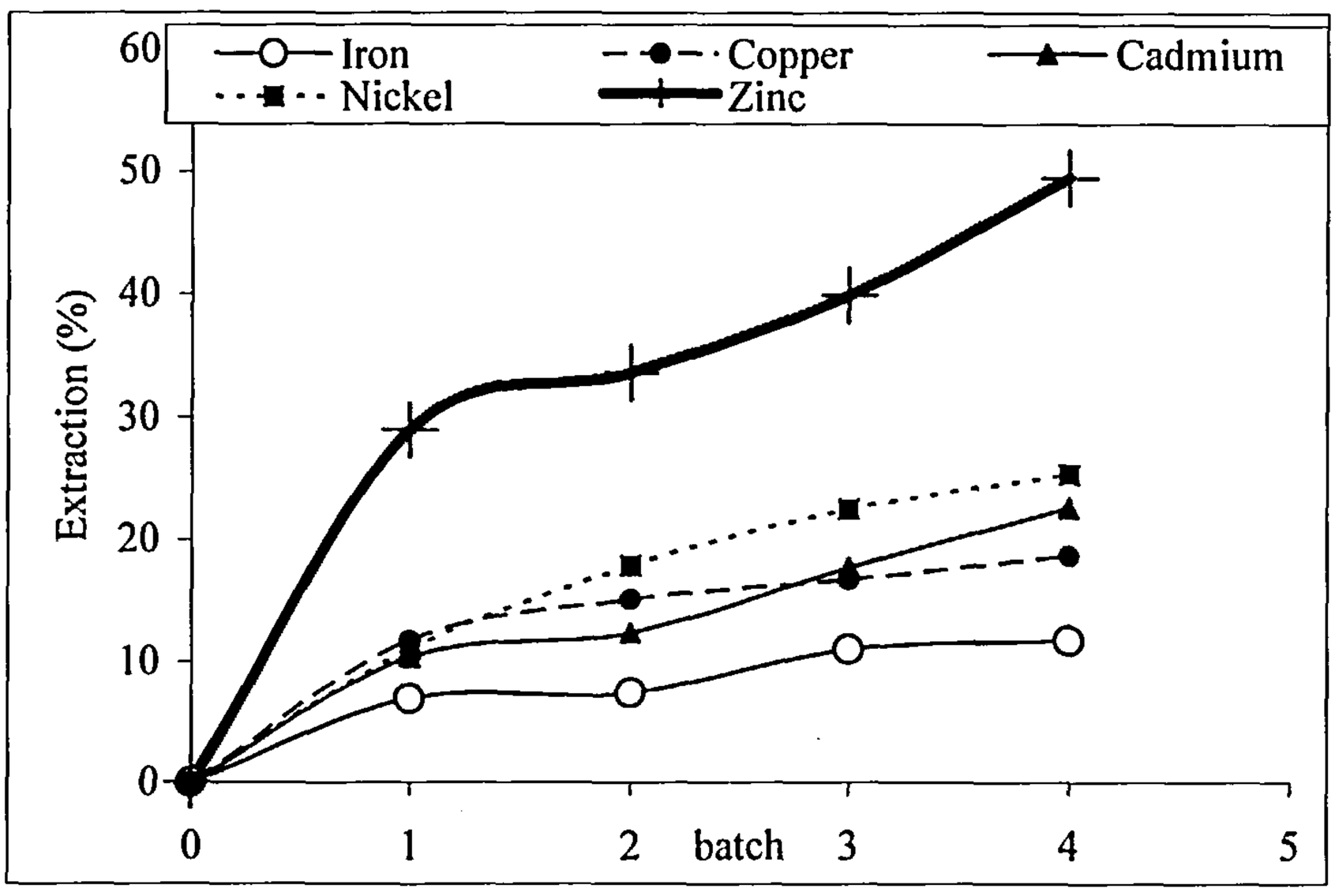

Figure 55: Extraction of zinc, copper, cadmium, nickel and iron from Rotterdam Fly Ash in four batches using Hacac
(mean of two experiments presented in appendix 9 tables A9-34 to A9-38)

(b) Using H_2pnaa

Figure 56 shows a continuous increase in the extraction of zinc, copper, and extraction seems to be improved by increasing the number of extraction steps as no plateau appears for these two metals. The extraction of cadmium and nickel reaches a plateau after step 1 and no further improvement is observed. The extraction of these four metals (table 33) stays below the possible extraction suggested by the sequential

extraction results and this despite a higher contact time between the Rotterdam Fly ash and H_2pnaa. Again, the temperature used in the second reactor, where complexation occurs, was chosen to ensure the volatilisation of all H_2pnaa metal complexes, i.e. 270°C.

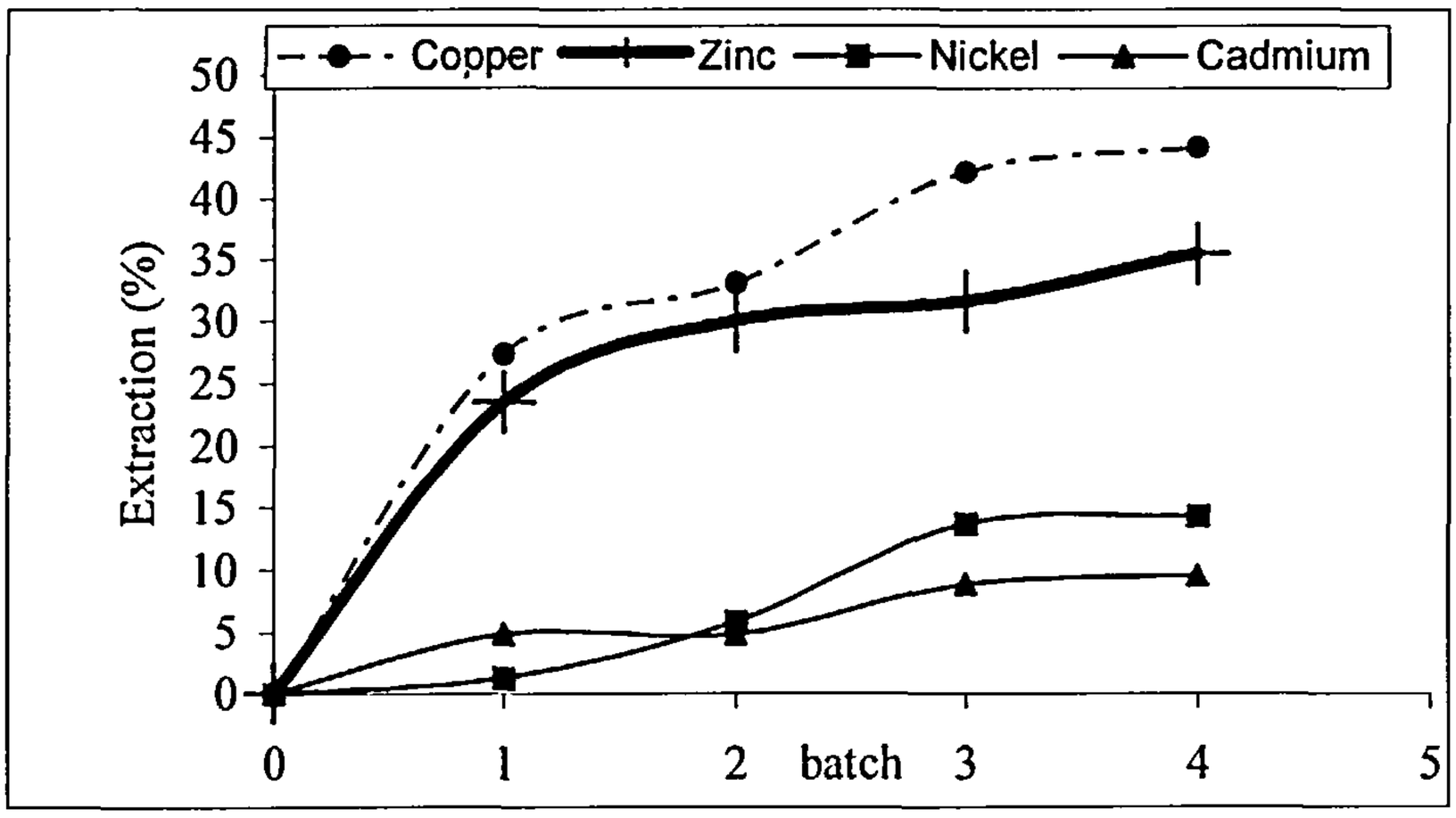

Figure 56: Extraction of zinc, cadmium, nickel and copper from Rotterdam Fly Ash in four batches using H_2pnaa
(mean of two experiments presented in appendix 9 tables A9-24 to A9-27)

The incomplete extraction of "extractable" metals can be explained by incomplete formation of the H_2pnaa metal complexes. The mechanism of complexation proposed Dr A.A. Pichugin [111] for H_2pnaa suggests that the extractant condenses on the feed material where it reacts with the metal salts. Therefore the incomplete formation of the H_2pnaa metal complexes might be due to incomplete condensation of the extractant in the pores of the Rotterdam Fly ash. This mechanistic study [111] also showed that the size of the feed material was important and the smaller the particle the higher the possible condensation of the extractant and the higher the extraction. The size of the Rotterdam Fly ash particles used here are in the range 1.4 – 2 mm. Grinding the ash followed by agglomeration using clay as carried out with the Puertollano Fly ash might improve condensation of the extractant in the pores of the Rotterdam Fly ash and thus improve extraction. The mineralogy of Rotterdam Fly ash might also prevent ready access of the extractant to the metal salts.

	Cu (1050 µg g^{-1})	Zn (13500 µg g^{-1})	Ni (480 µg g^{-1})	Cd (310 µg g^{-1})
Step 1	317 ± 9 (27.3%)	2751 ± 144 (23.5%)	6.4 ± 1.3 (1.2 %)	11.8 ± 4.8 (4.8%)
Step 2	383 ± 7 (33%)	3519 ± 203 (30.0%)	31.2 ± 10.8 (5.9%)	11.7 ± 2.0 (4.8%)
Step 3	489 ± 18 (42.1%)	3702 ± 55 (31.6%)	72.2 ± 11.4 (13.6%)	21.4 ± 5.1 (8.8%)
Step 4	512 ± 21 (44.2%)	4162 ± 197 (35.5%)	75.7 ±1.9 (14.3%)	23.2 ± 6.8 (9.5%)

Table 33: Concentration of copper, zinc, nickel and cadmium (µg g^{-1}) extracted from Rotterdam Fly Ash in four steps using H_2pnaa
(mean of two experiments presented in appendix 9 tables A9-24 to A9-27)

(c)Using Hprps:

Figure 57 shows that after two steps the extraction of iron (8.8%), lead (75.1%), cadmium (80.7%) and copper (82.8%) reach a plateau that is close (except for copper) to the full recovery of extractable metals as indicated by the sequential extraction results. Even though copper should be extracted up to 93%, only 83% is extracted by Hprps. $Cu(prps)_2$ is known to be thermally unstable (§2.2.3.9, 14.5% residue at 275°C), therefore some decomposition of $Cu(prps)_2$ may have occurred. As with Hacac, iron extraction is not required and would interfere with the extraction of other metals. Zinc, that should be fully extractable from the sequential extraction results, is only extracted to 69.2%. However the extraction curve does not tend to a plateau and thus further extraction may be possible by increasing the number of steps. This extraction is nevertheless better than that observed using Hacac or H_2pnaa. Nickel, has the lowest extraction of the desired metals, with only 27.2% of a possible 64.6% nickel salts being extracted. As for zinc, the nickel extraction curve does not tend to a plateau and better extraction might be obtained by increasing the number of steps. $Ni(prps)_2$ and $Zn(prps)_2$ are quite thermally stable with respectively only 1.45% and 0.7% thermal degradation at 300°C, therefore thermal degradation is probably not the reason for this incomplete extraction.

The incomplete extraction of zinc and nickel can be explained by the mineralogy of the Rotterdam Fly ash, where nickel and zinc would be contained in a structure not readily accessible to the extractant, e.g. a nickeliferous iron chlorite phase.

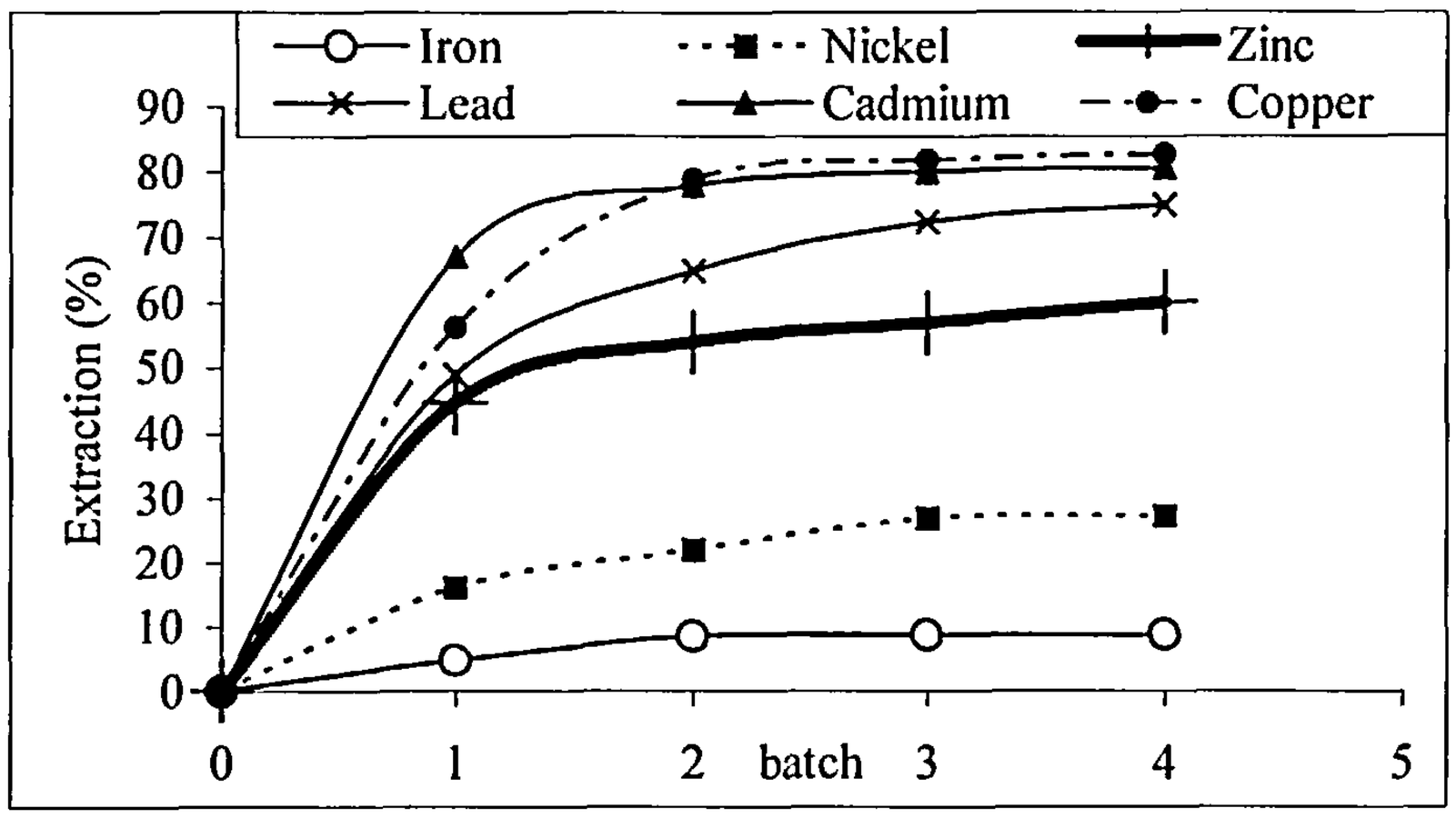

Figure 57: Extraction of lead, zinc, cadmium, nickel, copper and lead from Rotterdam Fly Ash in four batches using Hprps
(mean of two experiments presented in appendix 9 tables A9-28 to A9-33)

	Cu ($1050\ \mu g\ g^{-1}$)	Zn ($13500\ \mu g\ g^{-1}$)	Ni ($480\ \mu g\ g^{-1}$)	Pb ($4850\ \mu g\ g^{-1}$)	Fe ($8400\ \mu g\ g^{-1}$)	Cd ($310\ \mu g\ g^{-1}$)
Step 1	651 ± 17 (56.1%)	5232 ± 1013 (44.7%)	85 ± 6.4 (16.0%)	2330 ± 81 (48.9%)	430 ± 42 (4.7%)	163 ± 7 (67%)
Step 2	914 ± 30 (78.8%)	6309 ± 373 (53.8%)	116 ± 8 (21.9%)	3095 ± 102 (65.0%)	785 ± 137 (8.5%)	190 ± 10 (78%)
Step 3	948 ± 11 (81.8%)	6661 ± 498 (56.9%)	142 ± 5 (26.8%)	3456 ± 44 (72.5%)	794 ± 93 (8.6%)	195 ± 12 (80%)
Step 4	960 ± 16 (82.8%)	7054 ± 244 (69.2%)	144 ± 7 (27.2%)	3578 ± 1 (75.1%)	815 ± 91 (8.8%)	196 ± 7 (80.7%)

Table 34: Concentration of copper, zinc, nickel, lead, iron and cadmium extracted from Rotterdam Fly Ash in four steps using Hprps
(mean of two experiments presented in appendix 9 tables A9-28 to A9-33)

4.2.4 Conclusion

The higher contact time between the Rotterdam Fly ash and the extractants did improve the extraction of all metals using the three extractants.

Nickel is the least extracted of all the metals by H_2pnaa (14.3% ± 0.4) and Hprps (27.2% ± 1.3), but it is extracted equally well by Hacac or Hprps. The nickel complex with Hprps is more thermally stable (1.5% residue at 300°C) than that

formed with Hacac (28.6% residue at 300°C), therefore Hprps would be preferred for the extraction of nickel.

Optimum iron extraction is obtained using Hprps or Hacac but such extraction is not required and would constrain the extraction of other metals, H_2pnaa offers the advantage of not extracting this metal.

Copper extraction obtained using Hprps is good and reaches a plateau at 83% (92% of the "extractable" content), but the complex formed, $Cu(prps)_2$, is thermally unstable and some decomposition might have occurred that could explain the incomplete extraction. The figure for the extraction of copper using H_2pnaa (44% extraction after four steps) shows no indication of reaching a plateau so further steps might increase this result. Copper is the easiest of the metals to be extracted by H_2pnaa (27% in the first step) and as the complex formed with H_2pnaa is more thermally stable (1.6% at 192 °C) than that with Hprps, H_2pnaa would be preferred for copper extraction.

Cadmium is the easiest metal extracted by Hprps (67% in the first step) but its complex formed with Hprps decomposes at 300 °C leaving a 6.3% residue.

Lead is also easily extracted by Hprps, its extraction curve shows a smooth increase up to a plateau that correspond to the total extractable lead, and $Pb(PrPS)_2$ is thermally stable with only 1.5% residue left at 300 °C.

Zinc is the only metal from those studied that is fully extractable from the Rotterdam Fly ash, but after four steps complete extraction was not observed with the three extractants and no plateaus were reached. Zinc is most easily extracted by Hacac (29% in the first step), but the zinc complex is not thermally stable with 9.7% decomposition at 200°C. The best zinc extraction (69%) is obtained using Hprps and the complex formed is thermally stable (0.7% degradation at 300°C).

The complete extraction of the extractable lead and cadmium after two steps and the thermal stability of the complexes formed with nickel and zinc, makes Hprps the best of the three extractants studied. H_2pnaa is the preferred extractant for copper because of the thermal stability of the complex, and is also preferred in the presence of iron. Finally Hacac would not be selected for the extraction of metals from Rotterdam Fly ash because of thermally unstable complexes or a low extraction.

4.3 Orimulsion Ash

4.3.1 Analysis of Orimulsion Ash:

Analysis of the Orimulsion ash powder following acid digestion, table 35, gave results comparable to literature. [119]

Concentration μg g^{-1}	Zn	Cu	V	Fe	Mo	Ni	Cr
Digestion analysis	0	0	76990 ±314	3 356 ±190	444 ±16.6	20 573 ±377	93 ±10
Literature value [119]	60	30	76 000	3 000	>700	17 300	60

Table 35: Analysis of Orimulsion ash
(mean of three replicates presented in appendix 9 table A9-42)

The major components are magnesium sulphate and magnesium oxides, vanadium pentoxide, nickel sulphate, oxygen compounds and residual carbon. [37] X-Ray powder diffraction study of the fly ash showed an extremely complex system that is difficult to interpret with only some crystalline components giving lines that could not be easily assigned (appendix 10). Another study based on XRD and TG-DTA analysis [41] indicated that vanadium may be present as vanadium(IV) oxysulphate and the following major constituents were proposed (table 36).

Metal salts	$VOSO_4$	$(NH_4)_2Ni(SO_4)_2$	$(NH_4)_2Mg(SO_4)_2$
Composition	11.2%	6.8%	74.8%
Metal salts	$Al_2(SO_4)_3$	$(NH_4)_2Fe(SO_4)_2$	
Composition	10.1%	3.7%	

Table 36: Major constituent analysis of Orimulsion fly ash [41]

The sum of these constituents exceeds 100% but this could be due to the presence of some sulphates, sulphides or oxides of some of these metals. [41]

4.3.2 Sequential Extraction of Orimulsion Ash

The sequential extraction results obtained from Orimulsion ash powder (figure 58 and table 37) show that nickel and vanadium are both easily leachable in steps 1, 2 and 3 leaving no residue after step 3. This ease of leaching is one of the

major problems with the disposal of this ash. Because of their high concentration and easy leachability the SERVO process should extract both nickel and vanadium.

	V (77 000 µg g^{-1})	Ni (20 570 µg g^{-1})
Step 1 (available)	47262 ± 973 (59.8%)	14826 ± 301 (67.7%)
Step 2 (reducible)	22063 ± 797 (27.9%)	4261± 214 (19.5%)
Step 3 (oxidisable)	9669 ± 387 (12.2%)	2809 ± 109 (12.8%)
Step 4 (residual)	0	0
Total	78994	21896
Recovery (%)	102.6	106.5

Table 37: Sequential Extraction of Orimulsion Ash
(mean of five replicates presented in appendix 9 tables A9-43 and A9-44)

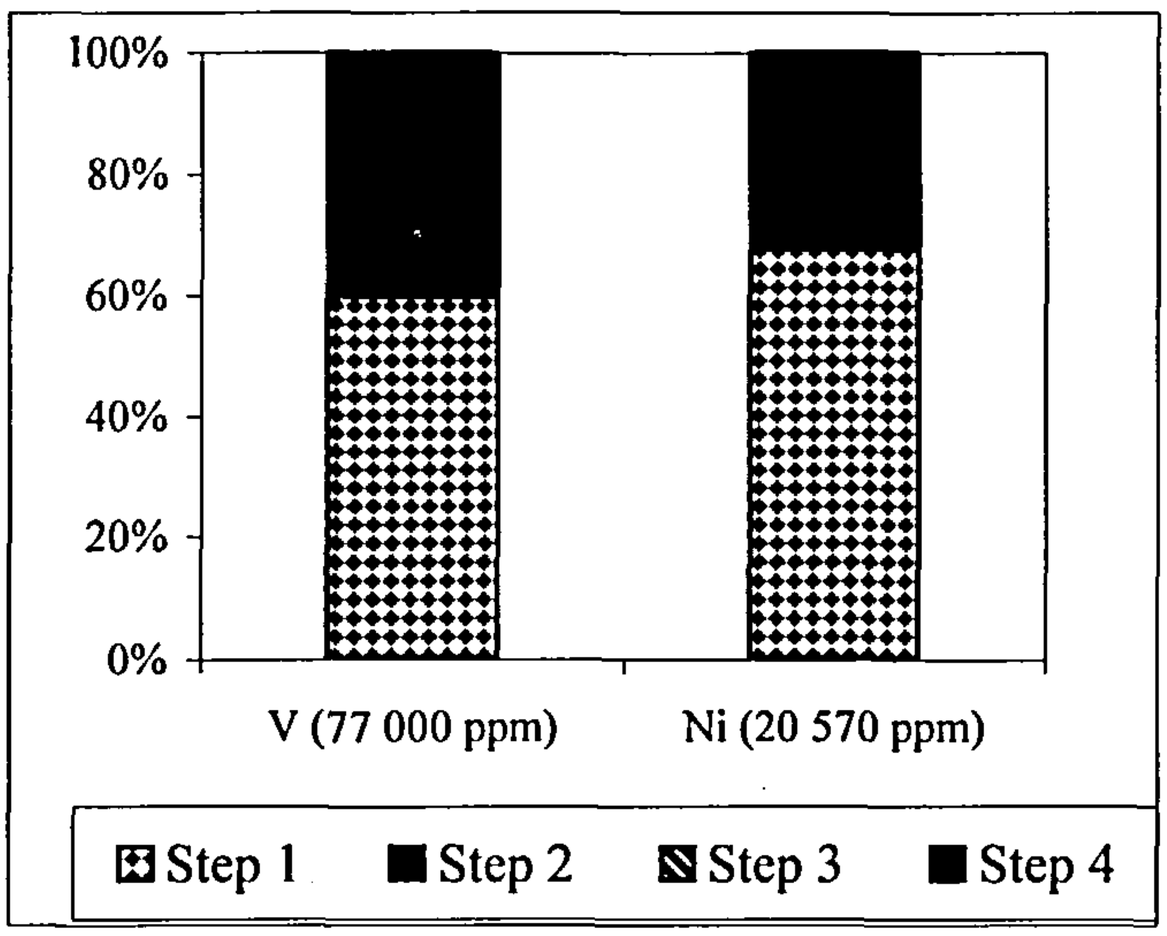

Figure 58: Sequential Extraction of Orimulsion Ash
(mean of five replicates presented in appendix 9 tables A9-43 and A9-44)

4.3.3 SERVO Extraction Results:

Studies were performed with a single extraction under the conditions specified in §3.3.4.2, using pellets prepared with 10% clay (figure 59 and table 38).

Both nickel and vanadium (82% and 80.0% respectively) are easily extracted with Hprps, with lower extractions for H_2pnaa (43% and 23% respectively) and Hacac (64% and 15% respectively).

	Hprps(μg g^{-1})	H_2pnaa(μg g^{-1})	Hacac(μg g^{-1})
Ni (20 600 μg g^{-1})	16920 ±1100 (82%)	8850 ±210 (43%)	13250 ± 1310 (64%)
V (77 000 μg g^{-1})	61950 ±2220 (80%)	17660 ±570 (23%)	11630 ±1480 (15%)

Table 38: Concentration of nickel and vanadium extracted from Orimulsion Ash in one step using Hprps, H_2pnaa and Hacac
(mean of two experiments presented in appendix 9 tables A9-45 to A9-50)

Scanning electronic microscope examination of the Orimulsion Ash residue after the SERVO treatment showed *no* increase of carbon content (appendix 10), so no absorption of ligand onto the surface of the Orimulsion Ash had occurred. Also the greenish colour of the Orimulsion Ash before processing completely disappears giving a light grey coloured residue.

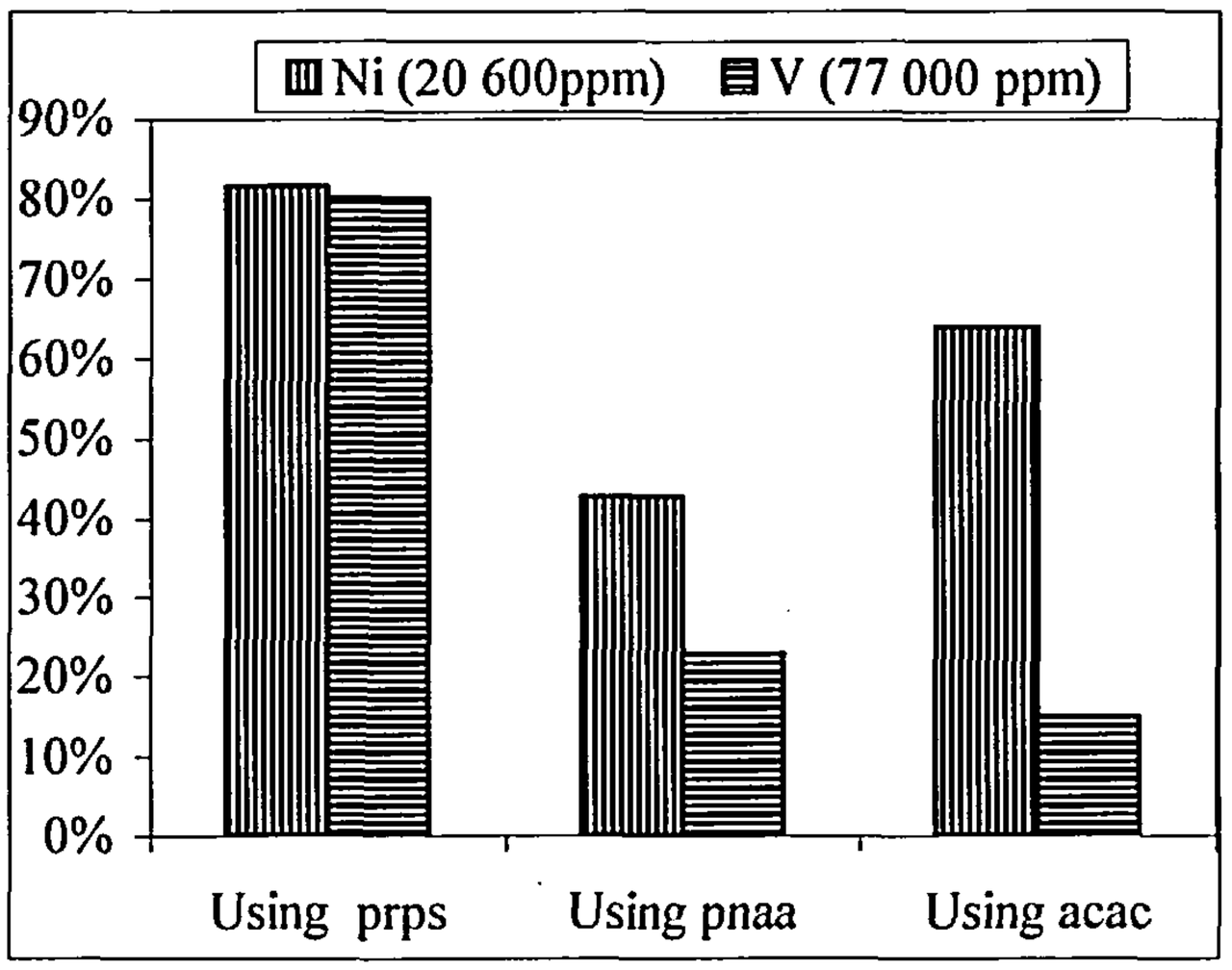

Figure 59: Results of a single extraction of Orimulsion Ash with Hprps, H_2pnaa and Hacac
(mean of two experiments presented in appendix 9 tables A9-45 to A9-50)

4.3.4 Conclusion:

These results are quite encouraging; however, speciation studies suggest that total extraction of these elements should be possible. Hprps extractant is the most thermally stable and is more effective than either Hacac or H_2pnaa as it is able to

extract most of the contaminating metals in one step, with the removal of vanadium (80.0% ±2.9) and nickel (81.6% ±5.3).

4.4 General Conclusion

From this series of experiments on the use of the SERVO process to treat different types of ash, some overall conclusions can be drawn.

4.4.1 Most suitable type of ash for the process

The type of ash that is most suitable for the process is the one that has the best physico-chemical characteristics of both the metal and the ash (e.g. porosity, pore size distribution, surface characteristics, adsorption parameters and solid structure, but also metal speciation). Therefore the physical comparison of the different ashes and their metal speciation are reviewed here to determine the matrix to which the SERVO process is most applicable.

(a) Puertollano Fly ash

As received, the Puertollano Fly ash showed low moisture content (1%) and the major crystalline phases were identified as 17% quartz (SiO_2), 3.2% mullite ($Al_6Si_2O_{13}$), 1.3% magnetite (Fe_3O_4) and 78.5% glass (aluminosilicate). The exchange capacity of these fly ashes is low because they are free of anhydrite ($CaSO_4$), lime (CaO), calcite ($CaCO_3$), and the feldspar group of potassium, calcium, and/or sodium aluminium silicates, and they are characterised by a relative low iron oxide content. [23] Particles of fly ash were agglomerated at room temperature using clay (2.5%) and distilled water to form pellets (diameter ~1-1.5mm) that were left at room temperature to dry for 24 hours. The moisture content of the pellets measured after 24 hours showed low moisture content (1%) and therefore they do not retain water. The results of the speciation studies showed that iron, lead, copper, and nickel are either present within the silicate phase of the fly ash or as resistant oxides so should be resistant to extraction using the SERVO process or leaching.

(b) MSW Rotterdam Fly ash:

MSW Rotterdam fly ashes as received were sieved, and particles in the range 1.4 – 2 mm used. Moisture content was about 5%, and the major crystalline phases

identified were more like a characteristic combustion fly ash with high concentrations of quartz, some anhydrite ($CaSO_4$), calcite ($CaCO_3$), and halite (NaCl). The speciation studies actually showed that most of the metals are easily leachable in the first three stages of the BCR procedure, except for nickel and iron that seem to be mainly contained in the silicate phase. Zinc is fully removed within the first three steps of the sequential procedure, making it the most suitable for extraction with the SERVO process. Zinc is also present at the highest concentration with most of it (57%) easily leached by dilute acetic acid (step 1 of BCR sequential procedure).

(c) Orimulsion ash:

The size distribution of the as received Orimulsion ash showed that more than 70% of the particles were in the range 0.5 - 4mm with less than 10% under 0.2 mm. The moisture content was about 15%, and the density 2.2. Sulphate is the major constituent of the ash and the metals examined (V and Ni) are also present as sulphates, and therefore easily leachable. [41] Particles of fly ash were agglomerated at room temperature using clay (10%) and distilled water to form pellets (diameter ~1-1.5mm) that were left at room temperature to dry for 24 hours. The sequential extraction results showed that vanadium and nickel are both easily leachable in step 1 (60% and 68% respectively), step 2 (28% and 19% respectively), and step 3 (12% and 13% respectively) leaving no residue after step 3.

From these results the least convenient material for the SERVO process is the Puertollano Fly ash, not only because of all metals are bound to the silicate phase, but also it requires pelletisation, is too dry, and has low permeability, aeration and porosity.

The second least convenient source is the MSW Rotterdam fly ash, with a typical fly ash physical structure with some anhydrite ($CaSO_4$), calcite ($CaCO_3$) and chloride that can retain metals and easily exchange with them. However no preparation is necessary and the MSW Rotterdam fly ash can be treated as received.

Overall the best material for the SERVO process is Orimulsion ash where all the metals studied are extractable in the first three steps of the BCR sequential extraction, and it has high permeability, aeration, porosity, and sorptive capacity.

4.4.2 Efficiency of the extractants

The efficiency of the three extractant is reviewed here. Table 39 shows the extractable elements from the MSW Rotterdam fly ash, Orimulsion ash, and Puertollano fly ash. To provide a better view of the elements extracted with the different ligands the following three tables provide a summary of the extraction results for the three different fly ashes.

Element ($\mu g\ g^{-1}$)	MSW Rotterdam fly ash	Puertollano fly ash	Orimulsion ash
Zn	14220 ±1189	74 ±13	0
Cu	850 ±84	0	0
Cd	256 ±8.4	0	0
Ni	300 ±15	0	20 573 ±377
Pb	3850 ±437	0	0
V	0	0	77 000 ±310

Table 39: Extractable elements (steps 1+2+3 from sequential extraction) from MSW Rotterdam fly ash, Puertollano fly ash and Orimulsion ash:

(a) Hprps

Hprps is able to remove extractable elements from a typical combustion fly ash structure (i.e. zinc from Puertollano fly ash). Extraction of nickel, cadmium, and zinc from MSW Rotterdam fly ash corresponds to the concentration of these elements present in Step 1 of the sequential extraction, (table 30). As nickel has the least concentration in this 'available' species (116 $\mu g\ g^{-1}$, 25.1%), its extraction is the lowest. In Orimulsion ash, nickel and vanadium (table 37) are mostly 'available' (14826 $\mu g\ g^{-1}$, 67.7% and 47262 $\mu g\ g^{-1}$, 59.8%), and their extractions with Hprps (table 38) is in the same order (16920 $\mu g\ g^{-1}$, 82% and 61959 $\mu g\ g^{-1}$, 80%), with some of the BCR 'reducible species' of nickel and vanadium also being extracted. Extraction of lead from MSW Rotterdam fly ash corresponds to the amount of this element present as 'available' and 'reducible' (BCR steps 1+2) and extraction of copper from MSW Rotterdam fly ash corresponds the amount present as 'available', 'reducible' and also 'oxidisable' (BCR steps 1+2+3).

Hprps will extract most of the nickel, vanadium, zinc and cadmium present as 'available' in the fly ash, but lead seems to have a better affinity with this sulfur donor ligand as the reducible lead is also extracted, finally copper is the element

preferred by Hprps as all the categories of 'available', 'reducible' and 'oxidisable' copper are removed.

Element ($\mu g\ g^{-1}$)	MSW Rotterdam fly ash	Puertollano fly ash	Orimulsion ash
Zn	6796 ± 378 (47.8%)	54.1 ±10.1 (73.1%)	0
Cu	571 ± 44 (67.2%)	0	0
Cd	234 ± 6 (91.4%)	0	0
Ni	100 ± 20 (33.3%)	0	16 920 ±1100 (82%)
Pb	1789 ± 270 (46.5%)	0	0
V	0	0	61 950 ±2220 (80%)

Table 40: Metal Extracted from MSW Rotterdam fly ash, Puertollano fly ash and Orimulsion ash using the SERVO process with Hprps after one step

It is now interesting to compare this last result with the thermal stability of the complexes formed between the elements and Hprps. Even though copper is the more widely extracted metal the complex formed, $Cu(prps)_2$, was shown to be thermally unstable (15% degradation), therefore careful temperature control will be required to recover the maximum amount of copper. $Zn(prps)_2$ is the most thermally stable complex, followed by $Pb(prps)_2$, $Ni(prps)_2$, $Cd(prps)_2$.

(b) H_2pnaa:

H_2pnaa is able to remove extractable elements from a typical combustion fly ash structure (i.e. zinc from Puertollano fly ash). In the MSW Rotterdam fly ash, nickel and cadmium are not extracted after one step, as might be expected. Zinc and copper are extracted but less than with Hprps. This can be explained by the fact that H_2pnaa is more selective and will only extract elements present in a certain form, in particular elements present as 'reducible' (BCR step 2). However, nickel and cadmium are also present in this material as 'available' and thus would have been expected to have been extracted. It has been shown that this extractant requires condensing in the pores of the matrix to complex with the metals, and maybe the

structure of the MSW Rotterdam fly ash might not allow this condensation readily to take place. In Orimulsion ash, nickel is still extracted but less than half of that with Hprps, and vanadium extraction is a quarter of that with Hprps. Orimulsion ash has a high porosity and will allow condensation of H_2pnaa in its pores.

$\mu g\ g^{-1}$	MSW Rotterdam fly ash	Puertollano fly ash	Orimulsion ash
Zn	4493 ± 344 (31.6%)	68.1±1.6 (92%))	0
Cu	241 ± 37 (38.4%)	0	0
Cd	0.0	0	0
Ni	0.0	0	8850 ±210 (43%)
Pb	0.0	0	0
V	0	0	17660 ±570 (23%)

Table 41: Metal Extracted from MSW Rotterdam fly ash, Puertollano fly ash and Orimulsion ash using the SERVO process with H_2pnaa after one step

Of all the elements studied, zinc in MSW Rotterdam fly ash and vanadium in Orimulsion ash are those that have the best affinity with H_2pnaa. Overall H_2pnaa is a poorer extractant than H_2prps, with lower extraction but is more selective.

(c) Hacac:

Hacac is not able to remove extractable elements from a typical combustion fly ash structure (no zinc extraction from Puertollano fly ash). It also extracted fewer elements than the other two compounds. Thus with the MSW Rotterdam fly ash, zinc and copper extraction are poorer than with Hprps and H_2pnaa, and with Orimulsion ash, nickel extraction is better, but vanadium extraction is lower than with H_2pnaa.

Element ($\mu g\ g^{-1}$)	MSW Rotterdam fly ash	Puertollano fly ash	Orimulsion ash
Zn	3387 ± 193 (23.8%)	0	0
Cu	58 ± 16 (7%)	0	0
Cd	0	0	0
Ni	0	0	13250 ± 1310 (64%)
Pb	0	0	0
V	0	0	11630 ±1480 (15%)

Table 42: Metal Extracted from MSW Rotterdam fly ash, Puertollano fly ash and Orimulsion ash using the SERVO process with Hacac after one step

Hacac is therefore the least efficient of the three ligands; and of the elements studied, zinc in MSW Rotterdam fly ash and nickel in Orimulsion ash are those that have the best affinity with Hacac.

Overall this study has shown that Hprps is the best of the three extractants. It is able to remove most of the extractable elements in a single step from the fly ashes that have a typical physico-chemical structure, and also gives good results with Orimulsion ash. A large variety of elements can be removed (Cd, Ni, Zn, Cu, Pb, V) with good efficiency in one step. The only disadvantage is that the synthetic route is difficult and the overall reagent cost will be high.

4.4.3 Overall conclusions

Originally devised for the treatment of low grade ores, the SERVO process has been studied for the treatment of different combustion fly ashes containing some new challenging metals to be extracted, i.e. cadmium, vanadium, lead, and zinc.

These sources differ in their structure: Orimulsion ash was obtained from combustion of a water-in-oil emulsion of a Venezuelan heavy crude oil with a magnesium stabiliser and the major components are sulphates (75%). Puertollano fly ash is a typical fly ash from Pulverised Coal Combustion with a low moisture content (1%)) and with 78.5% glass, and 17% quartz as major components. It also is free of anhydrite ($CaSO_4$), lime (CaO), and calcite ($CaCO_3$). MSW Rotterdam fly ash was obtained from a municipal waste incinerator and had a low moisture content (5%), also with major components of glass and quartz, but it also contained some anhydrite ($CaSO_4$), calcite ($CaCO_3$), and halite (NaCl).

The use of the SERVO process for the removal and recovery of heavy metals from these typical fly ashes has been demonstrated using the two ligands Hprps and H_2pnaa. Hprps can remove a larger variety of elements than H_2pnaa, with better extraction. The extraction of elements by Hacac is the lowest of the three ligands, therefore Hacac is not recommended for the process. Orimulsion ash has an open porous structure that is suitable for the SERVO process where most of the metals are present as sulphates or oxides. Typical fly ashes are also suitable for the SERVO process when they contain some kind of "absorbent" for metals such as anhydrite

($CaSO_4$), lime (CaO), and calcite ($CaCO_3$) and a minimum of moisture (5%).

These sources also differed in metal speciation. This is important as the extractants used in the SERVO process are weak organic acids without extensive oxidising or reducing properties, therefore the way in which the elements are contained within the fly ash determines the extractability. Thus the elements that were most easily extracted were found to be present mainly in those species contained in Steps 1 and 2 of the BCR procedure. This indicates that a detailed analysis (total analysis and a sequential analysis (BCR procedure)) of the elements is required to quantify the feasibility of the SERVO process.

Chapter 5: General Conclusions

5.1 Studies of Extractants

5.1.1 Thermal stability and volatility of the extractants and their metal complexes

Three ligands and their metal complexes have been synthesised to determine their thermal stability and volatility. A comparison of these data is undertaken here.

2,4-Pentanedione (acetylacetone, Hacac) is a commercially available liquid reagent (b.p. 140°C), volatile and thermally stable below 100°C. A wide range of volatile metal complexes can be produced and all are volatile above 165°C (table 43). However Hacac is not very selective and reacts readily with iron(III), which is a disadvantage in some applications like the extraction from sediments or soil where iron is naturally present in high concentration. However, the complexes are reasonably thermally stable at low temperature (below 170°C), and an order of stability has been established from the most stable to the least stable acetylacetonates: Hacac > $Cu(acac)_2$ > $Fe(acac)_3$ > $VO(acac)_2$ > $Ni(acac)_2$ > $Zn(acac)_2$ > $MoO_2(acac)_2$. Moreover, it has been shown that reduction of the nickel and copper acetylacetonates with hydrogen produces the metal in high purity.

Bis(pentane-2,4-dionato)propan-1,2-diimine, (H_2pnaa) is more suitable than H(acac) for application of the SERVO process to the extraction of metals from wastes, as it gives complete separation of the divalent metals from iron(III). It is a solid compound with melting point of 91°C, and easily synthesised from commercially available reagents (yield 73%) by slowly adding 1,2-diaminopropane (1 mol) to continuously stirred 2,4-pentanedione (2 mol). This ligand shows some thermal degradation at temperatures higher than 220°C to the extent of between 3 and 10% [110], and is sensitive to hydrolysis. The complexes of the divalent metals (table 43) are relatively thermally stable and can be reduced with hydrogen in the vapour phase. The temperature where all complexes are volatile is higher than the Hacac complexes (above 194°C), and the order of volatility is H_2pnaa > Cu(pnaa) > Co(pnaa) > Ni(pnaa), similar to that of the metal acetylacetonates.

Tetra-*iso*-propyldithiophosphoramide, $((i\text{-}Pr)_2PS)_2NH$, Hprps), is a solid compound (mp 173°C) prepared by a two-stage synthesis where the overall yield (57%) is low. But this ligand has good volatility and thermal stability with no observed degradation and also forms a wide range of volatile and thermally stable complexes with divalent metals (table 43). All the metal complexes are volatile at 190°C, and volatilisation is complete at 300°C or below. An order of volatility can be established: $Cd(prps)_2$ > Hprps > $Zn(prps)_2$ = $Cu(prps)_2$ > $Pb(prps)_2$ > $Co(prps)_2$ > $Ni(prps)_2$. To date hydrogen reduction of the metal complexes has not been successful and recovery of the metal and ligand has been achieved by absorption into dilute acid.

Metal	Compound:	Mp (°C)	Volatilisation Temperature (°C)	Stability (% residue)
-	Hacac	-	21 →100	1.4
Zn	$Zn(acac)_2$	137	122 → 200	9.7
Cu	$Cu(acac)_2$	127	163 →270	0.2
Ni	$Ni(acac)_2$	112	146 → 280	28.6
Fe	$Fe(acac)_3$	173	92 →275	3.6
Mo	$MoO_2(acac)_2$	Decompose at 210	130 →256	55.0
V	$VO(acac)_2$	Decompose at 172	131 →230	11.5
-	H_2pnaa	91	125 → 240	4.0
Cu	Cu(pnaa)	119	142 →292	1.6
Ni	Ni(pnaa)	145	194 →300	4.0
Co	Co(pnaa)	154	167 →292	0.4
-	Hprps	173	150 → 300	0.8
Zn	$Zn(PrPS)_2$	147	150 →300	0.7
Pb	$Pb(PrPS)_2$	125	175 →300	1.7
Cd	$Cd(PrPS)_2$	163	140 →300	7.6
Ni	$Ni(PrPS)_2$	175	190 →300	1.4
Co	$Co(PrPS)_2$	136	190 → 300	4.0
Cu	$Cu(PrPS)_2$	152	150 →300	14.9

Table 43: Summary of thermal properties of synthesised compounds

The volatility of the metal chelate is influenced in many ways [134]. The most important of these relates to the Lewis acidity of the metal and therefore its tendency to undergo interaction with Lewis-base sites involving nitrogen or oxygen donors in other molecules. This type of interaction is supported by the existence of stacking chains of the metal ions in crystal structures of ß-ketoimide compounds (figure 28, p88). This depresses the volatility of, in particular, cobalt and nickel thus resulting in the volatility order for Hacac, H_2pnaa and Hprps metal chelates: Zn > Cu > Co > Ni.

Hprps is the most thermally stable ligand with only 0.8% thermal degradation. It has been shown to complex with at least six metals of interest (Zn, Pb, Cd, Ni, Co, Cu) forming thermally stable complexes except for copper and cadmium that show 14.9% and 7.6% degradation respectively. Hacac is the second most thermally stable ligand with only 1.4% degradation. It can also complex with most metals, including iron(III) but only $Cu(acac)_2$ is thermally stable, as the other complexes prepared (Zn, Cu, Ni, Fe, Mo, V) show more than 10% degradation. The other disadvantage of this ligand is its ability to form a thermally stable complex with iron(III), that would be detrimental to the operation of the SERVO process as iron extraction would deplete the amount of extractant available in the system. H_2pnaa is the least stable ligand of the three studied with 4% thermal degradation and a tendency to hydrolysis. Only three metal complexes of the metals of interest have been successfully prepared for H_2pnaa (Co, Cu and Ni), and of these nickel shows some degradation (4%). During the extraction studies from Orimulsion ash, sediments, and the Rotterdam fly ash, H_2pnaa was also shown to complex with and extract zinc and vanadium, but the thermal stability of these complexes was not defined. Finally, H_2pnaa offers the advantage of being selective over iron(III).

Looking at the thermal properties, and the ability to form thermally stable complexes, Hprps is the preferred ligand, followed by H_2pnaa and finally Hacac.

5.1.2 Cost of Extractants

Another important factor in the evaluation of the best ligand for the feasible application of the SERVO process is the cost of the ligand. Therefore a ligand cost comparison has been calculated on the basis of the extraction of one mole of divalent metal. Prices and physical properties of the starting material were obtained from the

Aldrich catalogue (2002) and are shown in table 44. These prices are only applicable for bench scale quantities of starting materials, but the estimate based on these prices will nevertheless provide a cost for comparison that should be higher than the bulk price of starting materials. As a reminder, the production of one mole of H_2pnaa requires two moles of Hacac and one mole of 1,2 diaminopropane; and one mole of Hprps requires two moles of chlorodiisopropylphosphine, one mole of hexamethyldisilazane, two moles of sulphur and 14 moles of toluene (1.5 L). Moreover to extract one mole of divalent metal, two moles of Hacac, one mole of H_2pnaa and two moles of Hprps are required. The production yield is also considered in this calculation. Hacac ligand being the cheapest option, it will be considered as the basic price and the cost of the H_2pnaa and Hprps required for the extraction of one mole of divalent metal is compared relatively to Hacac in table 45.

Starting materials	Density ($g\ L^{-1}$)	Molecular weight ($g\ mol^{-1}$)	Price from Aldrich	Theoretical cost/mole (£)
2,4 pentanedione (Hacac)	975	100	£22 : 975g	2.26
1,2 diaminopropane	870	74.13	£22.5 : 870g	1.92
hexamethyldisilazane	765	161.4	£69.9 : 50g	225.63
chlorodiisopropyl-phosphine	959	152.61	£66 : 25g	403
sulphur powder, mesh-100	2360	32.07	£34.3 : 2000g	0.55
toluene, anhydrous, 99.8%	865	92.14	£175.3 : 20l	0.94

Table 44: Starting material costs from Sigma-Aldrich, 11/02 [146]

Ligand	Theoretical cost/mole (£)	Production Yield (%)	Cost/mole (£)	Cost required to extract 1 mole of divalent metal (£)	Relative cost
Hacac	2.26	100	2.26	4.5	1
H_2pnaa	6.4	73	8.8	8.8	2
Hprps	1046	57	1835	3670	814

Table 45: Relative ligand cost comparison.

From the results in table 45, Hprps is far more expensive than Hacac and H_2pnaa. Even if Hprps can complex with a wide range of divalent metals, and form volatile and thermally stable complexes, this cost factor is a big drawback for the use of Hprps in a SERVO pilot plant.

The cost of H_2pnaa (twice the cost of Hacac) means that this extractant can still be considered on cost to be an alternative to Hacac. It also offers the advantage, over Hacac, of being selective over ferric iron. Nevertheless, H_2pnaa shows some degradation [111], and some degradation products, both non-volatile or volatile, may accumulate in the sample being decontaminated causing additional costs of pollution control and affecting the quality of the final product.

5.1.3 Conclusion

In summary on the basis of their thermal properties, and the ability to form thermally stable complexes, Hprps is the preferred ligand, followed by H_2pnaa, and finally Hacac. On cost, Hacac is the cheapest ligand followed by H_2pnaa, twice as expensive, and H(prps) far more expensive (814 times than Hacac). The cost of H_2(pnaa) means that this is still comparable with H(acac), and has the advantage of selectivity over ferric iron. However although H(prps) can form volatile and thermally stable complexes with a range of divalent metals, the current cost of the extractant precludes its use in a SERVO pilot plant.

Therefore on balance H_2pnaa is the preferred extractant followed by Hacac and Hprps.

5.2 Physico-chemical characteristics of the contaminated sources studied and extraction of metals using SERVO process:

5.2.1 Physico-chemical characteristics of the contaminated sources

The extraction of metals present in the different sources depends on the physico-chemical characteristics of both the metal and the source. The mechanism of metal extraction by H_2pnaa in the SERVO process, proposed by Dr A.A. Pichugin [111], and confirmed by thermal analysis studies, suggests that the extractant condenses on the feed material where it reacts with the metal salts. It also showed that the quantity of H_2pnaa retained by the ore will depend on the physico-chemical

characteristics of the ore (e.g. porosity, pore size distribution, surface characteristics, adsorption parameters and structure of the solid).

Therefore the physical comparison of the different matrices (sediments, Orimulsion ash, Rotterdam fly ash and Puertollano fly ash) and the metal speciation in these samples are reviewed and summarised in table 46 to determine the most appropriate source for the SERVO process.

The least convenient matrix for the SERVO process is the Puertollano Fly ash, not only because all the metals are bound to the silicate phase, but also it requires pelletisation, has a low moisture content, and low exchange capacity, permeability, aeration and porosity.

The second least convenient matrix is the Rotterdam Fly Ash, this has a typical physical structure of a fly ash with some anhydrite ($CaSO_4$), calcite ($CaCO_3$) and chloride that can retain the available metals and easily exchange with them. However apart from size reduction no other sample preparation is necessary and the fly ash can be treated as received.

The second best matrix are the canal sediments that have high porosity, permeability, aeration and sorptive capacity, abundant organic matter and clay, significant amounts of carbonates, sulphates, and oxides and most of the metals are readily available for leaching.

Finally the best matrix is the Orimulsion ash, as it is mainly made of sulphates, has all the metals studied available of extraction, a high permeability, aeration, porosity, and sorptive capacity.

Matrices as used in SERVO process	Puertollano Fly ash	MSW Rotterdam Fly ash	Sediments	Orimulsion ash
Form and size	Pellets (2.5% Clay) 1-1.5 mm	Agglomerates 1.4-2 mm	Agglomerates 710 µm-1 mm	Pellets (10% clay) 1-1.5 mm
Moisture content	1%	5%	5%	5%
Permeability; Aeration and porosity; and sorptive capacity	Low	Low	High	High
Organic Matter	Absent	Absent	Abundant	Absent
Clay	Low	Low	Abundant	Low
Oxide	Low	Abundant	High	High
Carbonate	Absent	Low ($CaCO_3$)	High ($CaCO_3$)	Absent to low
Anions (phosphate, nitrate, chloride, sulphate)	Low	Low $CaSO_4$ High Cl^-	High	Abundant SO_4^{2-}
Metal available to SERVO process (%)*	Zn	Pb Cd Zn Cu Ni	Ni Cu Zn	V Ni
step 1:	1	17.3 65.8 57 20.1 25.1	42 0 27.2	59.8 67.7
step 2:	0.6	23.3 7.4 29 16 24.1	19 0 30.2	27.9 19.5
step 3:	4.6	41 2.9 14 55 15.4	39 83.3 30.5	12.2 12.8
steps 1+2+3	6.2	81.6 76 100 91.3 64.6	100 83.3 84.6	100 100

Table 46: physical characteristics of the different matrices as used in the SERVO process

* data from speciation studies

5.2.2 SERVO process extraction results:

A study with the modified TGA equipment confirmed the condensation of H_2pnaa in the pore structure of the clay where the complexation takes place. Moreover it was shown that the adsorption rate of the extractant though the clay is dependent on the temperature. Extraction studies with the modified TGA shows that H_2pnaa requires a long contact time with the clay and several cycles of extraction are required to obtain significant extraction. The extraction of copper is much improved by mixing H_2pnaa with the clay before running the experiment, but repeating the process ten times using a higher temperature in the reactor 2 did not release more Cu(pnaa).

In the case of the sediments, even though Hprps and Hacac extractants required only a single heating cycle of 5 hours, H_2pnaa remains the ligand of choice for the SERVO process. The reasons for this preference are that Hprps does not extract all the extractable copper and only a little nickel is removed, and Hacac extracts all the iron and no nickel. Despite its longer heating cycle, H_2pnaa removed all the available zinc and copper, did not extract iron, and the highest extraction of nickel (28%) was obtained.

The use of the SERVO process for the removal of heavy metals from typical fly ashes and Orimulsion ash is feasible using the two ligands, Hprps or H_2pnaa. Hprps can remove a larger variety of elements than H_2pnaa, with a better extraction and is therefore preferred. The extraction of elements obtained by Hacac is the lowest obtained from the three ligands, therefore Hacac is not recommended for the extraction of metals from fly ashes.

5.2.3 Conclusion

The SERVO process has been applied to four different sources contaminated by heavy metals that had different physico-chemical characteristics. These sources can be ranked from the best to the least applicable: Orimulsion ash > canal sediments > MSW Rotterdam fly ash > Puertollano fly ash. For the fly ashes, of the three ligands Hprps is the best followed by H_2pnaa. Hacac is not recommended for these sources because metal extraction was too low. For the canal sediments, H_2pnaa is the best followed by Hprps. Hacac is also not recommended for sediments because of its ability to remove iron(III).

Therefore balancing their thermal properties, ability to form thermally stable metal complexes and cost, and the extraction results obtained on the different sources studied, H_2pnaa is the preferred extractant followed by Hprps and Hacac.

5.3 Cost of the SERVO process and comparison to other relevant technologies

In general, costs are site-specific and based on parameters such as the size of the affected area, the characteristics of the contaminants, the required clean-up standards, the level of health and safety protection during the remediation, the type and number of chemical analyses, and any long-term, post-remedial actions required. Costs can generally be broken down into capital costs and operating costs.

Capital costs constitute one-time costs that occur at the beginning of a project and depend on the size of the plant. They include cost of all the installed equipment, construction of buildings and provision of facilities such as on-site labs and offices, one-off costs involved with obtaining licenses, site characterization and preparation, bench scale treatability tests, design, engineering, start-up, etc.

Operating costs include pre- and post-treatments (excavation and dewatering, replacement of cleaned sediments), labour, utilities, sampling and analysis, consumables, equipment repair and maintenance, waste disposal and transportation, project management, quality assurance measures, insurance, and leases.

Total costs for a full-scale remediation are found by adding the capital, operating, and also include contingency costs associated with unforeseen difficulties.

This section describes the budget cost estimates (±20% accuracy) to process 10,000 tons of sediments on site using the extractant H_2pnaa. The SERVO process costs provided the best basis for projecting the costs for a remediation operation. Only an approximate evaluation of capital and operating costs will be carried out based on catalogue reagent prices, process energy requirements and a typical cost breakdown from nickel laterite processing [147] and acid leaching. [146]

The cost of competing remediation technologies were standardised to the same currency and quantity of sediments processed to make them comparable with the SERVO process costs.

5.3.1 General Assumptions

It is assumed that the plant would be used for sites up to 10,000 tons, its performance will be maintained at 20 tons/hr, and will operate 330 days per annum. The process will operate on site and no sediment transportation is required. Power will be provided to the pilot plant substation within the plant battery limit. Nitrogen and hydrogen will be available at the plant battery limit. Reagents will be self-contained with regard to administration and engineering requirements. The battery limits include the following inputs: sediments on storage site, tonnage nitrogen and hydrogen, power, and bulk reagents; and the output: metal and residues.

Implicit in the scale-up cost projection is the assumption that some bench scale treatability tests on a 40 kg size reactor will have been performed to confirm the best operational conditions and the extraction results obtained in the present work (small scale) and that the plant would be required to meet similar extraction results to those obtained in the present work for the production of metal from sediments using the extractant H_2pnaa. For the purposes of this exercise zinc was considered as the metal to be recovered from canal sediments.

Some pre-treatment may be required on the sediments before applying the SERVO process. These may involve only physical separation like excavation, dewatering to remove most of the water present, and screening to remove oversize debris (if any). It is important to recover and possibly treat the water from the dewatering process because it may contain elevated levels of soluble and suspended metals. Commonly used processes for dewatering include filtration, expression, and centrifugation. A combination of these methods typically is used to obtain successively drier solids. The projected costs for these physical separation processes (dewatering and screening) were evaluated by the ESTCP [148]. This cost, for the treatment of 10,000 tons of sediments at a processing rate of 20 tons/hr, would be approximately £7.5/ton.

Total costs for technology applications were standardised for comparability, with adjustments made for both currency and quantity of sediments treated. It was assumed that 1$ = £0.5973, and 10,000 tons = 6850 cu.yd. No adjustments were made for time or location (using an inflation factor for time and a cost factor for location) [148, 149]. Moreover there are some correlation factors between technologies costs and quantity treated [150], as the unit costs decrease with increase

in the quantity treated. Again when adjustment was made to the amount of sediment treated, there was no consideration to these factors.

5.3.2 SERVO process costs

5.3.2.1 Capital cost

Different SERVO systems may vary in the manner in which the soils are transported through the second thermal reactor (mechanical design features), the method used to heat the soils (direct or indirect, heated or fired); the temperature at which the thermal reactors operate (process operating conditions); the time required to treat the soils (residence time); and the off-gas treatment used to control emissions (air pollution control system), and to method used to reduce the metal complexes to metal and recycle the ligand. Moreover systems may either be stationary facilities or mobile units. Various types of thermal reactors are currently used in thermal desorption technologies and are available in four configurations: rotary dryer, asphalt plant aggregate dryer, thermal screw and conveyor furnace. [151] Among these four types of desorption units, the latter seems to have the mechanical design features and process operating conditions that best fit the SERVO process requirements. A conveyor furnace uses a flexible metal belt to convey the sample through the heating chamber. A thin layer of sample is spread evenly over the belt. As the belt moves through the system, agitators lift the belt and turn the sample to enhance heat transfer. The conveyor furnace can heat the sample to temperatures from 150 to 430°C. This system is mobile and can treat 5-10 tons of sample per hour. A Low Temperature Thermal Desorption (LTTD) system using a conveyor furnace could be the basis for the SERVO process, and so the capital cost for the SERVO process will be based on the LTTD system. This was estimated to be £1 152 390 for excavation, thermal desorption and waste container management of sediments. [152]

5.3.2.2 Operating costs

Operating costs include physical separation processes cost, energy costs, reagent costs, maintenance, labour, administration and depreciation costs. The cost for physical separation processes (excavation, dewatering and screening) was estimated by the ESTCP to be £7.5/ton [146].

Thus the cost for 10,000 tons of sediments will be £74 700. It is assumed that the sediments will be dried to the same level as that obtained on the bench scale, i.e. to 5% moisture content.

Energy costs include the energy required to evaporate H_2pnaa, and to provide the heat required for the process. The energy cost was taken as an average unit cost in the U.K. as £0.055 $(kW\ hr)^{-1}$, with1 kW hr = 3.6×10^6 J.

Energy requirement for the evaporation of H_2pnaa has been assessed on the basis of the heat of evaporation of the extractant (112240 J/mol). [111]

Considering extraction of 95% zinc from 10 000 tons of sediments containing 0.855 % zinc, the production of zinc by the SERVO process would be:

$$10\,000\times\frac{0.855}{100}\times\frac{95}{100}=81225\text{ kg of zinc or }\frac{81225}{65.4}=124\,200\ \textit{moles}\text{ of zinc.}$$

So the energy requirement for the evaporation of the H_2pnaa used to process 10 000 tons of sediments is: $\frac{124\,200}{3.6\times10^6}\times112240=$ 38 722 kW hr.

Energy requirements to heat the SERVO process were estimated by Pichugin [111] to be about 7.02 kW hr/kg of metal produced. Therefore the energy requirements to heat 10 000 tons of sediments in the SERVO process is: 81 $225\times7.02=$ 57 020 kW hr.

Total energy cost is: (38 722 + 57 020) × 0.055 = £5 266

The H_2pnaa reagent cost for 1 mole of metal extracted is £8.8. Considering four heating cycles of 5 hours, with 4% H_2pnaa degradation in each cycle, this corresponds to 16% H_2pnaa degradation overall. With the possibility of recycling, the reagent costs for the extraction of 124 200 moles of zinc: $\frac{16}{100}\times124\,200\times8.8=$ £175 000

Maintenance, labour, operating supplies and depreciation costs for SERVO pilot plant have been estimated on the basis of the typical operating costs for electric furnace smelting for Ni-Fe alloy. [147]

The different operating costs detailed above have been summarised in table 47.

Operating costs	Cost for 10 000 tons of Sediments processed
Physical separation processes	£75 700
Energy costs	£5 266
H_2pnaa cost	£175 000
Maintenance and material	£1 572
Labour	£9 700
Operating supplies	£1 940
Contingency	£15 816
Indirect costs	£15 816
Depreciation (straight line over 5 years)	£63 070
Total operating costs	£ 363 750

Table 47: Operating cost of the SERVO process for 10 000 tons of sediments treated

The total cost to clean 10 000 tons of sediments using the SERVO process with H_2pnaa extractant is obtained by adding the capital cost and the operating costs: £1 152 390 + £363 750 = £1 516 140

Any zinc recovered by the SERVO process can be considered as a credit to the operating cost. This credit could be attributed to the sale of 81 220 kg of zinc produced at the current cost of £600/ton, which means a credit of £48 735.

5.3.3 Competing technologies

Cost of the following remediation technologies that could also be used to treat sediments contaminated with heavy metals have been standardised to the same currency (£) and quantity of sediments or soil processed (10 000 tons) to make them comparable with the SERVO process.

5.2.3.1 Dredging and Offsite disposal [148]

This is the simplest technique and would consist initially of dredging and dewatering the sediments. This would result in a very significant reduction in the mass of the contaminants. The sediments would then be transported off-site for disposal at a permitted landfill as hazardous material.

It must be mentioned that the landfill tax applied in this American reference, [148] in 1997, is different from that in the UK. The landfill tax was set up in 1996 by the UK government at an initial cost of £7/ton, and raised annually by £1 until April 2004. From April 2004, the annual increase will be £3-4/ton, until it reaches a rate of £35/ton in the medium to long term. Another important factor is that the number of hazardous waste sites in the UK is tending to decrease; so as a treatment option landfill is not viable in the long-term.

Capital costs $262 395 = £ 156 730

Operating costs (10 000 tons): $2 095 335 = £ 1 252 544

Total Project Cost (10 000 tons): £1 408 274

5.2.3.2 Containment/capping [153]

As an example of this process the cost data for a project concerning 2600 cu yd (3800 tons) of sediments (sediments and the upper six inches of underlying clay) excavated from Bayou Verdine (Louisiana) and containing elevated concentrations of 1,2-dichloroethane (EDC, 11400 $\mu g\ g^{-1}$) and also some zinc (620 $\mu g\ g^{-1}$) in a relatively localized portion (reach 2) of the Site Bayou Verdine has been chosen. The concentration for removal was set at 289 $\mu g\ g^{-1}$ EDC. Three layers were specified to cover the sediments, from the bottom up: a barrier layer directly on top of the clay to impede the vertical movement of water and sediments; a protective layer to protect the barrier layer; and a sand/silt cover material to provide a substrate with a texture similar to natural conditions (minimum 1 ft thick). These layers form a physical, hydraulic and chemical resistant barrier that separates the contaminated sediments from the overlying water column and the biota in the river.

Capital costs $ 1 070 000 = £ 639 111

Operating costs (3800 tons): $ 25000 = £ 149 325

Total Project Cost (10 000 tons): £ 1 032 072

5.2.3.3 HCl acid leaching process [148]

This chosen example here concerned 835 tons of soil containing 4,117 $\mu g\ g^{-1}$ of lead in Louisiana processed by physical separation and hydrochloric acid leaching

at an average processing rate of 6.3 tons/hour over a period of 18 days. This system consistently met both the total and TCLP lead targets. The acid leaching was performed as a continuous process and involved four vessels. In the leaching tank the acid solution was mixed with the soil to leach out the metals at a pH of 1.4 to 1.5. It removed an average of 96% of the total lead. Precipitation of lead was conducted efficiently at a pH of around 9.5 by adding sodium hydroxide. About 7% of the lead was collected in the precipitate sludge.

Capital Costs $ 58 450= £ 34 912

Operating costs (835 tons): $50 100 = £ 26 720

Total Project Cost (10 000 tons): £ 634 912

5.2.3.4 Electrokinetic processing [155]

A site in California (½ acre in area) where electroplating and metal finishing operations had been conducted was selected for demonstration of electrokinetic remediation in 1994. This demonstration was carried out on 1 000 cu yd (1460 tons) of a soil matrix consisting of a mixture of 85% sand, 7% gravel, 6% silt, 1% clay, with a pH of 5.84, an hydraulic conductivity of 0.045 cm sec^{-1}, and a CEC of 3.9. Levels of chromium and cadmium were up to 25,100 μg g^{-1} and 1,810 μg g^{-1}, respectively.

The available literature from the equipment manufacturer typically quote costs only in terms of power and chemical amendments used. These costs reflect full-scale costs extrapolated from the costs incurred on the demonstration-scale project. Also, these costs do not reflect turnkey costs because effective treatment was not achieved during the demonstration.

Total Capital costs $890,988 = £532 187

Total Operating costs (1460 tons) $302,062 = £180 421

Total Project Cost (10 000 tons): £1 768 075

5.2.3.5 In Situ Lead Fixation - Fox River, Wisconsin [154]

An *in-situ* underwater treatment system was designed to fix contamination by lead to the sediment of the Fox River (Wisconsin, USA), and avoid complications and cost of dealing with removal of contaminated sediments. This was a relatively small-scale treatment involving 500 tons of sediment. First, cofferdams were driven into the bedrock to a total depth of 15 feet (the water depth ranged from 7 to 8 feet in the treatment area) and sealed. Water was then pumped out of the cofferdams to maintain an inward gradient. Next, a mixture of chemical additives: fertilizer grade phosphate, magnesium oxide, and a reactive form of limestone, were incorporated into the sediment. Adequate time was allowed for complete reaction, and then the stabilized sediment was dredged and put into a containment basin, from which the pore water was allowed to drain and the stabilized sediment was then sent to a landfill as a non-hazardous waste in USA. The leachable lead from the stabilized sediments was reduced to less than 0.26% of the highest observed untreated value. It must be mentioned that this value would not be allowed by the hazardous waste regulations in the UK (UK ICRCL threshold values for lead are between 500-2000 g/kg [appendix 2]).

Total Capital costs $100 000 = £59 730

Total Operating costs (500 tons) $32 000 = £19 114

Total Project Cost (10 000 tons): £442 000

5.2.3.7 Comparison of Technologies:

The cost of the above technologies have been normalised to provide a standard basis for comparison with the SERVO process and the results ranked from the cheapest to the most expensive in table 48.

From this table, the cheapest option is the *in-situ* fixation, mainly due to the fact that fixation uses simpler equipment and therefore incurs lower capital costs. But the strength of the solidified sediment is important to prevent its erosion and the release of contaminants over time. Since mixing and curing temperature are the principal factors that influence solidified sediment strength, it is difficult to control *in-situ* solidification.

Technologies	Capital costs	Operating costs	Total cost
In Situ Fixation (lead)	59 730	382 270	442 000
HCl acid leaching process	34 912	600 000	634 912
Containment/capping	639 111	392 961	1 032 072
Dredging and offsite disposal	156 730	1 251 544	1 408 274
SERVO process	**1 152 390**	**363 750**	**1 516 140**
Electrokinetic	532 187	1 235 888	1 768 075

Table 48: Comparison of technologies costs for 10 000 tons (£)

The second cheapest treatment is acid leaching that removes the heavy metals off-site, and this eliminates any further leaching problems and long term maintenance and monitoring of the site. Acid leaching uses simple equipment and therefore incurs lower capital costs, however although hydrochloric acid is cheap it is also corrosive that can lead to problems with equipment selection. However the treated soil still retains its loose texture and can be returned on site and recycled metals can be recovered and considered as a credit to the operating cost. However, the efficacy of this acid treatment will vary with soil type, especially the content of acid-consuming minerals; the metal species and complexing characteristics, and the capability of metal oxidation.

The third cheapest treatment is on-site containment and capping. However, the potential for erosion and compatibility with site conditions would have to be determined prior to placement of the barrier layers. Incomplete coverage and technical difficulties in placing the cover is also a concern, especially in sites that are difficult to reach. Long term maintenance and monitoring of the cover is subject to estimation and might lead to variation in costs.

Dredging and off-site disposal is often the preferred option at sites with less than about 2,600 tons of soil, because it is the cheapest option, and it offers a rapid

and cost effective process that completely remove the liability. [148] At larger sites, on-site technologies become cheaper because the fixed costs for site preparation, plant equipment, etc., are spread over a larger tonnage of soil processed. But the number of hazardous waste sites in the UK are tending to decrease; and the landfill tax cost is increasing drastically until it reaches a rate of £35 /ton in the medium to long term. So overall landfill is not a viable option in the long-term.

The SERVO process cost is in the same range as the dredging and offsite disposal technique. It offers the advantage of removing and recovering soil heavy metals, and eliminating any further leaching problem and long term maintenance and monitoring. The treated sediment still retains its texture and can be returned on site. At larger sites, the capital cost could be spread over the greater amount of sediments processed, and thus the unit cost per ton of sediments processed would be expected to be much lower. The processing rate, which affects the costs incurred for labour, utilities, chemicals and other consumable supplies, depends on type of sediment. Thus some reductions may be possible. Bulk purchases of consumables may also be feasible for larger operations. Any recycled metals recovered by the SERVO process are considered as a credit to the variable cost, and higher value metal production and sale would reduce further the cost. SERVO process remains a process that has been only tested at a bench scale and a small pilot scale is required to confirm the extraction obtained here.

Electrokinetic treatment is also a new technology that has only been tested on a small scale (1460 tons). Issues such as control of contaminant movement, ability to achieve clean-up goals, by-product formation, and treatment effects on the soil matrix have not been addressed. Like the SERVO process, electrokinetic processing will eliminate the long-term liability that is incurred by land-filling of contaminants. Nevertheless, this is an on-site treatment that remains more expensive than dredging and off-site disposal, and the unit cost per ton would not decrease much for application on a larger scale, because the capital cost is not important compared to operating cost that represents more than 2/3 of the total cost.

5.3.4 Conclusion

The total cost for the SERVO process to treat 10 000 tons of sediment is estimated at an average cost of £1 516 000, or £151.6/ton. Several benefits of the SERVO process may outweigh the cost disadvantage over other remediation processes, irrespective of the amount of soil requiring processing, and these should be considered by sites trying to identify the best alternative.

With solidification and containment/capping techniques, although the metals have been immobilized or contained, the liability remains. With extraction technologies like the SERVO process, the metals should be removed, recovered, and reused and any recycled metals would reduce further the cost. Sediments treated with the SERVO process are physically unchanged and can be recycled to the site, whereas solidification may result in a hardened treated material that is physically unsuitable for replacement.

Due to issues of technical feasibility, containment and capping is often more difficult to implement than the dredging alternatives when sites are not easily reached. After dredging the SERVO process can be applied instead of sending the material to off-site disposal thus satisfying future demands to reduce land-filling.

Electrokinetic offers the advantages of an extraction process, but it stays an expensive and unproven technology for metal removal.

Like the SERVO process, acid leaching also offers the same advantages of an extraction process and for both techniques the efficacy will vary with soil type, contained metal species, and metal speciation characteristics. Acid leaching being less expensive and being an established technology would generally be preferred over the SERVO process unless the sample contained a large proportion of acid-consuming minerals than could lead to downstream processing and waste disposal difficulties.

5.4 Future Studies

New methods for fly ash pelletization need to be considered to improve the extraction rate of the metals from fly ash and render them as porous as the Orimulsion ash pellets.

Although extraction of metals has been shown to be possible for new contaminated sources with different physico-chemical characteristics, the recovery of

the metals remains a problem. A study of the possible thermal separation of metals by careful temperature control needs to be considered, and other separation techniques need to be investigated to separate the metal complexes from each other and hence recycle pure extractant and pure metals for possible reuse.

If hydrogen reduction is used as a means of metal recovery, then the extractants can be recycled and reused. In this case the carrier gas will be a mixture of hydrogen and nitrogen, so the influence of hydrogen in the carrier gas on metal extraction and the reagents H_2pnaa and Hprps needs to be investigated. Earlier studies [134] have shown that the mixture of hydrogen and nitrogen has no effect on the extraction of copper with Hacac.

Recovery of metals from complexes with Hprps is also required to demonstrate the overall feasibility of the process using this extractant. However as Hprps is too expensive for the metals currently being studied, the extraction of more valuable metals should be investigated.

The contact residence time between the extractant and the feed to be decontaminated is a key parameter affecting the degree to which decontamination is achievable. This time depends upon the design and operation of the system, therefore optimization of the SERVO process reactors to improve the contact between the feed and the extractant could increase productivity.

Pilot testing of metal-contaminated soil, in which a quantity of soil from the site is processed through the SERVO system is required. The results of preliminary testing of soil samples should identify the relevant operating conditions, and examination of the overall performance records should indicate the effectiveness of the system. In any pilot testing it is important to ensure that the soil tested is representative of average conditions and that enough samples are analyzed before and after treatment to determine with confidence the overall process operating conditions.

References

[1] Stanners D. and Bourdeau P. "Soil, Europe's Environment: The Dobris Assessment", European Environment Agency, 2nd reprint. Chapter 7, (1995) Available from internet URL: http://reports.eea.eu.int

[2] Tyler G. and Miller J.R., "Living in the Environment" 11th edition, Wadsworth Publishing Company, Belmont, Calif., Chapter 1: Population, Resources, Environmental Degradation, and Pollution; 2-34 (2000).

[3] Miscra K.B. "Clean Production: Environmental and Economic Perspectives". Springer, Berlin and London: Chapter 1, 1-109 (1996).

[4] As reference 2, Chapter 22: Economics and Environment, 578-606.

[5] Rulkens W.H, Grotenhuis J.T.C. and Tichy R. "Methods for Cleaning Contaminated Soils and Sediments" in Heavy Metals: Problems and Solutions, Springer-Verlag, Berlin and New York: 165-191 (1995).

[6] EPA "Remediation of Contaminated Sediments", EPA/625/6-91/028, (1991).

[7] Greenwood N.N. and Earnshaw A. "Chemistry of the Elements" 2nd Edition, Pergamon Press, 355, (1997).

[8] Pendias A. K. "Trace Element in Soils and Plants", 2nd edition, CRC Press, Boca Raton, Fl. USA, 23-43, (1992).

[9] Velde B. "Introduction to Clay Minerals: Chemistry, Origins, Uses, and Environmental Significance" Chapman & Hall, Boston, Mass., Butterworth-Heinemann, 34-77, (1992).

[10] McLaren R.G. and Cameron K.C "Soil Science: Sustainable Production and Environmental Protection", 2nd edition, Oxford University Press, Chapter 5: Physical and Mechanical Characteristic of Soil, 57-71, (1996).

[11] Singer M.J. and Munns D.N. "Soils an Introduction" 3rd edition, Prentice-Hall, 43, (1996).

[12] Brady Nyle C. and Weil Ray R., "The Nature and Properties of Soils, 12th edition, Prentice Hall, Chapter 12: Soil Organic Matter, 446-489, (1999).

[13] Sparks D.L. "Environmental Soil Chemistry", Academic Press, Chapter 5: Ion Exchange Processes, 309-312, (1995).

[14] Vaugham D.J. and Pattrick R.A.D. "Mineral Surfaces", Chapman & Hall, London, Chapter 8, 265-283, (1995).

[15] Miller R.W and Gardinier D.T. "Soil in our Environment", 8th edition, Prentice Hall, Upper Saddle River, N.J. Chapter 5: Soil Colloids and Chemical Properties, 145-173, (1998).

[16] Sparks D.L. "Environmental Soil Chemistry", Academic Press, Chapter 8: Redox Chemistry of Soils, 187-202, (1995).

[17] Joshi R.C. and Lohtia R.P. "Fly Ash in Concrete, Production, Properties, and Uses" edited by V.M. Malhothra, Advanced Concrete Technology Program, CANMET, Ottawa, Ontario, Canada, (Gordon and Breach Science Publishers), Vol 2, Chapter 1, 1-11, (1997).

[18] Meyers R. A. "The Wiley Encyclopedia of Environmental Pollution and Cleanup", John Wiley & Sons, New York; Chichester: Vol 1, 397-417, (1999).

[19] Idem, Vol. 2, 1714-1718.

[20] Elliot T.C "Standard Handbook of Power Plant Engineering", McGraw-Hill, Section 3, Chapter 3.5: Wood Fuel and Wood Handling, 3.109-3.111, (1989).

[21] Idem, Section 1, Chapter1.8: Stokers, 1.183-1.206 (1989)

[22] As reference [18], Vol 2, Chapter 2, 15-42 (1995)

[23] Querol X., Umana J.C., Alastuey A., Bertrana C., Lopez-Soler A. and Plana F. "Physico-chemical characterization of Spanish fly ashes" *Energy Sources*, 21 (10) 883-898, (1999).

[24] As reference [17], Vol 2, 1791-1796.

[25] Idem, Vol 1, 751-754.

[26] Idem, Vol 2, 1036-1042.

[27] As reference [19], Section 3, Chapter 3.6: Waste Fuels, their Preparation, Handling and Firing, 3.117-3.151.

[28] As reference [19], Vol 1, 754-761.

[29] Poran C. J. and Ahtchi-Ali F., "Properties of Solid Waste Incinerator Fly Ash", *J. Geotech. Eng*, 115, (8), 1118-1133 (1989).

[30] Chermisinoff P. "Waste Incineration Handbook", Butterworth-Heinemann, Chapter 3: Incinerator Type, 49-64 (1992).

[31] Wiles C.C. "Municipal solid waste combustion ash: State of the knowledge" *Hazard. Mat.*, 47, 325-344 (1996).

[32] Onliveros J.L., Clapp T.L. and Kossen D.S. "Physical properties and chemical properties distribution within municipal waste combustor ashes" *Environ. Prog.* 8, 200-206 (1989).

[33] Nagib S. and Inoue K., "Recovery of lead and zinc from fly ash generated from municipal incineration plants by means of acid and/or alkaline leaching", *Hydrometallurgy*, 56, 269-292, (2000).

[34] Bodog I, Polyak K, Csikos-Hartyanyi Z and Hlavay J., "Sequential extraction procedure for the speciation of elements in fly as samples" *Microchem. J.*, 54, 3, (1996).

[35] Hasselriis F. and Licata A., "Analysis of heavy metal emission data from municipal waste combustion", *Hazard. Mat.*, 47, 77-102, (1996).

[36] Vitolo S, Seggiani M, Filippi S. and Brocchini C., "Recovery of vanadium from heavy oil and Orimulsion fly ashes" *Hydrometallurgy*, 57, 141-149 (2000).

[37] Longley J., Electricity Association "An alternative fossil fuel" Environmental Briefing 12, March 2000, Internet: www.electricity.org.uk.

[38] Bitor Energy News, Orimulsion Combustion, Internet: www.bitor-europe.co.uk/Gen/Gen_2.htm.

[39] Miller C.A. and Srivastava R.K. "The combustion of Orimulsion and its generation of air pollutants" *Progress in Energy and Combustion Science*, 26, 131-160 (2000).

[40] Bitor Energy News, Boiler Performance, available from internet: www.bitor-europe.co.uk/Gen/Gen_3.htm.

[41] Murase K, Nishikawa K, Ozaki T, Machida K, Adachi G. and Suda T., "Recovery of vanadium, nickel, and magnesium from a fly ash of bitumen-in-water emulsion by chlorination and chemical transport" *Alloys and Compounds*, 264, 151-156 (1998).

[42] Bourg A.C.M. "Speciation of heavy metals in soil and groundwater and implications for their natural and provoked mobility" from "Heavy Metals" Salomons, Fostner – Springer, 19-33, (1995).

[43] Mc Lean, J.E. and Bledsoe B.E. Behavior of Metals in Soils, EPA-540-S-92-018, (1992).

[44] Tessier A. "Sequential extraction procedure for the speciation of particulate trace metals" *Anal. Chem.*, 51, (7), 844-851, (1979).

[45] Gomez Ariza J.L., Giraldez I., Sanchez-Rodas D. and Morales E "Comparison of the feasibility of three extraction procedures for trace metal partitioning in sediments from south-west Spain" *Science of the Total Environment* 246, 271-283, (2000).

[46] Ure A.M. "Single extraction schemes for soil analysis and related applications" *Science of the Total Environment*, 178, 3-10 (1996).

[47] Sahuquillo A., Lopez-Sanchez J.F., Rubio R., Rauret G., Thomas R.P, Davidson C.M and Ure A.M. " Use of a certified reference material for extractable trace metals to assess sources of uncertainty in the BCR three-stage sequential extraction procedure" *Anal. Chim. Acta,* 382, 317-327 (1999).

[48] Petit M D. and Rucandio M. I. "Sequential extraction for determination of cadmium distribution in coal fly ash, soil, and sediment samples" *Anal. Chim. Acta*, 401, 183-291 (1999).

[49] McBride M.B., "Environmental Chemistry of Soils", Oxford University Press, New York and Oxford, Chapter 4: Chemisorption and Precipitation of Inorganic Ions, 121-169 (1994).

[50] Brummer G.W. "The Importance of Chemical Speciation in Environmental Processes" Springer Verlag, Berlin, (1986).

[51] Sparks D.L. "Environmental Soil Chemistry", Academic Press, Chapter 3: Chemistry of Soil Organic Matter, 53-79, (1995).

[52] Alloway B.J. "Heavy Metals in Soils", 2nd edition, Blackie Academic and Professional, Glasgow, Chapter 14: Soil Pollution and Land Contamination, 319-339 (1995).

[53] Information obtained from web, URL: www.contaminatedland.co.uk/std-guid.htm, 03-25-98.

[54] Brusseau M.L. and Miller R.M. "Basic Concept of Remediation" Academic Press, Chapter 11, in "Pollution Science", (1996).

[55] Novotny V. "Diffuse Sources of Pollution by Toxic Metals and Impact on Receiving Waters" in "Heavy Metals", Salomons, Forstner, Mader (eds) Springer, Verlag, Berlin, 33-52 (1995).

[56] Fergusson, J.E. The Heavy Elements. Chemistry, Environmental Impact and Health Effects, Pergamon Press, Oxford, Chapter 3: Chemistry, 35-84 (1990).

[57] Kot A., and Namesnik J. "The role of speciation in analytical chemistry", *Trends in Analytical Chemistry,* 19, (2/3), 69-79, (2000).

[58] Artiola J.F. "Waste disposal" Chapter 10, in "Pollution Science", Academic Press, 135-149, (1996).

[59] As reference [19], Vol 2, p1681-1682

[60] Remediation Technologies Screening Matrix and Reference Guide (EPA, USAF, 1993). http://solaris.frtr.gov./matrix/section3/sec3_int.html (04/98).

[61] Bardos P. "Overview of the state of the art remediation technologies" presented at the Environment Agency and British Geological Survey interactive workshop: Co-operative to Manage Contaminated Land, (1998) Nottingham, information obtained from web: http://www.r3-bardos.demon.co.uk/papers/.

[62] Ernst W.H.O "Decontamination or Consolidation of Metal Contaminated Soil by Biological Means" in "Heavy Metals" Salomons, Forstner, Mader (eds), Springer, Verlag, Berlin, 141-151 (1995).

[63] Ellis, B. and Gorder, K. Intrinsic bioremediation: an economic option for cleaning up contaminated land. *Chem. and Ind.*, (3) 95-99, (1997)

[64] Private communication from Scott D. McGregor, Agricultural, Food and Environmental Chemistry. University of Glasgow, Glasgow, G12 8QQ

[65] Roane T. M., Pepper I.L. and Miller R.M. "Microbial Remediation of Metals" in "Bioremediation: Principles and Applications", L.Crawford and D.L.Crawford (eds), Cambridge University Press, 312-340, (1996).

[66] Smith L.A., Alleman B.C. and Graves C. L., "Biological Treatment Options" in "Emerging Technology for Bioremediation of Metals" Means J. and Hinckee R. (ed), Lewis, (1993).

[67] Lodi A., Del Borghi M. and Ferraiolo G "Biological Leaching of Inorganic Materials" *Biological Waste Treatment*, 133-158, (1989).

[68] Torma A.E, Walden C.C and Branion R.M.R " Microbiological leaching of a zinc sulphide concentrate" *Biotechnol. Bioeng.* 12, 501, (1970).

[69] Summers A.O. "The hard stuff: Metals in bioremediation" *Current Opinion in Biotechnology*, 3, 271-276, (1992).

[70] Tichy R., Grotenhuis J.T.C., Janssen A., van Houten R., Rulkens W.H. and Lettinga G., "Application of the Sulphur Cycle for Bioremediation of Soils Polluted with Heavy Metals" *Contaminated Soil*, 93, 1461-1462, (1993).

[71] Brombacher C., Bachofen R and Brandl H., "Development of a laboratory-scale leaching plant for metal extraction from fly ash by thiobacillus strains" *Appl. Environ. Microbiol.* 64, (4), 1237-1241, (1996).

[72] Anderson W.C., Innovative Site Remediation Technology, Vol. 5, Solvent/Chemical Extraction, Springer, Verlag, Berlin, (1995).

[73] "A Citizen's Guide to Solvent Extraction" US-EPA 542-F-96-003, (1996).

[74] Andrew Hong P.K. "Extraction, recovery, and biostability of EDTA for the remediation of heavy metals-contaminated soil" *J. Soil Contamination*, 8, (1), 81-103, (1999).

[75] Hong K.-J., Tokunaga S. and Kajiuchi T. "Extraction of heavy metals from MSW incinerator fly ashes by chelating agents" *J. Hazard. Mat.* B75 57-73, (2000).

[76] Chmielewski A.G., Urbanski T.S. and Migdal W "Separation technologies for metals recovery from industrial wastes" *Hydrometallurgy* 45, 333-344 (1997).

[77] Bipp H.-P., Wunsch P., Fischer K., Bieniek D. and Kettrup A., "Heavy metal leaching of fly ash from waste incineration with gluconic acid and a molasses hydrolysate" *Chemosphere,* 36, (11), 2523-2533, (1998).

[78] Nugteren H. W., Janssen-Jurkovicova M. and Scarlett B. "Removal of heavy metals from fly ash and the impact on its quality" *J. Chem. Tech. Biotechnol.*, 76 (3), 389-395, (2001).

[79] Anderson W.C., "Innovative Site Remediation Technology", Springer, Verlag, Berlin, Vol. 3, "Soil Washing/Soil Flushing", (1993).

[80] Kedziorek M.A.M. and Bourg A.C.M. "Solubilisation of lead and cadmium during the percolation of EDTA through a soil polluted by smelting activities" *J.Contaminant Hydrology*, 40, 381-392, (2000).

[81] "A Citizen's Guide to Soil Washing" US-EPA 542-F-96-002, (1996).

[82] Soil Washing at the King of Prussia Technical Corporation Superfund Site. information obtained from web URL: www.clu-in.com/kop.htm.

[83] Barkay T. and Schaefer J., "Metal and radionucleides bioremediation: issues, considerations and potentials" *Current Opinion in Microbiology*, 4, 318-323, (2001).

[84] Gadd G. M. "Bioremedial potential of microbial mechanisms of metal mobilization and immobilization" *Current Opinion in Biotechnology*, 11, 271-279, (2000).

[85] White C., Sayer J.A. and Gadd G.M. "Microbial solubilisation and immobilization of toxic metals: Key biogeochemical processes for treatment of contamination" *FEMS Microbiology Reviews*, 20, 303-316 (1997).

[86] White C., Sherman A.K. and Gadd G.M., "An integrated microbial process for the bioremediation of soil contaminated with toxic metals" *Natural Biotechnology*, 16, 572-575, (1998).

[87] Groudev S.N., Spasova I.I. and Goergiev P.S. "In situ bioremediation of soil contaminated with radioactive elements and toxic heavy metals" *Int. J. Min. Proc.* 62, 301-308, (2001).

[88] Thomas R.A.P., Beswick A.J., Basnakova G., Moller R. and Macaskie L.E., "Growth of naturally occurring microbial isolates in metal-citrate medium and bioremediation of metal-citrate wastes" *J. Chem. Tech. Biotechnol.*, 75, 187-195, (2000).

[89] Mehlhorn R.J., Buchanan B.B. and Leighton T. "Bacterial Chromate Reduction and Production Characterisation" in "Emerging Technology for Bioremediation of Metals" Means J. and Hinckee R. (editors), Lewis, (1993).

[90] White C., Wilkinson S.C and Gadd G. M. "The role of microorganisms in biosorption of toxic metals and radionucleides" *Int. Biodeter. Biodegrad.* 17-40, (1995)

[91] Wong P.K. and Kwok S.C. "Accumulation of nickel ion by immobilized cells of *Enterobacter* species" *Biotech. Letters* 14 (7), 629-634, (1992)

[92] Mejare M. and Bulow L., "Metal binding proteins and peptides in bioremediation and phytoremediation of heavy metals" *TRENDS in Biotechnology*, 19, (2), 67-73, (2001).

[93] Anderson W.C., "Innovative Site Remediation Technology", Vol. 4, "Stabilisation/Solidification", Springer edition, (1994).

[94] THIO RED Technology. Information obtained from web, URL: www.env-sol.com/etus/hp-detox.html (09-07-98).

[95] Crannell B. S., Eighmy T.T., Krzanowski J.E., Dykstra Eusden Jr J., Shaw E.L. and Francis C.A., "Heavy metal stabilization in municipal solid waste combustion bottom ash using soluble phosphate" *Waste Management* 20, 135-148, (2000).

[96] Bardos P. Overview of the state of the art remediation technologies, presented at the Environment Agency & British Geological Survey interactive workshop: Co-operative to Manage Contaminated Land, British Geological Survey, Keyworth, Nottingham, (1998).

[97] Comans R. N. J., Maima J. A. and Geelhoed P.A., "Reduction of contaminant leaching from MSWI bottom ash by addition of sorbing components" *Waste Management* 20, 125-133 (2000).

[98] US-EPA Report, Cost and Performance Report: In-situ vitrification at the Parson Chemical/ETM Enterprises Superfund Site Grand Ledge, Michigan. information obtained from web: http://clu-in.com/parsons.htm.

[99] US-EPA report EPA/540/S-97/500, Technology alternatives for the remediation of soil contaminated with As, Cd, Cr, Hg, and Pb, (1997).

[100] Cox, M., Duke P.W. and Gray M.J. "Winning metal from an ore" *Patent GB* 213 5984 A (1984).

[101] Davies D.J., and Oelman L.A., "Metallurgical Processes and Production Technology", Pitman, London, Chapter 2, 15-68, (1985).

[102] Gilchrist J.D. "Extraction Metallurgy" 2nd edition, Pergamon Press, Oxford: 274-354, (1979).

[103] Jackson E. "Hydrometallurgical Extraction and Reclamation", Ellis Horwood, Chichester: (1986).

[104] Conard B.R., "The role of hydrometallurgy in achieving sustainable development" *Hydrometallurgy*, 30, 1-28, (1992).

[105] Betteridge W. "Nickel and its Alloys", Ellis Horwood, Chichester Chapter 2: occurrence and extraction of nickel, section 2.2: sulphide ores, 32-34, (1984).

[106] Barr D. W. "The Extraction of Nickel using Volatile Organic Reagents" PhD thesis, University of Hertfordshire, (1989).

[107] Mosier R.W. and Sievers R.L "Gas Chromatography of Metal Chelates" Pergamon Press, Oxford, (1965).

[108] Duke P.W. "Thermal stability and reactivity of metal extraction coordination compounds" M.Phil. Thesis, (1985).

[109] Cox M., Duke P.W., and Gray M.J. 'Extraction of metals by the direct thermal attack of organic reagents' Extraction Metallurgy'85, IMM London, 33-41, (1985).

[110] Barr D.W. Cox M., Flett D.S. and Holt G., 'The extraction of nickel from low grade ores by volatile organic reagents' Extraction Metallurgy'89, IMM London, 27-44, (1989).

[111] Pichugin A.A. and Cox M., "Direct recovery of nickel from Greek Laterite ore using SERVO Process" Nickel Cobalt'97 Vol II, Pyrometallurgical

fundamentals and process development. Levrac L.A. and Bergmann R.A.,(eds) Metallurgical Society of CIM, 125-136 (1997).

[112] Rouessac F. and Rouessac A., "Chemical Analysis, Modern Instrumentation Methods Analysis", 4th Edition, John Wiley, New York, Chapter 10, 161-186, (2000).

[113] Idem, Chapter 16, 289-315.

[114] Hatakeyama T. and Zehenhai Lui, "Handbook of Thermal Analysis", Wiley, Chichester, Chapter 1: Introduction, 3-13, (1998)

[115] Willard H.M., Merritt L.L., Dean J.A. and Settle F.A., "Instrumental Methods of Analysis", 7th Edition, Wadsworth Publishing Company, Belmont, Calif., Chapter 10, 260-282 (1988).

[116] As reference 115 Chapter 13, 340-398.

[117] Anon. American Allied, Volclay Minerals Ltd, Technical data sheet, Sodium Montmorillonite grade MPS-1.

[118] Private communication from France.

[119] Private communication from Venezuela.

[120] Maruyama T., and Shirai T. "Copper thin films prepared by chemical vapour deposition from copper (II) acetylacetonate" *J. Mater. Sci.*, 30, 5551-5553, (1995).

[121] Maruyama T. and Tago T. "Nickel thin films prepared by chemical vapour deposition from nickel acetylacetonate" *J. Mater. Sci.*, 28, 5345-5348, (1993).

[122] Bell C.F. "Properties of ligands and chelate rings" in "Metal chelation: principles and applications". Oxford Chemistry Series, Atkins P.W., Holker J.S.E, and Holliday A.K (eds), Oxford University Press, UK, Chapter 1, (1977).

[123] Hassanein M. and Hewaidy I.F., "A simple method for the preparation of zinc, cadmium, mercuric and cobalt acetylacetonate" *Anorg. und Allgem. Chem.*, 373, 80-82, (1970).

[124] Berg E.W. and Truemper J.T. "A study of the volatile characteristic of various metal β-diketone chelates" *J. Phy. Chem.*, 64, 487-490 (1960).

[125] Graddon D.P. "Divalent transition metal β-keto-enolate complexes as Lewis acids" *Coord. Chem. Reviews*, 4, 1-28 (1969).

[126] Murray J.P. and Hill J.O., " DSC determination of the sublimation enthalpy of tris(2,4-pentanedianoto)cobalt(III) and bis(2,4-pentanedionato)nickel(II) and copper(II)", *Thermochim. Acta*, 109, 383-390 (1987).

[127] P Fackler, "Metal β-ketoenolate complexes", in "Progress in Inorganic Chemistry", F.Albert Cotton (editor), Interscience Publishers, USA, Ohio, Vol 7 (1966).

[128] Belcher R., Martin R.J., Stephen W.I., Henderson D.E., Kamalizad A. and Uden P.C. "Gas chromatography of divalent transition metal chelates" *Anal. Chem.*, 45 (7), 1197-1203, (1973).

[129] Ohrbach K.-H., Radhoff G. and Kettrup A., "Thermal degradation of metal acetylacetonates with divalent metals by a combined TG-DTA-MS technique", *Thermochim. Acta*, 67, 189-195, (1983).

[130] Murray J.P. and Hill J.O. "DSC determination of the sublimation enthalpy of tris(2,4-pentanedianoto)chromium (III) and iron (III)" *Thermochim. Acta*, 72, 341-347, (1984).

[131] Gilby L.M. and Piggott B. "The synthesis and X-ray structure of cobalt(II) complexes of iminobis(phosphinechalcogenides), $[Co\{N(XPR_2)_2\text{-}X,X'\}_2]$ (X=S or Se; R=Ph or Pr^i)" *Polyhedron*, 18, 1077-1082 (1999).

[132] Murray J.P. and Hill J.O. "DSC determination of the sublimation enthalpy of Bis(2,4-pentanedianoto)oxovanadium(IV) and tetrakis(2,4-pentanedianoto) zirconium(IV) " *Thermochim. Acta*, 109, 391-396, (1987).

[133] Rietzel M., Roesky H. W., Katti K. V., Schmidt H, Herbst-Irmer R., Noltemeyer M. and Sheldrick G. M. " Unexpected nitrogen-oxygen exchange reaction in cyclic metalphosphazenes; Synthesis and X-Rays crystal structures of $[Mo(OPPh_2NPPh_2O)_2Cl_2]$, [Mo(OPPh2NPPh2O)2(O)Cl] and $[Mo(OPPh_2NPPh_2O)_2O_2]$", *J. Chem. Soc Dalton Trans.*, 2387-2392 (1990).

[134] Barr D.W., "The Extraction of Nickel using Volatile Organic Reagents", PhD Thesis, University of Hertfordshire, Hatfield, UK, Chapter 2, (1989).

[135] Duke P.W. "Thermal stability and volatility studies" in "Thermal stability and reactivity of metal extraction coordination compounds" M.Phil. Thesis, University of Hertfordshire, Hatfield, UK, Chapter 3, (1985).

[136] D.C. Cupertino, R.W. Keyte, A.M.Z. Slawin, D.J. Williams and J.D. Woolings, "Preparation and singlecrystal characterization of $^iPr_2(S)NP(S)^iPr_2$ and

homoleptic [$^{i}Pr_2(S)NP(S)^{i}Pr_2$]$^-$ complexes of zinc, cadmium and nickel" *Inorg. Chem.* 35, 2695-2697, (1996).

[137] Siiman O. and Vetuskey J. "Synthesis of copper thioxo- and dithioimido-phosphinates. Infrared and Raman spectra of imidodiphosphinates" *Inorg. Chem.*, 19, 1672-1680 (1980).

[138] Rietzel M., Roesky H. W., Katti K. V., Noltemeyer M., Symons M.C.R. and Abu-Raqabah A. "Formation of spirocyclic imidophosphinato complexes: Crystal structures of [$V(OPPh_2NPPh_2O)_2O$] and [$Mo(NPPh_2NPPh_2O)_2Cl_2$]" *J. Chem. Soc Dalton Trans.*, 1285-1290 (1991).

[139] McQuillan G.P. and Oxton I.A. "Vibrational spectrum, structure and complex forming reactions of imidobis(diphenylphosphine sulphide)" *Inorg. Chim. Acta*, 29, 69-75, (1978).

[140] Schmidpeter A. and Groeger H., Z. *Anorg. Allgem. Chem.*, 106, 345, (1966).

[141] Davidson A. and Switkes E.S. "The stereochemistry of four coordinate bis(imidophosphinato)metal(II) chelate complexes" *Inorg. Chem.*, 10, (4), (1971).

[142] Birdsall D.J., Slawin A. M. Z. and Woollins J.D. "The preparation and coordination chemistry of $R_2P(S)NHP(S)R'_2$" *Polyhedron*, 20, 125-134 (2001).

[143] Duke P.W. "Reduction Studies" in "Thermal Stability and Reactivity of Metal Extraction Coordination Compounds" M.Phil.Thesis, University of Hertfordshire, Hatfield, UK, Chapter 5, (1985).

[144] Davidson C.M., Thomas R.P., McVey S.E., Perala R., Littlejohn D. and Ure A.M. "Evaluation of a sequential extraction procedure for the speciation of heavy metals in sediments" *Anal. Chim. Acta*, 291, 277-286 (1994).

[145] Miller J.C., Miller J.M., "Statistics for analytical chemistry" Ellis Horwood, Chichester, England, 33-79 (1984).

[146] Sigma-Aldrich, Information obtained from web, URL: http://www.sigmaaldrich.com/europe/ (10-11-02).

[147] Taylor A. 'Nickel laterites processing', *Mining magazine*, 100-103, (1996)

[148] ESTCP, US department of defense, cost and performance data 'Joint Small-Arms Range Remediation' (1997)

[149] information obtained from the web: www.enr.com/cost/coctcci.asp

[150] information obtained from the web: www.hq.usace.army.mil/cemp/e/es/pax/paxtoc.htm

[151] US-EPA Report, Remediation Technology Cost Compendium. Information obtained from web: http://epa.gov, EPA. 542R-01-009, (2001)

[152] US-EPA Report, Cost and Performance summary report, "Thermal Desorption at the Waldick Aerospace Device Site, Wall Township, New Jersey", (1993)

[153] URS Corporation, URS File No. 35-00009574.00 'Draft Final EE/CA, "Engineering Evaluation /Cost Analysis, Bayou Verdine Area of Concern" Section 5: Identification and Analysis of Removal Action Alternatives (2002)

[154] Renholds J., US EPA report, "In Situ Treatment of Contaminated Sediments", (1998)

[155] ESTCP, US Army Environmental Center "In-Situ Electrokinetic Remediation of Metal Contaminated Soils", Technology Status Report Number: SFIM-AEC-ET-CR-99022 (2000)